ISSN 0021-9673

VOL. 518 NO. 1 SEPTEMBER 28, 1990

JOURNAL OF

CHROMATOGRAPHY

INTERNATIONAL JOURNAL ON CHROMATOGRAPHY, ELECTROPHORESIS AND RELATED METHODS

ELSEVIER

JOURNAL OF CHROMATOGRAPHY

Scope. The *Journal of Chromatography* publishes papers on all aspects of chromatography, electrophoresis and related methods. Contributions consist mainly of research papers dealing with chromatographic theory, instrumental development and their applications. The section *Biomedical Applications*, which is under separate editorship, deals with the following aspects: developments in and applications of chromatographic and electrophoretic techniques related to clinical diagnosis or alterations during medical treatment; screening and profiling of body fluids or tissues with special reference to metabolic disorders; results from basic medical research with direct consequences in clinical practice; drug level monitoring and pharmacokinetic studies; clinical toxicology; analytical studies in occupational medicine.

Submission of Papers. Manuscripts (in English; *four* copies are required) should be submitted to: The Editor of *Journal of Chromatography*, P.O. Box 681, 1000 AR Amsterdam, The Netherlands, or to: The Editor of *Journal of Chromatography, Biomedical Applications*, P.O. Box 681, 1000 AR Amsterdam, The Netherlands. Review articles are invited or proposed by letter to the Editors. An outline of the proposed review should first be forwarded to the Editors for preliminary discussion prior to preparation. Submission of an article is understood to imply that the article is original and unpublished and is not being considered for publication elsewhere. For copyright regulations, see below.

Subscription Orders. Subscription orders should be sent to: Elsevier Science Publishers B.V., P.O. Box 211, 1000 AE Amsterdam, The Netherlands, Tel. 5803 911, Telex 18582 ESPA NL. The *Journal of Chromatography* and the *Biomedical Applications* section can be subscribed to separately.

Publication. The *Journal of Chromatography* (incl. *Biomedical Applications*) has 37 volumes in 1990. The subscription prices for 1990 are:

J. Chromatogr. (incl. *Cum. Indexes, Vols. 451–500*) + *Biomed. Appl.* (Vols. 498–534):
Dfl. 6734.00 plus Dfl. 1036.00 (p.p.h.) (total *ca.* US$ 3885.00)

J. Chromatogr. (incl. *Cum. Indexes, Vols. 451–500*) only (Vols. 498–524):
Dfl. 5616.00 plus Dfl. 756.00 (p.p.h.) (total *ca.* US$ 3186.00)

Biomed. Appl. only (Vols. 525–534):
Dfl. 2080.00 plus Dfl. 280.00 (p.p.h.) (total *ca.* US$ 1180.00).

Our p.p.h. (postage, package and handling) charge includes surface delivery of all issues, except to subscribers in Argentina, Australia, Brasil, Canada, China, Hong Kong, India, Israel, Malaysia, Mexico, New Zealand, Pakistan, Singapore, South Africa, South Korea, Taiwan, Thailand and the U.S.A. who receive all issues by air delivery (S.A.L. — Surface Air Lifted) at no extra cost. For Japan, air delivery requires 50% additional charge; for all other countries airmail and S.A.L. charges are available upon request. Back volumes of the *Journal of Chromatography* (Vols. 1–497) are available at Dfl. 195.00 (plus postage). Claims for missing issues will be honoured, free of charge, within three months after publication of the issue. Customers in the U.S.A. and Canada wishing information on this and other Elsevier journals, please contact Journal Information Center, Elsevier Science Publishing Co. Inc., 655 Avenue of the Americas, New York, NY 10010. Tel. (212) 633-3750.

Abstracts/Contents Lists published in Analytical Abstracts, ASCA, Biochemical Abstracts, Biological Abstracts, Chemical Abstracts, Chemical Titles, Chromatography Abstracts, Clinical Chemistry Lookout, Current Contents/Life Sciences, Current Contents/Physical, Chemical & Earth Sciences, Deep-Sea Research/Part B: Oceanographic Literature Review, Excerpta Medica, Index Medicus, Mass Spectrometry Bulletin, PASCAL-CNRS, Pharmaceutical Abstracts, Referativnyi Zhurnal, Science Citation Index and Trends in Biotechnology.

See inside back cover for Publication Schedule, Information for Authors and information on Advertisements.

0021-9673/90/$03.50

CONTENTS

(Abstracts/Contents Lists published in Analytical Abstracts, ASCA, Biochemical Abstracts, Biological Abstracts, Chemical Abstracts, Chemical Titles, Chromatography Abstracts, Current Contents/Life Sciences, Current Contents/Physical, Chemical & Earth Sciences, Deep-Sea Research/Part B: Oceanographic Literature Review, Excerpta Medica, Index Medicus, Mass Spectrometry Bulletin, PASCAL-CNRS, Referativnyi Zhurnal and Science Citation Index)

(Continued overleaf)

In articles with more than one author, the name of the author to whom correspondence should be addressed is indicated in the article heading by a 6-pointed asterisk (*)

JOURNAL OF CHROMATOGRAPHY
VOL. 518 (1990)

JOURNAL *of* CHROMATOGRAPHY

INTERNATIONAL JOURNAL ON CHROMATOGRAPHY,
ELECTROPHORESIS AND RELATED METHODS

ELSEVIER
AMSTERDAM — OXFORD — NEW YORK — TOKYO

0021-9673/90/$03.50

Printed in The Netherlands

Journal of Chromatography, 518 (1990) 1–8
Elsevier Science Publishers B.V., Amsterdam

CHROM. 22 587

Systematic errors with the use of internal standard calibration in gas chromatographic headspace analysis

JOSEF DROZD* and ZDENA VODÁKOVÁ
Institute of Analytical Chemistry, Czechoslovak Academy of Sciences, 611 42 Brno (Czechoslovakia)
and
PAVEL KOUPIL
Department of Clinical Biochemistry, Hospital, 792 01 Bruntál (Czechoslovakia)
(First received December 14th, 1989; revised manuscript received May 28th, 1990)

ABSTRACT

The specificity of the use of internal standard calibration in headspace analysis was studied. An equation was derived that differed from the conventional equation by a factor $(V_g + K_sV_l)/(V_g + K_iV_l)$, where V_g and V_l are the volumes of the gaseous and the liquid phases, respectively, and K_i and K_s are the distribution constants between the phases of the analyte i and the internal standard s, respectively. This factor is generally not equal to unity. Its magnitude, and hence that of the systematic error, is demonstrated by using literature values and experimental data obtained by analyses of model blood and water samples. It is shown that the use of the internal standard technique does not generally eliminate the matrix effect which is a serious problem in quantitative headspace analysis.

INTRODUCTION

Nowadays headspace analysis is widely used for the determination of volatile substances in condensed materials [1–3]. In this method of sample treatment, gas (air) in contact with the material to be analysed is injected into the chromatograph rather than the material itself.

The effect of the matrix composition has long been regarded as a crucial problem in quantitative headspace analysis [4–6]. The composition of the liquid (and/or condensed) sample being analysed influences, sometimes very strongly, the concentration of analyte in the gaseous phase, and thereby the accuracy of the results (the so-called "matrix effect"). In order to compensate for this effect, and to obtain accurate results, analysts often use the internal standard technique for calibration [7–11]. This technique consists in adding to the sample a known amount of a substance (internal standard) different from that being analysed, and relating the peak area of the analyte to that of the internal standard. A calibration graph can be constructed and used for evaluation of this procedure, *viz.*, the ratio of the masses of the analyte and internal standard is plotted against the ratio of the corresponding peak areas. This technique is generally widely used to compensate for imprecisions in injected sample volume measurements and other experimental variables. As far as headspace analysis is concerned, it must be realized that both the analyte and the internal standard are

0021-9673/90/$03.50

distributed between the condensed and gaseous phases and these distributions are influenced by the composition of the condensed phase in different ways. The proportions of analytes and the internal standard in the gaseous phase are therefore generally different from those in the original condensed sample, and might also be different from those in reference calibration. Hence the calibration graph measured for a matrix of a certain composition should be used for headspace analysis of the same matrix, otherwise the results obtained can suffer from systematic errors.

This aspect seems often to be overlooked in this field, even though it has already been discussed in the literature [5], and methods that generally eliminate the matrix effect have been proposed, *e.g.*, the method of standard addition [4–6] and the method of multiple gas extraction [12,13], and also a practical approach to the decision as to whether these methods are necessary in a particular case has been described [14]. Hence, it is felt that a paper defining and demonstrating the problem clearly is lacking.

In this paper the relationships that describe the use of the internal standard technique in headspace analysis and allow an estimate of the magnitude of the systematic error are derived; the estimation was demonstrated using literature values and comparing them with experimental data.

THEORETICAL

Let us consider liquid material enclosed in a vessel to be subjected to headspace analysis, the volatile analyte i being distributed between the liquid and the gaseous phases of this two-phase system. At equilibrium, the mass balance of the distribution can be expressed as

$$m_{io} = m_{ig} + m_{il} \tag{1}$$

and described by the distribution constant, K_i:

$$K_i = \frac{c_{il}}{c_{ig}} = \frac{m_{il}/V_l}{m_{ig}/V_g} \tag{2}$$

where m_{io}, m_{ig} and m_{il} are the mass of the analyte i originally present in a liquid sample and the equilibrium mass of analyte i present in the gaseous and the liquid phases, respectively; c_{ig} and c_{il} are equilibrium concentrations of the analyte i in the gaseous and the liquid phases, respectively and formally V_g and V_l are the volumes of the gaseous and the liquid phases, respectively. By combining the above two equations we obtain

$$m_{io} = c_{ig}(V_g + K_i V_l) = \frac{m_{ig}}{V_g}(V_g + K_i V_l) \tag{3}$$

a well known equation which is the basis of quantitative evaluation in headspace analysis. The gaseous phase sample, of volume v_g, containing the mass of the volatile analyte m_i, is subjected to analysis. To this mass of analyte the peak area of the analyte in the chromatogram, A_i, corrected by a mass response factor, f_i^m, is proportional.

Thus we can write

$$A_i f_i^m = k m_i \tag{4}$$

where k is a proportionality constant characteristic for an apparatus employed [15].

The mass of the analyte in the gaseous phase, m_{ig}, can then be expressed as

$$m_{ig} = \frac{s_i f_i^m}{k} \cdot \frac{V_g}{v_g} \tag{5}$$

By rearranging this expression and substituting for m_{ig} from eqn. 3, we obtain

$$A_i = \frac{k m_{ig} v_g}{f_i^m V_g} = \frac{m_{io}}{V_g + K_i V_l} \cdot \frac{k v_g}{f_i^m} \tag{6}$$

The same situation occurs with the internal standard and a corresponding relationship can also be written:

$$A_s = \frac{m_{so}}{V_g + K_s V_l} \cdot \frac{k v_g}{f_s^m} \tag{7}$$

Division of eqns. 6 and 7 results in

$$\frac{A_i}{A_s} = \frac{m_{io} f_s}{m_{so} f_i^m} \left(\frac{V_g + K_s V_l}{V_g + K_i V_l} \right) \tag{8}$$

This equation describes the use of an internal standard in headspace analysis and differs from that used for this technique in a conventional manner by containing the expression in parentheses. This expression describes the effect of matrix material on the ratios of the concentrations in the gaseous phase of the analyte and the internal standard. In other words, when constructing the calibration graph in a conventional way by plotting various ratios of masses of the analyte and the internal standard against ratios of the corresponding peak areas, we have to multiply the slope of the curve by the magnitude of the factor in parentheses so that we can use this calibration for headspace analysis. It is obvious that the magnitude of this factor is generally not equal to unity and in most practical instances such an operation cannot be made owing to a lack of knowledge of the distribution constants, but the magnitude of the factor corresponds to that of systematic errors from which the results of headspace analysis suffer if the internal standard technique is employed. In further work we calculated values of the slopes of the calibration graphs for different matrix materials from the literature and measured values of the distribution constants with the use of a flame ionization detector, and demonstrated the occurrence of systematic errors in the determination of volatile substances in water and blood on models samples.

EXPERIMENTAL

The measurements of distribution constants were based on the mass balance expressed by eqn. 3. For blood, a known amount of analyte (1–5 μl of a particular substance) was added to 1.5 ml of blood in an 8.2-ml vial, which was closed tightly with a septum. After equilibration for 30 min at 52°C, 0.2 ml of the gaseous phase was withdrawn with a 1-ml gas-tight syringe (Hamilton, Bonaduz, Switzerland) preheated to about 60°C to suppress condensation and adsorption. The gas chromatographic (GC) analyses were performed on a Chrom-5 instrument (Laboratory Instruments, Prague, Czechoslovakia) equipped with a flame ionization detector and a glass column (2.5 m × 3 mm I.D.) packed with Porapak P (80–100 mesh) (Waters Assoc., Milford, MA, U.S.A.), with nitrogen as the carrier gas at a flow-rate of 35 ml/min. The column temperature was 160°C and the injection port and detector temperatures were 180 and 240°C, respectively.

With water and aqueous solutions, a known amount of the analyte was added to 50 ml of water or aqueous phase in a 100-ml bottle fitted with a septum. The bottle was thermostated at 40°C for 20 min and 1 ml of the gaseous phase was withdrawn for analysis as above with a gas-tight syringe preheated to about 60°C. The GC analyses were carried out on a Shimadzu GC4A instrument (Shimadzu Seisakusho, Kyoto, Japan) with a flame ionization detector and a stainless-steel column (1.5 m × 3 mm I.D.) packed with 15% (w/w) Carbowax 20M on Chromosorb G (100–120 mesh) (Carlo Erba) with nitrogen as the carrier gas at a flow-rate of 35 ml/min. The column temperature was 70°C and the injection port and detector temperatures were 150°C, respectively. The peak areas were measured with a CI-100 electronic integrator (Laboratory Instruments) in all instances.

Similarly, the calibration graphs were measured and constructed for several analyte–internal standard pairs, the range of concentrations being from tens to hundreds of μg/ml in distilled water, in 0.34 g/ml aqueous sodium chloride solution and in blood.

All chemicals were of analytical-reagent grade from various suppliers.

RESULTS AND DISCUSSION

To obtain an idea of how serious the systematic error in headspace analysis with internal standard calibration could be, we calculated the values of the slopes of calibration graphs obtained with eqn. 8. For this purpose we used the K values published by Sato and Nakajima [16], who measured the distribution constants in two-phase systems with the gaseous phase being air and the other phase water, blood and/or oil. The mass response factors for the flame ionization detector were taken from ref. 17. The magnitudes of the slopes were calculated for the pairs of various substances, one being considered as the analyte and the other as the internal standard. The results are illustrated in Table I for a ratio of the volumes of the phases of $V_g/V_l = 4$.

It is obvious from Table I that for different liquid phases the value of the slope is not the same for a particular pair of compounds, *i.e.*, that the effect of the matrix composition is not eliminated by an internal standard technique. The ratio of the slopes gives an idea of the systematic error due to the evaluation of the analysis of one

TABLE I

SLOPES OF THE CALIBRATION GRAPHS CALCULATED WITH K VALUES FROM REF. 5

Analyte (i)	Internal standard (s)	Distribution constant		Slope	Liquid phase[a]
		K_i	K_s		
Toluene	Ethylbenzene	2.23	1.69	0.998	w
		15.60	28.40	0.591	b
		1471	3791	0.384	o
Toluene	Benzene	2.23	2.78	0.865	w
		15.60	7.80	1.611	b
		1471	492	3.003	o
m-Xylene	*p*-Xylene	1.66	1.57	0.932	w
		26.4	37.6	0.722	b
		3842	3694	1.04	o
Diethyl ketone	Methyl ethyl ketone	181	254	0.641	w
		168	202	0.746	b
		808	263	2.719	o

[a] w = Water, b = blood, o = oil.

matrix material by calibration with another condensed phase. For instance, if we determine toluene in blood with benzene as an internal standard and the calibration graph is constructed with distilled water, we obtain systematically results that are roughly twice as high. The differences are not very significant only with compounds that are chemically very similar, such as *m*- and *p*-xylene.

To show influence on the results of very small differences in the composition of the matrix of the same character, we measured the distribution constants of acetone and propanol in a blood–air system as described under Experimental. The three blood samples differed in the content of lipophilic substances, *viz.*, blood sample 1 having 3.7 nmol/l of cholesterol and 1.13 nmol/l of triglycerides, sample 2 having 4.2 and 1.28 nmol/l and sample 3 4.5 and 1.5 nmol/l, respectively. The results are given in Table II; the relative standard deviations of the K values are *ca.* 5%. From the magnitude of the slopes calculated according to eqn. 8, again for the phase volume ratio $V_g/V_l = 4$, one can estimate that even with a matrix material of such a similar composition the systematic error can reach up to 20%. One should be aware that in our particular instance such an accuracy might be tolerable, but in other instances the error might be

TABLE II

SLOPES OF CALIBRATION GRAPHS FOR DIFFERENT BLOOD SAMPLES

Analyte, acetone; internal standard, *n*-propanol.

Distribution constant		Slope	Liquid phase
K_i	K_s		
205	935	0.269	Blood sample 1
261	1053	0.303	Blood sample 2
297	1115	0.323	Blood sample 3

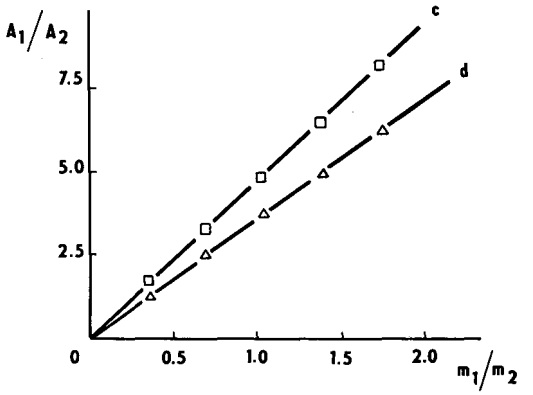

Fig. 1. Example of calibration graphs for the determination of acetone (subscript 1) in blood in headspace analysis with *n*-propanol (subscript 2) as the internal standard. Line c, blood sample 4; line d, blood sample 5.

even higher. For example, the internal standard technique used in headspace analysis for the determination of ethanol in blood has been intensively studied and used [18,19] with an accuracy that was found to be acceptable.

The magnitude of the error is illustrated graphically in Fig. 1, where calibration graphs are plotted for the determination of acetone (subscript 1) in blood by headspace analysis with *n*-propanol as the internal standard (subscript 2). Under the conditions described under Experimental, line c was measured for blood sample 4 containing 7.9 nmol/l of cholesterol and 2.1 nmol/l of triglycerides and line d was measured for blood sample 5 containing 3.8 nmol/l of cholesterol and 1.6 nmol/l of triglycerides. Fig. 1 demonstrates the error made if blood with a composition that is accidentally close to that of sample 5 is analysed and if the evaluation is carried out according to line c.

In another model situation we measured the calibration graphs for pairs of compounds in distilled water and in 0.34 g/ml aqueous sodium chloride solution. The resulting slopes for six chosen pairs are given in Table III, and the calibration graph for acetone with isopropanol as an internal standard is shown in Fig. 2. It is obvious that only very similar compounds such as *n*-propanol and isopropanol are influenced to the

TABLE III

SLOPES OF CALIBRATION GRAPHS OF THE INTERNAL STANDARD TECHNIQUE FOR VARIOUS PAIRS OF SUBSTANCES IN WATER AND IN 0.34 g/ml SODIUM CHLORIDE SOLUTION

Analyte	Internal standard	Slope of calibration graph		Ratio of slopes
		In water	In NaCl solution	
n-Propanol	Isopropanol	0.644	0.649	0.992
Acetone	Isopropanol	3.754	2.771	1.350
Acetone	*n*-Propanol	4.041	3.010	1.340
Ethanol	*n*-Propanol	0.482	0.385	1.260
Acetone	Methyl ethyl ketone	0.456	0.326	1.410

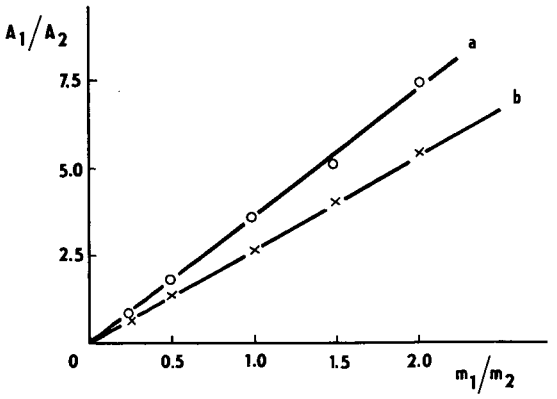

Fig. 2. Example of calibration graphs for the determination of acetone (subscript 1) by headspace analysis with isopropanol (subscript 2) as the internal standard. Line a, in water; line b, in 0.34 g/ml sodium chloride solution.

same extent by a change in the liquid phase composition, so that the calibration graphs are almost identical. With other pairs the relative error reaches 40%.

However, one also has to take account of the influence of adsorption that may possibly occur during the procedure, namely in the syringe used. Although the syringe was kept at an elevated temperature, adsorption may occur in it. If the effect of adsorption varies for different analytes, the result could be similar to that observed in this study or may, at least, contribute to it. According to our previous experience, these effects are not very pronounced and it is also difficult to imagine glass being a selective adsorbent towards the analytes that we studied. As the final consequence for the analytical results seemed to be the same, we did not carry out any special experiments to distinguish the extents of various fine particular effects.

CONCLUSIONS

When using internal standard calibration with headspace analysis, it should be realized that the use of the internal standard technique does not generally eliminate the matrix effect in headspace analysis and systematic errors may occur; the calibration graph for the internal standard technique should be applied to the evaluation of headspace analysis of the same matrix material for which that graph was measured; and one can only expect similar values of the slopes of calibration graphs for very closely chemically related compounds (*e.g.*, isomers).

REFERENCES

1 H. Hachenberg and A. P. Schmidt, *Gas Chromatographic Headspace Analysis*, Heyden, London, Philadelphia, PA, 1977.
2 B. Kolb, *Applied Headspace Gas Chromatography*, Heyden, London, Philadelphia, 1980.
3 B. V. Ioffe and A. G. Vitenberg, *Headspace Analysis and Related Methods in Gas Chromatography*, Wiley, New York, 1984.
4 J. Novák, *Quantitative Analysis by Gas Chromatography*, Marcel Dekker, New York, 1975, pp. 138–153.
5 B. Kolb, *J. Chromatogr.*, 122 (1976) 553.

6 J. Drozd and J. Novák, *J. Chromatogr.*, 165 (1979) 141.
7 C. L. Mendenhall, J. MacGee and E. S. Green, *J. Chromatogr.*, 190 (1980) 197.
8 E. Zuccato, F. Marcucci and E. Mussini, *Anal. Lett.*, 13 (1980) 363.
9 H. Radzikowska-Kintzi and M. Jakubowski, *Int. Arch. Occup. Environ. Health*, 49 (1981) 115.
10 E. Westerberg and L. Larsson, *J. Environ. Anal. Chem.*, 12 (1982) 233.
11 J. M. Christensen, K. Rasmussen and B. Koppen, *J. Chromatogr.*, 442 (1988) 317.
12 B. Kolb, P. Pospisil and M. Auer, *J. Chromatogr.*, 204 (1981) 371.
13 B. Kolb, *Chromatographia*, 15 (1982) 587.
14 R. W. Souter, *J. Chromatogr.*, 193 (1980) 207.
15 J. Novák, *Quantitative Analysis by Gas Chromatography*, Marcel Dekker, New York, 2nd ed., 1988, p. 82.
16 A. Sato and T. Nakajima, *Br. J. Ind. Med.*, 36 (1971) 231.
17 J. C. Sternberg, W. S. Gallaway and D. T. L. Jones, in N. Brenner, J. E. Callen and M. D. Weiss (Editors), *Gas Chromatography*, Academic Press, New York, 1962, p. 231.
18 G. Machata, *Clin. Chem. Newsl.*, 4 (1972) 29.
19 G. Machata, *Z. Rechtsmed.*, 75 (1975) 229.

Journal of Chromatography, 518 (1990) 9–19
Elsevier Science Publishers B.V., Amsterdam

CHROM. 22 546

Automatic sampler for Curie-point pyrolysis–gas chromatography with on-column introduction of pyrolysates

W. G. FISCHER* and P. KUSCH
Fischer Labor- und Verfahrenstechnik GmbH, Industriepark Kottenforst, D-5309 Meckenheim (F.R.G.)
(First received January 25th, 1990; revised manuscript received May 8th, 1990)

ABSTRACT

An automatic sampler for Curie-point pyrolysis–gas chromatography (GC) to be used in connection with a packed GC column for direct (on-column) introduction of pyrolysates is described. A comparison with the conventional method for pyrolysate introduction with the on-column method is given. Good reproducibility of the results obtained for poly(acrylonitrile–co-1,3-butadiene–co-styrene–co-α-methylstyrene) and poly(methyl methacrylate) pyrolysis products was observed (relative standard deviation <5%). Examples of other applications are presented.

INTRODUCTION

The Curie-point pyrolysis (CPPy) method, introduced by Simon and Giacobbo [1] in 1965, is one of two different commercially available pyrolysis systems [2]. In CPPy a ferromagnetic wire is centred in a glass or quartz tube, which is connected to the inlet of a gas chromatograph and through which the carrier gas flows. A Curie-point induction coil surrounds the tube and heats the wire by introduction. The wire heats up until its Curie-point is reached. This is the temperature at which the wire becomes paramagnetic and its energy intake drops, thus holding the temperature of the wire at this point. Different pyrolysis temperatures are obtained by using wires with different Curie-points. A range of temperatures is obtained by using alloys containing differing amounts of the common ferromagnetic metals, *i.e.*, iron, cobalt, nickel and chromium.

Curie-point pyrolysis combined with gas chromatography (CPPy–GC) has developed into a well established method for research into non-volatile compounds, especially in the field of synthetic products in macromolecular chemistry such as plastics, paints, varnishes and rubber, and also of natural substances, including plant materials, soils and minerals.

Many papers have been published, particularly over the past decade, on aspects of CPPy–GC [3]. A large number of different types of apparatus have been used, on a wide range of samples [4–7]. Some information has been given about automated Curie-point pyrolysis systems [8–11].

In a previous paper [12], the Fischer 0316 A pyrolyser with a Fischer AP-6 automatic sampler for CPPy–GC–mass spectrometric–Fouriertransform IR spectro-

0021-9673/90/$03.50

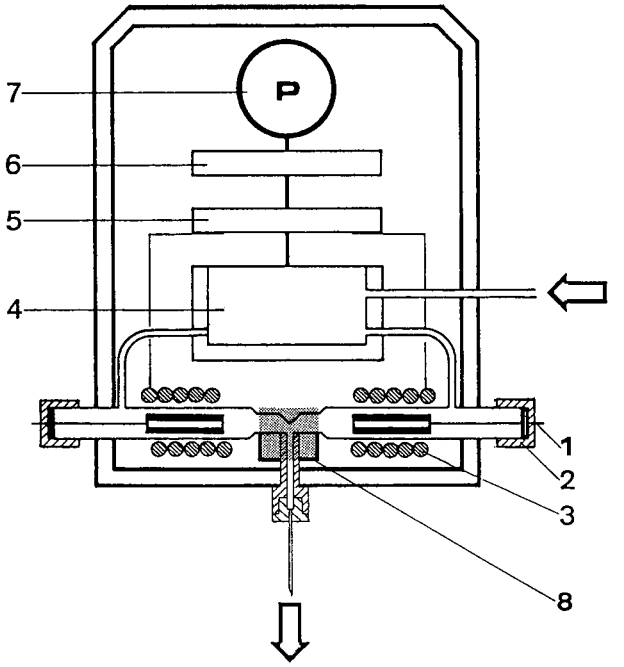

Fig. 1. Schematic sectional view of the Fischer AP-6 automatic sampler. 1 = Sample support; 2 = knurled screw-cap with septum; 3 = induction coil; 4 = carrier gas switching valve; 5 = sample switch; 6 = control switch; 7 = programmer; 8 = heating.

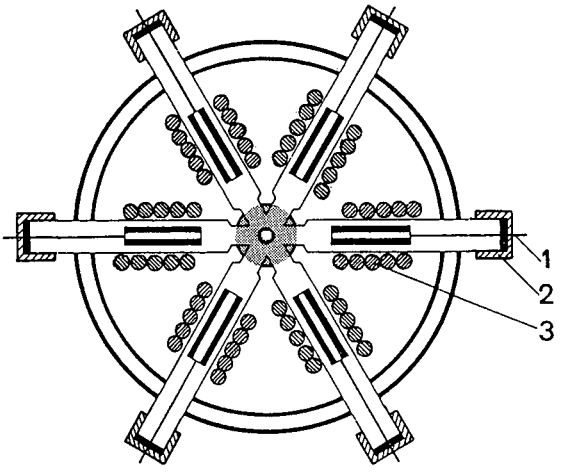

Fig. 2. Cross-section of the Fischer AP-6 automatic sampler at the level of chambers with sample supports.

metric applications was described. The most important features of the Fischer pyrolysis system are exactly reproducible temperatures of pyrolysis, "shock" heating-up within milliseconds, a wide temperature range by means of ferromagnetic filaments or tubes from 250 to 1200°C and high durability because of minor wear and tear [12]. It can be connected with any commercial gas chromatograph with horizontal or vertical injection ports.

The aim of this work was application of the Fischer automatic sampler to the direct (on-column) introduction of pyrolysates. An appropriate system and examples of applications in comparison with the conventional method of pyrolysate introduction are presented.

EXPERIMENTAL

Curie-point pyrolysis

Pyrolysis was performed using a Fischer Model 0316 A Curie-point pyrolyser of 2 kW at 1.1 MHz power supply (Fischer Labor- und Verfahrenstechnik, Meckenheim, F.R.G.), achieving a measured temperature-rise time of 20–30 ms. The pyrolyser was equipped with a digital adjuster for adjusting of pyrolysis times between 0.1 and 9.9 s and for adjusting pyrolysis sample numbers between 1 and 6 with a standby time between 1 and 99 min.

A Fischer Model AP-6 automatic sampler with six circularly arranged pyrolysis chambers made of stainless-steel with changeable glass inserts was used (Figs. 1 and 2). Removable quartz tubes (Fig. 3) were used to line the internal cavity of the pyrolysis chamber and the ferromagnetic pyrolysis tubes coated with sample. The quartz tubes also act to reduce the dead volume of the system to enable chromatographic resolution to be retained.

The central outlet of the pyrolysis chambers (see Figs. 1 and 3) was equipped with a built-in heater serving to prevent condensation of pyrolysates and to ensure a constant temperature distribution between the sample support and the GC column. The central outlet, maintained isothermally at 250°C, was directly connected to the GC column with a 1/8-in. Swagelok connection (Fig. 3).

About 1 mg of each sample was pyrolysed for 9.9 s at 700°C using ferromagnetic tubes composed of iron, nickel and cobalt (Fischer). Helium (for chromatography) from Linde (Munich, F.R.G.) was used as the carrier gas at a flow-rate of 15 cm^3/min.

Gas chromatography

GC analyses of pyrolysates were performed using a Fraktometer F-7 gas chromatograph (Perkin-Elmer, Überlingen, F.R.G.) equipped with a flame ionization detector connected to an Linseis (Selb, F.R.G.) Model L 6512 recorder with a chart speed of 1 cm/min.

A stainless-steel column (1.5 m × 1/8 in. O.D.) packed with 10% SE-30 on Chromosorb W AW (80–100 mesh) (WGA, Griesheim, F.R.G.) was used. The column temperature was programmed from 60 to 280°C at 5°C/min. The detector temperature was 300°C. The flame ionization detector was supplied with 35 cm^3/min of hydrogen and 250 cm^3/min of air.

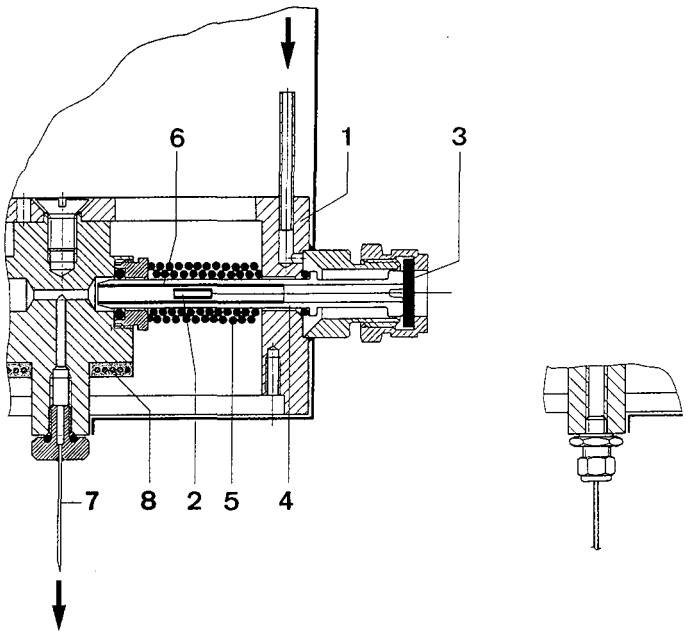

Fig. 3. Sectional enlargement of the construction of the pyrolysis chamber with the injection needle and with connected chromatographic column (right). 1 = Stainless-steel housing; 2 = ferromagnetic sample support; 3 = septum; 4 = glass tube insert; 5 = induction coil; 6 = quartz tube insert; 7 = injection needle; 8 = heater. Carrier gas flow is indicated with arrows.

Chemicals

Samples of poly(acrylonitrile–co-1,3-butadiene–co-styrene–co-α-methylstyrene) (ABS–α-MS), Plexiglas [poly(methyl methacrylate)] (PMMA), PMMA of MW 200 000 in mineral oil (1:1), supplied by the Burmah Oil (Deutschland) (Hamburg, F.R.G.) and commercially available poly(ethylene) and poly(propylene) were used. 1,3-Butadiene (research purity) obtained from Matheson Gas Products (Heusenstamm, F.R.G.) and acrylonitrile, methyl methacrylate, styrene, α-methylstyrene, 4-vinylcyclohexene, toluene and ethylbenzene of analytical-reagent grade from Riedel-de Haën (Seelze, F.R.G.) were used as standards. Hydrocarbon standards obtained from PolyScience (Niles, IL, U.S.A.) were used to measure retention indices.

RESULTS

Experimental conditions such as pyrolysis temperature, temperature-rise time, sample size, volume of pyrolysis chamber and the GC conditions should be carefully controlled in order to obtain a high reproducibility in CPPy–GC [13,14]. Figs. 4 and 5 show typical pyrograms of ABS–α-MS copolymer and PMMA, respectively, obtained at 700°C with on-column introduction of pyrolysates. The retention indices (I_p) of the separated components (Table I) are in agreement with values obtained for commercially available standards. The main degradation products of ABS–α-MS

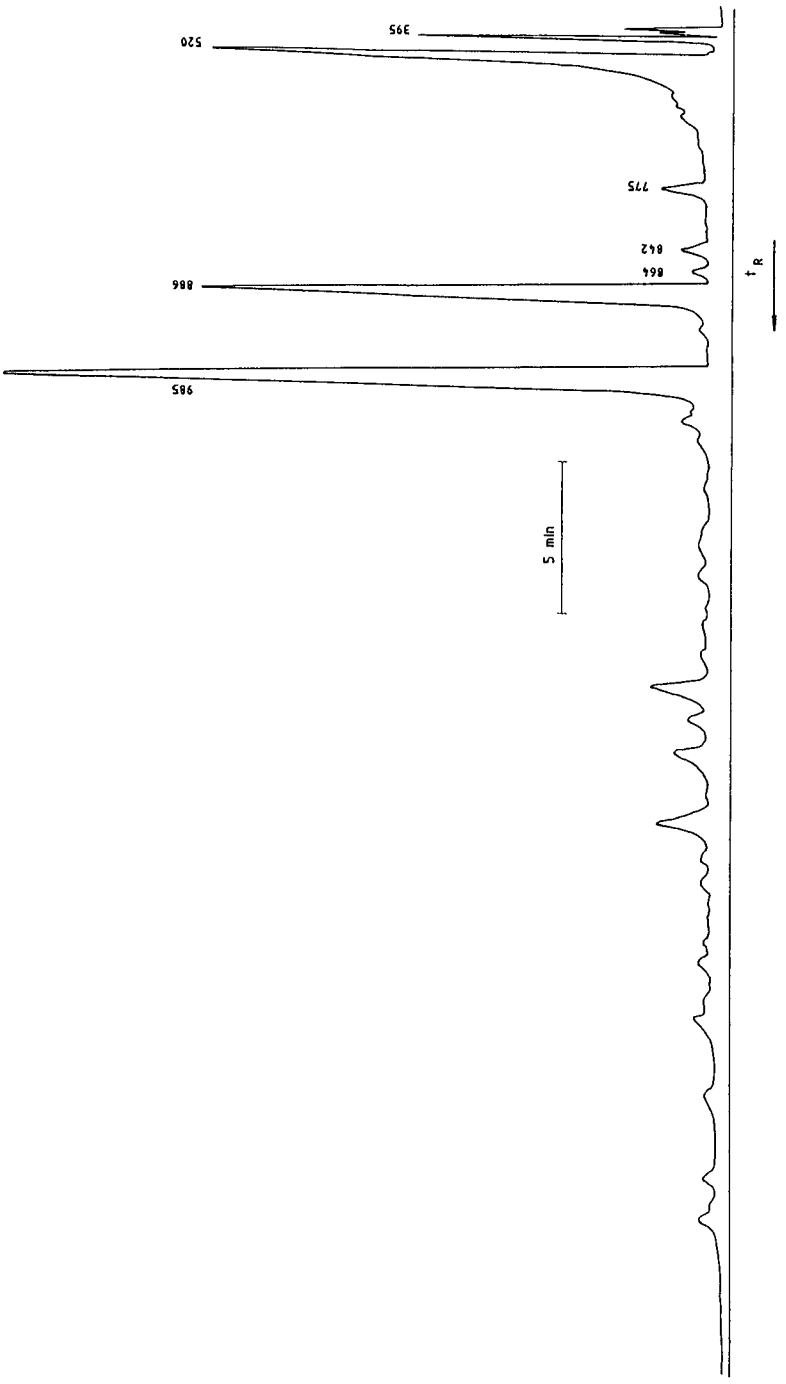

Fig. 4. Pyrogram of ABS–α-MS copolymer obtained at 700°C with the AP-6 automatic sampler and on-column introduction of pyrolysates. Analytical conditions as in Experimental. For peak identification, see Table I.

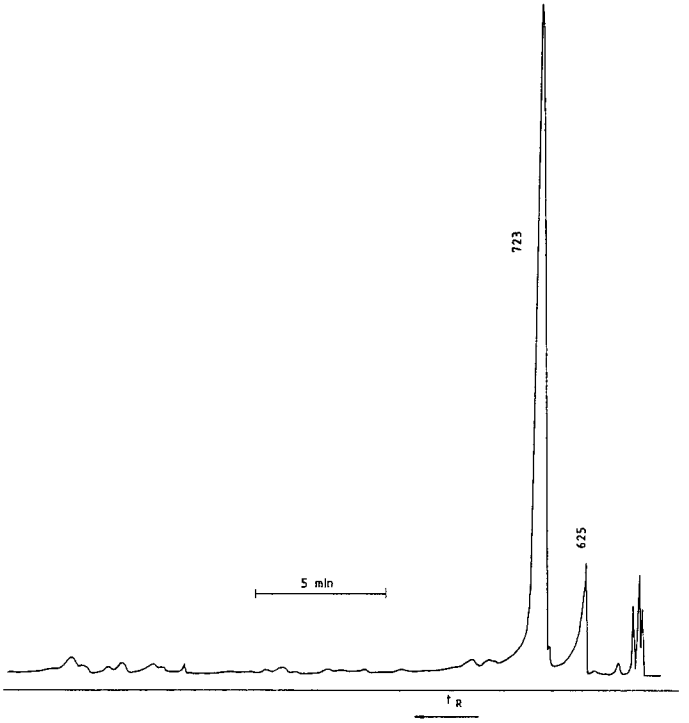

Fig. 5. Pyrogram of Plexiglas (PMMA) obtained at 700°C with the AP-6 automatic sampler and on-column introduction of pyrolysates. Analytical conditions as in Experimental. For peak identification, see Table I.

copolymer pyrolysis, with retention indices of 395, 520, 886 and 985, correspond to 1,3-butadiene, acrylonitrile, styrene and α-methylstyrene, respectively. Small amounts (<1%, w/w) of toluene (I_p = 775), 4-vinylcyclohexene (I_p = 842) and ethylbenzene (I_p = 864) were also observed. Other peaks (I_p > 985) were not identified.

TABLE I

RETENTION DATA OF THE CPPy PRODUCTS FROM ABS–α-MS COPOLYMER AND PMMA

Polymer/copolymer	CPPy product	Retention time, t_R (min)	Retention index, I_p[a]
ABS–α-MS copolymer	1,3-Butadiene	0.92	395
	Acrylonitrile	1.50	520
	Toluene	5.87	775
	4-Vinylcyclohexene	7.84	842
	Ethylbenzene	8.58	864
	Styrene	9.30	886
	α-Methylstyrene	12.38	985
Plexiglas (PMMA)	Methyl acrylate	2.90	625
	Methyl methacrylate	4.70	723

[a] I_p: Retention indices in temperature-programmed GC [17].

TABLE II

REPRODUCIBILITY OF CURIE-POINT PYROLYSIS OF ABS–α-MS COPOLYMER AT 700°C WITH THE AP-6 AUTOMATIC SAMPLER AND CONVENTIONAL INTRODUCTION OF PYROLYSATES

Normalized percentages of the major peaks.

Pyrolysis chamber	Component (peak area, %)			
	Acrylonitrile	1,3-Butadiene	Styrene	α-Methylstyrene
1	16.70	3.10	35.01	45.19
2	15.48	3.40	34.33	46.79
3	13.41	3.26	34.71	48.62
4	16.23	3.62	33.81	46.34
5	16.30	3.57	34.88	45.25
6	17.32	3.61	33.10	45.97
Average ($\bar{x}$)	15.91	3.43	34.31	46.36
$\bar{s}_x$	1.3639	0.2129	0.7334	1.2685
$\bar{s}_{x,r}$ (%)	8.57	6.21	2.14	2.74

The thermal decomposition of PMMA at temperatures >200°C yields nearly quantitatively (98%) methyl methacrylate (MMA) [15,16]. In our pyrograms the main peak obtained after PMMA pyrolysis is also monomeric MMA (I_p = 723). The peak with I_p = 625 was identified from the retention index increment (ΔI_p = 98) as methyl acrylate (MA).

TABLE III

REPRODUCIBILITY OF CURIE-POINT PYROLYSIS OF ABS–α-MS COPOLYMER AT 700°C WITH THE AP-6 AUTOMATIC SAMPLER AND ON-COLUMN INTRODUCTION OF PYROLYSATES

Normalized percentages of the major peaks.

Pyrolysis chamber	Component (peak area, %)			
	Acrylonitrile	1,3-Butadiene	Styrene	α-Methylstyrene
1	15.92	3.48	34.40	46.20
2	16.01	3.52	34.61	45.86
3	15.85	3.41	34.38	46.36
4	16.12	3.54	34.31	46.03
5	16.23	3.44	34.53	45.80
6	15.74	3.40	34.29	46.57
Average ($\bar{x}$)	15.98	3.46	34.42	46.14
$\bar{s}_x$	0.1795	0.0578	0.1259	0.2976
$\bar{s}_{x,r}$ (%)	1.12	1.67	0.37	0.64

TABLE IV

COMPARISON OF RESULTS OBTAINED BY CPPy–GC OF PMMA AT 700°C WITH THE AP-6 AUTOMATIC SAMPLER BY CONVENTIONAL AND ON-COLUMN INTRODUCTION OF PYROLYSATES

Normalized percentages of the major peaks.

Pyrolysis chamber	Conventional introdution of pyrolysates		On-column introduction of pyrolysates	
	MA (peak area, %)	MMA (peak area, %)	MA (peak area, %)	MMA (peak area, %)
1	6.93	93.07	7.58	92.42
2	8.40	91.60	7.95	92.05
3	8.03	91.97	7.43	92.57
4	7.30	92.70	6.97	93.03
5	9.16	91.84	7.29	92.71
6	6.86	93.14	7.49	92.51
Average ($\bar{x}$)	7.61	92.39	7.45	92.55
$\bar{s}_x$	0.6669	0.66669	0.3240	0.3240
$\bar{s}_{x,r}$ (%)	8.76	0.72	4.35	0.35

Similar pyrograms for ABS–α-MS copolymers and PMMA were obtained at 700°C with conventional introduction of pyrolysates (through the injection port), but the reproducibility of analysis was lower. The results obtained for the two methods of analysis (conventional and on-column introduction of pyrolysates) with a statistical assessment are given for ABS–α-MS copolymer in Tables II and III and for PMMA in Table IV. Tables III and IV show the very good reproducibility of the results obtained by means of the automatic sampler and on-column introduction of pyrolysates. The relative standard deviations ($\bar{s}_{x,r}$, %) of the mean values of peak areas (%) obtained for ABS–α-MS copolymer and PMMA pyrolysis products are nearly 5%.

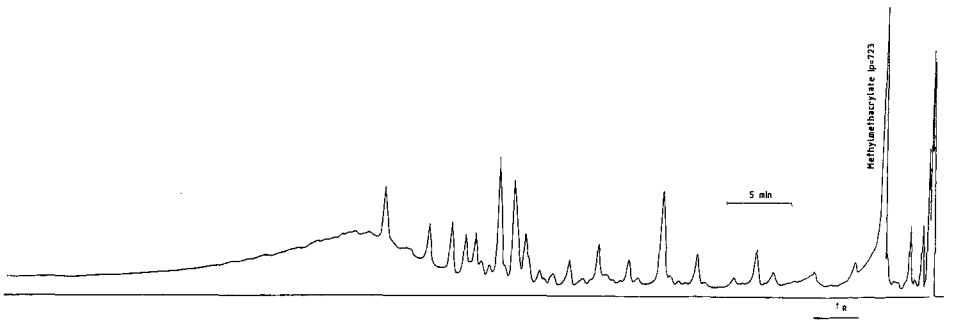

Fig. 6. Pyrogram of PMMA of MW 200 000 in mineral oil obtained at 700°C with the AP-6 automatic sampler and on-column introduction of pyrolysates. Analytical conditions as in Experimental.

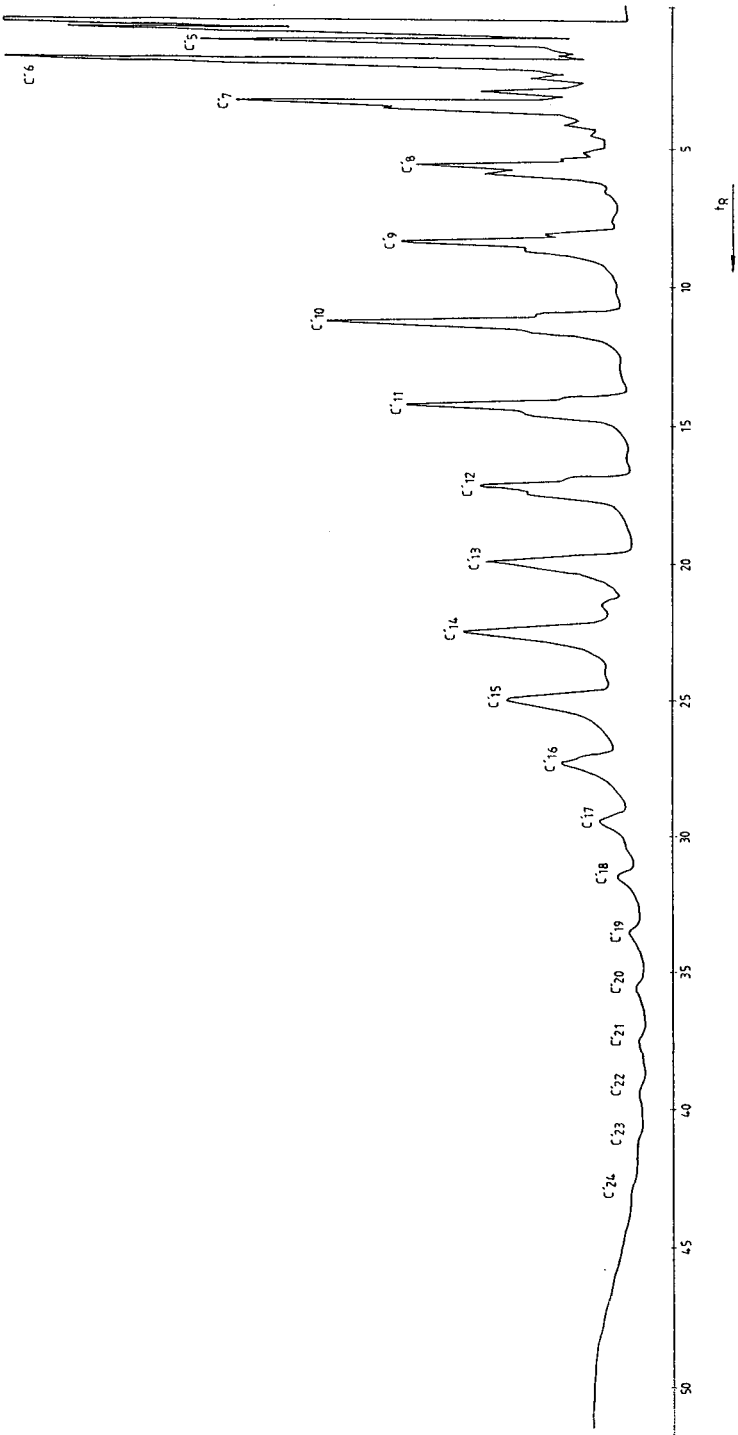

Fig. 7. Pyrogram of commercially available poly(ethylene) obtained at 700°C with the AP-6 automatic sampler and on-colum introduction of pyrolysates. Analytical conditions as in Experimental. Peak identification: for example, C'6 = hexane + hexene + hexadiene.

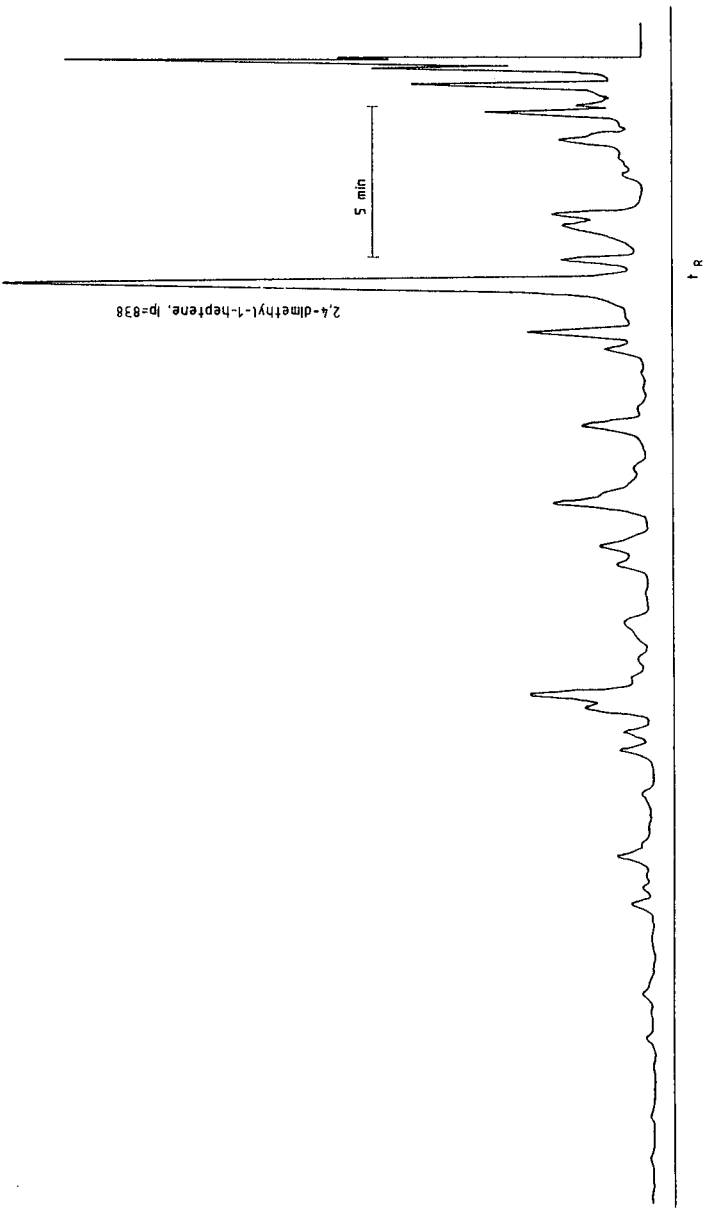

Fig. 8. Pyrogram of commercially available poly(propylene) obtained at 700°C with the AP-6 automatic sampler and on-column introduction of pyrolysates. Analytical conditions as in Experimental.

Some other examples of the application of CPPy–GC with the AP-6 automatic sampler and on-column introduction of pyrolysates are shown by the pyrograms obtained for PMMA in mineral oil (Fig. 6), commercially available poly(ethylene) (Fig. 7) and poly(propylene) (Fig. 8).

REFERENCES

1 W. Simon and H. Giacobbo, *Chem.-Ing.-Techn.*, 37 (1965) 709.
2 R. W. May, E. F. Pearson and D. Scothern, *Pyrolysis–Gas Chromatography*, Chemical Society, London, 1977.
3 T. P. Wampler, *J. Anal. Appl. Pyrol.*, 16 (1989) 291.
4 W. J. Irwin, *Analytical Pyrolysis*, Marcel Dekker, New York, 1982.
5 J. M. Halket and H. R. Schulten, *J. High Resolut. Chromatogr. Chromatogr. Commun.*, 9 (1986) 597.
6 R. S. Lehrle, *J. Anal. Appl. Pyrol.*, 11 (1987) 55.
7 R. S. Whiton and S. L. Morgan, *Anal. Chem.*, 57 (1985) 778.
8 H. L. C. Meuzelaar, H. G. Ficke and H. C. den Harink, *J. Chromatogr. Sci.*, 13 (1975) 12.
9 H. Fritsch, *Automatischer Probengeber für Curie-Punkt-Pyrolysator—ein Meilenstein in der Pyrolyse–GC, GC Philips Catalog No. 23*, Philips, Kassel, 1986.
10 H. Fritsch, *Labor Praxis*, 11 (1987) 1092.
11 R. Schrafft, paper presented at Philips GC Workshop, Kassel, F.R.G., 1982.
12 H. R. Schulten, W. G. Fischer and H. J. Wallstab, *J. High Resolut. Chromatogr. Chromatogr. Commun.*, 10 (1987) 467.
13 Ch. Bühler, *Beitrag zur Methodik der Curie-Punkt-Pyrolyse*, Diss. No. 4750, Eidgenössische Technische Hochschule, Zurich, Juris Druck u. Verlag, Zurich, 1971, p. 17.
14 X.-G. Jin and H.-M. Li, *J. Anal. Appl. Pyrol.*, 3 (1981) 49.
15 A. Zeman, *Angew. Makromol. Chem.*, 31 (1973) 1.
16 G. Buchhorn, I. Lüderwald, K. E. Müller and H. G. Willert, *Fresenius' Z. Anal. Chem.*, 312 (1982) 539.
17 P. Kusz and W. Czelakowski, *Int. Lab.*, Jan./Feb. (1987) 92.

Journal of Chromatography, 518 (1990) 21–40
Elsevier Science Publishers B.V., Amsterdam

CHROM. 22 118

Gas chromatographic and mass spectrometric determination of nitroaromatics in water

J. FELTES[a] and K. LEVSEN*
Fraunhofer Institut für Toxikologie und Aerosolforschung, Nikolai-Fuchs-Str. 1, D-3000 Hannover 61 (F.R.G.)
and
D. VOLMER and M. SPIEKERMANN
Fachhochschule Lübeck, Stephensonstr. 3, D-2400 Lübeck 1 (F.R.G.)
(Received May 14th, 1989)

ABSTRACT

Several methods for the extraction of nitroaromatic compounds from water were compared. High recoveries were achieved with discontinuous or continuous extraction of water with dichloromethane and by adsorption on Amberlite XAD-2, -4 and -8 resins (1:1:1) and elution with dichloromethane. The recoveries obtained with solid-phase extraction using cyano-, phenyl- or octadecyl-bonded phases varied, depending on the compounds studied, and were often low. Nitroaromatic compounds were determined by gas chromatography using an electron-capture or a chemiluminescence detector (thermal energy analyser) and by mass spectrometry using electron impact and positive- and negative-ion chemical ionization.

INTRODUCTION

Nitroaromatic compounds are widely used in the chemical industry, *e.g.*, for the production of explosives, dyes, pesticides and polyurethane foam, which may lead to their partial release into the environment. Nitroaromatics are toxic. They are readily adsorbed by skin contact and may lead to methemoglobinemia, anemia or liver damage [1]. Thus the LD_{50} value (rat) for 1-chloro-2-nitrobenzene is as low as 288 mg/kg and the LC_{50} value for goldorfe 5-10 mg/l [2].

Several nitroaromatic compounds are listed as priority pollutants by the U.S. Environmental Protection Agency [3] (nitrobenzene, 2,4-dinitrotoluene, 2,6-dinitrotoluene, 2-nitrophenol, 4-nitrophenol, 2,4-dinitrophenol and 4,6-dinitro-2-methylphenol) and by the European Community [2] (1-chloro-2-nitrobenzene, 1-chloro-3-nitrobenzene, 1-chloro-4-nitrobenzene, 4-chloro-2-nitrotoluene, 4-chloro-2-nitroaniline and parathion ethyl). Nitrobenzene, nitrotoluene isomers and chloronitrobenzenes have been observed repeatedly in samples from the river Rhine [4]. Acute pollution of the river Main led to concentrations of chloronitrobenzene isomers of *ca.*

[a] This paper is based on the Ph.D. Thesis of J. Feltes, University of Bonn, 1988.

0021-9673/90/$03.50

80 μg/l [5], which led to cessation of the withdrawal of Rhine water for drinking water supplies in The Netherlands.

In the past, relatively few studies have been exclusively directed towards the determination of nitroaromatic compounds in water. Explosives and related compounds have attracted particular attention. These compounds are usually determined by gas chromatography (GC) with flame ionization detection (FID) [6,7] or more selectively and sensitively using electron-capture detection (ECD) [8–13]. The use of chemiluminescence detection (thermal energy analysis, TEA) should be advantageous. This type of detection has been used for the selective GC determination of nitroaromatics in biosludge [14]. GC methods for the determination of nitroaromatics in water (in particular munition plant wastewater) [6,7,12] and sea water [10,11] have been published and the determination of nitrotoluidines (aminonitrotoluenes) in water by GC has been described [13].

Alternatively, high-performance liquid chromatography (HPLC) can be employed for the determination of nitroaromatics in water (mainly wastewater [15–18]).

In most instances the water samples were extracted by liquid–liquid extraction (using mainly benzene or toluene) [6-11,13]. Alternatively, resin adsorption using Porapack R, Porapack S or XAD-4 was used for sample extraction [12,18].

Nitrophenols represent a specific class of nitroaromatic compounds. They are usually determined using methods optimized for phenols, as reviewed by Tesarova and Pacakova [19]. Owing to their high polarity, the GC of these compounds may be difficult and they are often first derivatized [19]. Nitropolycyclic aromatic hydrocarbons represent another class of nitroaromatic compounds for which specific analytical schemes have been developed, as reviewed by White [20].

The methods discussed above were usually based on a few compounds and in general tested only with spiked water samples.

We report here the optimized determination of a large number of nitro compounds with a variety of functional groups. Analysis is performed by GC with ECD and TEA or by combined GC–mass spectrometry (MS) using electron impact (EI), positive-ion chemical ionization (PICI) or negative-ion chemical ionization (NICI). Nitrophenols are discussed only briefly as they have been considered in detail elsewhere [21–23]. Nitropolycyclic aromatic hydrocarbons have also been dealt with elsewhere [24].

EXPERIMENTAL

Instrument

All GC measurements were carried out on a Varian Model 3700 instrument equipped with a Varian ^{63}Ni electron-capture detector and a Model 543 chemiluminescence detector (TEA) from Thermedics (Woburn, MA, U.S.A.). Pyrolysis was effected at 950°C. The pressure in the reaction chamber was 0.8 Torr. Separation was achieved on both a DB-17 and an OV-225 column (30 m × 0.32 mm I.D., d_f 0.25 μm) with a column temperature of 70°C for 1 min, then raised from 70 to 250°C at 3°C/min, using nitrogen (ECD) or helium (TEA) as the carrier gas.

Mass spectrometric measurements were carried out on a Finnigan Model 4500 and a Vacuum Generator Model VG70 SQ instrument using an electron energy of 70 eV and a source temperature of 120°C (Finnigan) or 200°C (VG). PICI was achieved

with methane (0.5 Torr) or isobutane (0.05 Torr) as reagent gas and both methane and argon were used for NICI (0.5 Torr). Samples were introduced via the GC system using a DB-5 column with a temperature of 70°C for 1 min, then increased from 70 to 260°C at 3°C/min.

Extraction

Discontinuous extraction was carried out with a separation funnel using 1 l of water spiked with the internal standards and shaking three times with 30 ml of dichloromethane. The combined organic phases were dried over anhydrous sodium sulphate and reduced in volume to *ca.* 1 ml in a rotary evaporator after exchange of the solvent (methanol instead of dichloromethane). Concentration to 1 ml at 40°C and reduced pressure does not lead to evaporation losses as determined by recovery studies (recovery >96%).

Continuous extraction was carried out for 5 h in a rotary perforator using 0.5 l of water and dichloromethane as solvent followed by concentration and solvent exchange as described above.

Solid-phase extraction was performed using Amberlite (residue-free) XAD-2, XAD-4, XAD-8 resins from Alltech and Rohm & Haas, C_{18} phases (500-mg cartridges) from Baker (Baker 10 SPE), Analytichem (Bond-Elut) and Merck (Adsorbex), phenyl phases (500-mg cartridges) from Baker (Baker 10 SPE) and Analytichem (Bond-Elut) and cyano phases from Baker (Baker 10 SPE). XAD resin (2.5 g) was filled into a 15 × 1 cm I.D. glass column plugged with silanized glass-wool and flushed with methanol and water prior to use by forcing the solvent through the column with nitrogen at enhanced pressure. After forcing 1 l of the sample through the column at a flow-rate of 30 ml/min, the column was dried in a stream of nitrogen for about 15 min and eluted twice with 15 and 10 ml of dichloromethane. The C_{18}, phenyl and cyano cartridges were eluted with 1 ml of dichloromethane at reduced pressure. Drying, concentration and solvent exchange were carried out as described above.

Chemicals

Nitroaromatic reference compounds of 97–99% purity from Merck, Fluka, Riedel-de Haën and Aldrich were used without further purification. Solvents were purchased from Baker and Rathburn Chemicals.

RESULTS AND DISCUSSION

Gas chromatography

Nitroaromatic compounds were determined by GC with either ECD or TEA. In the TEA detector nitro compounds are pyrolysed to form $NO^{\cdot}$ radicals that react with ozone to form triplet excited NO_2, which relaxes to the ground state with emission of light in the near-infrared region (>0.6 μm), which is monitored. Slightly polar (DB-17) to moderately polar columns (OV-225 or DB-225) are well suited for the separation of nitroaromatics. Fig. 1 compares the chromatograms of 40 nitroaromatic compounds obtained on a DB-17 column with ECD (upper part) and TEA (lower part), and in Fig. 2 the chromatogram (ECD) of a mixture of explosives and their metabolites is presented. In Tables I and II retention times and capacity factors (k')

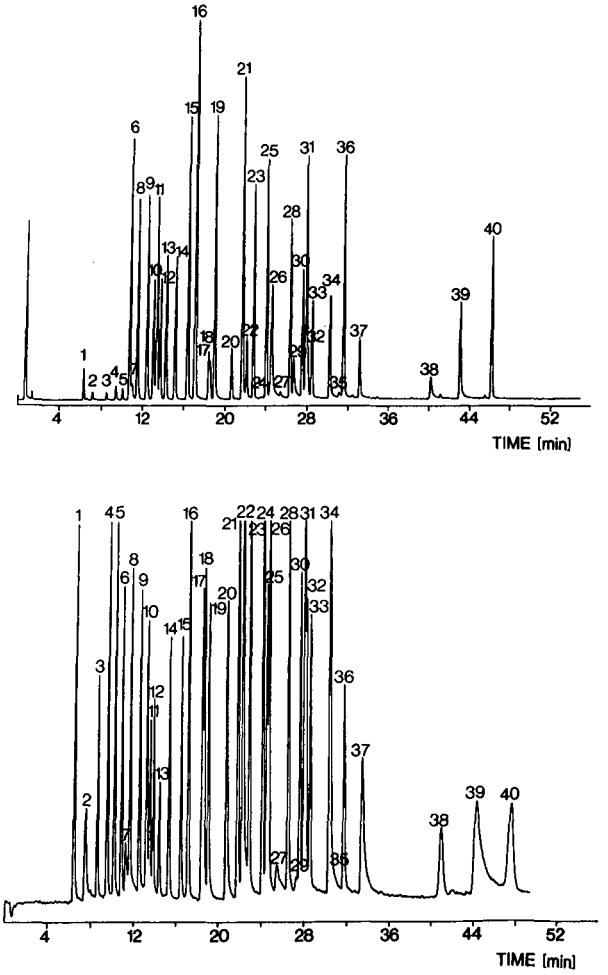

Fig. 1. Gas chromatograms of 40 nitroaromatic compounds on a DB-17 column (top, ECD; bottom, TEA). For peak assignment, see Table I.

are summarized for the DB-17 and OV-225 columns. 1-Chloro-2,4-dinitrobenzene and 2,2′-dinitrobiphenyl were used as internal standards. With the TEA detector substantial peak broadening is observed at high retention times, probably owing to adsorption within the transfer line.

Nitroaromatics can be determined by ECD as a result of their high electron affinity. However, Fig. 1 reveals that the response for nitroaromatics depends strongly on the individual compound. Thus, for instance, the ECD response of 3,4-dinitrotoluene is 61 times that of 2-nitrotoluene. On the other hand, the TEA response is more similar for all the compounds, as is evident from Fig. 1 (the response of 3,4-dinitrotoluene is 3.4 times that of 2-nitrotoluene). A low response is observed for the nitrophenols. This is particularly true for the dinitrophenols, such as 2,4-dinitro-6-*sec.*-butylphenol (dinoseb), which is probably due to irreversible adsorption of the

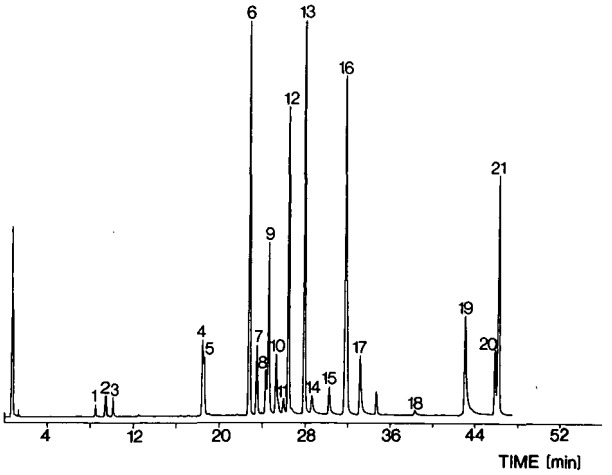

Fig. 2. Gas chromatogram of 21 nitroaromatic compounds used in ammunition production (including the degradation products) (ECD). For peak assignment, see Table II.

phenol at the active centres of the column. Hence it is preferable to derivatize nitrophenols [19].

The TEA detector responds specifically to nitro and nitroso compounds and is therefore better suited for the analysis of complex environmental samples than ECD, which is less selective. On the other hand, the selectivity of GC with ECD can be enhanced if the samples are chromatographed on two columns with phases of different polarities. As stated above, DB-5 and OV-225 (DB-225) are well suited for this purpose.

The linearity of the detectors for nitro compounds was studied using both ECD and TEA for five compounds. The results in Fig. 3 show that the ECD response (top) levels off at concentrations >10 ng, whereas the TEA detector (bottom) shows good linearity even at higher concentrations.

The detection limit of the detector (defined at three times the standard deviation of the noise) is summarized for 15 compounds in Table III for both ECD and TEA. With ECD the detection limit ranges from $0.8 \cdot 10^{-14}$ to $109 \cdot 10^{-14}$ g/s and that with TEA from $6 \cdot 10^{-11}$ to $34 \cdot 10^{-11}$ g/s. Hence ECD is about three orders of magnitude more sensitive than TEA.

Gas chromatography–mass spectrometry

A mass spectrometer is a considerably more specific GC detector than either electron-capture or TEA detectors. Nitroaromatic compounds were determined using EI, PICI and NICI. Mass spectrometry is particularly suitable for the analysis of this class of compounds as their ionization leads to the formation of structure-specific fragments, as summarized in Table IV for all three ionization methods. Under EI conditions, nitroaromatic compounds fragment predominantly by loss of NO$^{\bullet}$ or NO_2. In general, loss of NO_2 prevails. An *ortho* effect may lead to an abundant loss of OH$^{\bullet}$ [25] if a methyl or amino group is in an *ortho* position to the nitro group. In addition, dinitro and trinitro derivatives show in part the loss of two nitro groups. An

TABLE I

ELUTION ORDER, RETENTION TIMES AND CAPACITY FACTORS OF NITROAROMATIC COMPOUNDS CHROMATOGRAPHED ON A DB-17 AND OV-225 COLUMN

Compound	DB-17			OV-225		
	Elution order	t_R (min)	k'	Elution order	t_R (min)	k'
Nitrobenzene	1	6.32	13.04	1	5.94	17.56
2-Nitrophenol	2	7.16	14.91	2	6.70	19.94
2-Nitrotoluene	3	8.50	17.89	3	7.46	22.31
3-Nitrotoluene	4	9.42	19.93	4	8.71	26.22
4-Nitrotoluene	5	10.07	21.38	5	9.70	29.31
1-Chloro-3-nitrobenzene	6	10.74	22.87	9	12.06	36.69
3-Methyl-6-nitrophenol	7	10.94	23.31	6	10.34	31.31
1-Chloro-4-nitrobenzene	8	11.52	24.60	7	10.57	32.03
1-Chloro-2-nitrobenzene	9	12.45	26.67	5	9.70	29.31
2-Chloro-5-nitropyridine	10	13.08	28.07	11	13.66	41.69
4-Chloro-2-nitrotoluene	11	13.41	28.80	9	12.06	36.69
6-Chloro-2-nitrotoluene	12	13.74	29.53	8	11.50	34.94
5-Chloro-2-nitrotoluene	13	14.31	30.80	10	12.68	38.63
2-Chloro-4-nitrotoluene	14	15.20	32.78	12	13.98	42.69
1,4-Dichloro-2-nitrobenzene	15	16.41	35.47	13	15.58	47.69
1,2-Dichloro-4-nitrobenzene	16	17.12	37.04	13	15.58	47.69
1,3-Dichloro-4-nitrobenzene	16	17.12	27.04	14	15.84	48.50
2-Nitroanisole	17	18.45	40.00	15	19.27	59.22
4-Nitroanisole	18	18.59	40.31	15	19.27	59.22
4-Nitrobenzonitrile	19	19.00	41.22	16	21.31	65.59
2-Nitroaniline	20	20.67	44.93	20	23.93	73.78
1,4-Dinitrobenzene	21	21.71	47.24	19	23.84	73.50
1,3-Dinitrobenzene	22	22.15	48.22	21	24.93	76.91
3-Nitrophenol	22	22.15	48.22	32	34.10	105.56
2,6-Dinitrotoluene	23	22.84	49.76	18	23.63	72.84
2,4-Dinitrophenol	24	23.56	51.36	17	22.48	69.25
1,2-Dinitrobenzene	25	24.12	52.60	25	28.06	86.69
3-Nitroaniline	26	24.61	53.69	27	29.75	91.97
2,4-Dinitrotoluene	26	24.61	53.69	23	27.27	84.21
4-Nitrophenol	27	25.49	55.64	35	40.50	125.56
1-Chloro-2,4-dinitrobenzene[a]	28	26.44	57.76	26	29.35	90.72
2-Methyl-3-nitrophenol	29	26.79	58.53	28	30.71	94.97
1-Nitronaphthalene	30	27.61	60.36	22	26.24	81.00
3,4-Dinitrotoluene	31	27.94	61.09	30	32.23	99.72
4-Chloro-2-nitroaniline	32	28.09	61.42	29	31.66	97.94
2-Nitronaphthalene	33	28.55	62.44	24	27.78	85.81
4-Methoxy-2-nitroaniline	34	30.27	66.27	31	33.05	102.28
4-Nitroaniline	34	30.27	66.27	33	37.70	116.81
Dinoseb	35	31.23	68.40	32	34.10	105.56
2,6-Dichloro-4-nitroaniline	36	31.65	69.33	32	34.10	105.56
2-Methyl-4-nitroaniline	37	33.22	72.82	34	39.42	122.19
Parathion ethyl	38	40.26	88.47	38	51.60	160.25
2,4-Dinitroaniline	39	43.16	94.91	37	51.49	159.91
2,2'-Dinitrobiphenyl[a]	40	46.24	101.76	36	47.23	146.59

[a] Internal standard.

TABLE II

ELUTION ORDER, RETENTION TIMES AND CAPACITY FACTORS OF NITROAROMATICS USED IN AMMUNITION PRODUCTION (INCLUDING POSSIBLE METABOLITES)

Compound	DB-17			OV-225		
	Elution order	t_R (min)	k'	Elution order	t_R (min)	k'
2-Nitrotoluene	1	8.50	17.89	1	7.46	22.31
3-Nitrotoluene	2	9.42	19.93	2	8.71	26.22
4-Nitrotoluene	3	10.07	21.37	3	9.71	29.34
2-Nitroanisole	4	18.45	40.00	4	19.25	59.16
4-Nitroanisole	5	18.59	40.31	4	19.25	59.16
2,6-Dinitrotoluene	6	22.84	49.76	5	23.64	72.88
2-Methyl-6-nitroaniline	7	23.51	51.24	6	25.63	79.09
4-Methyl-2-nitroaniline	8	24.33	53.07	7	27.25	84.16
2,4-Dinitrotoluene	9	24.61	53.69	7	27.25	84.16
5-Methyl-2-nitroaniline	10	25.28	55.18	8	28.32	87.50
2-Methyl-3-nitroaniline	11	25.96	56.69	10	30.23	93.47
1-Chloro-2,4-dinitrobenzene[a]	12	26.44	57.76	9	29.28	90.50
3,4-Dinitrotoluene	13	27.94	61.09	11	32.23	99.72
2-Methyl-5-nitroaniline	14	28.65	62.67	12	32.94	101.94
4-Methoxy-2-nitroaniline	15	30.27	66.27	12	32.94	101.94
1,3,5-Trinitrobenzene	16	31.80	69.67	15	39.75	123.22
2,4,6.Trinitrotoluene	16	31.80	69.67	13	37.96	117.63
2-Methyl-4-nitroaniline	17	33.20	72.78	14	39.43	122.22
2,4,6-Trinitrophenol	18	38.40	84.33	17	49.50	153.69
2,4-Dinitroaniline	19	43.13	94.84	18	51.52	160.00
N,2,4,6-Tetranitro--N-methylaniline	20	45.93	101.07	19	51.89	161.16
2,2'-Dinitrobiphenyl[a]	21	46.24	101.76	16	47.25	146.66

[a] Internal standard.

abundant molecular ion is usually observed under EI conditions. As expected, this ion is of low abundance with dinitrotoluenes and absent (<1% relative abundance) with trinitrotoluene.

Only a few nitroaromatic compounds have been studied previously under PICI

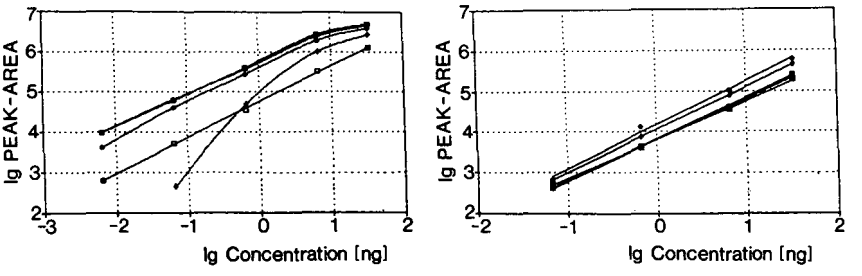

Fig. 3. Linearity of the detectors (left, ECD; right, TEA). □, Nitrobenzene; ○, 1-chloro-2-nitrobenzene; ■, 1,4-dichloro-2-nitrobenzene; ●, 2,6-dinitrotoluene; +, 2-nitroaniline.

TABLE III

DETECTION LIMITS OF THE ELECTRON-CAPTURE AND TEA DETECTORS

Compound	ECD		TEA	
	Detection limit (g/s)	R.S.D. (%)	Detection limit (g/s)	R.S.D. (%)
Nitrobenzene	$2.33 \cdot 10^{-13}$	8.1	$1.35 \cdot 10^{-11}$	7.8
2-Nitrophenol	$1.09 \cdot 10^{-12}$	6.2	$3.43 \cdot 10^{-11}$	6.5
3-Nirotoluene	$5.44 \cdot 10^{-13}$	3.9	$1.09 \cdot 10^{-11}$	7.1
1-Chloro-3-nitrobenzene	$1.18 \cdot 10^{-14}$	4.9	$1.42 \cdot 10^{-11}$	12.3
1,4-Dichloro-2-nitrobenzene	$8.28 \cdot 10^{-15}$	7.6	$1.12 \cdot 10^{-11}$	3.3
6-Chloro-2-nitrotoluene	$2.87 \cdot 10^{-14}$	5.2	$2.50 \cdot 10^{-11}$	9.2
4-Nitroanisole	$1.15 \cdot 10^{-13}$	9.7	$1.85 \cdot 10^{-11}$	4.7
2-Nitroaniline	$9.92 \cdot 10^{-14}$	11.2	$1.98 \cdot 10^{-11}$	8.8
2,4-Dinitrotoluene	$3.80 \cdot 10^{-14}$	7.9	$1.77 \cdot 10^{-11}$	4.9
1-Nitronaphthalene	$2.32 \cdot 10^{-14}$	2.2	$1.15 \cdot 10^{-11}$	6.6
2-Methyl-6-nitroaniline	$6.08 \cdot 10^{-14}$	5.8	$2.42 \cdot 10^{-11}$	7.5
4-Chloro-2-nitroaniline	$1.44 \cdot 10^{-13}$	8.4	$1.14 \cdot 10^{-11}$	9.2
Parathion ethyl	$2.25 \cdot 10^{-13}$	10.8	$1.62 \cdot 10^{-11}$	13.1
2,4-Dinitroaniline	$4.85 \cdot 10^{-14}$	9.2	$6.54 \cdot 10^{-12}$	18.5
2,4,6-Trinitrotoluene	$2.70 \cdot 10^{-14}$	5.6	$9.89 \cdot 10^{-12}$	7.2

conditions [26,27]. In this study methane and isobutane were used as reactant gases. Under PICI conditions with methane the protonated molecule is usually the most abundant peak, as shown in Table IV. This is even the case for the very labile trinitrotoluene. An abundant loss of NO$^{\bullet}$ from $[M + H]^+$ is observed in almost all instances whereas the loss of NO_2 is less pronounced or often absent. Further fragments are due to loss of O$^{\bullet}$ or H_2O from the protonated molecule. NO$^{\bullet}$ loss allows a rapid structure assignment.

Nitroaromatic compounds have a relatively high electron affinity and therefore they can be readily ionized with electron-capture NICI. In this study both methane and argon were used as buffer gases. Characteristic fragments are summarized in Table IV. The NICI spectra of some of these compounds were reported previously [28]. It is evident from Table IV that fragmentation under NICI conditions is low except for dinitro compounds. Losses of OH$^{\bullet}$, NO$^{\bullet}$ and NO_2 lead to characteristic fragments. Further fragmentation occurs by loss of H_2O or O$^{\bullet}$. Unfortunately, not all compounds show the structure-specific loss of NO$^{\bullet}$, which makes a structure assignment of unknowns difficult. The fragmentation is further reduced if argon instead of methane is used as a buffer gas. The response factors of nitroaromatic compounds under NICI conditions vary substantially. As expected, dinitro compounds such as dinitrobenzene and dinitrotoluenes in general have a higher response than the mononitro compounds, although exceptions are observed. Thus, 1,4-dinitrobenzene has a five times higher response than 1,3-dinitrotoluene.

Mass spectrometric detection limits (signal-to-noise ratio = 3) were determined for several compounds, as summarized in Table V. These detection limits were determined on the Finnigan 4500 quadrupole instrument. It is conceivable that they would

TABLE IV

MAIN FRAGMENTS OBTAINED WITH EI, PICI AND NICI

The Table represents the m/z values and in parentheses the relative abundance.

Compound	EI				PICI (CH_4)			NICI (CH_4)			
	M^+	M−OH	M−NO	$M-NO_2$	MH	MH−NO	$MH-NO_2$	M^-	M−OH	M−NO	$M-NO_2$
Nitrobenzene	123	–	93	77	124			123	106		
	(80)		(15)	(100)	(100)			(100)	(20)		
2-Nitrotoluene	137	120	107	91	138	108		137	120	107	
	(20)	(93)	(2)	(70)	(100)	(70)		(100)	(30)	(<1)	
3-Nitrotoluene	137	–	107	91	138	108		137	120	107	
	(80)		(10)	(100)	(100)	(72)		(100)	(5)	(<1)	
4-Nitrotoluene	137	–	107	91	138	108		137	120	–	
	(95)		(18)	(100)	(100)	(70)		(100)	(5)		
2-Nitroaniline	138	121	108	92	139	109		138	121	–	
	(100)	(5)	(8)	(50)	(100)	(30)		(100)	(30)		
3-Nitroaniline	138	–	108	92	139	109		138	121	–	
	(95)		(8)	(85)	(100)	(85)		(100)	(30)		
4-Nitroaniline	138	–	108	92	139	109		138	121	–	
	(100)		(28)	(35)	(96)	(100)		(100)	(4)		
4-Nitrobenzonitrile	148	–	118	102	149	119	–	148	–	118	102
	(70)		(10)	(100)	(30)	(100)		(85)		(50)	(5)
2-Methyl-6-nitroaniline	152	135	122	106	153	123	107	152	135	122	–
	(100)	(10)	(5)	(35)	(100)	(25)	(6)	(100)	(10)	(<1)	
4-Methyl-2-nitroaniline	152	135	122	106	153	123	107	152	–	–	–
	(100)	(4)	(4)	(50)	(100)	(30)	(6)	(100)			
5-Methyl-2-nitroaniline	152	135	122	106	n.d.[a]			152	135	–	–
	(100)	(65)	(2)	(30)				(100)	(20)		
2-Methyl-5-nitroaniline	152	–	122	106	153	123	107	152	135	122	–
	(100)		(4)	(63)	(100)	(66)	(8)	(100)	(25)	(<0.5)	
2-Methyl-4-nitroaniline	152	–	122	106	153	123	–	152	–	–	–
	(100)		(30)	(30)	(100)	(73)		(100)			
2-Methyl-3-nitroaniline	n.d.				153	123	107	152	135	–	–
					(100)	(82)	(10)	(100)	(13)		
2-Nitroanisole	153	136	123	107	154	124	108	153	136	123	107
	(80)	(<1)	(36)	(5)	(100)	(90)	(4)	(100)	(10)	(2)	(2)

(Continued on p. 30)

TABLE IV *(continued)*

Compound	EI				PICI (CH_4)			NICI (CH_4)			
	M^+	M − OH	M − NO	$M - NO_2$	MH	MH − NO	$MH - NO_2$	M^-	M − OH	M − NO	$M - NO_2$
4-Nitroanisole	153	–	123	107	154	124	108	153	136	123	107
	(100)		(30)	(10)	(95)	(100)	(6)	(100)	(2)	(8)	(12)
1-Chloro-2-nitrobenzene	157	–	127	111	158	128	–	157	140	127	–
	(80)		(22)	(80)	(100)	(97)		(100)	(2)	(4)	
1-Chloro-3-nitrobenzene	157	–	127	111	158	128	–	157	140	127	–
	(73)		(7)	(100)	(100)	(78)		(100)	(5)	(<1)	
1-Chloro-4-nitrobenzene	157	–	127	111	158	128	112	157	140	–	–
	(94)		(35)	(93)	(68)	(100)	(2)	(100)	(5)		
1,4-Dinitrobenzene	168	–	138	122	169	139	123	168	–	138	122
	(100)		(1)	(26)	(75)	(28)	(30)	(100)		(50)	(12)
1,2-Dinitrobenzene	168	–	138	122	169	139	123	168	151	138	122
	(100)		(2)	(2)	(100)	(7)	(11)	(100)	(2)	(95)	(20)
1,3-Dinitrobenzene	168	–	138	122	169	139	123	168	151	138	122
	(100)		(2)	(30)	(100)	(11)	(14)	(100)	(5)	(68)	(6)
1,2-Dichloro-4-nitrobenzene	191	–	161	145	192	162	–	191	–	161	145
	(95)		(60)	(70)	(71)	(100)		(100)		(30)	(2)
1,3-Dichloro-4-nitrobenzene	191	–	161	145	192	162	–	191	–	161	–
	(98)		(30)	(100)	(73)	(100)		(100)		(2)	
1,4-Dichloro-2-nitrobenzene	191	–	161	145	192	162	146	191	–	161	145
	(100)		(6)	(95)	(100)	(100)	(12)	(100)		(50)	(10)
4-Chloro-2-nitrotoluene	171	154	141	125	172	142	126	171	154	141	–
	(36)	(100)	(3)	(28)	(70)	(100)	(3)	(100)	(4)	(<1)	
5-Chloro-2-nitrotoluene	171	154	141	125	172	142	126	171	154	141	–
	(40)	(100)	(1)	(30)	(100)	(85)	(5)	(100)	(4)	(1)	
6-Chloro-2-nitrotoluene	171	154	141	125	172	142	126	171	154	141	–
	(36)	(100)	(1)	(30)	(100)	(80)	(3)	(100)	(4)	(1)	–
2-Chloro-4-nitrotoluene	171	–	141	125	172	142	–	171	154	–	–
	(100)		(18)	(80)	(100)	(60)		(100)	(5)		

2,4-Dinitrotoluene	182	165	–	136	183	153	137	182	165	152	136
	(12)	(100)		(1)	(100)	(12)	(15)	(100)	(50)	(54)	(14)
3,4-Dinitrotoluene	182	–	152	136	183	153	137	182	–	152	136
	(100)		(4)	(1)	(100)	(6)	(10)	(100)		(32)	(10)
2,6-Dinitrotoluene	182	165	–	136	183	153	137	182	165	152	136
	(2)	(100)		(<1)	(100)	(22)	(20)	(100)	(35)	(85)	(20)
1-Nitronaphthalene	173	–	143	127	174	144	128	173	156	143	–
	(80)		(12)	(100)	(70)	(100)	(2)	(100)	(2)	(<1)	
2-Nitronaphthalene	173	–	143	127	174	144	128	173	–	–	–
	(90)		(2)	(100)	(85)	(100)	(3)	(100)			
1-Chloro-2,4-dinitrobenzene	202	–	172	156	203	173	157	202	185	172	156
	(100)		(8)	(8)	(100)	(15)	(18)	(100)	(4)	(50)	(10)
2-Chloro-4-nitroaniline	172	155	142	126	173	143	127	172	155	142	126
	(100)	(4)	(7)	(56)	(100)	(21)	(6)	(100)	(10)	(5)	(<1)
2,6-Dichloro-4-nitroaniline	206	–	176	160	207	177	161	207	190	–	–
	(100)		(50)	(50)	(73)	(100)	(3)	(85)	(60)		
4-Methoxy-2-nitroaniline	168	151	138	122	169	139	123	168	151	138	122
	(100)	(1)	(1)	(40)	(100)	(42)	(10)	(100)	(25)	(2)	(1)
Parathion ethyl	291	–	261	–	292	262	–	291	274	–	–
	(88)		(1)		(100)	(80)		(100)	(10)		
1,3,5-Trinitrobenzene	213	–	–	167	214	–	–	213	–	183	167
	(85)			(10)	(100)			(100)		(50)	(12)
2,4,6-Trinitrotoluene	227	210	197	–	228	198	–	227	210	197	181
	(–)	(100)	(<1)		(100)	(5)		(100)	(36)	(42)	(10)
3-Nitrophenol	139	–	109	93	140	110		139	122	109	
	(100)		(2)	(50)	(100)	(20)		(100)	(30)	(6)	
2-Nitrophenol	139	122	109	93	140	110		139	122	109	
	(100)	(5)	(12)	(10)	(100)	(11)		(100)	(20)	(8)	
2-Methyl-3-nitrophenol	n.d.				154	124	108	153		123	
					(100)	(21)	(10)	(100)		(4)	
3-Methyl-6-nitrophenol	153	136	123	107	154	124	108	153	136	123	–
	(100)	(4)	(20)	(5)	(100)	(12)	(5)	(100)	(35)	(8)	
2,2'-Dinitrobiphenyl	244	–	–	198	245	–	199	244	227	214	198
	(–)			(100)	(100)		(12)	(90)	(20)	(40)	(100)

[a] n.d. = not detected.

TABLE V

MASS SPECTROMETRIC DETECTION LIMITS (SIGNAL-TO-NOISE RATIO = 3) (pg)

Compound	EI (full scan)	EI (SIM[a])	PICI (isobutane)	NICI (methane)	NICI (argon)	NICE–SIM[a] (methane)	NICI–SIM[a] (argon)	NICI–SIM[b] (methane)
2-Nitrotoluene	21	7	44	3	2	0.6	0.3	n.d.
Nitrobenzene	43	4	206	2	3	0.3	0.3	n.d.
2,6-Dinitrotoluene	47	4	n.d.[c]	0.4	1	0.2	0.2	0.05
1,2-Dinitrobenzene	152	6	660	3	2	0.3	0.8	n.d.
2-Nitronaphthalene	32	17	7800	1	2	0.5	0.7	n.d.

[a] Ten masses are monitored.
[b] One mass is monitored.
[c] n.d. = not determined.

be one order of magnitude lower on modern sector field instuments. Whereas under full scan EI conditions an average detection limit of *ca.* 60 pg is achieved, the detection limit is higher by a factor of 2–200 under PICI conditions (isobutane). On the other hand, a substantial improvement in the detection limit is achieved under full-scan NICI conditions, ranging from 1 to 3 pg. Selective ion monitoring (SIM) using time windows with ten masses lowers the detection limit to below 1 pg, and a single mass can be monitored even at 0.05 pg.

If water samples are analysed for nitroaromatics by mass spectrometry, EI in general will be the method of choice as under these conditions abundant structure-specific fragments are formed and library searches can be carried out. NICI has the advantage of an at least ten times higher sensitivity and a substantially higher selectivity than EI and should be preferentially applied when traces of nitroaromatic compounds are to be determined in a complex aqueous mixture.

Extraction

Four different methods for the extraction of nitroaromatics from water were compared, *viz.*, discontinuous liquid–liquid extraction with dichloromethane, continuous liquid-liquid extraction with dichloromethane, solid-phase extraction with XAD resins and solid-phase extraction with octadecyl-, phenyl- and cyano-bonded phases. Moreover, the influence of different pH values and salt additions (sodium chloride) was studied. The most important results for the recovery of fifteen compounds are summarized in Table VI. The complete data are available on request.

The classical discontinuous extraction (separation funnel) with dichloromethane leads to good recoveries [$>78\%$, relative standard deviation (R.S.D.) $<11\%$]. Lowering the pH to 2.5 or increasing the salt content to 10 g/l NaCl does not influence the recoveries significantly. If the compounds are present in the sample at concentrations as low as 0.05 μg/l, they can still be recovered to a large extent ($>70\%$) although with higher R.S.D. Surprisingly, continuous extraction with dichloromethane for 5 h leads to poorer recoveries. The recovery of 2-nitrophenol is poor with both methods (46–49%). Poor recoveries were also observed for other nitrophenols.

Adsorption of nitroaromatic compounds on Amberlite XAD-2 and -4 resins leads to good recoveries ($>80\%$, R.S.D. $<7\%$) except for 2-nitrophenol (36%) and 2,4-dinitroaniline (58%). The recovery can even be enhanced for some compounds by using XAD-8. Solid-phase extraction (elution with dichloromethane) with phenyl- or octadecyl-bonded phases leads to recoveries that vary strongly from compound to compound. Although the recoveries are better with octadecyl- than phenyl-bonded phases (leading also to lower R.S.D.s), there are several compounds with unacceptably low recoveries, such as nitrobenzene, 2-nitroaniline and 1,2-dinitrobenzene. The recoveries are even poorer with cyano-bonded phases. Elution with other solvents such as methanol or diethyl ether does not improve the recovery. The poor recoveries observed for solid-phase extraction with phenyl- and octadecyl-bonded phases may be at least partially due to irreversible adsorption on the phase. If, after use, the C_{18} phase is extracted for 8 h with methanol in a Soxhlet the compounds with poor recovery can be obtained, although not quantitatively.

For the determination of the detection limit of the method, 1 l of water was spiked with 5, 50 or 500 ng/l of seventeen nitroaromatic compounds, extracted by adsorption with XAD-2 and -4 resins (1:1) and analysed by GC with ECD and TEA. If ECD is employed nitroaromatics can be determined at a concentration of 50 ng/l with recoveries comparable to those in Table VI and R.S.D. <9%. At 5 ng/l the R.S.D. rises to 10–30%. Similarly, nitroaromatic compounds can be detected with TEA with low R.S.D. (<10%) at a concentration of 500 ng/l, whereas 50 ng/l the R.S.D. rises to 10–30%. In favourable cases, detection at a level of 10 ng/l is possible. Thus, if the TEA detector is used the detection limit of the method is about one order of magnitude higher than if ECD is used. The relatively poor detection limit of the latter method is due to a substantial increase in the noise if a water sample is analysed.

Although TEA is less sensitive than ECD, compound assignment is more reliable as TEA is much more specific for nitroaromatic compounds than ECD (see below).

Analysis of surface water

A variety of surface waters were analysed for nitroaromatic compounds. Some results are reported below and additional data are available on request. The nitroaromatic compounds were extracted with Amberlite XAD-2, -4 and -8 resins (1:1:1). 1-Chloro-2,4-dinitrobenzene and 2,2′-dinitrobiphenyl were added as internal standards. The samples were chromatographed on both DB-17 and OV-225 columns. If

TABLE VI

RECOVERIES FOR THE EXTRACTION OF NITROAROMATIC COMPOUNDS FROM WATER[a]

Compound	Liquid–liquid extraction (continuous)[b]		Liquid–liquid extraction (discontinuous)[c]	
	Recovery (%)	R.S.D. (%)	Recovery (%)	R.S.D. (%)
Nitrobenzene	84	4	61	12
2-Nitrophenol	46	17	49	10
3-Nitrotoluene	83	3	77	6
1-Chloro-3-nitrobenzene	n.d.[e]		n.d.	
6-Chloro-2-nitrotoluene	78	6	66	11
1,4-Dichloro-2-nitrobenzene	97	5	86	5
4-Nitroanisole	94	9	82	3
2-Nitroaniline	91	7	74	8
1,2-Dinitrobenzene	93	5	78	4
1-Nitronaphthalene	92	5	78	6
4-Chloro-2-nitroaniline	105	6	89	3
Parathion ethyl	104	6	91	4
2,4-Dinitroaniline	94	11	55	9
2,4,6-Trinitrotoluene	n.d.		n.d.	
1-Chloro-2,4-dinitrobenzene	110	5	104	4

[a] Means of three determinations (relative to 2,2′-dinitrobiphenyl as internal standard, 2 μg/l per compound).
[b] pH 7.6 + 1 g/l NaCl.
[c] pH 7.6 + 0.5 g/l NaCl.
[d] pH 7.
[e] n.d. = not determined.

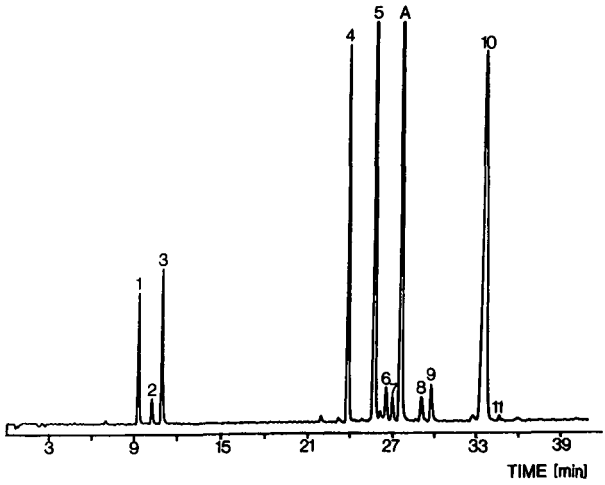

Fig. 4. Gas chromatogram (TEA) of a water sample taken from a brook near Hirschhagen/Waldhof (Hessia, F.R.G.). For peak assignment, see Table VII.

the retention times of unknown compounds coincide with those of reference compounds, the identification should be reliable, particularly if TEA is used.

Fig. 4 presents the chromatogram (obtained with TEA and a DB-5 column) of a

XAD-2/4[d]		XAD-8[d]		Phenyl[d]		C_{18}[d]	
Recovery (%)	R.S.D. (%)	Recovery (%)	R.S.D. (%)	Recovery (%)	R.S.D. (%)	Recovery (%)	R.S.D. (%)
93	3	97	5	7	30	18	15
36	10	<1		<1		<1	
86	3	112	13	27	23	78	15
86	7	105	8	21	16	72	10
100	3	98	4	69	11	94	4
110	1	96	5	58	3	92	3
96	3	109	7	65	5	67	4
86	2	90	4	<1		16	3
80	5	89	5	13	18	23	7
85	4	99	3	100	5	104	4
97	3	91	6	25	14	74	9
96	5	109	8	80	11	103	7
58	20	88	4	<1		62	4
95	7	n.d.		n.d.		n.d.	
102	4	99	1	107	–	104	–

sample taken from a brook near Hirschagen/Waldhof (Hessia, F.R.G.) which rises in an area where ammunition was produced in World War II. The chromatogram reveals the presence of nitrotoluenes, dinitrotoluenes, trinitrotoluene and also several methylnitroanilines. While the former compounds are the direct remains of the ammunition production which was terminated over 45 years ago, the latter compounds are probably biodegradation products. The compound assignment was corroborated by running the sample on an OV-225 column. As the brook is contaminated by relatively few compounds, analysis can be achieved reliably using ECD.

The brook is highly polluted by nitroaromatic compounds. Trinitrotoluene has been observed at a concentration of 19 μg/l. High concentrations of nitroaromatics were also found in a second brook nearby and in the river Losse, into which these brooks flow. The quantitative results are summarized in Table VII. Results obtained with ECD and TEA usually agree to within ± 10%. As mentioned above, TEA leads to substantial peak broadening at higher retention times, so that this part of the chromatogram could not be used to identify compounds unequivocally. Thus, in combination with GC–MS (both EI and NICI), 2,6-dinitro-4-aminotoluene and 2,6-diamino-4-nitrotoluene could be identified.

Nitroaromatic compounds were also detected in two ponds (1–10 m in depth) (Pfauenteiche) near Clausthal-Zellerfeld (Lower Saxony, F.R.G.), which again are located near a former ammunition plant closed after World War II. Fig. 5 shows the chromatogram obtained with the TEA detector for one of these ponds (Unterer Pfauenteich). In contrast to the sample in Fig. 4, where dinitrotoluenes and trinitrotoluene dominated, mononitrotoluenes were more abundant in this sample. 2-Nitrotoluene was found at a concentration of 22 μg/l. Again, several methylnitroanilines were observed, which are probably biodegradation products. Small amounts of dinitrotoluenes were also found in the river Oder near Bad Lauterbach. The concentrations were near the detection limit (TEA). Table VIII summarizes these results. In addition, with GC–MS 2,6-diamino-4-nitrotoluene and 2,6-dinitro-4-aminotoluene were identified.

TABLE VII

CONCENTRATIONS OF NITROAROMATIC COMPOUNDS IN TWO BROOKS AND THE RIVER LOSSE NEAR HIRSCHAGEN/WALDHOF

No.	Compound	Concentration (μg/l)		
		Brook I	Brook II	River Losse
1	2-Nitrotoluene	7.4	0.4	1.2
2	3-Nitrotoluene	0.9	0.1	0.1
3	4-Nitrotoluene	4.5	0.3	0.4
4	2,6-Dinitrotoluene	7.6	4.1	0.1
5	2,4-Dinitrotoluene	13.0	3.1	0.5
6	5-Methyl-2-nitroaniline	6.7	3.5	0.2
7	2-Methyl-3-nitroaniline	2.5	0.5	<0.03
8	3,4-Dinitrotoluene	0.8	0.5	<0.03
9	2-Methyl-5-nitroaniline	1.2	0.3	0.3
10	2,4,6-Trinitrotoluene	19.0	12.0	0.7
11	2-Methyl-4-nitroaniline	0.4	0.1	0.1

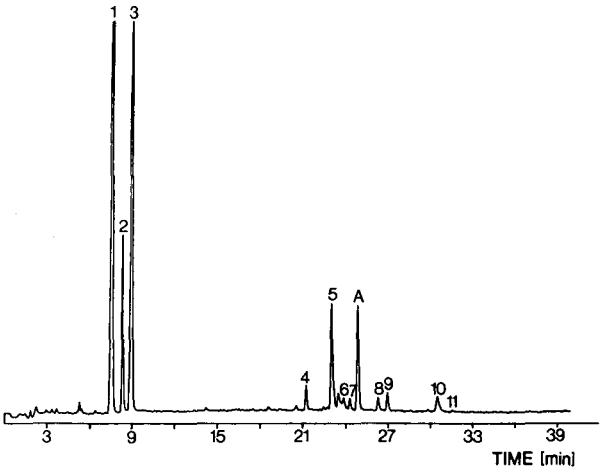

Fig. 5. Gas chromatogram (TEA) of a water sample taken form a pond near Clausthal-Zellerfeld (Lower Saxony, F.R.G.). For peak assignment, see Table VII.

Samples from several rivers in F.R.G. were analysed for nitroaromatic compounds. Fig. 6 compares the chromatograms of a sample from the Elbe (near Lauenburg) obtained using ECD (top) and TEA (bottom) on a DB-5 column. A variety of nitroaromatic compounds can be identified. Table IX summerizes the quantitative results. Compound assignment was again verified by running the sample on a second column (OV-225). As the river Elbe is a highly polluted surface water which contains many ECD-sensitive compounds, compound assignment and quantification based on the ECD chromatogram alone is not reliable. With ECD, a five times higher concentration of 2-nitrotoluene (as compared with TEA) was determined in this sample. In

TABLE VIII

CONCENTRATIONS OF NITROAROMATIC COMPOUNDS IN TWO PONDS AND THE RIVER ODER (HARZ)

No.	Compound	Concentration (μg/l)		
		Unterer Pfauenteich	Mittlerer Pfauenteich	River Oder
1	2-Nitrotoluene	22.0	0.4	<0.01
2	3-Nitrotoluene	1.5	0.1	<0.01
3	4-Nitrotoluene	4.8	0.2	<0.01
4	2,6-Dinitrotoluene	0.3	0.07	0.02
5	2,4-Dinitrotoluene	1.2	0.8	0.02
6	5-Methyl-2-nitroaniline	0.8	0.5	<0.01
7	2-Methyl-3-nitroaniline	0.7	0.1	<0.01
8	3,4-Dinitrotoluene	0.1	0.1	<0.01
9	2-Methyl-5-nitroaniline	0.2	0.2	<0.01
10	2,4,6-Trinitrotoluene	0.5	0.5	<0.01
11	2-Methyl-4-nitroaniline	<0.01	<0.01	<0.01

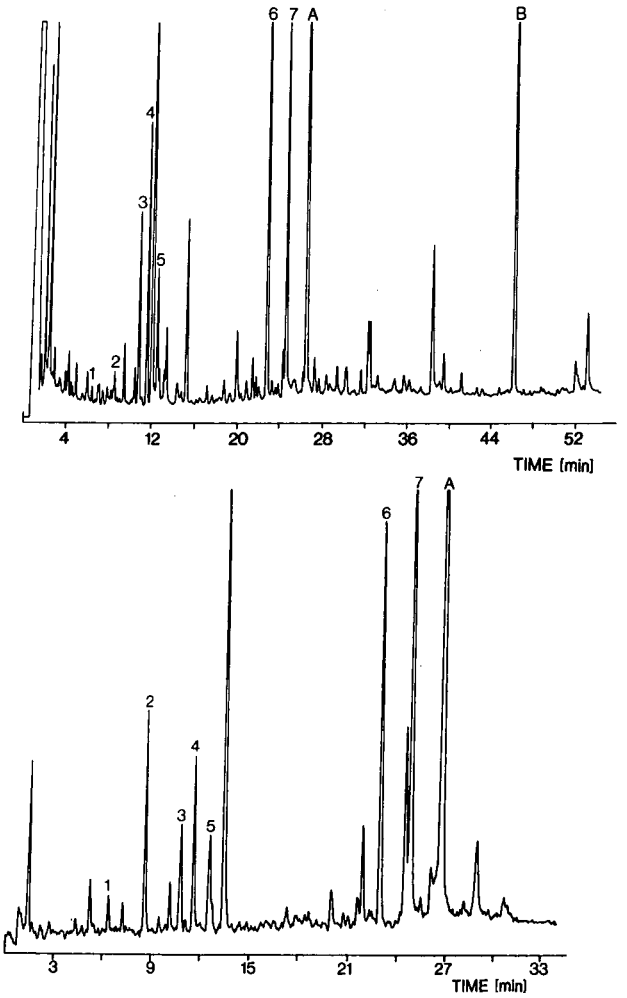

Fig. 6. Gas chromatogram of a water sample taken from the Elbe near Lauenburg (top, ECD; bottom, TEA). For peak assignment, see Table IX.

TABLE IX

CONCENTRATIONS OF NITROAROMATIC COMPOUNDS IN THE RIVER ELBE AT THREE LOCATIONS

No.	Compound	Concentration (μg/l)		
		Lauenburg	Brokdorf	Brunsbüttel
1	Nitrobenzene	0.1	0.03	0.02
2	2-Nitrotoluene	0.4	0.08	0.05
3	1-Chloro-3-nitrobenzene	0.2	0.04	<0.02
4	1-Chloro-4-nitrobenzene	0.3	0.1	0.04
5	1-Chloro-2-nitrobenzene	0.2	0.1	0.04
6	2,6-Dinitrotoluene	0.5	0.08	0.04
7	2,4-Dinitrotoluene	1.3	0.3	0.1

contrast, the much higher selectivity of the TEA detector allows a safe assignment of nitroaromatic compounds if reference compounds are available (The TEA chromatogram in Fig. 6 reveals the presence of an additional major unknown compound for which a reference compound was not available). With GC–MS the results in Table IX could also be corroborated.

CONCLUSIONS

Nitroaromatic compounds can be extracted from aqueous samples with high recoveries by liquid–liquid extraction with dichloromethane or by adsorption on Amberlite resins, while lower and strongly varying recoveries are found if solid-phase extraction with phenyl-, octadecyl- or cyano-bonded phases is employed. As a result of their high electron affinities, nitroaromatic compounds can be determined with high sensitivity by GC using ECD. If, however, highly polluted surface water is to be investigated, ECD is not sufficiently selective for an unambiguous compound assignment. In contrast, a chemiluminescence detector (TEA) is much more selective for nitro compounds, allowing a reliable peak assignment if reference compounds are available. The major disadvantage of the chemiluminescence detector is its lower sensitivity (compared with the electron capture detector), which precludes the analysis of weakly polluted water. Definite compound assignment can usually be achieved with GC–MS, where NICI is more sensitive and selective than EI, but gives fewer structure-specific fragments.

Some nitrophenols have also been studied. However, the analysis has not been optimized for this specific class of compounds, for which poor recoveries were observed with extraction as described above.

ACKNOWLEDGEMENT

We are gratefully to Mrs. S. Behnert for skillful technical assistance.

REFERENCES

1 W. Wirth and C. Gloxhuber, *Toxikologie*, Georg Thieme, Stuttgart, 1985.
2 K. G. Malle, *Z. Wasser Abwasser Forsch.*, 17 (1984) 75.
3 L. H. Keith and W. A. Telliard, *Environ. Sci. Technol.*, 13 (1979) 416.
4 *Arbeitsgemeinschaft Rhein-Wasserwerke*, 44th Report, Cologne, 1987.
5 F. Karrenbrock and K. Haberer, *Vom Wasser*, 60 (1983) 237.
6 R. J. Spanggord, B. W. Gibson, R. G. Keck, D. W. Thomas and J. J. Barkley, *Environ. Sci. Technol.*, 16 (1982) 229.
7 N. B. Jurinski, G. E. Podolak and T. L. Hess, *Am. Ind. Hyg. Assoc. J.*, 36 (1975) 497.
8 F. Belkin, R. W. Bishop and M. V. Sheely, *J. Chromatogr. Sci.*, 24 (1985) 532.
9 L. X. Tian and R. N. Fu, *Int. Jahrestag. Fraunhofer Inst. Treib-Explosivst. 17th (Anal. Propellants Explos.: Chem. Phys. Methods)*, 63-1, 1986.
10 A. Hashimoto, T. Kozima, H. Shakino and T. Akiyama, *Water Res.*, 13 (1979) 509.
11 A. Hashimoto, H. Sakino, E. Yamagami and S. Tateishi, *Analyst (London)*, 105 (1980) 787.
12 J. J. Richard and G. A. Junk, *Anal. Chem.*, 58 (1986) 723.
13 R. Haas, *Forum Städte-Hygiene*, 36 (1985) 86.
14 J. H. Phillips, R. J. Coraor and S. R. Prescott, *Anal. Chem.*, 55, (1983) 889.
15 J. T. Walsh, R. C. Chalk and C. Merritt, *Anal. Chem.*, 45 (1973) 1215.
16 C. F. Bauer, C. L. Grant and T. F. Jenkins, *Anal. Chem.*, 58 (1986) 176.

17 T. F. Jenkins, D. C. Leggett, C. L. Grant and C. F. Bauer, *Anal. Chem.*, 58 (1986) 170.
18 M. P. Mascarinec, D. L. Manning, R. W. Harvey, W. H. Griest and B. A. Tomkins, *J. Chromatogr.*, 302 (1984) 51.
19 E. Tesarova and V. Pacakova, *Chromatographia*, 17 (1983) 269.
20 C. M. White (Editor), *Nitrated Polycyclic Aromatic Hydrocarbons*, Hüthig, Heidelberg, 1985.
21 M. Alber, H. B. Böhm, J. Brodesser, J. Feltes, K. Levsen and H. F. Schöler, *Fresenius' Z. Anal. Chem.*, 334 (1989) 540.
22 H. B. Böhm, J. Feltes, D. Volmer and K. Levsen, *J. Chromatogr.*, 478 (1989) 399.
23 H. D. Winkeler and K. Levsen, *Fresenius' Z. Anal. Chem.*, 334 (1989) 340.
24 J. Schilhabel and K. Levsen, *Fresenius' Z. Anal. Chem.*, 333 (1989) 800.
25 H. Budzikiewicz, C. Djerassi and D. H. Williams, *Mass Spectrometry of Organic Compounds*, Holden-Day, San Francisco, 1967.
26 S. Zitrin and J. Yinon, *Org. Mass Spectrom.*, 11 (1976) 388.
27 J. Yinon, *Org. Mass Spectrom.*, 15 (1980) 637.
28 E. A. Stemmler, R. A. Hites, *Electron Capture Negative Ion Mass Spectra of Environmental Contaminants and Related Compounds*, VCH, Weinheim, 1988.

Journal of Chromatography, 518 (1990) 41–52
Elsevier Science Publishers B.V., Amsterdam

CHROM. 22 604

Determination of clenbuterol in bovine plasma and tissues by gas chromatography–negative-ion chemical ionization mass spectrometry

J. GIRAULT* and J. B. FOURTILLAN
CEMAF S.A., 144 rue de la Gibauderie, 86000 Poitiers (France)
(First received March 23rd, 1990; revised manuscript received May 31st, 1990)

ABSTRACT

A highly sensitive and specific assay was developed for the determination of clenbuterol in bovine plasma and tissues. Clenbuterol and the internal standard [$^2H_9$]clenbuterol were measured by gas chromatography–negative-ion chemical ionization mass spectrometry with methane as the reagent gas. Bovine tissues including muscle, liver, heart, kidney, lung, suet, brain, spinal cord and thymus were ground in a buffer of pH 7 and then extracted using ethyl acetate. After two subsequent purification steps, the cleaned-up organic extract was derivatized with pentafluoropropionic anhydride. The mass spectrometer was set to monitor the abundant ions *m/z* 368 and 377 of the perfluoroacyl derivatives. This assay was performed with 1 ml of plasma or 0.2 g of tissue. The feasibility of this method was demonstrated by the determination of clenbuterol residues as the femtomole level in a variety of tissues.

INTRODUCTION

Many drugs (hormones, antibiotics, anabolic agents) including clenbuterol are widely administered to farm animals for health reasons or to improve meat production. Clenbuterol {4-amino-α-[(*tert.*-butylamino)methyl]-3,5-dichlorobenzyl alcohol hydrochloride} is a broncholytic agent normally used in humans for the treatment of asthma [1]. This potent sympathomimetic drug with selective activity on adrenergic β_2-receptors is also used in veterinary medecine as bronchorelaxant and tocolytic agent. More recently, clenbuterol has been suggested as a bovine growth promotant and is currently, but illegally, used in many countries. Because the active dose is very low and the apparent distribution volume relatively high, the resulting plasma and tissue concentrations of clenbuterol following oral administration of the drug are in the parts per trillion (ppt) range.

The determination of a substance present at the femtomole level in complex biological matrices is a tremendous challenge. In order to investigate correctly the pharmacokinetic behaviour of clenbuterol involving absorption, distribution and elimination of the drug, and to monitor the residue levels in tissues intended for human use, a reliable and robust method is required.

As far as law is concerned, the maximum residue level (MRL) allowed in animal

0021-9673/90/$03.50

products is zero. Obviously, the MRL is based on the detection limit of the most sensitive analytical method available. Hence the zero level is greatly dependent on the procedure used to quantify, with sufficient specificity and sensitivity, the residue levels of compounds which are most often present in the lower parts per billion (ppb) range in complex matrices.

Most sympathomimetic drugs have been identified or measured in biological fluids by techniques such as high-performance liquid chomatography (HPLC) [2–9], gas chromatography–mass spectrometry (GC–MS) [10–24] or radioimmunoassay (RIA) [25]. High-resolution capillary GC–MS remains the method of choice for the determination of clenbuterol. We have previously reported an isotope dilution method using negative-ion chemical ionization (NICI) mass spectrometry with methane as the reagent gas for the precise and accurate determination of small amounts of clenbuterol following oral administration of the drug to healthy volunteers [26–28]. This assay was performed with 1 ml of plasma or 0.5 ml of urine. The extracts were reacted with pentafluoropropionic anhydride at ambient temperature. The perfluoroacyl derivatives gave rise to characteristic ions of m/z 368 (clenbuterol) and 377 ([$^2H_9$]clenbuterol) which were recorded by selected ion monitoring.

This assay has been successfully adapted to the determination of clenbuterol in bovine plasma and tissues. A study protocol was designed in order to generate a range of levels that illustrates the distribution of clenbuterol in a variety of bovine samples. The feasibility of this highly sensitive and specific assay was demonstrated by preliminary results on the determination of clenbuterol in bovine plasma and tissues from 12 animals receiving oral treatment with clenbuterol.

EXPERIMENTAL

Chemicals

Chemical standards were kindly supplied by Chiesi Farmaceutici Laboratories (Parma, Italy). All solvents and reagents were of analytical-reagent grade from Merck (Darmstadt, F.R.G.) and were used without further purification. Pentafluoropropionic anhydride (PFPA) was obtained from Pierce (Rockford, IL, U.S.A.).

All glassware was cleaned with a mechanical scaling brush, then left overnight in CrO_3–H_2SO_4 and finally rinsed with doubly distilled water. The PTFE caps of the tubes were also carefully cleaned to avoid any subsequent sample contamination.

Calibration graphs

Stock solutions of clenbuterol and [$^2H_9$]clenbuterol (internal standard) were prepared by dissolving each of the pure reference compounds in methanol in order to achieve a primary concentration of 0.1 mg ml^{-1}. Secondary standard solutions, obtained by appropriate dilutions with distilled water, were protected from light by aluminium foil and stored at 4°C until used.

Aliquots of 1 ml of drug-free human plasma were fortified with 50 μl of a 10 ng ml^{-1} [$^2H_9$]clenbuterol solution in water and various amounts of clenbuterol ranging from 5 to 250 pg ml^{-1}. For tissue samples (0.2 g) the added amount of internal standard was the same as for the plasma specimens and a calibration graph was constructed from 10 to 500 pg g^{-1}. Blank samples were prepared in a similar way by spiking 1 ml of control plasma (or 0.2 g of tissue) only with the internal standard solution.

Extraction from plasma samples

Plasma samples (1 ml), spiked as stated above with [$^2H_9$]clenbuterol, were placed in 20-ml screw-capped tubes with 1 ml of 2 *M* sodium hydroxide solution buffered at pH 12 with sodium hydrogencarbonate. After brief mixing, 6 ml of ethyl acetate were added to each tube. The extraction procedure was conducted over a 10-min period using a reciprocating shaker and the tubes were then centrifuged at 1600 *g* for 5 min. The organic layer was transferred into a 10-ml screw-capped tube containing 1 ml of 0.2 *M* sulphuric acid. After extraction and centrifugation as described, the organic solvent was removed under vacuum. The remaining aqueous phase was purified with 4 ml of ethyl acetate–hexane (2:1, v/v). Following a brief extraction and centrifugation, the upper organic layer was discarded. The sulphuric acid phase was made alkaline with 1 ml of 2 *M* sodium hydroxide solution and then extracted with 5 ml of ethyl acetate. The organic solvent was decanted into a 10-ml Quickfit glass tube and evaporated to dryness under nitrogen at 40°C.

Extraction from tissue samples

Tissue samples (0.2 g) were accurately weighed and placed in a 20-ml glas tube with 3 ml of a Sorensen buffer (pH 7) and 500 pg of [$^2H_9$]clenbuterol. Each sample was homogenized for 1 min using a Polytron tissue grinder powered by an overhead stirrer. The tubes were centrifuged for 15 min at 1800 *g* and the supernatant was decanted in another 20-ml screw-capped tube. The aqueous phase was made alkaline with 1 ml of 2 *M* sodium hydroxide solution and then extracted for 10 min with 6 ml of ethyl acetate. The samples were then purified as described above for plasma.

Derivatization procedure

In order to eliminate moisture, the inner sides of the vials were rinsed with 100 μl of acetone, previously dried over anhydrous sodium sulphate. The acetone was evaporated and 40 μl of PFPA were added to the residue in the vials, which were then tightly capped and allowed to stand at room temperature until analysis. A 1-μl aliquot of the derivatization mixture was injected into the gas chromatograph–mass spectrometer.

Precision, accuracy and limit of detection

To assess the precision and accuracy of the method for plasma samples, repeatability assays were carried out at four concentrations (5, 20, 100 and 200 pg ml^{-1}). The spiked plasma samples were analysed on the same day by the same person and for each concentration level the relative standard deviation and mean percentage error were calculated.

The limit of detection (LOD) was defined as the lowest detectable concentration yielding a signal significantly higher than that of blank control specimens [27–30]. First, to calculate the LOD of the method a repeatability assay was performed with ten blank plasma samples. The mean signal ($\bar{Y}_{bl}$) eventually observed at the retention time of clenbuterol and the associated standard deviation (S_{bl}) were used to calculate a theoretical value of the detection limit. Then, a repeatability assay was carried out with ten replicate plasma samples spiked at a concentration corresponding to this theoretical detection limit. The mean signal ($\bar{Y}_{LOD}$) was statistically compared with the mean signal ($\bar{Y}_{bl}$) obtained with the blank samples. After testing the variance

homogeneity ($p < 0.001$), a t-test or a Welch test was applied in order to demonstrate that $\bar{Y}_{LOD}$ was significantly higher than $\bar{Y}_{bl}$ ($p < 0.05$).

The precision and accuracy of the method for tissue samples were also investigated at two concentrations, 20 and 200 pg g^{-1}, of clenbuterol. The tissue samples were analysed as described above.

GC–MS analysis

The method was developed on an HP 5985 B gas chromatograph–mass spectrometer operated under the SIDS operating system. GC was carried out on a fused-silica capillary column (25 m × 0.35 mm O.D.) wall-coated with OV-1701. The film thickness and I.D. of the column were 0.11 μm and 0.22 mm, respectively.

Samples were injected with a falling needle injector with helium as the carrier gas (inlet pressure 14 p.s.i.). The injection port was maintained at 290°C. The oven temperature was raised from 180 to 230°C at 8°C min^{-1} and from 230 to 290°C at 20°C min^{-1}.

One end of the capillary column was connected to the glass solid injector 1 mm from the bottom of the moving needle. The other end was introduced directly near the ion source of the mass spectrometer via a 1/16-in. stainless-steel transfer line, the temperature of which was held at 280°C.

The GC–MS system was operated in the NICI mode with an electron energy of 100 eV, an emission current of 300 μA and an ion source temperature of 180°C. Prior to the analysis, the instrument was tuned in the NICI mode using the fragments of m/z 414, 595 and 633 from the perfluorotributylamine calibrant gas. The reagent gas methane was admitted via a gas-flow controller to an indicated ion source pressure of about 0.8 Torr.

The NICI mass spectra of clenbuterol and [$^2H_9$]clenbuterol perfluoroacyl derivatives were recorded during a GC run by scanning the quadrupole mass filter repetitively every 1.1 s from m/z 250 to 450. Determination of clenbuterol was performed by focusing the instrument in the single-ion monitoring mode in order to measure the fragments of m/z 368 (clenbuterol) and 377 (internal standard). The dwell time was 100 ms for each mass range.

Quality controls

Throughout the study quality controls were supplied blind to the analyst by spiking blank plasma and tissue samples with known amounts of clenbuterol. The experimenter in charge of the assay ignored the theoretical concentration of these samples, prepared independently by a technician who did not participate in the study. The standard solutions used to spike the control specimens were different from those used to obtain the calibration graphs. The quality control samples were stored at −20°C until analysis. Two samples were assayed each day together with the real life samples collected during the pharmacokinetic study. After calculating the results, the absence of any systematic bias in the assay of clenbuterol was controlled. For that reason, a regression analysis was carried out by plotting the found *versus* the theoretical values. The slope and intercept were then statistically compared with the theoretical values of 1 and 0, respectively, using a Student's t-test.

Drug administration

Twelve Holstein calves received an oral treatment with clenbuterol and during the administration period plasma and urine samples were collected for pharmacokinetic analysis. The calves were subsequently slaughtered and different tissues were collected. All plasma and tissue samples were stored frozen (−20°C) until analysis. Twelve other calves that did not receive clenbuterol were used as control animals.

RESULTS AND DISCUSSION

Sample pretreatment and analysis

The samples must be carefully purified to remove endogenous substances that could interfere during the selected ion monitoring determination of clenbuterol. The multiple-step extraction process leads to a "clean" residue devoid of most impurities. Owing to the use of a glass solid injector and despite this long sample pretreatment, the laboratory throughput can be up to 40 samples per day. The moving needle injection technique, which is very protective for the capillary column, allows an initial oven temperature that is much higher than that required for other sample inlets such as splitless or on-column injectors.

Under the analytical conditions adopted, the retention times of clenbuterol and [$^2H_9$]clenbuterol were 5.22 and 5.16 min, respectively. The two chromatographic peaks followed a Gaussian distribution and each derivative was totally eluted from the column in less than 4 s. The peak width at half-height was *ca.* 1.3 s. A dwell time of 0.1 s per mass unit led to a minimum of 18 measurements for each analyte.

Derivatization procedure

The determination of underivatized clenbuterol is unsuitable owing to the presence of hydroxy and amino groups, which are mainly responsible for tailing peaks in GC. We have already proposed to derivatize clenbuterol and the internal standard with hexamethyldisilazane (HMDS) [31,32]. This silylating reagent gave a low chemical background with highly volatile by-products. The extracts were heated with 30 μl of HMDS for 1 h at 80°C. A faster derivatization step yielded low sensitivity and poor reproducibility, with the formation of small amounts of reaction products. Moreover, the O-trimethylsilyl ether derivative of clenbuterol was prone to hydrolysis: glassware and solvents were carefully protected from moisture in order to hinder this interfering reaction process.

We have now developed another derivatization procedure that offers a more favourable starting point for a highly sensitive and specific assay of clenbuterol. Under the mild conditions applied, clenbuterol and [$^2H_9$]clenbuterol reacted completely with PFPA. A subsequent study of this derivatization process has shown that, at ambient temperature, the hydroxy and amino groups of the side-chain were acylated with PFPA to give the dipentafluoropropionyl derivative. Because of the immediate loss of one PFP substituent in the reaction medium followed by internal dehydration, the final and highly stable reaction product was the monosubstituted derivative.

When the reaction temperature was raised, the 4-amino function also reacted with PFPA, and another chromatographic peak corresponding to the disubstituted derivative was observed. From a quantitative point of view, this reaction at higher temperature was not reproducible and the relative proportions between the two products differed day by day.

Mass spectra

The NICI mass spectra of clenbuterol and [$^2H_9$]clenbuterol mono-PFP obtained with methane as the reagent gas exhibit characteristic ions in the high-mass region, as shown in Fig. 1.

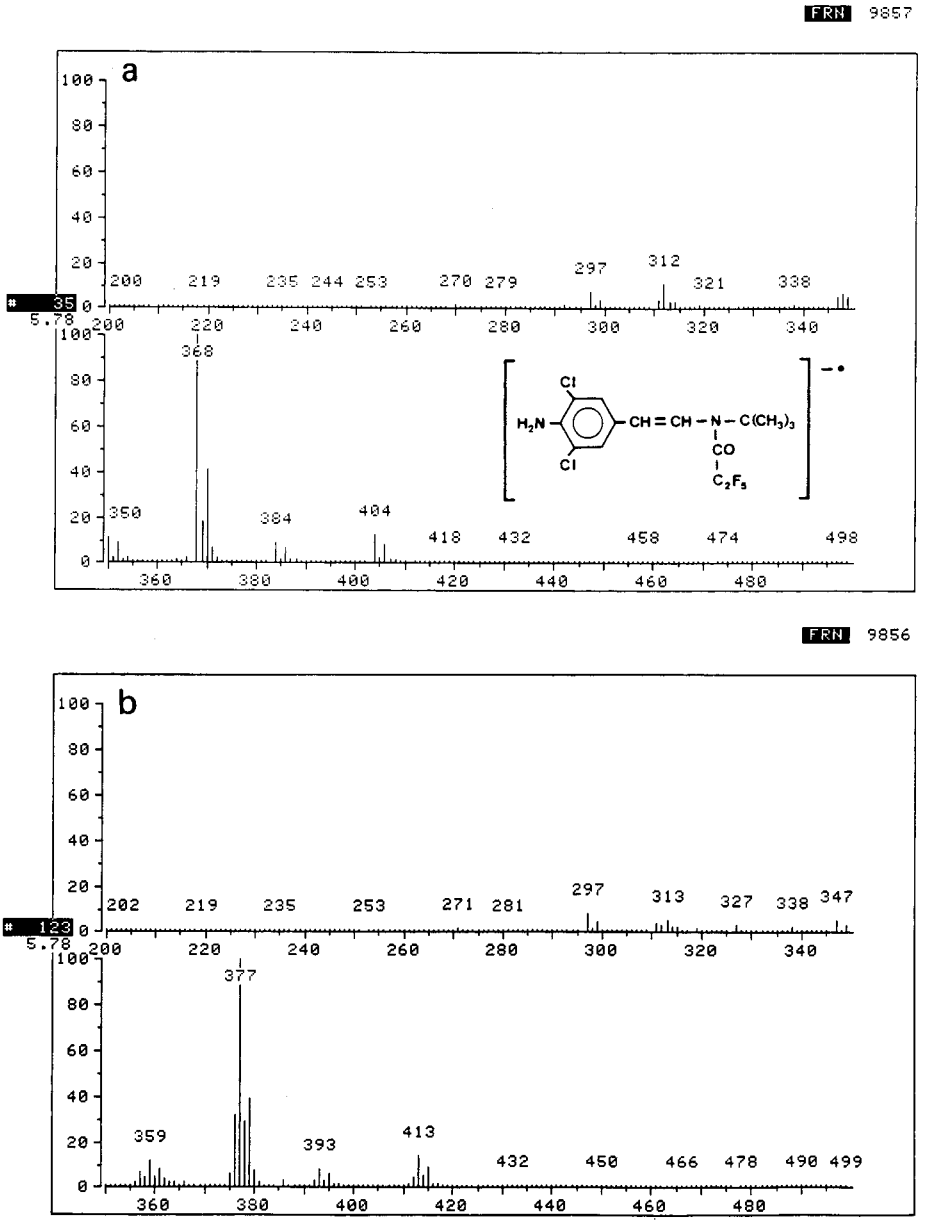

Fig. 1. Methane NICI mass spectra of the mono-PFP acyl derivatives of (a) pure clenbuterol and (b) [$^2H_9$]clenbuterol.

The molecular ions of *m/z* 404 and 413 are present with a relative intensity of about 15%. The two spectra are similar except for a mass shift of 9 u for most of the ions. The loss of one 36 u fragment ($[M-HCl]^-$) from the molecular ions could proceed from internal cyclization and gave rise to the base peaks observed at *m/z* 368 and 377. These two ions successively undergo the elimination of *tert.*-butyl and amino groups, leading to the formation of the ions of *m/z* 312, 313 and finally 297.

Calibration graphs

The seven-point plasma calibration graphs obtained each day of the assay by plotting the peak-area ratios of *m/z* 368 and 377 *versus* known plasma concentrations of clenbuterol were straight lines ($r = 0.9998$) over the concentration range 5–250 pg ml^{-1}. The slopes of the plasma calibration curves were reproducible from day to day, with a relative standard deviation of less than 4%. The least-squares regression analysis passed near the origin, with a mean intercept value close to zero.

The corresponding tissue calibration graphs were linear over the concentration range 10–500 pg g^{-1} for each tissue tested.

Precision and accuracy

The yield of the extraction was *ca.* 80% and all sources of variability were considerably reduced owing to the use of a stable isotopically labelled analogue as the internal standard. The relative standard deviations were less than 4% and the mean percentage error ranged from −1.9 to +0.2% for clenbuterol plasma concentrations between 20 and 200 pg ml^{-1} (Table I).

The precision and accuracy of the method were also tested with bovine tissue samples at two different concentrations. The relative standard deviations were 9.0 and 7.3%. The mean percentage error ranged from −5.5% to +6.4% for tissue spiked with 20 and 200 pg of clenbuterol (Table II).

Limit of detection

A signal-to-noise ratio $\geqslant 2.5$ is commonly used as a criterion for a significant response. Unfortunately, even if the low electronic noise is relatively constant day by day, the same does not apply to the chemical background, which is sometimes very different from one determination to another. This is principally due to the sample itself, the solvents, the glassware and/or the chromatographic system. In order to take

TABLE I

PRECISION AND ACCURACY OF THE CLENBUTEROL ASSAY PROCEDURE FOR PLASMA SAMPLES

Theoretical concentration (pg ml^{-1})	*n*	Mean observed concentration (pg ml^{-1})	S.D.	R.S.D. (%)	Error (%)
200	10	196.27	5.89	3.0	−1.9
100	5	99.30	3.41	3.4	−0.7
20	5	20.03	0.74	3.7	+0.2
5	10	4.78	0.61	12.8	−4.3

TABLE II

PRECISION AND ACCURACY OF THE CLENBUTEROL ASSAY PROCEDURE FOR TISSUE SAMPLES

Theoretical concentration (pg g^{-1})	n	Mean observed concentration (pg g^{-1})	S.D.	R.S.D. (%)	Error (%)
200	10	212.7	15.6	7.3	+6.4
20	10	18.9	1.7	9.0	−5.5

into account all of these soures of variation, we have developed a statistical determination of the detection limit based on the results obtained after GC–MS analysis of ten different blank plasma extracts. The mean signal ± S.D. (1.3482 ± 0.1114) calculated from the repeatability assay performed at 5 pg ml^{-1} was significantly different ($p<0.001$) from that observed with the ten blank specimens (0.4320 ± 0.0602). Owing to the relative standard deviation (12.8%) and mean percentage error (−4.3%), a 5 pg ml^{-1} concentration level was validated as the detection limit of the method for plasma samples.

For tissue samples the limit of detection was 10 pg g^{-1}. A representative selected ion chromatogram obtained after GC–MS analysis of a blank tissue specimen (kidney) is shown in Fig. 2. As examplified by this chromatogram, no interference from endogenous compounds was observed in the single-ion monitoring of the fragment of m/z 368.

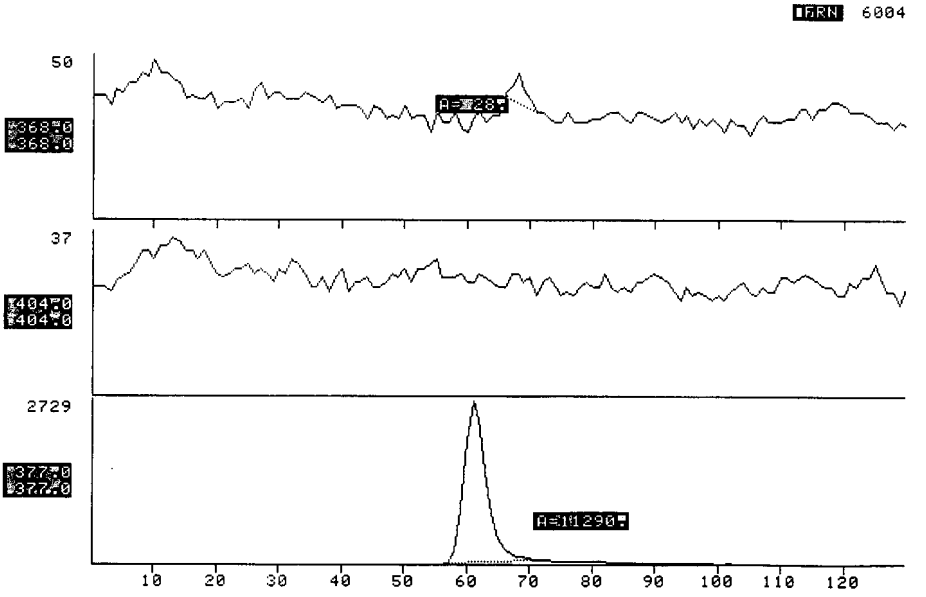

Fig. 2. Representative mass chromatogram obtained from a control kidney specimen (0.2 g) spiked with 500 pg of [$^2H_9$]clenbuterol.

Results for control tissue samples (back muscle and spinal cord), spiked with 10 and 250 pg of clenbuterol, respectively, are presented in Fig. 3.

Quality controls

Quality control analysis ($n=36$),showed that the found concentrations were

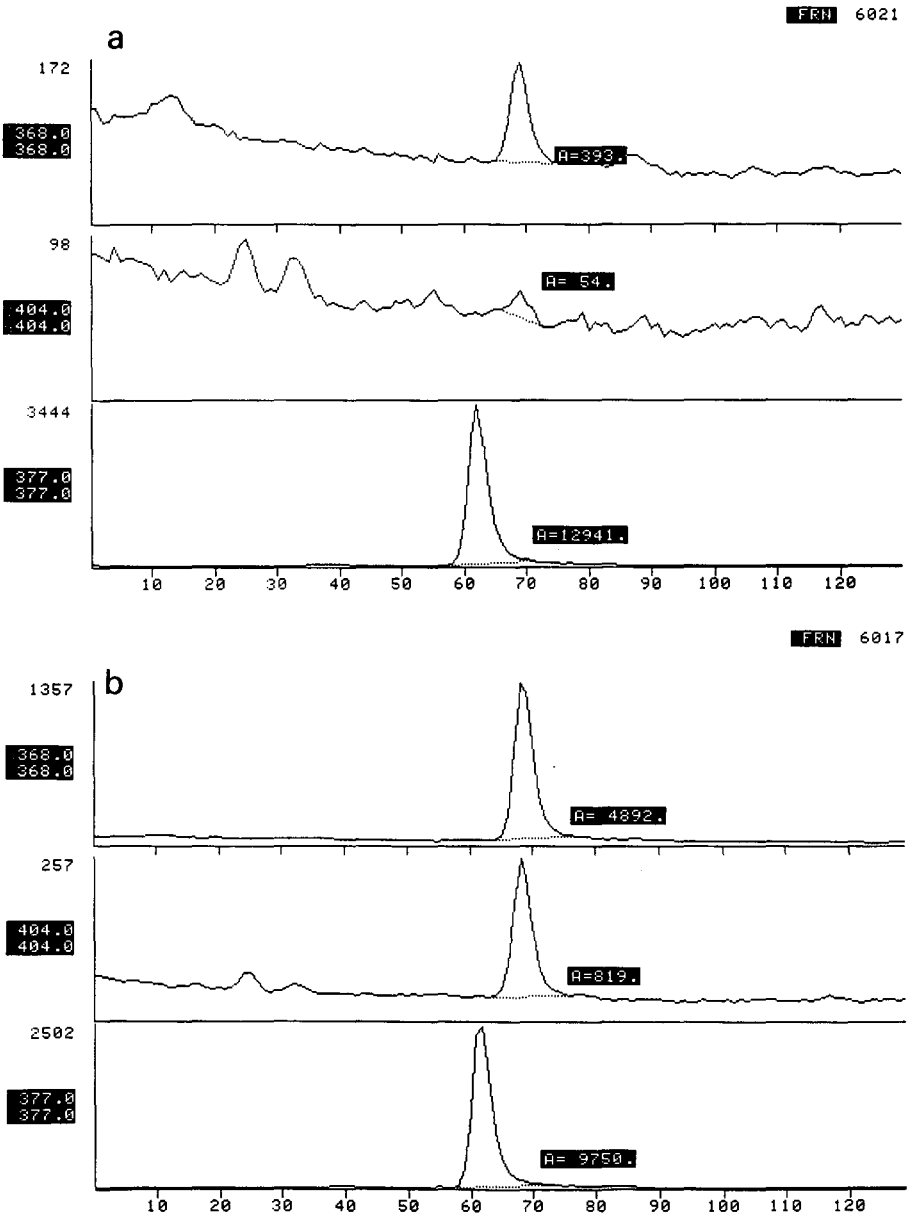

Fig. 3. Selected ion monitoring traces obtained from (a) a back muscle fortified with 10 pg of clenbuterol and (b) a spinal cord specimen spiked with 250 pg of clenbuterol and 500 pg of [$^2H_9$]clenbuterol.

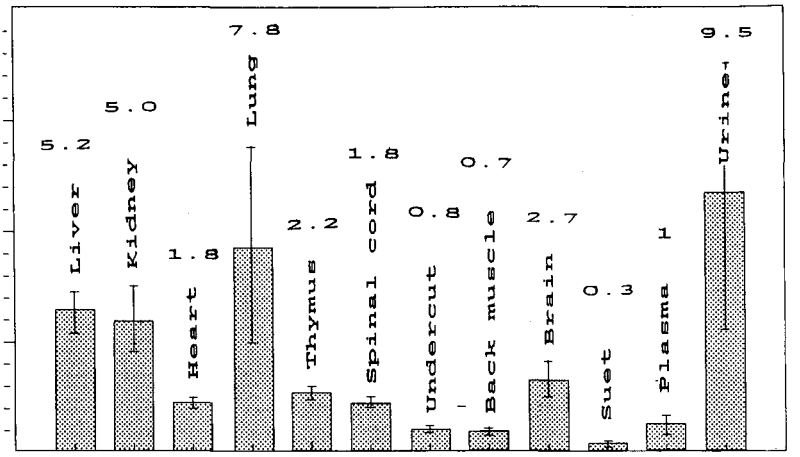

Fig. 4. Distribution of clenbuterol in different target tissues measured after oral administration of the drug.

correlated with the theoretical values ($r = 0.999$). A Student's t-test was carried out in order to demonstrate that the slope and intercept of the regression analysis were not significantly different from the theoretical values of 1 and 0, respectively, at a probability level of 95% for $n - 2$ degrees of freedom.

The values of $t_{slope} = 1.312$ and $t_{intercept} = -0.289$, were lower than the limit (1.960) of the t-table. Consequently, this assay was applied to the quantitative measurement of clenbuterol without any constant of proportional systematic error. The mean difference between the theoretical and actual values was 5.2% for clenbuterol plasma concentrations ranging from 0 to 250 pg ml^{-1}.

Distribution of clenbuterol in target tissues

The levels observed in different tissues are summarized in Fig. 4. The factor 1 was arbitrarily assigned to plasma and the other tissues were calculated on this basis.

Clenbuterol is a β_2-agonist drug initially used for the treatment of asthma in human, which is why the lungs normally contained the highest levels of clenbuterol. High concentrations of clenbuterol were also measured in liver, kidney and thymus, where the affinity of the drug for the β_1-adrenergic receptors of the heart was of minor importance. The muscles and the suet contained the lowest levels of clenbuterol. Clenbuterol is a lipophilic compound crossing the blood–brain barrier; relatively high levels of this drug were observed in the brain and spinal cord.

These results were in good agreement with those obtained previously when we compared the distribution of clenbuterol and salbutamol after intravenous administrations of the two drugs to six dogs [31,32].

CONCLUSION

The correct pharmacokinetic behaviour and the distribution of clenbuterol in target tissues can only be achieved if accurate and precise analytical data are obtained.

The method used to determine clenbuterol in biological matrices should be carefully optimized, so that the reliability of the analytical procedure depends greatly on the criteria used to validate the assay. The isotope dilution mass spectrometric assay described here afforded a sensitive and specific technique for measuring clenbuterol at the femtomole level in plasma and tissue. The monopentafluoropropionyl derivative of clenbuterol gave an intense signal and when the fragment of m/z 368 was monitored under NICI conditions the detection limit of this assay was 5 pg ml^{-1}. The relative standard deviations and mean percentage errors calculated during the different repeatability assays demonstrated that, even around this limit of detection, the precision and accuracy of the method were suitable for routine analysis for clenbuterol.

This method was successfully applied to the analysis of bovine tissues including muscle, liver, heart, kidney, lung, suet, brain, spinal cord and thymus after the administration of an oral dose of clenbuterol to twelve calves. This assay has been routinely applied for 4 years in many pharmacokinetic and bioavailability studies following oral or intravenous administration of clenbuterol to humans or animals.

ACKNOWLEDGEMENTS

The authors thank P. Gobin for technical assistance and veterinarians J. P. Tafani and J. Moreau for monitoring the clinical part of this study.

REFERENCES

1 G. Engelhardt, *Arzneim. Forsch./Drug Res.*, 26 (1976) 1404.
2 L. E. Edholm, B. M. Kennedy and S. Bergquist, *Chromatographia*, 16 (1982) 341.
3 B. Oosterhuis and C. J. van Boxtel, *J. Chromatogr.*, 232 (1982) 327.
4 G. B. Park, R. F. Koss, J. Utter and J. Edelson, *J. Chromatogr.*, 273 (1983) 481.
5 R. J. J. Hageman, J. E. Greving, J. H. G. Jonkman and R. A. de Zeeuw, *J. Chromatogr.*, 274 (1983) 239.
6 S. Bergquist and L. E. Edholm, *J. Liq. Chromatogr.*, 6 (1983) 559.
7 L. E. Edholm, B. M. Kennedy and S. Bergquist, *Eur. J. Resp. Dis.*, 65 (1984) 11.
8 N. Kurosawa, S. Morishima, E. Owada and K. Ito, *J. Chromatogr.*, 305 (1984) 485.
9 Y. K. Tan and Q. J. Soldin, *J. Chromatogr.*, 422 (1987) 187.
10 L. E. Martin, J. Rees and R. J. N. Tanner, *Biomed. Mass Spectrom.*, 3 (1976) 184.
11 F. C. Falkner and H. M. McLhenny, *Biomed. Mass Spectrom.*, 3 (1976) 207.
12 J. C. Leferink, I. Wagemaker-Engels, R. A. A. Maes, J. Lamont, R. Pauwels and M. van der Straeten, *J. Chromatogr.*, 143 (1977) 299.
13 R. A. Clare, D. S. Davis and T. A. Baillie, *Biomed. Mass Spectrom.*, 6 (1979) 31.
14 M. Ishigami, K. Saburomaru, K. Niino, M. Kido, S. Morita, G. Miyamoto and H. Kohri, *Arzneim. Forsch./Drug Res.*, 29 (1979) 266.
15 L. E. Martin, J. Oxford, R. J. N. Tanner and M. J. Hetheridge, *Biomed. Mass Spectrom.*, 6 (1979) 460.
16 S. E. Jacobsson, S. Jönsson, C. Lindberg and L. A. Svensson, *Biomed. Mass Spectrom.*, 7 (1980) 265.
17 K. Matsumura, O. Kubo, T. Tsukada, K. Nishide, H. Kato, K. Watanabe and M. Hirobe, *J. Chromatogr.*, 230 (1982) 148.
18 H. Kamimura, H. Sasaki, S. Higuchi and Y. Shiobara, *J. Chromatogr.*, 229 (1982) 337.
19 J. G. Leferink, J. Dankers and R. A. A. Maes, *J. Chromatogr.*, 229 (1982) 217.
20 R. J. N. Tanner, L E. Martin and J. Oxford, *Anal. Proc.*, 20 (1983) 38.
21 J. G. Leferink, T. A. Baillie and C. Lindberg, *Eur. J. Resp. Dis.*, 35 (1984) 25.
22 M. L. Powell, M. Weisberger, R. Gural, M. Chung, J. E. Patrick, E. Radwanski and S. S. Symchowicz, *J. Pharm. Sci.*, 74 (1985) 217.
23 J. Bress, A. M. Clauzel, H. Rachmat, B. Martinot, J. Dupouy, F. Bressolle and G. Doucet, *J. Pharm. Clin.*, 4 (1985) 109.

24 L. M. R. Thienpont, P. G. Verhaeghe and P. de Leenher, *Biomed. Mass Spectrom.*, 14 (1987) 613.
25 I. Yamamoto and K. Iwata, *J. Immunoassay*, 3 (1982) 155.
26 J. Girault, M. A. Lefebvre, I. Ingrand, A. Mignot and J. B. Fourtillan, paper presented at the *Sixth International Symposium on Mass Spectrometry in Life Sciences, Ghent, 1986.*
27 J. Girault, *Thèse de Doctorat d'État es Sciences Pharmaceutiques*, Poitiers, 1986.
28 J. Girault, B. Istin and J. B. Fourtillan, *Biomed. Environ. Mass Spectrom.*, 19 (1990) 88.
29 J. Girault and J. B. Fourtillan, *Biomed. Mass Spectrom.*, 17 (1988) 443.
30 *Statistique Appliquée à l'Exploitation des Mesures*, Masson, Paris, 1978.
31 J. B. Fourtillan, J. Girault, M. A. Lefebvre, S. Bouquet and P. Courtois, paper presented at the *Symposium Bronches et Sympathomimetiques, La Grande Motte, 1984.*
32 M. C. Saux, J. Girault, S. Bouquet, J. B. Fourtillan and P. Courtois, *J. Pharmacol.*, 17 (1986) 150.

Journal of Chromatography, 518 (1990) 53–58
Elsevier Science Publishers B.V., Amsterdam

CHROM. 22 573

Determination of gas chromatographic plate heights for hydrocarbon adsorption by superactivated carbon AX21

P. J. M. CARROTT*
Departamento de Química, Faculdade de Ciências, Universidade de Lisboa, Rua da Escola Politécnica 58, 1200 Lisbon (Portugal)
and
K. S. W. SING
Department of Chemistry, Brunel University, Uxbridge, Middlesex UB8 3PH (U.K.)
(Received March 13th, 1990)

ABSTRACT

Values of the height equivalent to a theoretical plate (HETP) were determined for the adsorption of several hydrocarbons by the petroleum pitch-based superactivated carbon AX21 over the temperature range 90–120°C. It was found that the HETP values were independent of both the adsorptive and the temperature of measurement. This surprising result is interpreted in terms of a very high degree of interconnectivity of the micropore structure of AX21. It is also concluded that considerable caution is required in interpreting micropore diffusivities determined from gas chromatographic measurements.

INTRODUCTION

Gas chromatography (GC) can provide a convenient and effective technique for the study of the physical adsorption of gases by microporous solids [1], provided that certain conditions are fulfilled. For instance, it is important to ensure that all contributions to band spreading arising from sources other than adsorption itself are minimized. As part of the (unpublished) preliminaries to our previous work [2–4], this was checked by making use of the well known Van Deemter equation [5]:

$$h = A + B/\bar{u} + C\bar{u} \tag{1}$$

where h is the height equivalent to a theoretical plate (HETP), defined as the peak variance per unit column length [6], and $\bar{u}$ is the linear velocity of the carrier gas. The coefficients A, B and C account for eddy diffusion, molecular diffusion and resistance to mass transfer, respectively [7]. Ideally, GC measurements at infinite dilution should be made at flow-rates corresponding to the minimum in the Van Deemter plot.

For most of the adsorbents that we studied previously, the HETP values were found to vary with flow-rate, column temperature and molecular weight of the adsorptive in the expected manner [1,7,8]. The most notable exception was the

0021-9673/90/$03.50

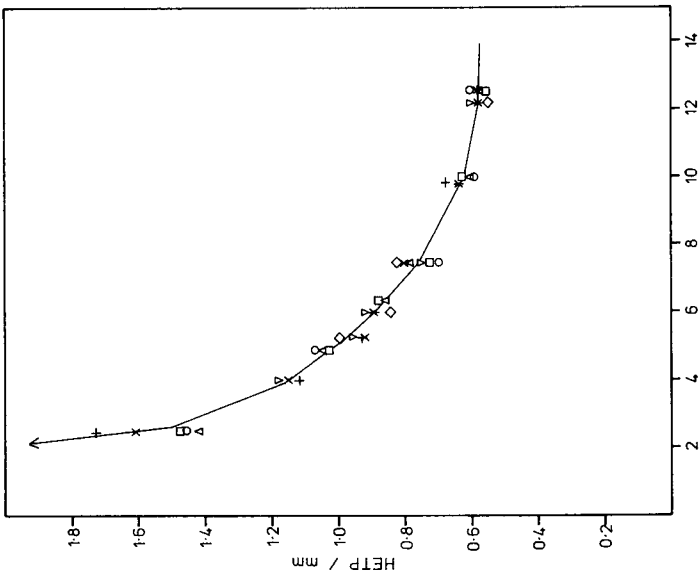

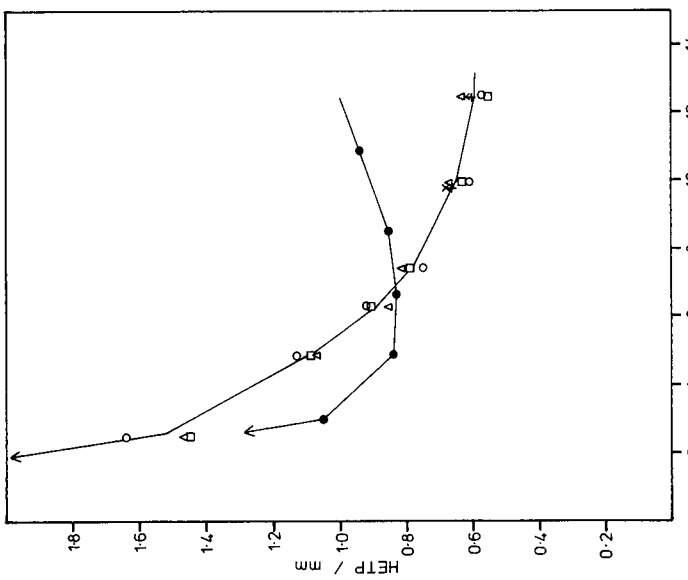

Fig. 1. Variation of HETP with linear carrier gas velocity, $\bar{u}$, for Carbosieve and AX21 at 150°C. ○ = Ethane; □ = propane; △ = butane; + = isobutane; × = neopentane; ● = methane on Carbosieve.

Fig. 2. Variation of HETP with linear carrier gas velocity, $\bar{u}$, for AX21 at 210°C. ○ = Ethane; □ = propane; △ = butane; ▽ = pentane; ◇ = hexane; + = isobutane; × = neopentane; * = cyclohexane.

superactivated carbon AX21, for which the more detailed results given here were subsequently obtained.

EXPERIMENTAL

GC measurements were made using a Perkin-Elmer Model 8310 gas chromatograph fitted with a flame ionization detector. The carrier gas was helium at flow-rates of 10–50 cm^3 (STP) min^{-1}. Measurements were made mainly over the temperature range 90–210°C. More complete details of the experimental procedure were given previously [3,4]. Linear carrier gas velocities were calculated from [7]

$$\bar{u} = L/t_m \tag{2}$$

where L is the column length and t_m the gas hold-up time (determined using hydrogen). The HETP was calculated from [7]

$$h = (L/5.545)/(d/z)^2 \tag{3}$$

where d is the peak width at half-height and z is the distance to the peak maximum.

The adsorbent AX21 is a petroleum pitch-based active carbon of exceptionally high adsorption capacity manufactured by Anderson Development (Adrian, MI, U.S.A.). Its micropore volume is 1.5 cm^3g^{-1} contained in pores of width up to 2 nm [9,10]. For purposes of comparison, some results are also presented for chromatographic measurements carried out using Carbosieve, which is a polymer-based molecular sieve carbon manufactured by Supelco (Bellefonte, PA, U.S.A.) and supplied by Bioscan (Canvey Island, U.K.). Its micropore volume is 0.43 cm^3g^{-1} contained predominantly in pores of width <0.8 nm [9,10].

The chromatographic columns were made from 2 mm I.D. aluminium tubing of length 30 cm for AX21 and 29 cm for Carbosieve. The particle size and weight of adsorbent in the column were 210–360 μm and 0.6091 g for AX21 and 105–125 μm and 0.7769 g for Carbosieve.

RESULTS

Van Deemter plots for the adsorption of eight saturated hydrocarbons by AX21 at column temperatures of 150 and 210°C are shown in Figs. 1 and 2. Also shown in Fig. 1 are results obtained for the adsorption of methane by Carbosieve. The latter are in accordance with the general form of eqn. 1: as $\bar{u}$ is increased the HETP initially decreases fairly rapidly, reaches a minimum and then begins to increase again at higher flow-rates. On the other hand, it is evident that, under the conditions of the experiments carried out using AX21, only part of the curve, corresponding to the terms in A and B, was determined. The most remarkable feature of the Van Deemter plots for AX21 shown in Figs. 1 and 2, and also those obtained at other column temperatures, is that they appear to be independent of both the adsorptive and the temperature of measurement.

HETP values for AX21, averaged over all temperatures, are plotted as a function of $1/\bar{u}$ in Fig. 3. Also indicated is the spread of values obtained at different

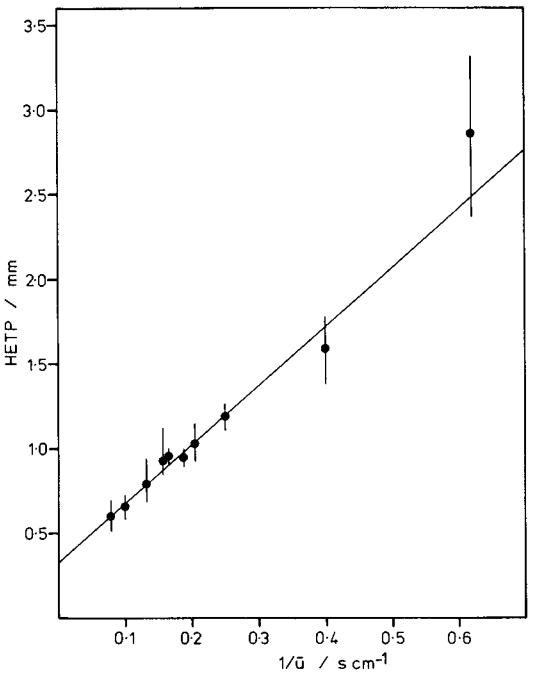

Fig. 3. Variation of HETP with reciprocal of linear carrier gas velocity, $1/\bar{u}$, for AX21 at temperatures between 90 and 210°C and for all adsorptives studied. The spread of HETP values at each temperature is indicated.

temperatures. At $1/\bar{u} = 0.62$ s cm^{-1} (corresponding to $\bar{u} = 1.61$ cm s^{-1} and off-scale on Figs. 1 and 2), the HETP value tends to decrease as the molecular weight of the adsorptive increases, which would be expected if gas-phase diffusion was making a significant contribution to band spreading [7,8]. At higher flow-rates, however, the spread of HETP values at each value of $1/\bar{u}$ appears to arise solely as a result of experimental uncertainty.

If the term in C in eqn. 1 is neglected, an estimate of the values of A and B can be obtained from the intercept and slope of the straight line drawn in Fig. 3. The results obtained are $A = 0.32$ mm and $B = 0.35$ cm^2 s^{-1}. Typical values for A reported in the

TABLE I

LIMITING ISOSTERIC HEATS OF ADSORPTION, q_0^{st}, OF HYDROCARBONS BY AX21

Adsorptive	q_0^{st} (kJ mol^{-1})	Adsorptive	q_0^{st} (kJ mol^{-1})
Ethane	28	Isobutane	49
Propane	39	Neopentane	57
Butane	52	Cyclohexane	66
Pentane	63		
Hexane	75		

literature [1,7,8,11,12] are 1–2 mm. The lower value obtained here is consistent with the very low HETP values observed at all flow-rates.

Specific retention volumes were calculated from the data in the manner described previously [2–4] and were found to be independent of the flow-rate and the amount of adsorptive injected. The plots of $\ln V_g$ *vs.* $1/T$ were found to be linear and, from the slopes of the plots, the limiting isosteric heats of adsorption given in Table I were determined.

DISCUSSION

The most remarkable feature of the results is that the HETP values for AX21 appear to be independent of both the adsorptive and the temperature. This indicates that the adsorptive molecules cannot have spent much time in the gas phase and that adsorption must therefore have occurred extremely rapidly. It might be thought that the results also indicate that molecular diffusion through the micropore structure was very rapid. However, in view of the magnitude of the heats of adsorption given in Table I, it is likely that this interpretation is oversimplified.

Previous work [3,9,10] has shown that although a high proportion of the micropores of AX21 are of width between 1 and 2 nm, there are also present a significant number of narrower micropores. Little, if any, enhancement in the heat of adsorption would be expected in the wider micropores [13] and it therefore seems reasonable to assume that diffusion of molecules through these pores could occur rapidly. In narrow micropores, on the other hand, it is well known that the heat of adsorption will be enhanced [3,4,11,13,14] and, further, that elevated temperatures will generally be required to bring about complete desorption of higher molecular weight adsorptives such as neopentane or nonane [15]. Hence, even at the comparatively high temperatures used here, some restriction on the mobility of the adsorbed molecules might have been expected. It is not possible to state with certainty the reason why this effect was not detected by our GC measurements. However, it is possible that the absence of this effect may arise, in part, as a result of a very high degree of interconnectivity of the micropore structure of AX21.

Results obtained using, for example, porous silicas [1], have shown that a decrease in particle size affects the Van Deemter plot in the following ways: HETP values decrease; curves for different adsorptives come closer together; the minimum shifts to higher $\bar{u}$; and the plot tends to become flat, or nearly so, at high $\bar{u}$. Complementary results have also been obtained with, for example, steam-activated coconut shell charcoals [11]. The origin of these changes lies in an increase in the accessibility of the internal pore structure as the particles become smaller [1]. Our results for AX21 may represent a limiting case in which the combination of small particle size and a high intrinsic degree of interconnectivity result in the whole of the pore structure being freely accessible.

If this is so, then adsorption ought to occur readily in those micropores which give the highest isostetic heat of adsorption, q_0^{st}. Bearing in mind that the enhancement in q_0^{st}, in comparison with that obtained on a non-porous surface, depends on the ratio of micropore width to molecular diameter [13], it follows that adsorptive molecules of different size will tend to adsorb preferentially in slightly different parts of the micropore structure. This argument supports previous conclusions [3] that the results

of GC measurements carried out at infinite dilution are not representative of the entire micropore structure, but are weighted in favour of certain groups of pores (or possibly certain active sites, in the case of specific physisorption [4]). One corollary of this is that considerable caution is required in interpreting diffusivities obtained from, for example, the coefficients of the Van Deemter equation.

ACKNOWLEDGEMENT

The Procurement Executive, Ministry of Defence, U.K., is thanked for the provision of research contracts under which this work was carried out.

REFERENCES

1 A. V. Kiselev, *Adv. Chromatogr.*, 4 (1967) 113.
2 P. J. M. Carrott and K. S. M. Sing, *Chem. Ind. (London)*, (1986) 360.
3 P. J. M. Carrott and K. S. W. Sing, *J. Chromatogr.*, 406 (1987) 139.
4 P. J. M. Carrott, M. Brotas de Carvalho and K. S. W. Sing, *Adsorption Sci. Technol.*, 6 (1989) 93.
5 J. J. Van Deemter, F. J. Zuiderweg and A. Klinkenberg, *Chem. Eng. Sci.*, 5 (1956) 271.
6 M. J. P. Martin and R. L. M. Synge, *Biochemistry*, 35 (1941) 1359.
7 J. R. Conder and C. L. Young, *Physicochemical Measurement by Gas Chromatography*, Wiley, Chichester, 1979.
8 T. Paryjczak, *Gas Chromatography in Adsorption and Catalysis*, Ellis Horwood, Chichester, 1986.
9 P. J. M. Carrott, R. A. Roberts and K. S. W. Sing, *Carbon*, 25 (1987) 59.
10 P. J. M. Carrott, R. A. Roberts and K. S. W. Sing, in K. K. Unger, J. Rouquerol, K. S. W. Sing and H. Kral (Editors), *Characterization of Porous Solids*, Elsevier, Amsterdam, 1988, p. 89.
11 H. W. Habgood and J. F. Hanlan, *Can. J. Chem.*, 37 (1959) 843.
12 D. M. Ruthven, *Principles of Adsorption and Adsorption Processes*, Wiley, New York, 1984.
13 D. H. Everett and J. C. Powl, *J. Chem. Soc., Faraday Trans. I*, 72 (1976) 619.
14 D. Atkinson, P. J. M. Carrott, Y. Grillet, J. Rouquerol and K. S. W. Sing, in A. I. Liapis (Editor), *Fundamentals of Adsorption*, Engineering Foundation, New York, 1987, p. 89.
15 P. J. M. Carrott, F. C. Drummond, M. B. Kenny, R. A. Roberts and K. S. W. Sing, *Colloids Surf.*, 37 (1989) 1.

Journal of Chromatography, 518 (1990) 59–67
Elsevier Science Publishers B.V., Amsterdam

CHROM. 22 574

Gas chromatographic determination of phenol compounds with automatic continuous extraction and derivatization

E. BALLESTEROS, M. GALLEGO and M. VALCÁRCEL*
Department of Analytical Chemistry, Faculty of Sciences, University of Córdoba, Córdoba 14004 (Spain)
(Received January 12th, 1990)

ABSTRACT

Two gas chromatographic procedures for the determination of a variety of substituted phenols in water samples are described. The phenols were extracted or extracted–derivatized by using a continuous liquid–liquid extraction–derivatizaton system and quantified with flame ionization detection. Ethyl acetate was found to be the most efficient solvent for phenols whereas *n*-hexane yielded essentially the same recoveries for derivatized phenols. Between 0.1 and 300 mg/l of the different phenols can be detected with a relative standard deviation 1.1 and 3.7%. The acetate esters of six phenols were formed by the direct addition of acetic anhydride to the organic extractant. The stable acetate esters thus formed were isolated by using a standard dimethyl polysiloxane gas chromatographic column.

INTRODUCTION

Phenol compounds enter the environment in various ways: directly, as industrial effluents, and indirectly, as conversion products from natural and synthetic chemicals, including pesticides. These compounds, and particularly chlorophenols, possess odour and taste-spoiling properties [1–4] which makes it desirable to establish their concentration levels in the environment. Methods for the determination of trace phenol pollutants in aqueous samples generally include an extraction and/or concentration step prior to their separation and quantification by gas chromatography. The concentration step in most commonly accomplished by direct solvent extraction [5–13] or by adsorption and subsequent elution [14–16]. Because of the high polarity and low vapour pressure of phenols, a derivatization step is often used in their analysis to improve the chromatographic performance and, occassionally, more efficient extraction from aqueous samples. Reagents such as 1-fluoro-2,4-dinitrobenzene [17,18], heptafluorobutyrylimidazole [19], diazomethane [20], silanizing agents [21–24], pentafluorobenzoyl derivatives [25,26] and acetic anhydride [26,27–33] have been employed for this purpose. However, derivatization has some drawbacks such as the additional errors that it introduces. Sterically hindered phenols may react incompletely and partial decomposition of derivatives may occur during their storage. Moreover, many reagents used for derivatization are toxic, carcinogenic or explosive [34,35].

0021-9673/90/$03.50

Flow-injection techniques have also been employed for the determination of phenols. Thus, phenol was analysed for in waters by using liquid dialysis for isolation prior to its photometric detection [36]. The standard photometric 4-aminoantipyrine method has been automated for the determination of pentachlorophenol from conventional and stopped-flow measurements [37]. Electrochemical techniques have also frequently been used with flow systems for the determination of phenolic compounds [38–40].

The only method using a modified steam-distillation extraction device for the continuous extraction and preconcentration of phenol, *o*-, *m*- and *p*-cresols and 2,6-, 2,5-, 3,5-, 2,3- and 3,4-xylenols was reported by Curvers *et al.* [41]. Subsequent analysis was carried out by gas chromatography on a instrument equipped with a glass capillary column coated with OV-1 with helium as carrier gas. The relative standard deviation was 3% for ethyl acetate extractant.

The aim of this study was to overcome the drawbacks posed by operations preceding sample introduction in gas chromatography (GC) (*e.g.*, decrease sample manipulations, prevent solvents and derivatizing reagents from coming into contact with air and the operator). This was accomplished by using a continuous liquid–liquid extractor allowing the simultaneous extraction and derivatization of various phenolic compounds. By optimizing all the experimental variables involved in the system a method was developed that combines the efficiency of extraction and the sensitivity and selectivity of GC. The performance of the continuous extraction–derivatization system was studied by using phenols, cresols and chlorophenols. The acetate esters of six phenol compounds were obtained by adding acetic anhydride to the *n*-hexane extractant used.

EXPERIMENTAL

Apparatus

A Hewlett-Packard 5890 A gas chromatograph furnished with a flame ionization detector was used. Chromatographic assays were performed on a 10 m × 0.53 mm I.D. dimethyl polysiloxane (film thickness 2.65 μm) coated fused-silica column obtained from Hewlett-Packard (HP-1). Nitrogen was used as the carrier gas (44 ml/min). The temperature of the injector was 150°C and the detector was kept at 250°C. The oven was kept at either 60°C for 2 min and then increased at 10°C/min to 150°C (2 min), or at 45°C for 5 min and then increased at 5°C/min to 150°C (2 min) for separation of phenols or acetate phenols, respectively. The injected sample volume was 2 μl and peak areas were measured by using a Hewlett-Packard 3392 A integrator. The flow extraction–derivatization system consisted of a peristaltic pump (Gilson Minipuls-2), an A-10T solvent segmenter (Tecator) and a custom-made phase separator with a Fluoropore membrane (1.0 μm pore size, FALP; Millipore) as described elsewhere [42]. Poly(vinyl chloride) and Solvaflex pumping tubes for aqueous and organic solutions, respectively, and Teflon tubing for the coils were used. A thermostated water-bath was also used.

Standards and reagents

Phenol, 3,4-dimethylphenol, 2-*tert.*-butylphenol, 2-*tert.*-butyl-4-methylphenol and naphthalene (internal standard) were obtained from Aldrich. All other phenols

and reagents used (*o*-cresol, *m*-cresol, 2-chlorophenol, 4-chlorophenol, acetic anhydride, ethyl acetate, toluene, *n*-hexane, sodium hydrogencarbonate and sodium sulphate) were obtained from Merck.

Preparation of samples and reagents solutions

Stock standard solutions of phenol, 3,4-dimethylphenol, 2-*tert.*-butylphenol, 2-*tert.*-butyl-4-methylphenol, *o*- and *m*-cresol and 2- and 4-chlorophenol were prepared at a concentration of 1 g/l in 95% ethanol and stored in glass-stoppered bottles at 4°C.

For extraction, appropriate amounts of each stock solution were further diluted with distilled water to prepare 25 ml of solutions containing between 0.1 and 300 mg/l of each phenol (phenol, 3,4-dimethylphenol, 2-*tert.*-butylphenol and 2-*tert.*-butyl-4-methylphenol); the extractant consisted ethyl acetate containing 300 mg/l of naphthalene as internal standard.

For extraction and derivatization, appropriate amounts of each stock solution (phenol, 3,4-dimethylphenol, *o*-cresol, *m*-cresol, 2-chlorophenol and 4-chlorophenol) and 0.5 ml 2 *M* sodium hydrogencarbonate were added to 25-ml calibrated flasks and diluted with distilled water to prepare solutions containing 0.2–300 mg/l of each phenol compound in 0.04 *M* sodium hydrogencarbonate (pH 8.5). The extractant was *n*-hexane containing 300 mg/l of naphthalene (internal standard) and 6% (v/v) acetic anhydride (derivatization reagent).

Procedure

The manifold employed in depicted in Fig. 1. The sample solution was pumped continuously into the system and merged with a stream of ethyl acetate (for extraction only) or *n*-hexane (for simultaneous extraction and derivatization). The extraction (and derivatization) process took place in the extraction coil and the organic phase was isolated in the membrane phase separator. The ethyl acetate or *n*-hexane extracts of underivatized phenols or acetate derivatives, respectively, was collected in a 4-ml glass vial, containing anhydrous sodium sulphate as a desiccant, from which 2-μl portions were extracted with syringes and introduced into the chromatograph. Although the acetate esters were volatile, nothing was lost in their transfer to the chromatograph.

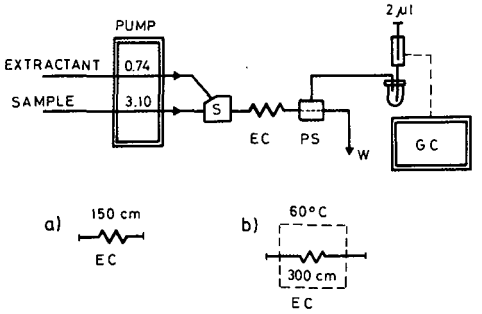

Fig. 1. Manifold for the chromatographic determination of underivatized or derivatized phenols. All tubes are made of Teflon (0.5 mm I.D.). S, solvent segmenter; EC, extraction coil, (a) for extraction and (b) for extraction and derivatization; PS, phase separator; W, waste. Flow-rates are given in ml/min.

TABLE I

RECOVERY (%) OF PHENOLS

Extractant: (A) for underivatized phenols; (B) extractant containing 6% (v/v) acetic anhydride for derivatization.

Compound	Ethyl acetate		Toluene		*n*-Hexane	
	A	B	A	B	A	B
Phenol	65.1	60.4	39.4	40.1	8.1	70.2
3,4-Dimethylphenol	76.2	70.2	80.1	75.1	18.3	75.4
2-*tert.*-Butylphenol	78.0	–	80.0	–	75.0	–
2-*tert.*-Butyl-4-methylphenol	56.9	–	55.6	–	61.2	–
o-Cresol	–	66.2	–	70.2	–	80.1
m-Cresol	–	58.4	–	76.4	–	78.9
2-Chlorophenol	–	65.1	–	66.2	–	69.5
4-Chlorophenol	–	55.8	–	70.5	–	77.8

RESULTS AND DISCUSSION

Ethyl acetate was found to be the most efficient extraction solvent for underivatized phenols, followed by toluene and *n*-hexane. Simultaneous acylation with acetic anhydride and extraction with *n*-hexane was comparable to the use of ethyl acetate alone in efficiency (Table I). The recoveries of phenol compounds was never higher than 80% because the extraction efficiencies in continuous extraction systems usually range between 70 and 80%, as chemical equilibrium is never reached; however, the recoveries were always reproducible. The recoveries listed in Table I were calculated by dividing the peak areas obtained in the continuous extraction mode into the corresponding peak area obtained by dissolving each phenol in its respective solvent at the same concentration. The conversion of the phenols to their corresponding esters yielded better GC peak symmetry than underivatized compounds and also allowed phenols, cresols and chlorophenols to be sequentially isolated (the bands of the underivatized phenols are usually overlapped).

Continuous extraction of underivatized phenols

Optimization of the method. For this study, a sample solution containing 30 mg/l of each phenol compound (phenol, 3,4-dimethylphenol, 2-*tert.*-butylphenol and 2-*tert.*-butyl-4-methylphenol) was prepared in distilled water. The extractant was ethyl acetate containing 300 mg/l of naphthalene as internal standard.

The effect of the sample pH was studied in the range 2–10; it was found to have no effect on the signals in the range 2–8. Above pH 8, the signals decreased owing to the formation of the corresponding phenolates, which decreased the phenol concentration. The ionic strength, adjusted with potassium nitrate, did not affect the signal up to 1 *M*.

The flow-rates of the aqueous and organic phases were also optimized. Fig. 2A shows the effect of the sample flow-rate at a constant flow-rate of ethyl acetate. Higher sample flow-rates resulted in greater peak areas owing to the increased preconcentra-

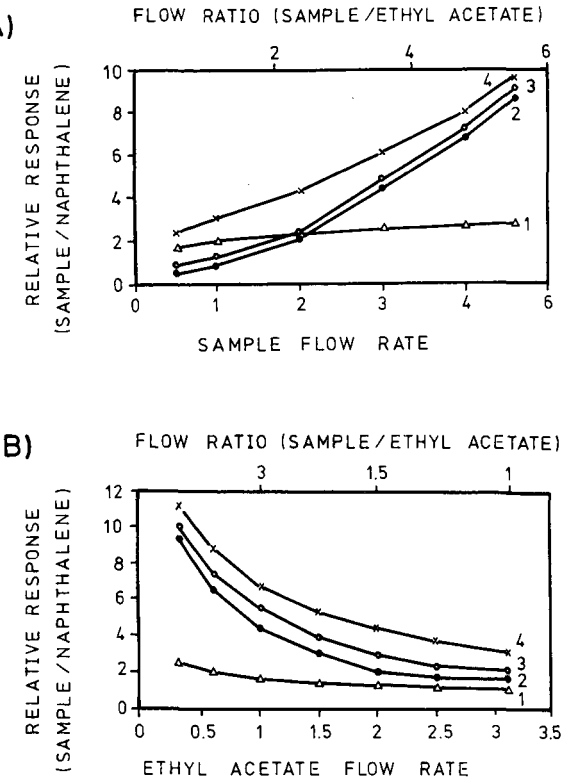

Fig. 2. Effect of (A) sample flow-rate (organic phase flow-rate = 0.84 ml/min) and (B) organic flow-rate (sample flow-rate = 3.1 ml/min). 1 = Phenol; 2 = 2-*tert.*-butylphenol; 3 = 2-*tert.*-butyl-4-methylphenol; 4 = 3,4-dimethylphenol. For GC conditions, see text.

tion ratio. The phenol signals remained virtually constant because of a potential mutual compensation of factors: increased signal from an increased preconcentration factor and decreased signal from decreased contact time between phases resulting from a decreased residence time of the analyte arising from increased flow-rates. Fig. 2B shows the variation of the signals as a function of the flow-rate of the organic phase. As expected, the peak area increased with decreasing organic phase flow-rate. Again, the phenol was the compound least affected by this variable. A sample flow-rate of 3.1 ml/min and an ethyl acetate flow-rate of 0.74 ml/min were chosen, taking into account the mutual influence of reproducibility, concentration ratio and sampling frequency. The influence of the residence time was also studied by varying the length of the extraction coil between 50 and 300 cm; the peak area was not affected by this variable. A length of 150 cm was therefore selected, which yielded a residence time of 5 s.

Calibration graphs for the underivatized phenols. The calibration graphs obtained by plotting the ratio of analyte peak area/internal standard peak area *versus* the analyte concentration in the aqueous medium were reproducible and linear over the range tested (0.1–300 mg/l). The features of these graphs and those of the analytical

TABLE II

FEATURES OF THE CALIBRATION GRAPHS AND DETERMINATION OF UNDERIVATIZED PHENOLS

Compound	Regression equation[a]	r[b]	Linear range (mg/l)	Detection limit (mg/l)	Relative standard deviation (%)
Phenol	$A = 7.80 \cdot 10^{-3} X + 2.23 \cdot 10^{-4}$	0.9992	0.2–3	0.15	2.81
3,4-Dimethylphenol	$A = 8.66 \cdot 10^{-3} X + 1.19 \cdot 10^{-3}$	0.9993	0.3–3	0.20	3.56
2-*tert.*-Butylphenol	$A = 9.16 \cdot 10^{-3} X + 1.21 \cdot 10^{-3}$	0.9994	0.1–3	0.10	3.53
2-*tert.*-Butyl-4-methylphenol	$A = 6.82 \cdot 10^{-3} X - 1.90 \cdot 10^{-4}$	0.9994	0.1–3	0.10	3.32
Phenol	$A = 6.58 \cdot 10^{-3} X + 2.20 \cdot 10^{-3}$	0.9996			1.82
3,4-Dimethylphenol	$A = 6.81 \cdot 10^{-3} X + 5.46 \cdot 10^{-3}$	0.9996	3 –30		2.24
2-*tert.*-Butylphenol	$A = 4.96 \cdot 10^{-3} X + 1.11 \cdot 10^{-2}$	0.9995			2.44
2-*tert.*-Butyl-4-methylphenol	$A = 5.42 \cdot 10^{-3} X + 5.06 \cdot 10^{-3}$	0.9995			2.62
Phenol	$A = 7.93 \cdot 10^{-3} X - 1.18 \cdot 10^{-2}$	0.9997			1.11
3,4-Dimethylphenol	$A = 8.92 \cdot 10^{-3} X - 2.52 \cdot 10^{-4}$	0.9997	30 –300		1.55
2-*tert.*-Butylphenol	$A = 7.53 \cdot 10^{-3} X - 8.63 \cdot 10^{-4}$	0.9997			1.75
2-*tert.*-Butyl-4-methylphenol	$A = 7.44 \cdot 10^{-3} X - 7.88 \cdot 10^{-3}$	0.9996			2.05

[a] A = analyte peak area/internal standard peak area ratio; X = concentration in mg/l.
[b] r= Correlation coefficient.

procedure are summarized in Table II at three integrator sensitivities. The practical detection limit was calculated as the concentration yielding the minimum detectable signal in the chromatogram. The relative standard deviation was checked on eleven samples containing 1, 15 or 35 mg/l of each phenolic compound in the linear range assayed, 0.2–3, 3–30 and 30–300 mg/l, respectively.

Simultaneous extraction and derivatization of phenol compounds

The proposed method for the continuous extraction and GC determination of phenolic compounds allows the isolation and identification of the four phenols assayed; however, if the samples also contain cresols and/or chlorophenols, their separation is not sequential and the chromatogram contains overlapped peaks. The conversion of the phenols, cresols and chlorophenols to their corresponding esters simultaneously with extraction into *n*-hexane ostensibly improved the chromatographic resolution.

Optimization of the method. First we studied the optimum pH for the derivatization reaction. For this purpose, two aqueous phenolic solutions of 30 mg/l of each phenol (phenol, 3,4-dimethylphenol, *o*-cresol, *m*-cresol, 2-chlorophenol and 4-chlorophenol) at a final pH of 3 or 8.5 were prepared. The extractant was *n*-hexane containing 300 mg/l of naphthalene and 6% acetic anhydride.

The yields of the acetate derivatives of the phenols obtained from an acidified water sample (pH 3) was lower than those obtained with an alkaline water sample (pH 8.5), thus indicating that acylation with acetic anhydride proceeded far more rapidly on the phenolate ions than on the undissociated compounds. The acetylation yields were not influenced by the hydrogencarbonate concentration over the range 0.03–0.05 *M*. For continuous derivatization–extraction, the aqueous samples were

prepared in 0.04 *M* sodium hydrogencarbonate solution (pH 8.5). The influence of the ionic strength on the aqueous samples (adjusted with potassium nitrate) was also tested; it had no effect up to a concentration of 1 *M* (similarly to the extraction of the underivatized phenols).

To study the influence of the concentration of acetic anhydride on the yield of acetate derivatives, several solutions in the range 0.2–7% in *n*-hexane were prepared. A 4% solution of the organic reagent was found to be sufficient for maximum response; lower concentrations resulted in incomplete derivatization and thus in the co-occurrence of peaks from the underivatized and derivatized phenols in the chromatogram. The relative response (sample/naphthalene) remained constant at higher concentrations. A 6% content of acetic anhydride in *n*-hexane was selected as extractant for routine analyses.

In manual procedures, the derivatization of phenolic compounds is favoured by heating [30] as it is in the continuous mode. The effect of temperature was studied in the range 20–75°C; the yield of the derivatization reaction was optimum above 40°C, below which the chromatogram obtained showed peaks corresponding to the underivatized phenols and esters. Fig. 3 shows the influence of temperature on the derivatization process for four phenolic compounds; the cresols assayed behaved similarly. The extraction coil was kept at 60°C by using a thermostated water-bath.

The influence of the extraction–derivatization coil length was investigated in the range 50–500 cm. Above 150 cm the signal remained virtually constant. There is a difference with the continuous method with extraction only (where this variable has no effect) as it requires some time for the esters to be formed. A thermostated (60°C) reaction coil of length 300 cm, which resulted in a residence time of 9 s, was chosen.

Determination of phenols, cresols and chlorophenols. The GC separation of the underivatized and acetylated phenols is illustrated in Fig. 4A and B, respectively. As can be seen, the peaks of the underivatized phenols and chlorophenols extracted into *n*-hexane are completely overlapped. In the manual preparation of esters of phenols, several workers have claimed [43] that the excess of anhydride must be removed prior to GC. As shown in Fig. 4B, excess of acetic anhydride did not interfere with the quantification of the derivatives, and thus need not be removed.

The calibration graphs for the acetic anhydride derivatives of phenol, 3,4-di-

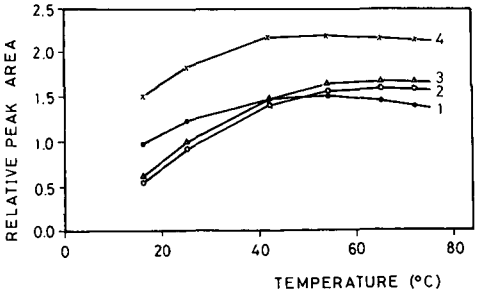

Fig. 3. Influence of temperature on the derivatization reaction. 1 = 2-Chlorophenyl acetate; 2 = 3,4-dimethylphenyl acetate; 3 = phenyl acetate; 4 = 4-chlorophenyl acetate. Extractant: *n*-hexane containing 6% acetic anhydride.

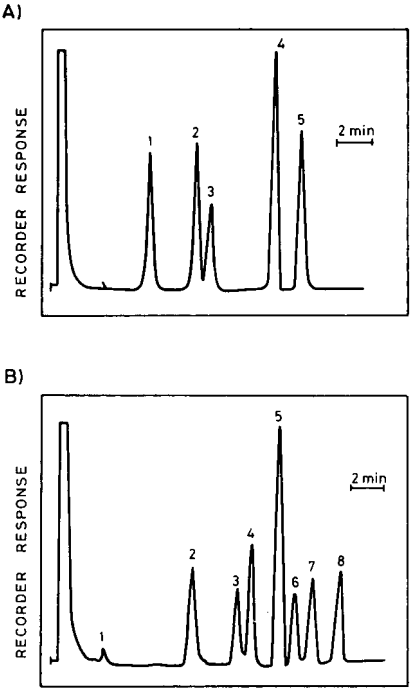

Fig. 4. (A) Gas chromatogram of underivatized phenols. Peaks: 1 = phenol + *o*-cresol; 2 = *m*-cresol; 3 = 2-chlorophenol; 4 = naphthalene; 5 = 3,4-dimethylphenol + 4-chlorophenol. (B) Gas chromatogram of acetate derivatives. Peaks: 1 = acetic anhydride; 2 = phenyl acetate; 3 = *o*-cresyl acetate; 4 = *m*-cresyl acetate; 5 = naphthalene; 6 = 2-chlorophenyl acetate; 7 = 4-chlorophenyl acetate; 8 = 3,4-dimethylphenyl acetate. The extractant was *n*-hexane and the column temperature was 45°C for 5 min, increased to 150°C at 5°C/min and held at 150°C for 2 min.

methylphenol, *o*-cresol, *m*-cresol, 2-chlorophenol and 4-chlorophenol were linear at concentrations between 5 and 7500 μg in 25 ml of distilled water at pH 8.5. The relative standard deviation ranged between 1.5 and 3.5%.

CONCLUSIONS

Phenols are usually derivatized in order to improve their GC features or enhance their extractability from aqueous solutions. However, the manual procedures used for this purpose are lengthy and require several steps, which gives rise to losses and low reproducibility; on the other hand, the method proposed here permits the direct acetylation of the aqueous test solution simultaneously with the extraction in a single step.

The two continuous methods proposed here for the extraction and extraction–derivatization of phenols feature all the inherent advantages of automatic methods (*viz.*, low sample and reagent consumption, minimal manipulation and contact with the reagents, accurate and reproducible results, high sampling frequencies, etc.). These automatic methods allow the derivatization and extraction of phenol compounds with

a sampling frequency of $35 \pm 5\ h^{-1}$. Such a high rate, however, is limited by the oven temperature programming.

ACKNOWLEDGEMENT

This work was financially supported by the Spanish CICYT (Grant No. PA86-0146).

REFERENCES

1 A. L. Buikema, M. J. McGinniss and J. Cairns, *Mar. Environ. Res.*, 2 (1979) 87.
2 Lawrence Berkeley Laboratory Environmental Instrumentation Survey, *Instrumentation for Environmental Monitoring*, Vol. 2, 2nd ed., Wiley, New York, 1986, pp. 497–532.
3 I. H. Suffet and M. Malaiyandi (Editors), *Organic Pollutants in Water. Sampling, Analysis and Toxicity Testing*, American Chemical Society, Washington, DC, 1987.
4 R. A. Minear and L. Keith (Editors), *Water Analysis. Organic Species*, Vol. III, Academic Press, Orlando, 1984.
5 D. A. Kalman, *J. Chromatogr. Sci.*, 22 (1984) 452.
6 L. L. Needham, S. L. Head and R. E. Cline, *Anal. Lett.*, 17 (1984) 1555.
7 O. I. Kalchenko, V. O. Volovenko, K. I. Sakodynskii and V. P. Svitelskii, *J. Chromatogr.*, 364 (1986) 339.
8 H. Lohse, M. Heyer and J. Kunze, *Fresenius' Z. Anal. Chem.*, 328 (1987) 592.
9 Ya I. Korenman, A. T. Alymova and V. N. Fokin, *Zh. Anal. Khim.*, 43 (1988) 901.
10 Ya I. Korenman, V. A. Minasyants and V. N. Fokin, *Zh. Anal. Khim.*, 43 (1988) 1303.
11 C. N. Ong, B. L. Lee, H. Y. Ong and L. E. Heng, *J. Anal. Toxicol.*, 12 (1988) 159.
12 J. Krupcik, D. Repka, E. Benicka, T. Hevesi, J. Nolte, B. Paschold and H. Mayer, *J. Chromatogr.*, 448 (1988) 203.
13 M. M. Kopecni, M. V. Tarana, S. D. Cupic and J. J. Comor, *J. Chromatogr.*, 462 (1989) 392.
14 P. van Rossum and R. G. Webb, *J. Chromatogr.*, 150 (1978) 381.
15 A. Tateda and J. S. Fritz, *J. Chromatogr.*, 152 (1978) 329.
16 U. Knecht and H. J. Nitsch, *Fresenius' Z. Anal. Chem.*, 324 (1986) 142.
17 M. Lehtonen, *J. Chromatogr.*, 202 (1980) 413.
18 M. Lehtonen, *Chromatographia*, 16 (1982) 201.
19 L. L. Lamparski and T. J. Nestrick, *J. Chromatogr.*, 156 (1978) 143.
20 B. Zimmerli, T. Marschall and B. Marek, *Anal. Abstr.*, 39 (1980) 1D87.
21 H. Kieninger and D. Boeck, *Anal. Abstr.*, 34 (1978) 6F36.
22 L. Heinrich and W. Baltes, *Anal. Abstr.*, 50 (1988) 2F53.
23 A. R. Gholson, R. H. St. Louis and H. H. Hill, *J. Assoc. Off. Anal. Chem.*, 70 (1987) 897.
24 C. W. Ford and R. D. Hartley, *J. Chromatogr.*, 436 (1988) 484.
25 Y. Osaki and T. Matsueda, *Bunseki Kagaku*, 37 (1988) 253.
26 J. Hajslova, V. Kocourek, I. Zemanova, F. Pudil and J. Davidek, *J. Chromatogr.*, 439 (1988) 307.
27 W. Krijgsman and C. van de Kamp, *J. Chromatogr.*, 131 (1977) 412.
28 R. T. Coutts, E. E. Hargesheimer and F. M. Pasutto, *J. Chromatogr.*, 179 (1979) 291.
29 J. Knuutinem and I. O. Korhonen, *J. Chromatogr.*, 257 (1983) 127.
30 G. Bengtsson, *J. Chromatogr. Sci.*, 23 (1985) 397.
31 H. B. Lee, Y. D. Stokker and A. S. Chan, *J. Assoc. Anal. Chem.*, 70 (1987) 1003.
32 K. Takami, T. Okumura, H. Yamasaki and M. Nakamoto, *Bunseki Kagaku*, 37 (1988) 349.
33 F. A. Maris, G. J. De Jong, G. W. Somsen and V. A. T. Brinkman, *Chemosphere*, 17 (1988) 1301.
34 T. M. Shafik, H. C. Sullivan and H. F. Euos, *J. Agric. Food Chem.*, 21 (1973) 295.
35 E. Tesarova and V. Pacakova, *Chromatographia*, 17 (1983) 268.
36 J. Moller and M. Martin, *Fresenius' Z. Anal. Chem.*, 329 (1988) 728.
37 M. Rodriguez-Alcala, P. Yañez-Sedeño and L. M. Polo Diez, *Talanta*, 35 (1988) 601.
38 A. Trojanek and S. Bruckenstein, *Anal. Chem.*, 58 (1986) 983.
39 H. Yan, F. Li and Y. Li, *Fenxi Huaxue*, 14 (1986) 359.
40 F. Cañete, A. Rios, M. D. Luque de Castro and M. Valcárcel, *Anal. Chim. Acta*, 214 (1988) 375.
41 J. Curvers, T. Noij, C. Cramers and J. Rijks, *Chromatographia*, 19 (1984) 225.
42 M. Gallego, M. Silva and M. Valcárcel, *Anal. Chem.*, 58 (1986) 2269.
43 E. Ehrsson, T. Walle and H. Brotell, *Acta Pharm. Suec.*, 8 (1971) 319.

Journal of Chromatography, 518 (1990) 69–75
Elsevier Science Publishers B.V., Amsterdam

CHROM. 22 592

Effect of carbon dioxide flow-rate on the separation of triacylglycerols by capillary supercritical fluid chromatography

HEIKKI KALLIO* and PÄIVI LAAKSO
Department of Chemistry and Biochemistry, Laboratory of Food Chemistry, University of Turku, SF-20500 Turku 50 (Finland)
(First received February 9th, 1990; revised manuscript received May 28th, 1990)

ABSTRACT

Triacylglycerols (TAGs) were separated using capillary supercritical fluid chromatography at various carbon dioxide densities and flow-rates at 150°C. The flow-rate was controlled with integral restrictors made directly at the end of the column. With a 50 μm I.D., d_f 0.20 μm, DB-5 [(95%)dimethyl(5%) diphenylpolysiloxane] column, separation numbers (*Tz*) of up to one per one triacylglycerol carbon number difference per metre were achieved at a practical optimum carrier flow-rate at 0.3–0.4 cm/s. Height equivalent to an effective theoretical plate–average linear carrier velocity–triacylglycerol carbon number three-dimensional plots at different pressures are presented.

INTRODUCTION

Capillary supercritical fluid chromatography (SFC) is a method that is often compared with capillary gas–liquid chromatography (GLC) with regard to efficiency. In practice, GLC always gives a better resolution per unit time than does SFC. In many laboratories the slowness of the latter method has led to the use of high carrier flow-rates in order to increase the speed of the analyses [1]. However, this approach brings about a reduced number of effective chromatographic plates.

Capillary SFC is applied to the analysis of sensitive and labile natural compounds in order to avoid thermal decomposition. As a tool in bioscience fields such as food and clinical chemistry, all the resolution and selectivity that an optimized capillary SFC analysis can provide are usually required. This is the case even at the expense of an increased duration of the analyses. Another limitation to increasing the flow-rate is a reduction in sensitivity and ionization accuracy in mass spectrometric analyses. For this reason, high carrier flow-rates cannot be recommended.

Most calculations concerning the number of theoretical plates (n) and the height equivalent to a theoretical plate (HETP) in SFC follow the Golay equation for non-adjusted retention times [2,3]. The height equivalent to a plate is the length of the column occupied by one theoretical plate (HETP) or by one effective theoretical plate (HEETP). This definition is always of primary importance when comparing experimental results with those reported in the literature.

0021-9673/90/$03.50

The number of theoretical plates and the relative retentions of analyte mixtures in SFC are more difficult to predict according to theoretical definitions than in GLC. This is due in part to the solubility factor, which changes in relation to the density of the carrier fluid. The term "solubility" includes all the factors that affect the interactions between a solute and the mobile phase and is difficult to define accurately with a universal equation.

Increasing the carrier pressure at constant temperature results in a decrease in the k' values and resolution [4–6], even though the correlation is in practice never really smooth and regular, as was shown, *e.g.*, by Klesper [7] with naphthalene, anthracene, pyrene and chrysene with *n*-pentane as the mobile phase. At a constant pressure, k' has a maximum at a certain temperature. The shape of this curve can be explained on thermodynamic principles [8] and is independent of the mobile and stationary phases [9].

This optimization work was done to improve the mass spectrometric analysis of butter fat and fish oil triacylglycerols (TAGs). Electron impact mass spectrometry (EI-MS) in the single-ion monitoring (SIM) mode has been used in order to determine the level of unsaturation of TAGs having the same carbon numbers [10]. The main goal, however, was the determination of the positional isomers of the fatty acids in individual TAGs of natural origin. Flow-rates far above the optimum are not recommended because of the distinct decrease in sensitivity in the EI-MS analyses. For positional isomer analyses, sufficiently large α-values between the TAGs eluting close to each other are needed, although complete resolution is unnecessary. The minimum requirement is the possibility of discriminating the SIM signals of adjacent compounds from each other according to their different retentions.

The aim of this research was to optimize the size of the integral restrictor and the linear flow-rate of the supercritical carbon dioxide carrier at a constant temperature for the separation of triacylglycerols by capillary SFC using a flame ionization detector.

EXPERIMENTAL

Saturated monoacid triacylglycerols of even-numbered fatty acids from trioctanoylglycerol (3 × 8:0) to trioctadecanoylglycerol (3 × 18:0) were subjected to capillary SFC. The chromatographic system was as described previously [10]. The only difference was the 100-nl loop injector with a pneumatic helium actuator. The mobile phase was SFC-grade carbon dioxide. The column temperature was kept at 150°C and that of the detector at 320°C. The TAG samples dissolved in tricholoromethane were introduced into the fused-silica capillary column (DB-5, 3.8 m × 50 μm I.D., d_f 0.20 μm) (J&W Scientific) and a linear capillary split with a flow ratio of *ca.* 1:15 measured at a 24.1-MPa inlet pressure was used.

The carbon dioxide flow-rate was regulated with integral restrictors [11] attached directly to the end of the column. The mixture of the homologous series of TAGs was analysed at carrier inlet pressures of 24.1, 26.2, 28.3, 30.3, 32.4 and 34.4 MPa at least three times at each pressure. The analyses were carried out with seven restrictors of various sizes at each pressure. The restrictors resulted in average linear flow-rates of carbon dioxide varying from 0.34 to 1.70 cm/s at the highest column inlet pressure of 34.4 MPa.

The column hold-up time (t_0) was measured at the front slope of the solvent, trichloromethane. Overloading of the column with the solvent resulted in a t_0 value very close to the theoretical hold-up time.

RESULTS AND DISCUSSION

Optimization of the carrier flow-rate in order to reach the minimum height equivalent to a chromatographic plate was achieved by selecting the size and construction of the restrictor. The integral restrictors were attached directly to the end of the fused-silica capillary column, thus the evident dead volumes caused by the capillary–capillary connectors could be avoided. The extremely rapid pressure drop in the short restriction area also prevented the solutes from precipitating prior to the detector flame. Some clogging problems occurred, however, with very narrow pinholes yielding linear flow-rates less than the optimum on the van Deemter curve. The results presented in this paper concern conditions at and slightly above the optimum flow-rate.

All the analyses were performed isothermally at 150°C. This fairly low temperature was chosen as preliminary studies showed only a slight increase in resolution at temperatures above 150°C. The conditions were safe for TAGs, as was also shown by Proot *et al.* [1].

The splitting ratio of the carrier flow between the column and the exit was on average only 1:15. The injector device was located outside the oven and the supercritical conditions chosen for the analyses were only reached after the splitting point. The injection system with the subsequent splitting area was responsible, at least in part, for a reduced separation efficiency in comparison with the theoretical column efficiency [12].

When starting up a "cold" chromatographic system, which had been at ambient pressure and temperature with the pumps depressurized, it could take as long as 1 h before acceptable analyses were obtained. During the first run(s) the k' values of the TAG solutes were higher than those with continuously repeated, reproducible analyses.

With tight restrictors the pressure drop along the column is minimized. In this work the widest hole used generated an average linear flow-rate of 1.57 cm/s at 24.1 MPa pressure and 1.70 cm/s at 34.4 MPa. The correlation between the inlet pressure and the average linear flow-rate (measured at six pressures) was highly linear (r = 0.989) and the increase in the flow-rate was only 7.8% when the pressure was increased from 24.1 to 34.4 MPa. The observed strong influence of the fluid density on linear velocity [13,14] can, in practice, be reduced by optimizing the flow-rate of the capillary column with a tight restrictor.

Height equivalent to an effective theoretical plate (HEETP)–average linear carrier velocity ($\bar{\mu}$)–triacylglycerol carbon number (CN) three-dimensional plots at different pressures are presented in Fig. 1. When the TAG size increased, the HEETP values decreased at constant pressure. The same phenomenon was clearly shown, *e.g.* by Leyendecker *et al.* [9] with polyaromatic hydrocarbons by using *n*-pentane as the mobile phase. On the other hand, the HETP values increased with increasing triacylglycerol carbon number in isobaric runs (Fig. 2). The increase in plate height with increasing fluid velocity can be seen clearly in Figs. 1 and 2. The same effect was

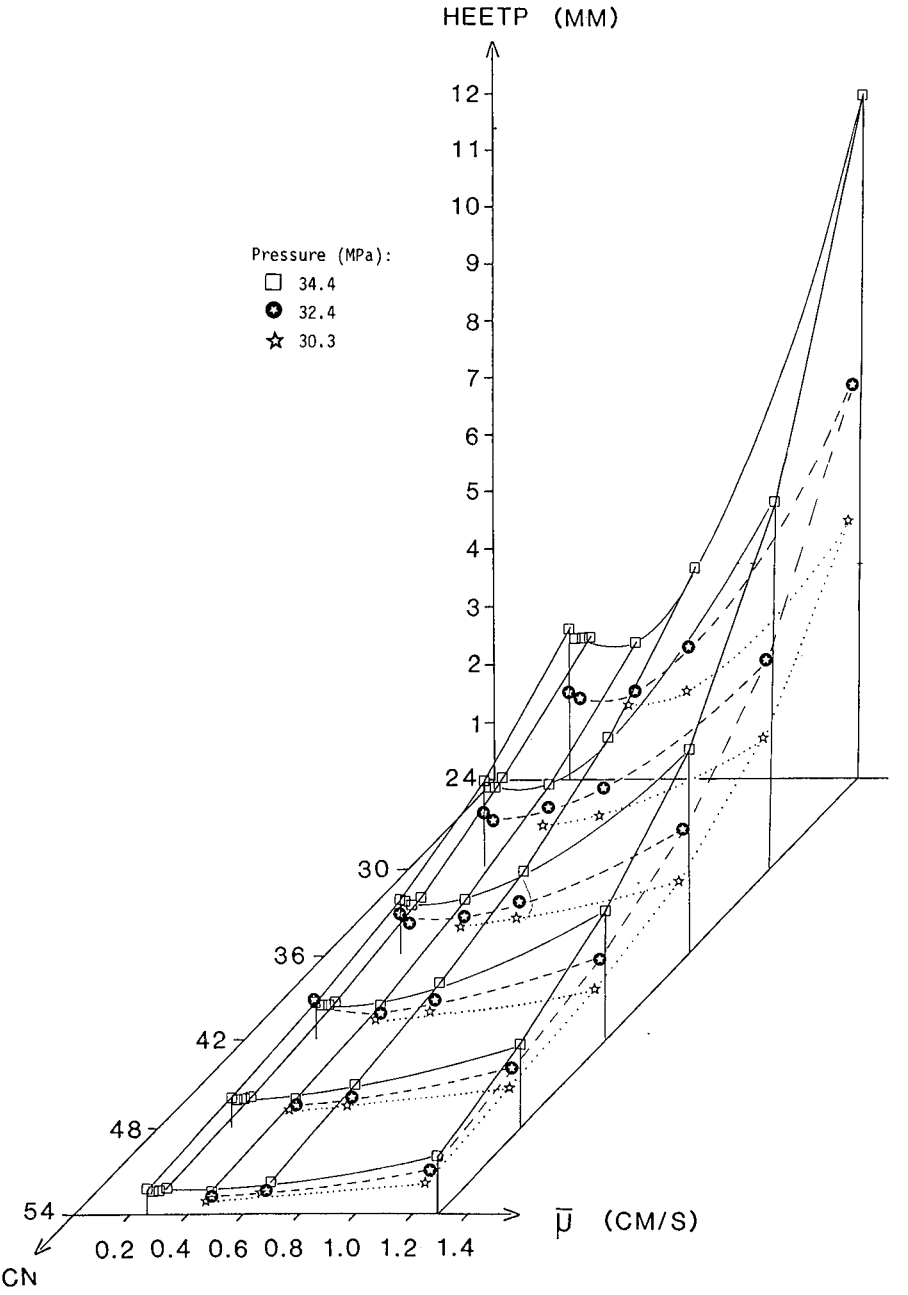

Fig. 1. Isothermal (150°C) plot of the height equivalent to an effective theoretical plate (HEETP) for saturated monoacid triacylglycerols (TAGs) containing fatty acids with an even number of carbon atoms *versus* average linear CO_2 carrier flow-rate ($\bar{\mu}$) and triacylglycerol carbon number (CN). Column, 3.8 m × 50 μm I.D., d_f 0.20 μm, DB-5.

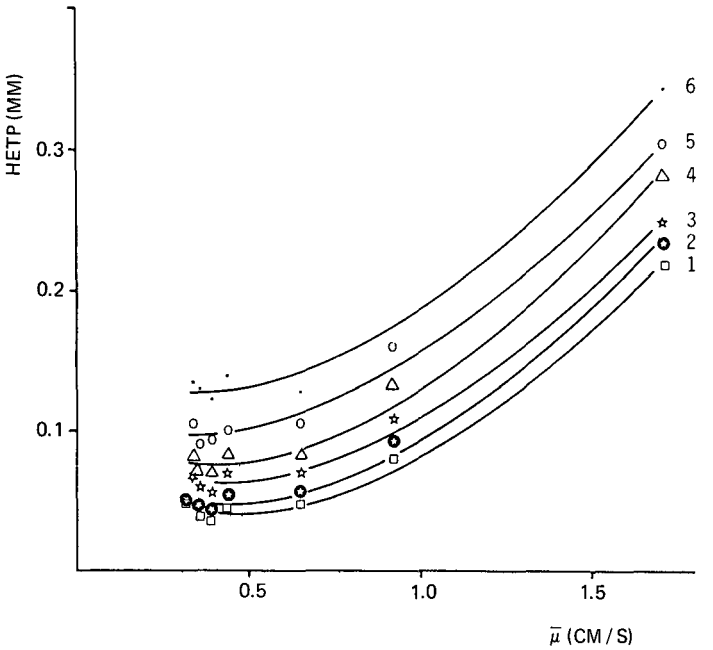

Fig. 2. Isothermal (150°C), isobaric (34.4 MPa) plot of the height equivalent to a theoretical plate (HETP) *versus* linear CO_2 carrier flow-rate ($\bar{\mu}$) for monoacid TAGs. Curves: 1 = 3 × 8:0; 2 = 3 × 10:0; 3 = 3 × 12:0; 4 = 3 × 14:0; 5 = 3 × 16:0; 6 = 3 × 18:0.

previously shown in practice by Sie and Rijnders in 1967 [15]. By increasing the average linear flow-rate of the supercritical carbon dioxide from 0.5 to 1.5 cm/s by changing the restrictor, increases in plate height of up to 3–5-fold were achieved. Losses in plate numbers were greater for the compounds having the lowest capacity factors (k'). An even steeper decline in the plate numbers per unit time was observed at flow-rate higher than 1.5 cm/s. In practice, this shows that when faster analyses are needed, shorter columns with optimized flow-rates are useful alternatives to longer columns run, *e.g.*, at ten times the optimum flow-rate. With packed fused-silica microcolumns the effect of flow-rate on efficiency is much less [5].

The approximated curves presented in Figs. 1 and 2 show reasonable symmetry and the coefficient of variation of the number of theoretical plates achieved with one restrictor was typically of the order of 5%. The $HETP_{min}$ values (Fig. 2) increased at constant pressure with increasing capacity factors (k'), whereas the $HEETP_{min}$ values (Fig. 1) showed the opposite behaviour.

Isothermal (150°C) plots of $HEETP_{min}$ of TAGs as a function of the capacity factor k' and average linear velocity $\bar{\mu}$ are shown in Fig. 3. The experimental $HEETP_{min}$ values are compared with theoretical values calculated according to the equations

$$HEETP_{min} = HETP_{min} [(k' + 1) / k']^2$$

and

$$HETP_{min} = r [(1 + 6k' + 11k'^2) / 3(1 + k')^2]^{1/2}$$

where r is the radius of the column (25 μm).

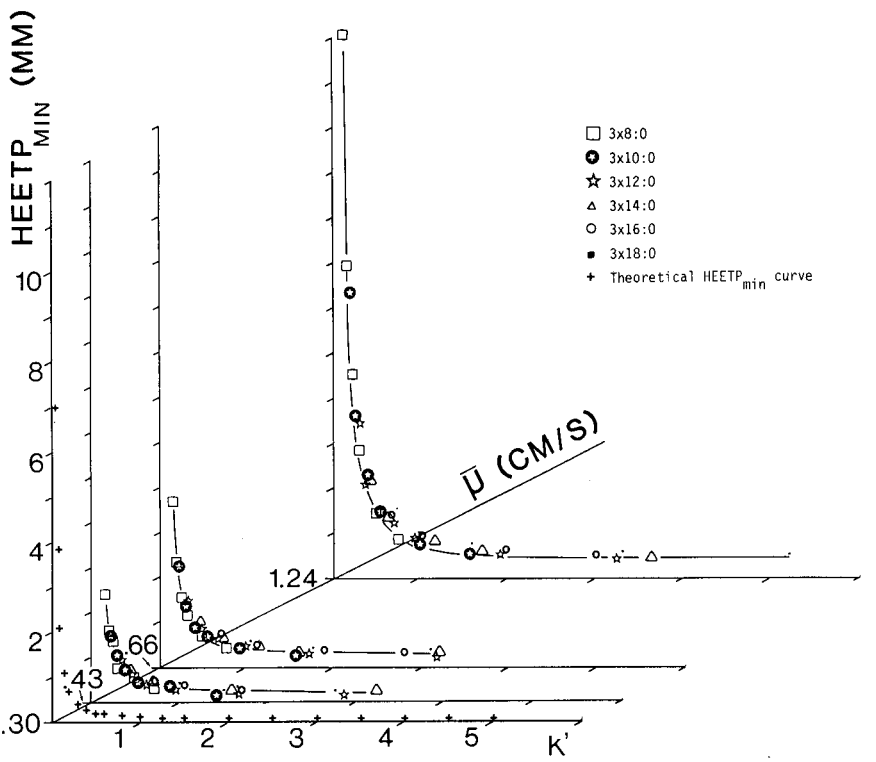

Fig. 3. Isothermal (150°C) plot of $HEETP_{min}$ of TAGs *versus* capacity factor (k') and $\bar{\mu}$.

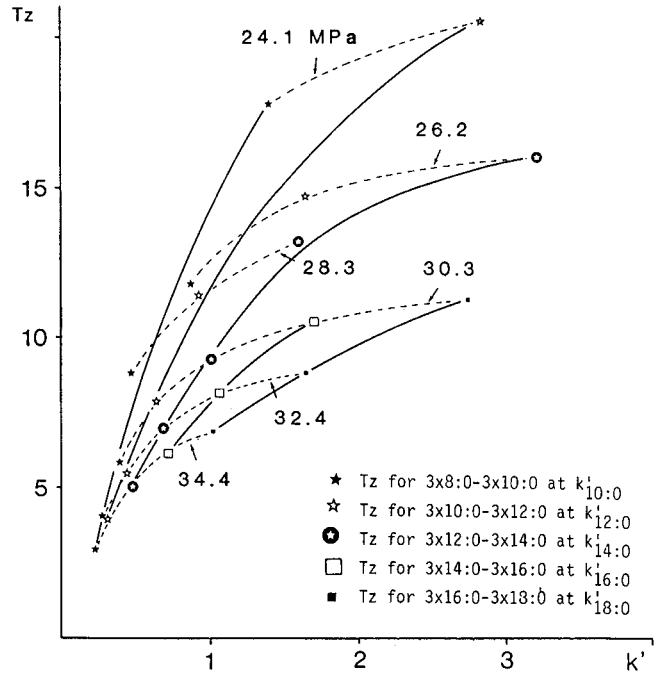

Fig. 4. Separation number (Tz) of adjacent TAGs as a function of capacity factor (k').

The plate heights obtained with the smallest TAG studied (trioctanoylglycerol) were 1.3–2 times the theoretical values, and this difference did not clearly depend on the pressure or k' value.

The plate numbers, or plate heights as such, do not yield sufficient information about the resolving power and usefulness of the column for TAG analysis. The separation number (Tz), which defines the number of average TAG peaks that can be placed between the adjacent compounds, is plotted against k' in Fig. 4. With high carbon dioxide density (pressure 34.4 MPa, $k' < 1$), the Tz between the smallest TAGs (CN = 24–30) was only 43% of the Tz of the largest compounds (CN = 48–54). With decreasing carbon dioxide density the relative difference between the Tz values of various TAG pairs decreased. At a pressure of 24.1 MPa, when the large molecules could no longer be analysed, the Tz of TAGs with CN = 30–36 exceeded 20.

Fig. 4 clearly shows that the smaller the compounds in a homologous series, the higher are the Tz values that can be generated. When increasing the capacity factor of each compound by decreasing the carbon dioxide density, one practical limitation will be the shape of the peak and the detection sensitivity lost when the peaks become broader. All the molecules are present but the misshaped peaks and the inaccuracy of the integration raise the standard deviations to unacceptable levels. At the same time, the improvement in the separation power by decreasing the fluid density becomes less and less in unit time. There are no empirical definitions to be followed when selecting the density or density programming of carbon dioxide for TAG analysis. According to our experience with the method used in this work, k' values higher than 3 cannot be recommended with the DB-5 column.

ACKNOWLEDGEMENT

Financial support by the foundation for Nutrition Research in Finland is gratefully acknowledged.

REFERENCES

1 M. Proot, P. Sandra and E. Geeraert, *J. High Resolut. Chromatogr. Chromatogr. Commun.*. 9 (1986) 189.
2 S. M. Fields, R. C. Kong, J. C. Fjelsted, M. L. Lee and P. A. Peaden, *J. High Resolut. Chromatogr. Chromatogr. Commun.*, 7 (1984) 312.
3 S. M. Fields, R. C. Kong, M. L. Lee and P. A. Peaden, *J. High Resolut. Chromatogr. Chromatogr. Commun.*, 7 (1984) 423.
4 M. Novotny, W. Bertsch and A. Zlatkis, *J. Chromatogr.*, 61 (1971) 17.
5 Y. Hirata and F. Nakata, *J. Chromatogr.*, 295 (1984) 315.
6 F. P. Schmitz, D. Leyendecker, D. Leyendecker and B. Gemmel, *J. Chromatogr.*, 395 (1987) 111.
7 E. Klesper, *Fresenius' Z. Anal. Chem.*, 330 (1988) 200.
8 C. R. Yonker, B. W. Wright, R. C. Petersen and R. D. Smith, *J. Phys. Chem.*, 89 (1985) 5526.
9 D. Leyendecker, F. P. Schmitz, D. Leyendecker and E. Klesper, *J. Chromatogr.*, 321 (1985) 273.
10 H. Kallio, P. Laakso, R. Huopalahti, R. R. Linko and P. Oksman, *Anal. Chem.*, 61 (1989) 698.
11 E. J. Guthrie and H. E. Schwartz, *J. Chromatogr. Sci.*, 24 (1986) 236.
12 J. Köhler, A. Rose and G. Schomburg, *J. High Resolut. Chromatogr. Chromatogr. Commun.*, 11 (1988) 191.
13 R. D. Smith, J. L. Fulton, R. C. Petersen, A. J. Kopriva and B. W. Wright, *Anal. Chem.*, 58 (1986) 2057.
14 H. E. Schwartz, P. J. Barthel, S. E. Moring and H. H. Lauer, *LC · GC*, 5 (1987) 490.
15 S. T. Sie and G. W. A. Rijnders, *Sep. Sci.*, 2 (1967) 699.

Journal of Chromatography, 518 (1990) 77–97
Elsevier Science Publishers B.V., Amsterdam

CHROM. 22 510

Multi-component elution overload chromatography of compounds with S-shaped isotherms

A theoretical study

VRATISLAV SVOBODA
Institute for Research, Production and Application of Radioisotopes, Radiová 1, 10227 Prague 10 (Czechoslovakia)
(First received October 12th, 1989; revised manuscript received April 9th, 1990)

ABSTRACT

An equation describing two-step adsorption was used for computation in overload elution chromatography of compounds with S-shaped isotherms. An equilibrium mixed cells model permits the study of the separation of multi-component mixtures. The band profiles of compounds with S-shaped isotherms exhibit two local maxima under certain conditions. Minor components may be dragged within the band of a major component.

INTRODUCTION

The preparative chromatography of compounds from biotechnological processes has been gaining in importance recently. Usually the starting point for this separation is analytical chromatography, but with increasing load the mechanism of separation becomes more and more complicated, as the non-linear part of the isotherm and the mutual influence of compounds play a greater role.

The first approach to gain an insight into these complicated mechanisms was the introduction of a simple model based on Langmuir isotherms [1]. No matter what computation method was used, either based on the study of solutions of systems of partial differential equations [2] or the use of a multi-cell equilibrium model [1], this approach may provide results that are in qualitative agreement with those of everyday practical preparative chromatography. On the other hand, there are some results that are impossible to explain by using this simple model, such as peaks with two maxima, the reversal of peak expansion under overload conditions and the dragging of one compound within the band of another.

A theoretical study of band profiles of compounds with S-shaped isotherms was published recently [3], but was limited to isolated bands of compounds without any extension toward the mutual influence of separated compounds. In that paper no

0021-9673/90/$03.50

indication was given of the possible mechanism by which the S-shaped isotherm is formed.

In principle, the deformation of the Langmuir isotherm to an isotherm with an inflection point may be caused by some secondary processes in the mobile or solid phase, *e.g.*, limited solubility of a solute in the mobile phase, two-stage adsorption on homogeneous adsorption sites or two or more kinds of adsorption sites in the solid phase, or by a combination of these influences.

There are only a few published experimental studies of S-shaped isotherms [4–6]. On the other hand, many unusual peak shapes resembling those predicted for S-shaped isotherms can be explained by the interaction of two compounds with Langmuir isotherms [7].

In this paper we postulate two-stage adsorption and extend this approach to solutes with limited solubility. Only elution chromatography will be considered; studies of the displacement chromatography of compounds with S-shaped isotherms and chromatography on solid phases with two or more kinds of adsorption sites will be reported later.

BASIC RELATIONSHIPS

The equilibrium distribution of a compound i between a mobile and a solid phase in a two-step process may be described by a set of equations similar to those used previously for the simple one-step system [1,8]. The first-step equation is identical:

$$\frac{c_{iF}}{c_i c_F} = K_i \tag{1}$$

where c_i, c_{iF} and c_F are concentrations of compound i in the mobile and solid phase and the concentration of sorption sites, respectively, and K_i is the equilibrium constant.

In the next step, compound i is sorbed on the already covered sorption site:

$$\frac{c_{2iF}}{c_i c_{iF}} = L_i \tag{2}$$

where c_{2iF} is concentration of sites in the solid phase binding two molecules of compound i. The amount of this compound in one cell, G_i, is therefore

$$G_i = c_i V_M + V_S (c_{iF} + 2c_{2iF}) \tag{3}$$

where V_M and V_S are volumes of the mobile and solid phase, respectively, in one equilibrium mixed cell.

The capacity of the sorbent in one cell is the sum of all free sorption sites, sorption sites covered by one molecule and sorption sites covered by two molecules:

$$G_D = V_S \left[c_F + \sum_{i=1}^{n} c_i K_i (R_i + c_i L_i T_i) \right] \tag{4}$$

where R_i is the blocking factor for the first-step sorption and T_i that for the second step. The blocking factor R_i may be understood as the average number of sorption sites covered by one molecule of compound bound to one adsorption site.

For the concentration of a compound j in the mobile phase (in one equilibrium mixed cell) one obtains

$$c_j = \frac{G_j}{V_M + G_D (K_j + 2L_jK_jc_j)/\left[1 + \sum_{i=1}^{n} c_iK_i(R_i + c_iL_iT_i)\right]} \tag{5}$$

The isotherm for one compound is simply

$$c_{iA} = c_{iF} + 2c_{ZiF} = \frac{G_D}{V_S}\left[\frac{K_ic_i(1+2L_ic_i)}{1 + c_iK_i(R_i+c_iL_iT_i)}\right] \tag{6}$$

Recently a similar equation for S-shaped isotherms was published [3]:

$$Q = \frac{25c\ (1+Ac)}{1+2Bc+ABc^2}$$

Obviously, these equations are equivalent with simple relationships between coefficients.

If $L_i = 0$, then eqn. 6 is reduced to the simple Langmuir-type isotherms (see eqn. 5 in ref. 1). For small values of c_i:

$$c_{iA} = \frac{G_DK_ic_i}{V_S} \tag{7}$$

(linear part of isotherms), and for very high values of c_i:

$$c_{iA} \rightarrow \frac{2G_D}{V_ST_i} \tag{8}$$

The shape of the isotherm is governed by the values of the constants R_i, K_i, L_i and T_i. If all are positive, then the isotherm is defined for all positive values of c_i. If R_i is negative, then the isotherm is defined for all positive values of c_i only if

$$T_i > \frac{R_i^2\ K_i}{4L_i} \tag{9}$$

If T_i is lower than this limiting value or if T_i is negative (all other constants being positive), then the isotherm is defined only in range from zero to the critical concentration, which is equal to the lower positive root of

$$c_{i,K} = \left(-R_i + \sqrt{R_i^2 - 4T_iL_i/K_i}\right)/2T_iL_i \tag{10}$$

Near this critical solute concentration the adsorbed concentration increases above all limits. This obviously does not correspond to any real system. Therefore, isotherms that do not obey condition 9 may introduce severe errors in model computation, as has been shown previously [1], and these results have to be examined very carefully.

If Lc is negligibly small in comparison with 1 and LT is negative, we obtain an equation that is similar to that used for the description of the adsorption of liquids with limited solubility [5,6]. The critical concentration then corresponds to the concentration of a saturated solution.

On isotherms with positive R, L and K a maximum of $c_{i,A}$ is observed in range of positive c_i if

$$T_i > \frac{4L_i}{K_i} + 2R_i \tag{11}$$

Isotherms conforming to condition 9 always show a maximum. The maximum occurs at a concentration

$$c_{i,\max} = \frac{1 + \sqrt{1+K_i\ (T_i-2R_i)/4L_i}}{K_i(T_i/2-R_i)} \tag{12}$$

In this instance the isotherm has two inflection points. No simple equation for their localization was found.

It should be pointed out that the binding of two different compounds to one site probably occurs in real systems (*i.e.*, c_{ijF}). This mechanism was not considered here. It is believed that the approach presented is flexible enough to describe most observed cases with satisfactory precision.

Table I and Fig. 1 demonstrate typical shapes of isotherms, all with the distribution coefficient $K_1 = 1.5$. Isotherm 1 is just a simple linear isotherm. The next isotherm (2) is the Langmuir isotherm (single-step adsorption). Isotherms 3, 4 and 5 differ only in the value of T (second-step blocking factor). When $T = 0.3$ (less than the critical value of 0.375 according to eqn. 9), then the isotherm is hyperbolic (curve

TABLE I

INFLUENCE OF CONSTANTS IN EQN. 6 ON ISOTHERM SHAPES

Curve No.[a]	K	R	L	T	Shape of isotherm
1	1.5	0.0	0.0	0.0	Linear
2	1.5	1.0	0.0	0.0	Langmuir
3	1.5	−1.0	1.0	0.3	Hyperbolic (convex)
4	1.5	−1.0	1.0	0.5	S-shaped, with maximum
5	1.5	−1.0	2.0	2.0	S-shaped, with maximum
6	1.5	1.0	1.0	1.0	S-shaped, no maximum
7	1.5	1.0	1.0	5.0	S-shaped, with maximum
8	1.5	1.0	0.01	−10.666	S-shaped, hyperbolic

[a] See Fig. 1.

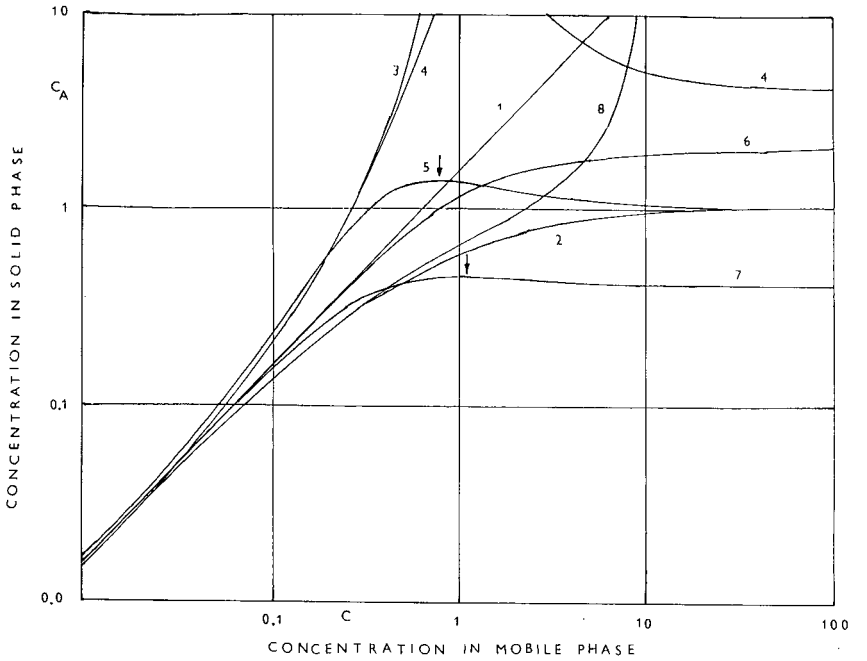

Fig. 1. Various shapes of two-step isotherms. Concentrations in arbitrary units. For values of the constants for the various curves, see Table I. Arrows indicate maxima.

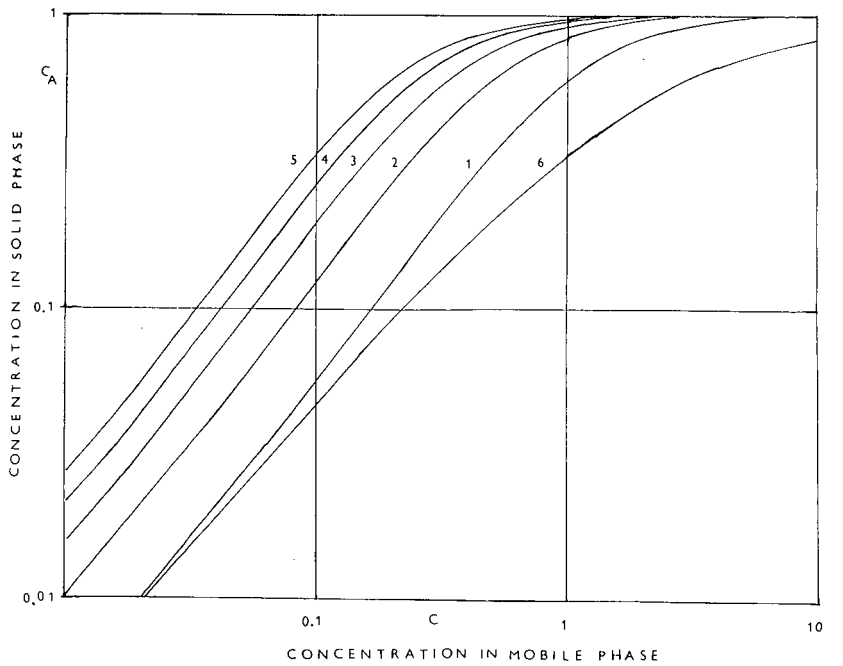

Fig. 2. Family of five parallel isotherms (log–log scale) and a Langmuir isotherm. Curve 1, $K = 0.5$, $L = 1.0$; curve 2, $K = 1.0$, $L = 2.0$; curve 3, $K = 1.5$, $L = 3.0$; curve 4, $K = 2.0$, $L = 4.0$; curve 5, $K = 2.5$, $L = 5.0$. For all these curves $R = 1.0$ and $T = 2.0$. Curve 6: Langmuir isotherm, $K = 0.5$; $R = 1.0$.

3). When T increases (above 0.375), then the isotherms exhibit a maximum (curves 4 and 5). With increasing value of T, the asymptotic value of the concentration adsorbed decreases according to eqn. 8. Isotherm 6 has all four constants positive; it has an inflection point on the ascending part, but no maximum. If its T value is increased above the critical value of 4.666 (eqn. 11), then a maximum appears (curve 7).

The isotherm with $L = 0.01$ and $T = -10.666$ (critical concentration = 10) is plotted as curve 8. This S-shaped isotherm has the first part concave, as in the Langmuir isotherm, and the second hyperbolic part convex toward the mobile phase concentration axis.

A set of parallel S-shaped isothems is depicted in Fig. 2. Compare curves 1 (S-shaped) and 6 (Langmuir).

The multi-component isotherm is an extension of eqn. 6:

$$c_{iA} = \frac{\frac{G_D}{V_S} \cdot K_i c_i \, (1 + 2L_i c_i)}{1 + \sum_{j=1}^{n} c_j K_j (R_j + c_j L_j T_j)} \tag{13}$$

The equilibrium model described by eqns. 1–4 neglects the volumes of solutes; in most instances this omission will not introduce severe errors.

As in the previous paper [1], the equilibrium mixed cells model is considered to

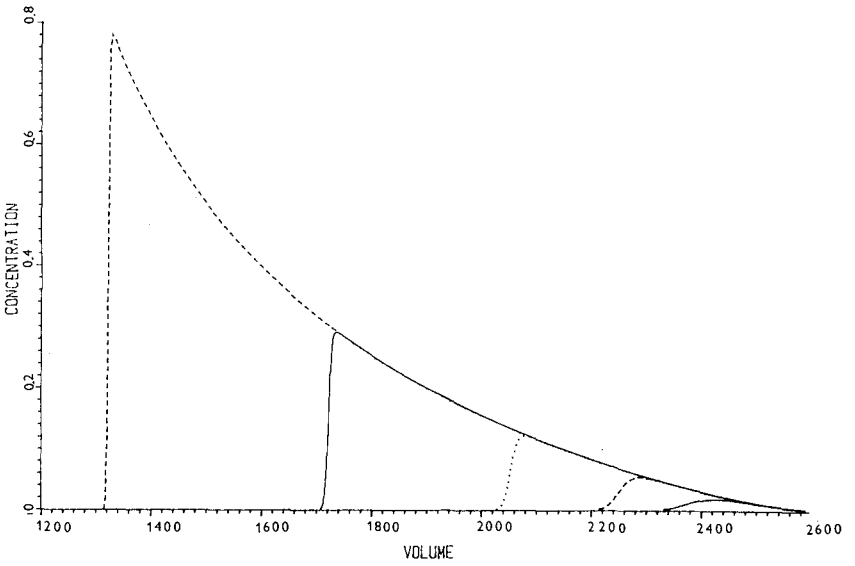

Fig. 3. Peak shapes of a compound with a Langmuir isotherm ($K = 1.5, R = 1, L = T = 0$); various amounts injected (3, 10, 30, 100, 300). Number of equilibrium cells: 1000. Amounts are measured in sorption capacity of one equilibrium cell. Injected volume (in volumes of sample solution divided by volume of one equilibrium cell): 1. Both sample amount and volume (in examples) are therefore dimensionless.

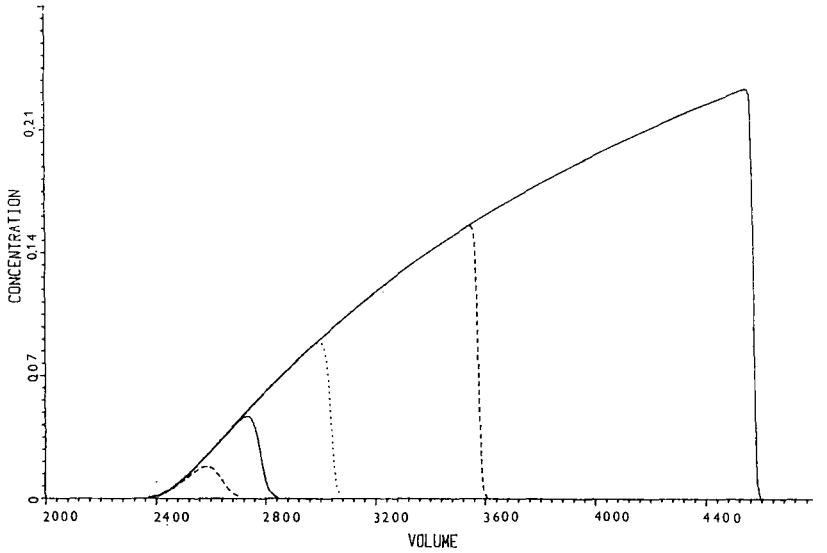

Fig. 4. Peak shapes of a compound with a hyperbolic isotherm ($K = 1.5$, $R = -1$, $L = T = 0$); injected amounts and column length (number of equilibrium cells) as in Fig. 3.

represent the number of theoretical plates in the chromatographic column. As has been pointed out earlier, the relationship between the number of cells and the number of theoretical plates holds exactly only for high enough numbers of these elements and for high values of K. The comparison between the equilibrium mixed cells model [1] and the description of chromatographic separation by a differential equation with a constant axial dispersion coefficient [8] will be published elsewhere.

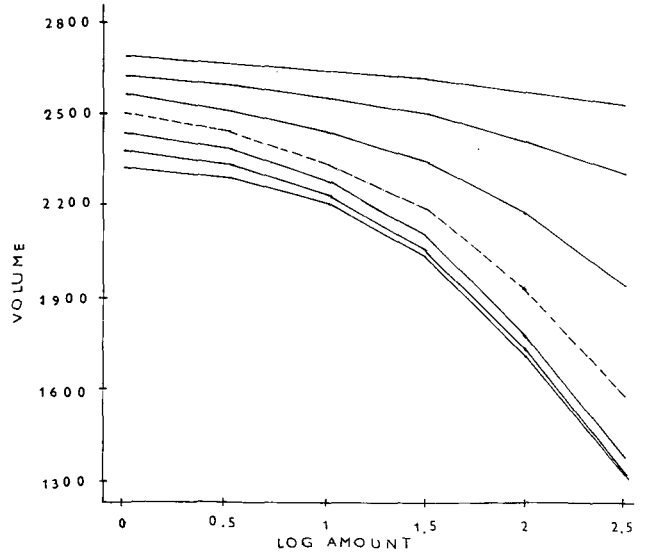

Fig. 5. Peak section positions for compound from Fig. 3 (Langmuir isotherm). Dashed line: median. For further explanation see text.

COMPUTATION

The course of computation follows the procedure described previously [1]. The key equation for computation is eqn. 5. The coverage of binding sites in the solid phase is estimated (from the previous step or set equal to zero) and then the concentration of all components is computed. If the coverage corresponding to these concentrations differs from the previously estimated value by less than $1 \cdot 10^{-5}$, then the computation is finished; if not, the iterative computation proceeds until the desired precision is attained. The amount of injected sample is expressed as sample amount divided by sorption capacity of one equilibrium cell (G_D), sample volume in multiples of V_M. Other details were described previously [1].

RESULTS AND DISCUSSION

Single compounds

Typical peak shapes for simple Langmuir-type isotherms are displayed in Figs. 3 and 4. Similar band profiles have been published for overload column chromatography when a solution based on the difference method was used as the method of computation. For a quantitative description of peak shapes we divided the peak area into seven sections, whose normalized areas (0.00135, 0.02140, 0.13591, 0.34134, 0.34134, 0.13591, ...) were selected so that for an ideal Gaussian peak the distances between section borders are equal to integral multiples of sigma (standard deviation) from the peak centre. When we plot these positions for our two peak families, we obtain for the Langmuir isotherm monotonously descending curves (Fig. 5) and for the hyperbolic (convex) isotherm curves which increase monotonously (Fig. 6).

The band profies of compounds with S-shaped isotherms change their shape

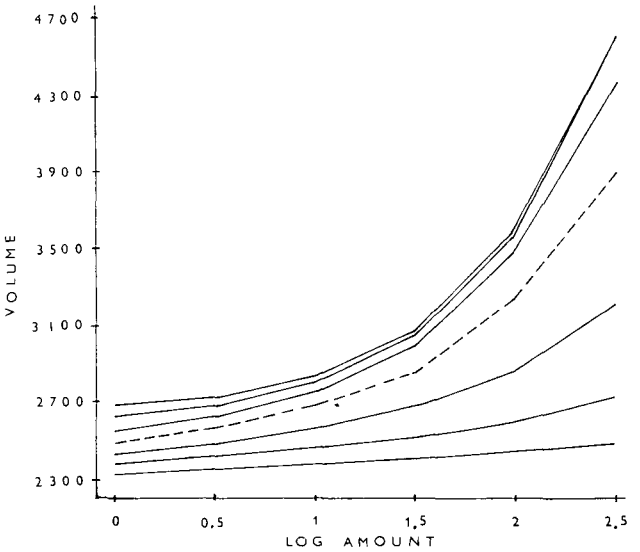

Fig. 6. Peak section positions for compound from Fig. 4 (hyperbolic isotherm). Dashed line: median. For further explanation, see text.

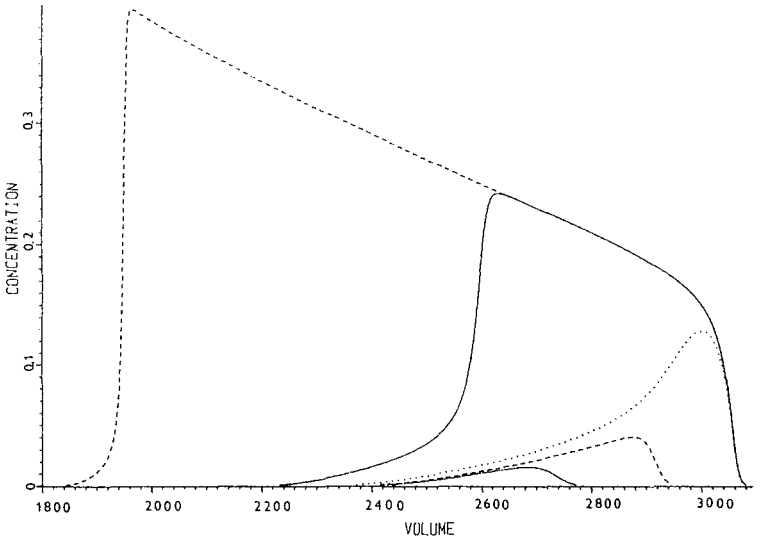

Fig. 7. Peak shapes of a compound with an S-shaped isotherm without a maximum ($K = 1.5$, $R = 1$, $L = 3$, $T = 2$). Isotherm is plotted in Fig. 2 (curve 3). Injected amounts: 3, 10, 30, 100, 300. Number of cells: 1000.

with increasing amount in a more complicated manner. At first, when the convex part of the isotherm predominates the peak extends its rear edge toward higher elution volumes (see Fig. 7) and its front edge remains diffuse. At higher overloadings, when the main role is played by the concave part of isotherm, similarly to the Langmuir isotherm, the front edge of the peak starts to extend to lower elution volumes and

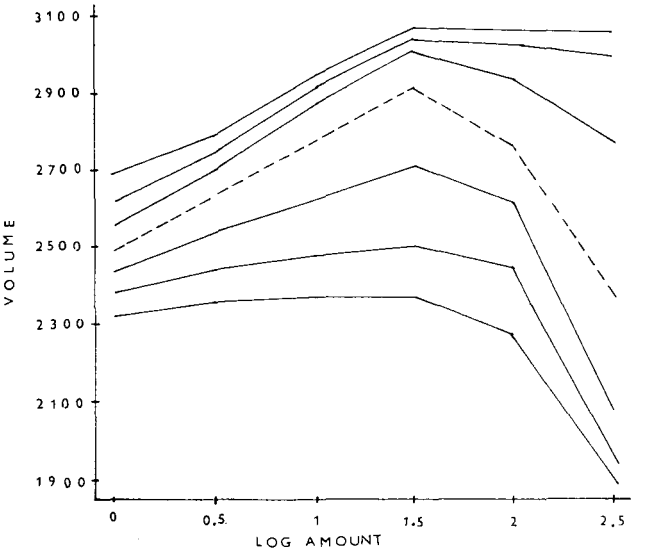

Fig. 8. Peak section positions for a compound with an S-shaped isotherm without a maximum (see Fig. 7). Dashed line: median. For further explanation, see text.

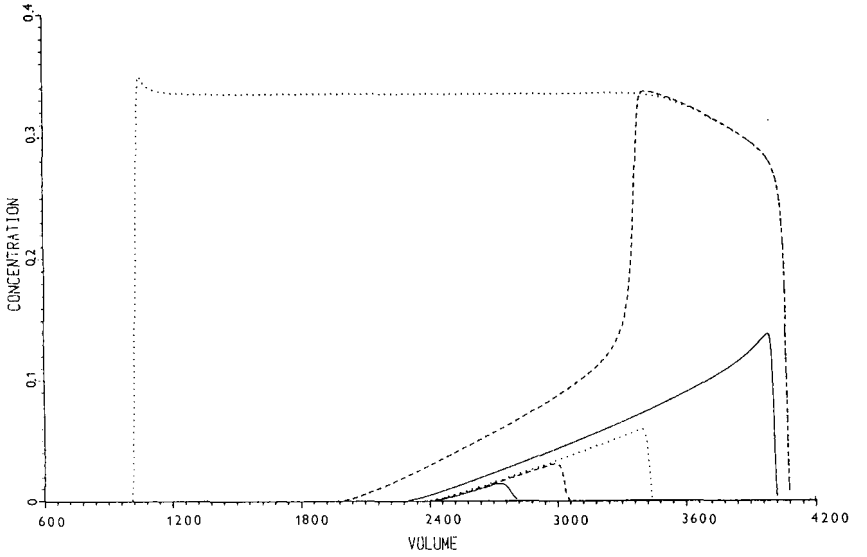

Fig. 9. Peak shapes of a compound with an S-shaped isotherm with a maximum ($K = 1.5$, $R = -1$, $L = 2$, $T = 2$). Isotherm is plotted in Fig. 1, curve 5. Injected amounts: 3, 10, 30, 100, 300, 1000. Number of cells: 1000.

becomes sharper, whereas the rear becomes diffuse and its position remains unchanged. This two-fold character of band profile dynamics is reflected in the plot of peak section positions by the at first ascending and descending shape of the plotted curves (Fig. 8). If the peak shapes of a compound with Langmuir and S-shaped

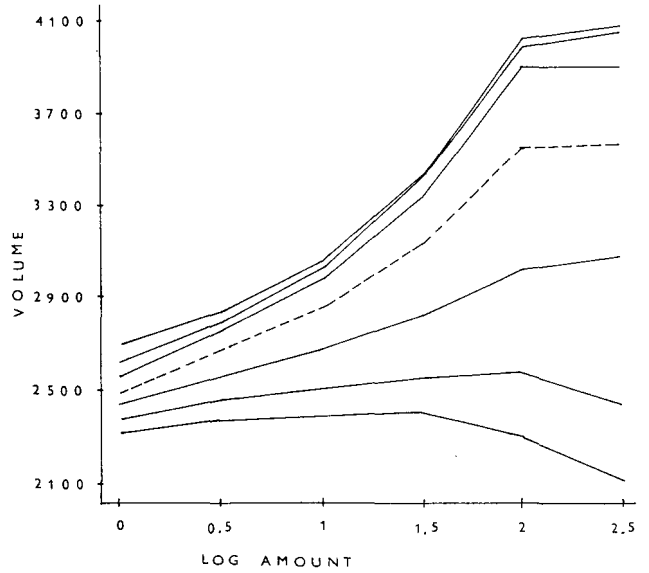

Fig. 10. Peak section positions for a compound with an S-shaped isotherm with a maximum; for parameters, see Fig. 9. Dashed line: median. For further explanation, see text.

isotherms are compared, then the heavily overloaded peak of the former is much broader and its maximum concentration is therefore lower (Figs. 3 and 7).

In the preceding example we examined isolated peaks corresponding to an S-shaped isotherm without a maximum (Fig. 2). The peaks corresponding to the S-shaped isotherm with a maximum (Fig. 1, curve 5) change their forms in a similar manner (Fig. 9). The overloading occurs at higher amounts owing to the higher concentrations at which isotherm maximum occurs; this is also reflected in the plot of peak section positions (Fig. 10). The stabilization of the rear edge position occurs at higher volumes than in the preceding example.

The influence of column efficiency and capacity on the band profile is illustrated in Fig. 11. With increasing column length, and hence with increasing column capacity, the peak form is transformed similarly to when the injected amount is decreased at a constant column length. At the same time, with increasing column efficiency, the relative effect of dispersion decreases.

The band profiles of compounds with limited solubility with isotherms similar to that depicted as curve 8 in Fig. 1 change their shape with increasing overloading in a different manner. At first they behave like bands corresponding to a normal Langmuir isotherm: the front edge is steep and the desorption part of the profile is long. When the load is increased, the profile becomes steeper also at the rear and finally we obtain a peak shape (Fig. 12) that is similar to the peak corresponding to an isotherm with the first part convex (Figs. 7 and 9). The computed shape resembles that published in an experimental study [6].

Comparison of the band profiles of four compounds with moderate (Fig. 13) and heavy overloading (Fig. 14) demonstrates how drastically may be the change in the elution volumes of bands which in linear region all elute as Gaussian profiles at 2500 volume units.

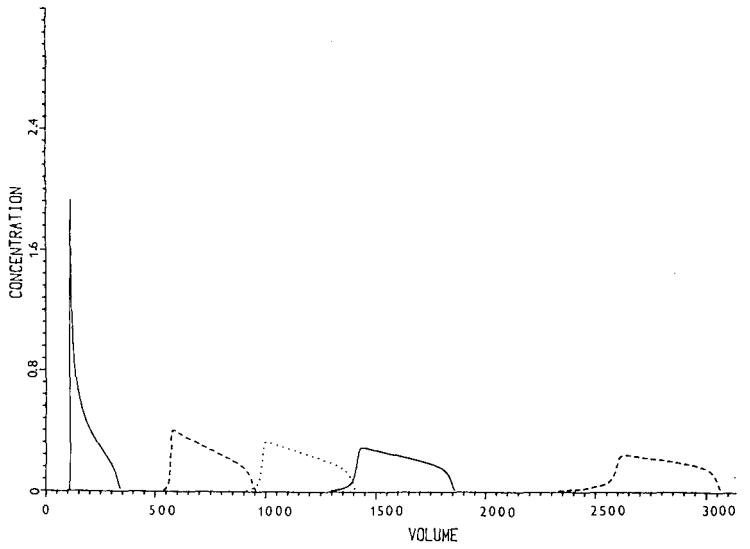

Fig. 11. Peak shapes at various column lengths. Isotherm as in Fig. 9, injected amount: 100 (volume, 10; concentration, 10). Number of cells: 1000, 600, 450, 300, 100.

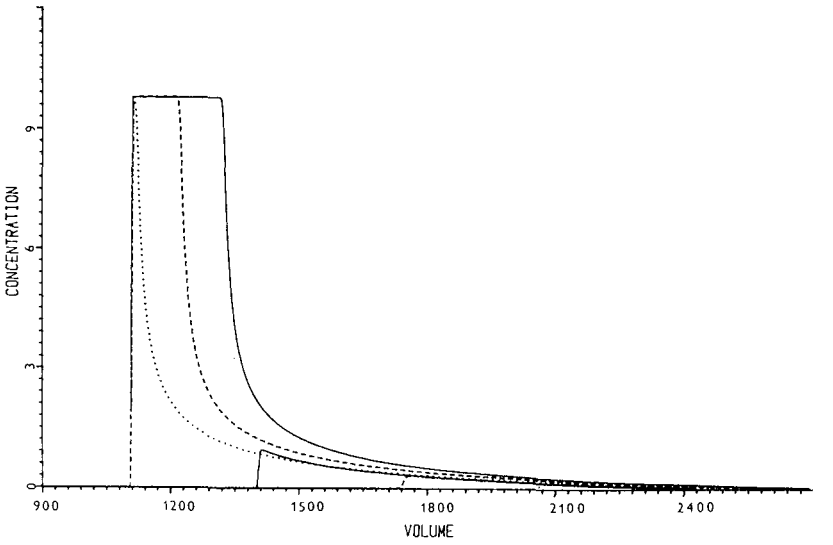

Fig. 12. Peak shapes of a compound with limited solubility (isotherm 8 in Fig. 1). Injected amounts: 3000, 2000, 1000, 300, 100, 30. Number of cells: 1000. Concentration of injected sample (all cases): 9.8.

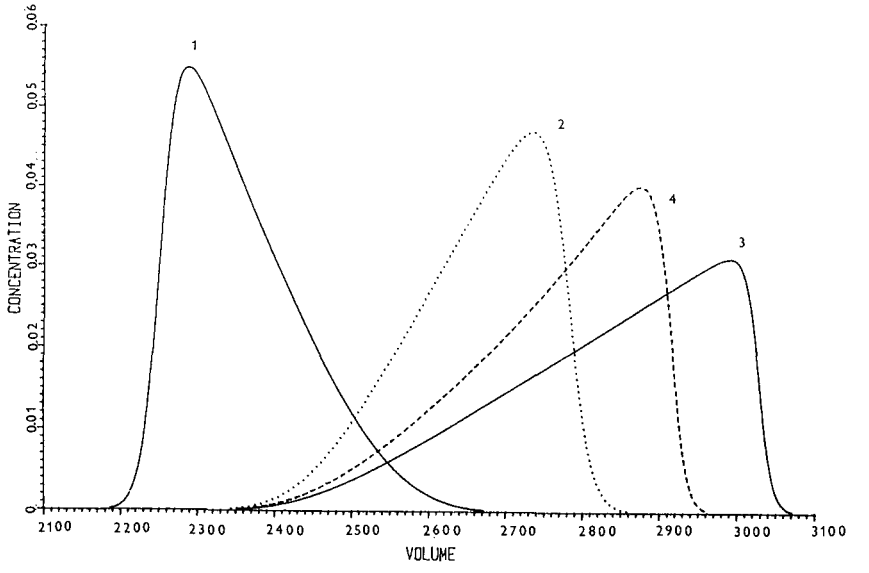

Fig. 13. Four band profiles at moderate overloading. In all instances $K = 1.5$. Injected amount: 10. Number of cells: 1000. Curve 1, Langmuir isotherm, $R = 1$; curve 2, hyperbolic (quasi-Langmuir), $R = -1$; curve 3, S-shaped, $R = -1$, $L = 2$, $T = 2$; curve 4, $R = 1$, $L = 3$, $T = 2$.

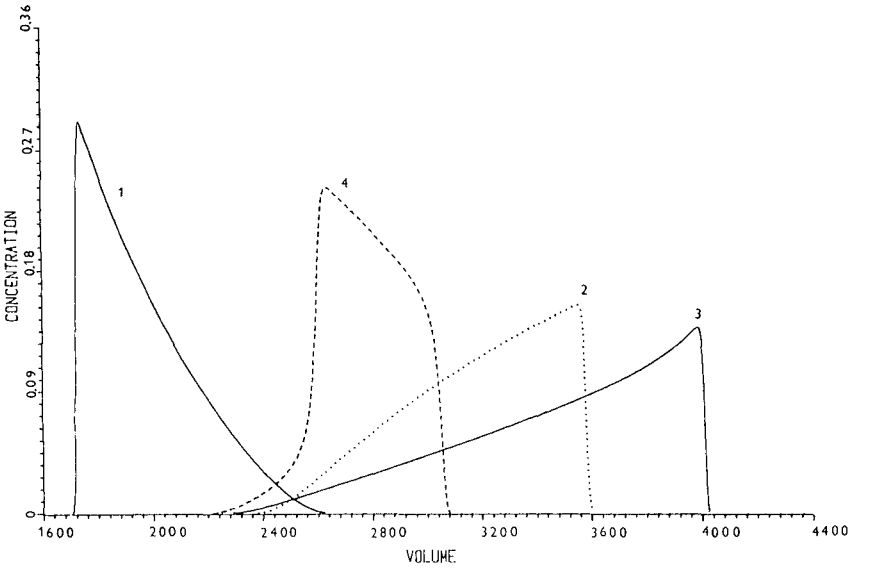

Fig. 14. Same as Fig. 13 but amount = 100.

Interaction of two compounds

Interaction of two bands with normal Langmuir isotherms in the overload region has been described previously [1,7,9] and similar interactions are observed when two compounds with hyperbolic isotherms are eluted (Fig. 15). In the region of

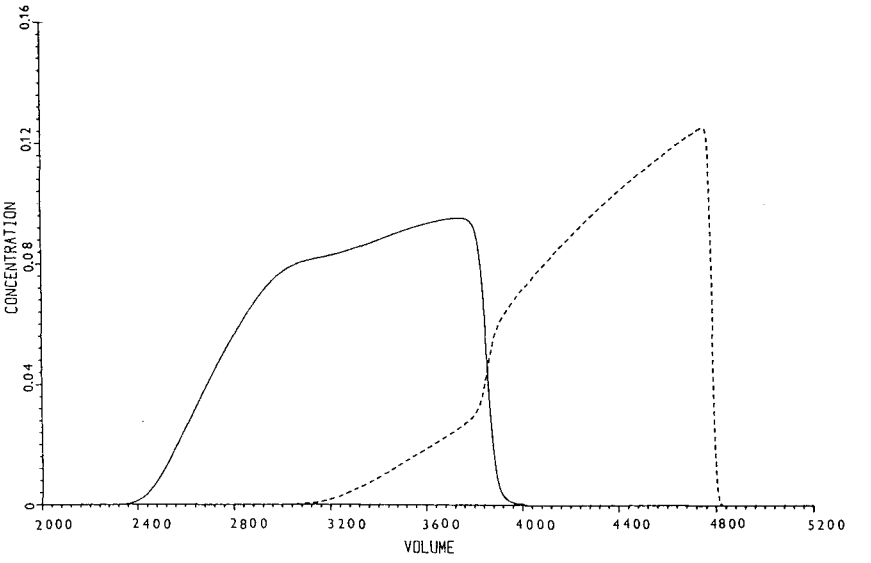

Fig. 15. Band profiles of two compounds with hyperbolic (quasi-Langmuir) isotherms, heavy overloading. Both bands: amount = 100, $R = -1$. Full line, $K = 1.5$; dashed line, $K = 2$. Number of cells: 1000.

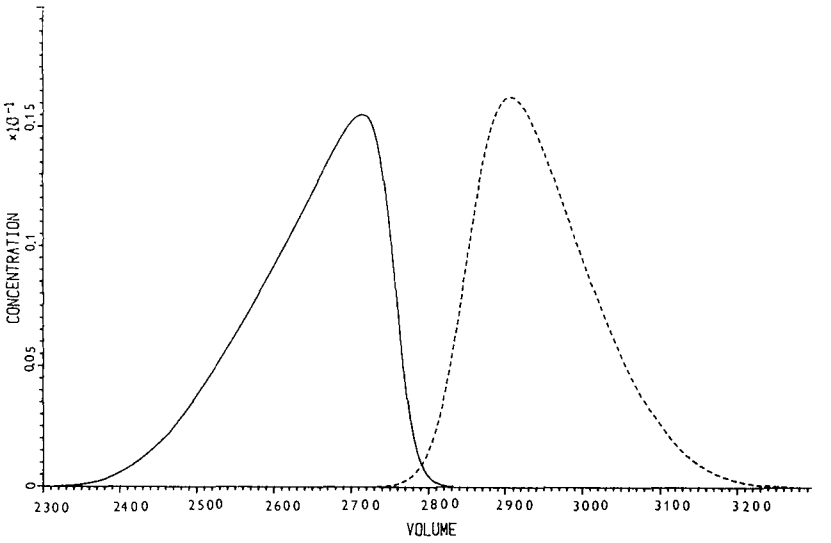

Fig. 16. Two compounds with different types of isotherms. Full line, $K = 1.5$, $R = -1$ (hyperbolic, quasi-Langmuir); dashed line, $K = 2$, $R = 1$ (Langmuir). Injected amount: 3. Injection volume: 10. Number of cells: 1000.

overlap, the compounds seemingly displace each other and the tendency to form bands of pure compounds manifests itself by the formation of an indentation in the front part of the second peak and of a hump in the front part of the first peak. A different situation occurs if one compound has a Langmuir isotherm and the second

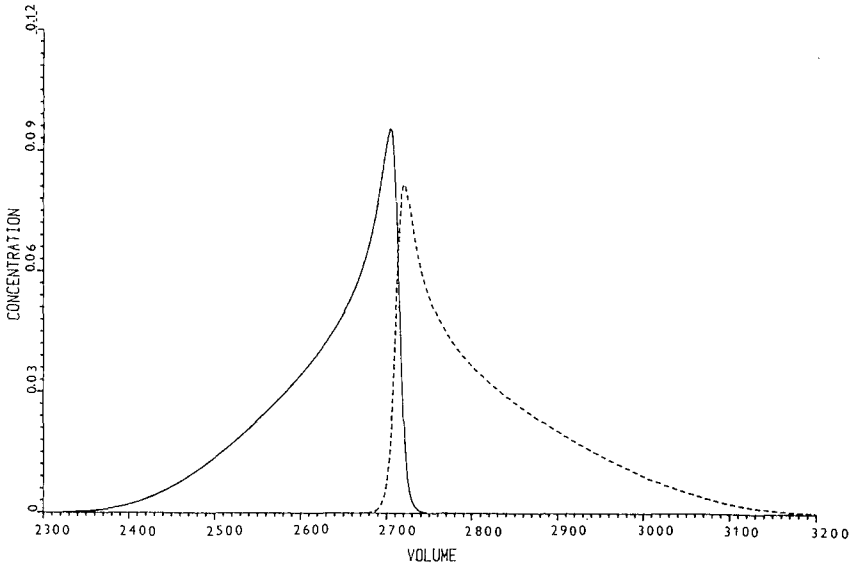

Fig. 17. Same as Fig. 16 but injected amount = 10.

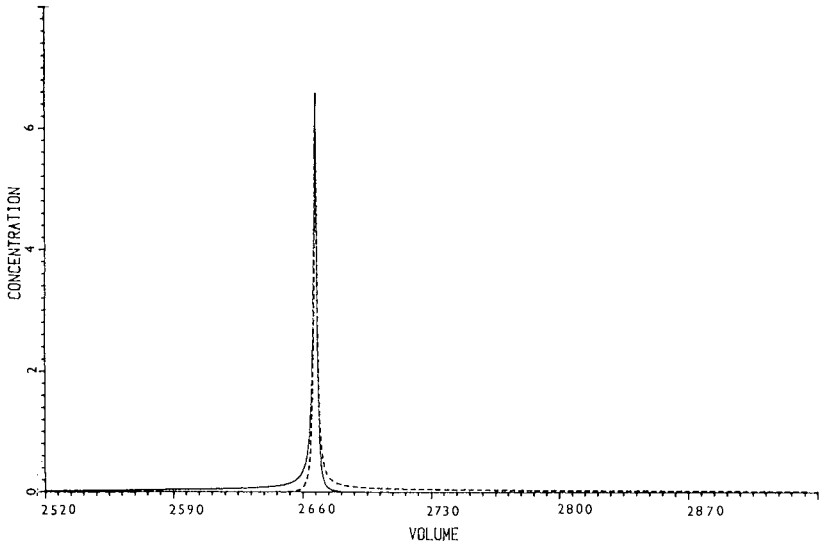

Fig. 18. Same as Fig. 16 but injected amount = 30.

a hyperbolic isotherm. Then at higher overloadings the band profiles do not overlap, but form a region with increased concentration (Figs. 16–18). This tendency for a decreasing width and increasing concentration finally leads to extremely narrow twin band profiles [1].

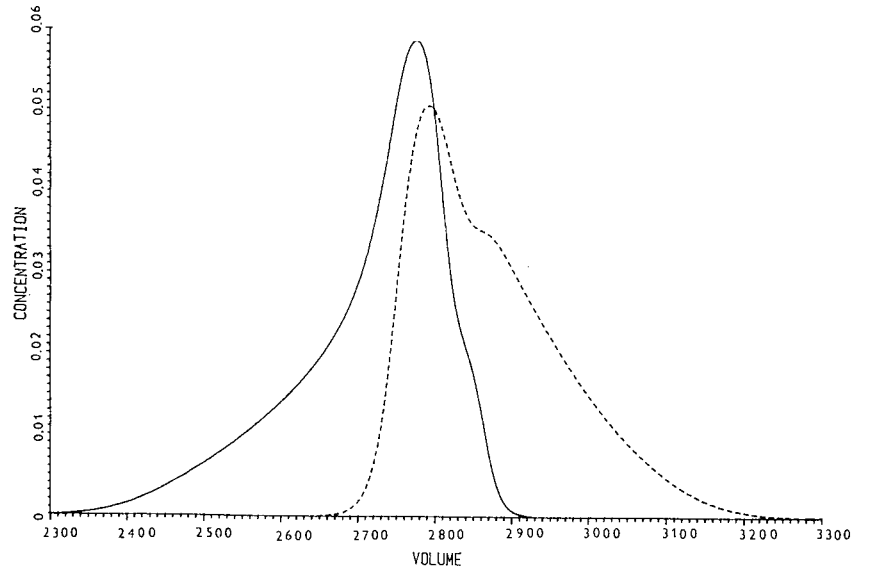

Fig. 19. Two compounds with different types of isotherms. Full line, S-shaped isotherm, $K = 1.5$, $R = -1.0$, $L = 2.0$, $T = 2.0$; dashed line, Langmuir isotherm, $K = 2.0$, $R = 1.0$, $L = T = 0$. Number of cells: 1000, Injected amount: 10.

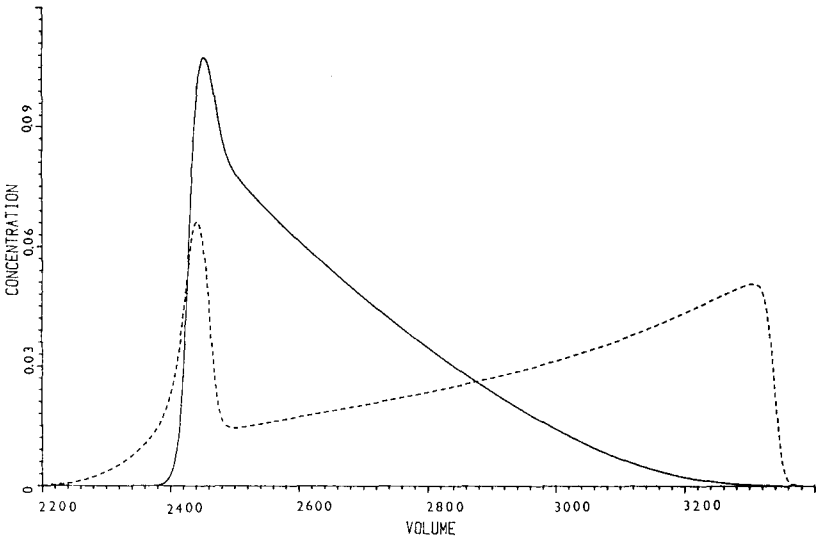

Fig. 20. Same as Fig. 19 but injected amount = 30.

When, instead of a compound with a hyperbolic isotherm together with a compound with a Langmuir isotherm, a compound with an S-shaped isotherm having the first two constants identical is eluted, at low concentrations the band profile is identical with that in Fig. 16. When the injected amount is increased, a narrow twin peak is formed (Fig. 19), similarly to the previous case (Fig. 17) with larger injected amounts, but then the peaks start to overlap (Fig. 20) and at still higher amounts the

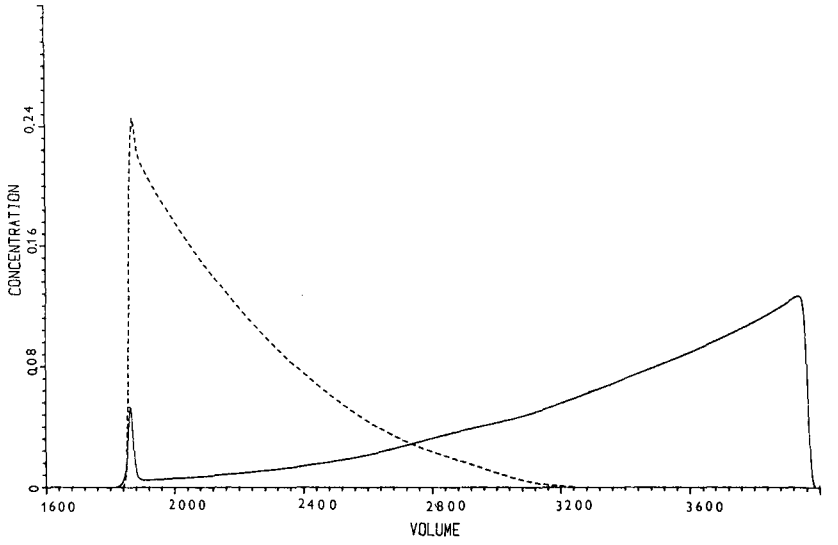

Fig. 21. Same as Fig. 19 but injected amount = 100.

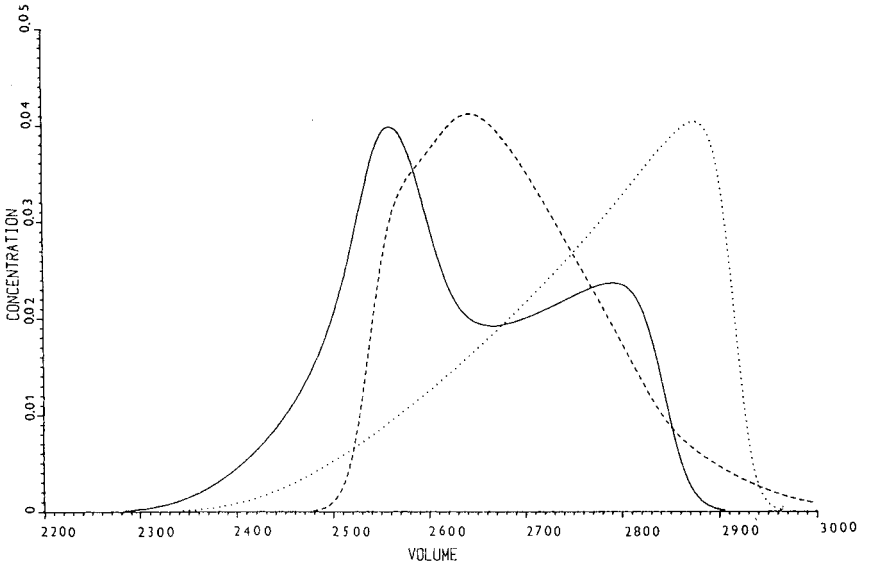

Fig. 22. Band profiles of compounds with S-shaped and Langmuir isotherms. Full line, $K = 1.5$, $R = 1.0$, $L = 3.0$, $T = 2.0$; dashed line, $K = 2.0$, $R = 1.0$, $L = T = 0$; dotted line, same as full line, but compound eluted alone, without interaction. Number of cells: 1000. Injected amount: 10.

band profiles are quite similar to those for pure compounds. The only indication of this inflection point on the isotherm of the compound with a lower distribution coefficient is the formation of a spike on the ascending part of the peak profile. This spike is also reflected on the front edge of the compound with a regular Langmuir isotherm (Fig. 21).

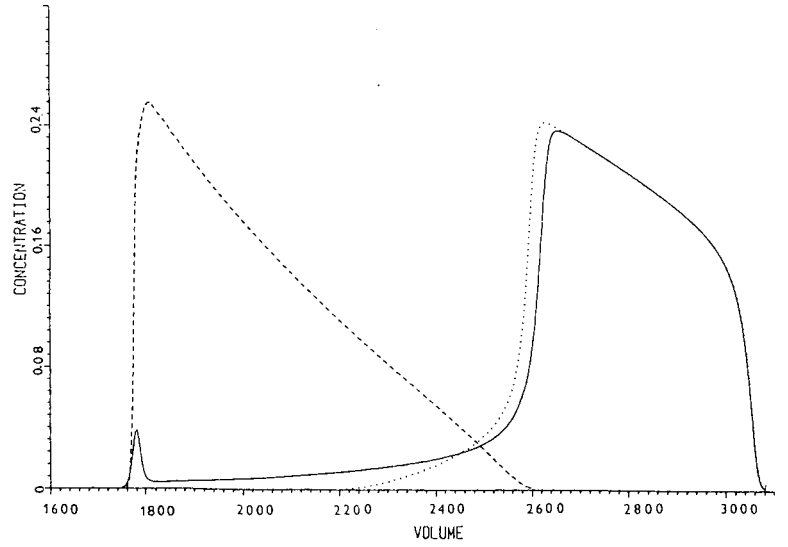

Fig. 23. Same as Fig. 22 but injected amount = 100.

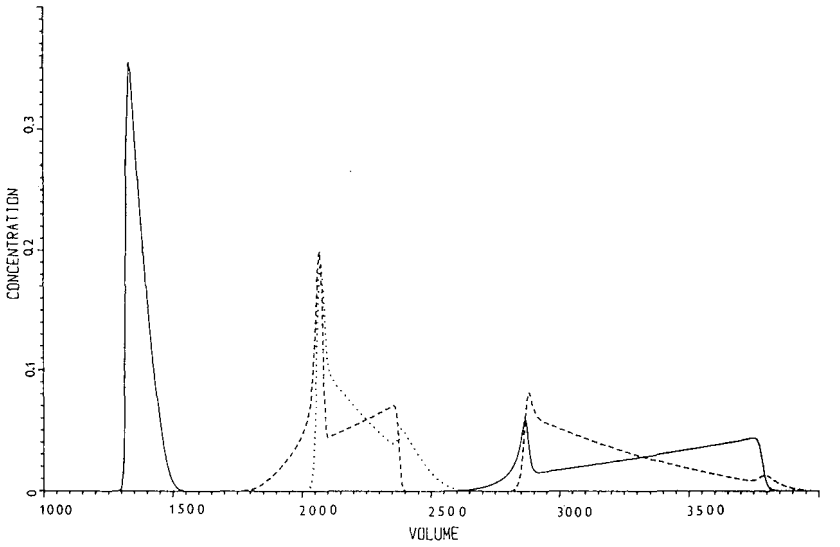

Fig. 24. Separation of five-component mixture. Three components with Langmuir isotherms, $K = 0.5$, 1.5 and 2.5; for all three $R = 1.0$, $L = T = 0$. Two component with S-shaped isotherms: $K = 1.0$, $R = -1.0$, $L = 1.0$ and $T = 0.3$ and $K = 2.0$, $R = -1$, $L = 1.0$ and $T = 1.2$. Injected amount (all components): 30. Number of cells: 1000.

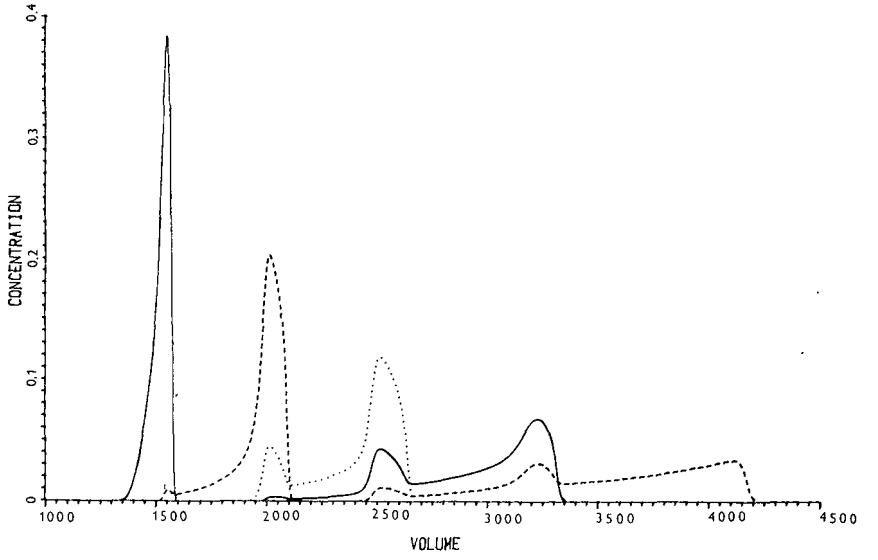

Fig. 25. Separation of five-component mixture. All components: S-shaped isotherms as in Fig. 2. Injected amount (all components): 30. Number of cells: 1000.

TABLE II

RECOVERY OF COMPOUNDS WITH S-SHAPED ISOTHERMS (AS IN FIG. 2) AS PERCENTAGE OF AMOUNT INJECTED

Injected amount	Volume of load	Compound[a]				
		1	2	3	4	5
5 × 10	1	100	80.57	31.92	6.03	40.36
5 × 20	200	100	100.00	37.14	10.16	85.77
5 × 30	1	50.87	16.32	0	0	0

[a] The numbers correspond to the curve numbers in Fig. 2.

The general character of the interaction between compound bands with S-shaped and Langmuir isotherms is preserved even when the isotherm contains only positive constants and does not exhibit a maximum. If small amounts are injected, Gaussian peaks at 2500 and 3000 volume units are eluted. At higher concentrations, the band profile of the first compound is extended towards higher elution volumes and *vice versa*. At the same time, the peak of the first compound is pushed backwards by interaction with the band of the second compound and a secondary peak is formed (Fig. 22). At higher loads the bands change their mutual position, and the band of the compound with an S-shaped isotherm shows a secondary spike at the elution volume of the sharp front of the compound with a Langmuir isotherm (Fig. 23).

Multi-component separations

The five-component mixture of compounds with regular Langmuir and with

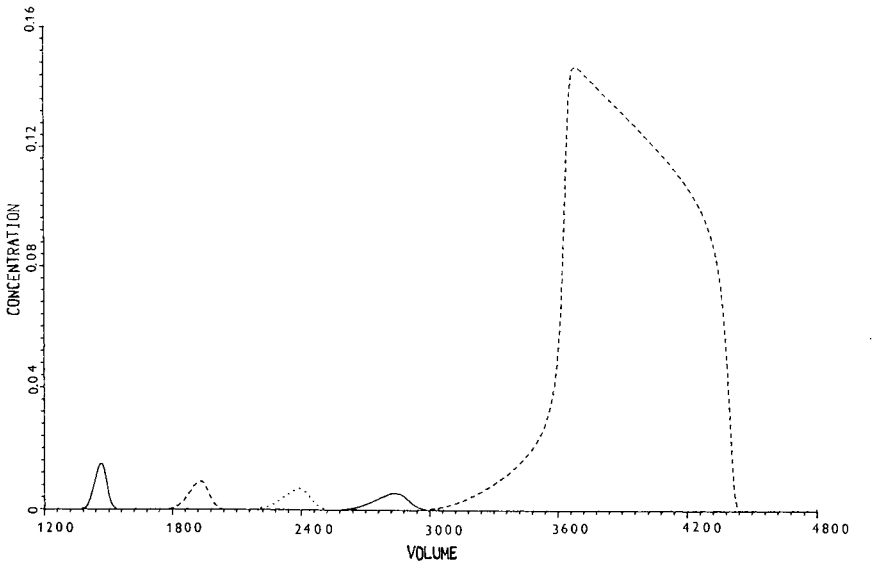

Fig. 26. Separation of five components as in Fig. 25. Injected amounts: component with $K = 2.5$, 100; other four, 1. Number of cells: 1000.

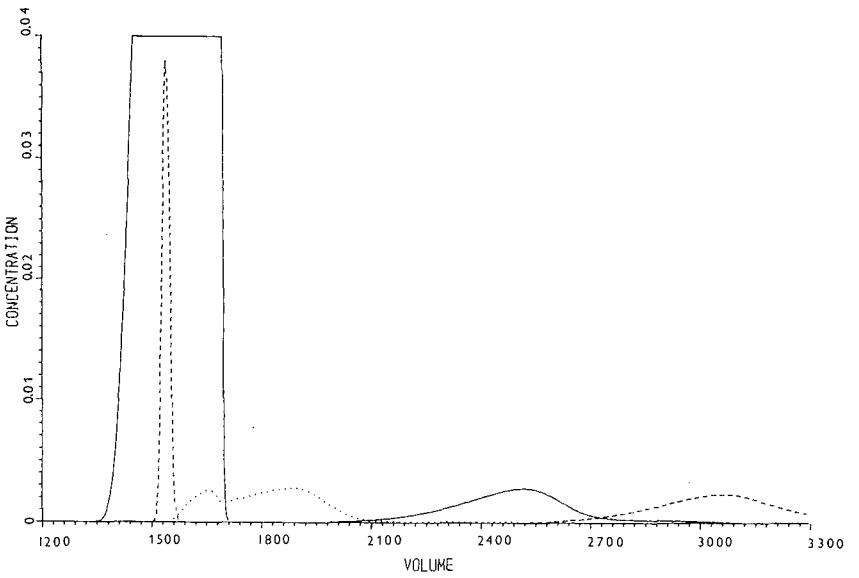

Fig. 27. Separation of five components as in Fig. 26. Injected amounts: component with $K = 0.5$: 100; other four, 1. Number of cells: 1000.

S-shaped isotherms reveals (Fig. 24) similar band profiles to those found for the two-component mixture (Fig. 20). The loading is relatively low in comparison with similar separations of compounds with Langmuir isotherms [1], but the overlap of bands is so severe that the recoveries (with the exception of the first compound) are only a few percent.

Another example is presented by compounds with S-shaped isotherms without a maximum and with all four constants positive (Fig. 2).

Injection of the same amount of compounds as in preceding example leads to severe interferences between all components (Fig. 25). Only after the load has been decreased 3-fold may a small percentage of all components be recovered with the desired purity (99%). As in similar instances, when severe interactions between chromatographic bands exist, dilution of the injected mixture may lead to an improvement in separation. In our case, even when the injected amount is double that in the preceding case the recovery increases (see Table II).

The recovery of trace components from compounds with S-shaped isotherms does not seem to present special problems if the major component is eluted in the last position. All four minor components are then eluted in isolated bands, only their elution volumes are shifted to lower values compared with elution of pure components (Fig. 26). In contrast, when the major compound is eluted first, the first minor component is completely overlapped by the major band and even a substantial part of the second minor component is lost in the first peak (Fig. 27). The shift of elution volumes to lower values is more pronounced than in the previous instance.

CONCLUSION

Two-step adsorption has been postulated as the mechanism for the formation of isotherms with inflection points. The band profiles of isolated peaks can then be computed using the equilibrium mixed cells model. This model permits the computation of multi-component separations and interesting features, not observed when compounds with simple Langmuir isotherms are separated, may be discerned.

However, it must be stressed that similarity of computed and experimental chromatograms may be only circumstantial. Only a thorough study of multi-component isotherms may establish that the hypothetical chromatograms presented in this paper describe real systems. On the other hand, the simplicity of the original postulate increases the validity of the results presented.

SYMBOLS

c_i concentration of ith compound in mobile phase (mol l^{-1})
c_{iA} concentration of ith compound (all adsorbed forms) in solid phase (mol l^{-1})
c_{iF} concentration of sorption sites with one adsorbed molecule of ith compound (mol l^{-1})
c_F concentration of free sorption sites in solid phase (mol l^{-1})
c_{2iF} concentration of sorption sites with two adsorbed molecules of ith compound (mol l^{-1})
G_D sorption capacity of sorbent in one equilibrium cell (mol) (see eqn. 4)
G_i amount of ith compound in one equilibrium cell (mol)
K_i equilibrium constant in single-step adsorption (l mol^{-1}) (see eqn. 1)
L_i equilibrium constant of the second adsorption step (l mol^{-1}) (see eqn. 2)
R_i blocking factor for the first adsorption step (dimensionless)
T_i blocking factor for the second adsorption step (dimensionless)
V_M volume of mobile phase in one equilibrium cell (l)
V_S volume of solid phase in one equilibrium cell (l)

REFERENCES

1 V. Svoboda, *J. Chromatogr.*, 464 (1989) 1.
2 S. Ghodbane and G. Guiochon, *J. Chromatogr.*, 440 (1988) 9.
3 G. Guiochon, S. Golshan-Shirazi and A. Jauches, *Anal. Chem.*, 60 (1988) 1856.
4 C. Souteyrand, M. Thibert, M. Caude and R. Roset, *J. Chromatogr.*, 262 (1989) 1.
5 E. B. Guglya and S. M. Yanovskiy, *Zh. Fiz. Khim.*, 60 (1986) 3069.
6 E. B. Guglya and S. M. Yanovskiy, *Zh. Fiz. Khim.*, 60 (1986) 108.
7 S. Golshan-Shirazi and G. Guiochon, *J. Chromatogr.*, 461 (1989) 1 and 19.
8 J. Plicka, V. Svoboda, I. Kleinmann and A. Uhlířová, *J. Chromatogr.*, 469 (1989) 29.
9 S. Ghodbane and G. Guiochon, *J. Chromatogr.*, 452 (1988) 209.

Journal of Chromatography, 518 (1990) 99–110
Elsevier Science Publishers B.V., Amsterdam

CHROM. 22 634

Surfactant-mediated hydrophobic interaction chromatography of proteins: gradient elution

J. J. BUCKLEY and D. B. WETLAUFER*
Department of Chemistry and Biochemistry, University of Delaware, Newark, DE 19716 (U.S.A.)
(First received February 27th, 1990; revised manuscript received June 14th, 1990)

ABSTRACT

Addition of 3-[(3-cholamidopropyl)dimethylammonio]-1-propanesulphonate (CHAPS) to mobile phases in gradient elution hydrophobic interaction chromatography (HIC) on SynChropak Propyl causes changes in observed elution times for nine globular proteins. The nine proteins showed different percentage reductions in capacity factor, k', demonstrating the ability of CHAPS to change the selectivity of the separations. Three basic types of gradient experiments have been explored for surfactant-mediated gradient elution HIC. Type I gradients are conducted with constant salt and variable surfactant concentration. Type II gradients with variable salt and constant surfactant concentration, and Type III gradients with variable salt and surfactant concentrations. By the criterion of a linear relationship between gradient time and retention time the linear solvent strength condition applies to Type II and Type III gradients. Type III gradients, with the fastest re-equilibration time, are preferable for repetitive analyses. Type I gradients are relatively ineffective in making use of the solvent strength of CHAPS, and Types I and II gradients require long equilibration times due to large changes in surface concentration of CHAPS which occur during elution. The presence of CHAPS had a negligible effect on peak shapes of the proteins examined, except for bovine serum albumin which yielded a narrower, less distorted peak in the presence of CHAPS.

INTRODUCTION

High-performance hydrophobic interaction chromatography (HIC) is growing in prominence for separation of proteins [1–5]. In this technique proteins are eluted from weakly hydrophobic stationary phases using decreasing salt gradients. These relatively mild conditions favor the recovery of proteins in their native condition (*i.e.* with retention of biological activity) [6]. This contrasts with reversed-phase (RP) HPLC separations of proteins where the use of acidic conditions, organic solvents and more hydrophobic stationary phases commonly induces protein denaturation [8-11].

Surfactants, due to fact that they may interact both with proteins [12] and stationary phase surfaces [13-18], are expected to have potential as eluting agents in HIC. Recent studies from this laboratory have shown some of the potential of surfactants in HIC as eluting agents [19,20]. It is suggested that non-ionic or zero net charge surfactants will have the highest potential for practical non-denaturing protein separations. This is due to the fact that these materials are known to be gentler in their action towards proteins, with less tendency to cause denaturation [21].

Recent isocratic HIC elution studies in this laboratory [20] with the zero net charge surfactant 3-[(3-cholamidopropyl)dimethylammonio]-1-propanesulphonate

0021-9673/90/$03.50

(CHAPS), have shown that this surfactant can act as an eluting agent for proteins and can also provide increased selectivity in protein separations.

However, most practical protein separations employ gradient elution to obtain maximum peak capacity and resolution. Since most proteins exhibit steep elution isotherms on RP-HPLC (and to a lesser degree on HIC stationary phases), they generally elute over a narrow range of solvent strength, making development of suitable conditions for isocratic elution of a protein mixture more difficult. For these and other well-known advantages of gradient elution, it was necessary to examine surfactant-mediated HIC in the gradient mode.

Recent studies of protein retention characteristics in both gradient elution HIC and RP-HPLC have shown them to be predictable in terms of the linear solvent-strength formalism [22–26]. Linear relationships have been observed between log k' (where k' is the capacity factor) and salt concentration for proteins in isocratic HIC [27–29]. As a consequence, protein retention in gradient elution HIC can also be modeled in terms of the linear solvent-strength formalism [24]. Thus standard HPLC optimization techniques can be applied to gradient elution protein separations by HIC.

Results from this laboratory [20] have shown that the linear relationships between the log k' and salt concentration in HIC are also observed in the presence of the surfactant CHAPS. Thus addition of a surfactant to HIC mobile phases does not affect the chromatographic predictability of the system, although changes in the eluting power and selectivity of the mobile phase are introduced. We therefore decided to determine whether chromatographically useful modifications of protein retention and selectivity can be obtained with CHAPS under various gradient conditions.

EXPERIMENTAL

Carbonic anhydrase B (human erythrocyte), ribonuclease A (bovine pancreatic), bovine pancreatic trypsin inhibitor (BPTI), enolase (Yeast Type III), α-amylase (from Bacillus, Type IIA), α-chymotrypsinogen A, aldolase (rabbit muscle, Type III) and bovine serum albumin (BSA) were obtained from Sigma (St. Louis, MO, U.S.A.). Lysozyme (hen eggwhite) was obtained from Miles Labs. (Elkhart, IN, U.S.A.). The proteins were used without further purification. Ammonium sulfate (ultra pure) was obtained from Schwarz Mann (Cambridge, MA, U.S.A.) and potassium phosphate (A.C.S. reagent) was obtained from Fisher (Fair Lawn, NJ, U.S.A.). HPLC-grade water was produced with a Milli-Q purification system. CHAPS was synthesized according to the procedure of Hjelmeland [26] and twice recrystallized from methanol.

The chromatographic system consisted of a Perkin-Elmer Model Series 3B pumping system (Norwalk, CT, U.S.A.), Perkin-Elmer Model LC75 variable-wavelength UV detector and a Waters WISP automatic sample injector (Milford, MA, U.S.A.). The chromatograms were integrated with a Spectra-Physics Model 4270 computing integrator and stored on a Spectra-Physics Chromstation AT. The chromatographic stationary phase used was 6.5-μm SynChropak Propyl HIC packing obtained from SynChrom (Linden, IN, U.S.A.). This material was packed into a 10 cm × 4.6 mm I.D. HPLC column. The column was thermostatted with a circulating water bath at 30.0 ± 0.1°C.

TABLE I

CLASSIFICATION OF GRADIENTS

All these gradients were linear, both in salt and in CHAPS.

Initial concentration		Final concentration		Gradient type
Ammonium sulfate (*M*)	CHAPS (m*M*)	Ammonium sulfate (*M*)	CHAPS (m*M*)	
1.7	0.0	1.7	0.6	I
1.7	0.6	0.0	0.6	II
1.7	0.1	0.0	3.0	III
1.7	0.6	0.0	3.0	III

Chromatographic mobile phases were prepared according to standard methods and filtered through 0.5-μm filters prior to use. All mobile phases contained 0.02 *M* potassium phosphate buffer at pH 6.1. All gradients contained an initial ammonium sulfate concentration of 1.7 *M*, with CHAPS concentrations ranging from 0 to 0.6 m*M*. The final buffer was in all cases 0.02 *M* potassium phosphate buffer with CHAPS concentrations ranging from 0 to 3 m*M*. CHAPS concentrations were chosen to be below the critical micelle concentrations [20]. All gradients were linear, with gradient times ranging from 10 to 60 min. The elution of proteins was routinely accomplished at a flow-rate of 1 ml/min, and monitored at a detector wavelength of 280 nm. Column equilibration experiments were conducted with a detector wavelength of 215 nm for the amide chromophore of CHAPS. Protein solutions were prepared at a concentration of *ca.* 1 mg/ml in 0.02 *M* phosphate buffer, pH 6.1 without CHAPS, and filtered through a 0.5-μm filter prior to injection. The injection volume was 25 μl for all the proteins.

Three basic combinations of surfactant and salt gradient are possible and were investigated in this study. They are as follows:

Type I: hold salt concentration constant while varying surfactant concentration.

Type II: vary salt concentration while holding surfactant concentration constant.

Type III: vary salt and surfactant concentrations simultaneously.

Description of the specific gradients used in this study is summarized in Table I; all gradients employed were linear. In the plots of retention time *vs.* gradient time (Figs. 1, 2, 4 and 5), lines were fit to the data with a linear least-squares program.

RESULTS AND DISCUSSION

Linear solvent strength theory

Since a linear relationship between log k' and salt concentration is observed in HIC, the linearly decreasing salt concentration gradients commonly employed for elution will yield a linear relationship between log k' and time [24]. Therefore, under these conditions the linear solvent strength (LSS) theory may be employed. This theory has been successfully employed in describing small-molecule gradient sep-

arations [22,25], and for a general description of large-molecule separations [23]. We also find an example of its application to HIC gradient separations of proteins [24]. The basic retention relation for linear solvent-strength conditions is as follows:

$$\log k_i = \log k_0 - b(t/t_0) \tag{1}$$

Where k_i is the value of k' at the column inlet during the gradient at time t, t_0 is the column dead time and k_0 is the value of k' at $t = 0$. The implication of eqn. 1 is that a linear relationship between the log of the instantaneous k' at the column head and time must apply during the gradient. The gradient steepness parameter may be described as:

$$b = \Delta\varphi S V_m / t_G F \tag{2}$$

Here $\Delta\varphi$ is the change in volume fraction of strong solvent in the gradient (*i.e.* for a 0–100% gradient $\Delta\varphi$ is 1.0), S is the slope of log k' *vs.* φ, V_m is the column dead volume, F the flow-rate, and t_G the gradient time. It can be shown that retention in gradient elution then may be expressed as:

$$t_g = (t_0/b)\log(2.3k_0 b + 1) + t_0 + t_D \tag{3}$$

Here, t_D is the correction for instrumental dwell time. In order to simplify this relationship we make the approximation $2.3bk_0 \gg 1$. Thus eqn. 3 simplifies to the following relationship:

$$t_g = t_G/\Delta\varphi S \log k_0 + t_0 + t_D \tag{4}$$

According to eqn. 4, we expect that retention time, t_g, will be linearly related to the gradient time, t_G. Since we previously observed that linear relationships are observed for log k' *vs.* salt concentration in the presence of the surfactant CHAPS in HIC [20], we would like to know if gradients containing CHAPS can be run under LSS conditions. To test this hypothesis t_g was plotted *vs.* t_G for the nine proteins in this study under Type III gradient conditions. Linear relationships were observed for all nine

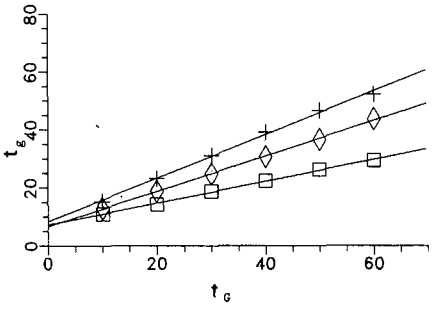

Fig. 1. Dependence of retention time (min) on gradient time (min) for the proteins carbonic anhydrase B (□), α-chymotrypsinogen A (+) and aldolase (◇). Linear gradient without CHAPS, 100% 1.7 *M* ammonium sulfate + 0.02 *M* potassium phosphate, pH 6.1 to 100% 0.02 *M* potassium phosphate, pH 6.1.

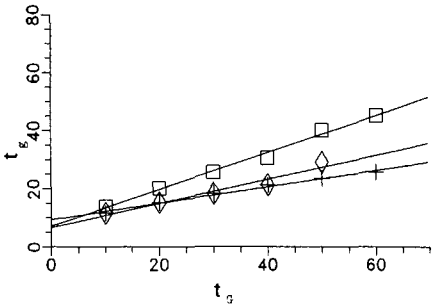

Fig. 2. Dependence of retention time (min) on gradient time (min) for the proteins α-amylase (□), BPTI (+) and enolase (◇). LSS gradient analysis, Type III bilinear gradient elution with CHAPS, 100% 1.7 *M* ammonium sulfate + 0.1 m*M* CHAPS + 0.02 *M* potassium phosphate, pH 6.1 to 100% 3.0 m*M* CHAPS + 0.02 *M* potassium phosphate, pH 6.1.

proteins. In Fig. 1, t_g *vs.* t_G is plotted for three representative proteins under gradient elution conditions without CHAPS in the mobile phase. In Fig. 2, t_g *vs.* t_G is plotted for representative data collected under Type III gradient conditions (with CHAPS present). As can easily be seen in Fig. 2, linear relationships between t_g and t_G are also observed for CHAPS-containing mobile phases in gradient elution HIC of proteins. Similarly, linear plots are obtained for Type II gradients and for the other six proteins under Type III conditions. Therefore we find that HIC separations with CHAPS can be modeled in terms of the LSS theory.

Selectivity

In order to examine the effects of CHAPS on selectivity, t_g was determined as $f(t_G)$ for the nine proteins with CHAPS (Type III gradients) and without CHAPS. Linear relationships for t_g *vs.* t_G were found in all cases, consistent with the LSS model. As shown in Table II, the effect of CHAPS varied greatly, depending on the

TABLE II

CHANGES IN t_g DUE TO CHAPS

Gradients of 60 min. Type III gradients were employed, with salt decreasing linearly from 1.70 *M* to 0 *M* ammonium sulfate, and [CHAPS] increasing linearly from 0.6 m*M* to 3.0 m*M*. With values of t_G ranging from 10 to 60 min, plots of t_g *vs.* t_G were fit with a linear least-squares program. Least-squares values of t_g with and without CHAPS were used to obtain $\Delta t_g = t_g$ (with CHAPS) $- t_g$ (without CHAPS).

Protein	t_g (without CHAPS)	Δt_g (min)
α-Amylase	45.9	− 3.7
Aldolase	43.1	− 0.8
BPTI	31.1	− 6.9
BSA	60.6	−17.5
Carbonic anhydrase	29.8	− 9.5
α-Chymotrypsinogen	53.3	− 7.9
Enolase	28.0	−13.7
Lysozyme	29.9	− 7.1
Ribonuclease A	16.7	− 4.9

protein. With t_g = 60 min the decrease in t_g due to CHAPS ranged from 0.8 min (aldolase) to 17.5 min (BSA). These reductions in t_g correspond to 1.8% and 30% respectively. It is therefore evident that the CHAPS shows strong selectivity in the gradient mode, consistent with what we have already shown for isocratic HIC [20].

Operational characteristics

Selectivity effects in Type I gradient elution were not investigated, as this mode of chromatography is more difficult to carry out. This is because of the difficulty of finding a suitable retention window of salt and surfactant concentrations such that proteins are retained strongly without CHAPS and weakly retained with CHAPS in the mobile phase. However, one such window was found for the protein carbonic anhydrase B. Fig. 3 shows the elution of this protein under Type I gradient conditions. The Type I gradient experiment was carried out using an initial CHAPS step gradient of 0–0.6 m*M* at a constant ammonium sulfate concentration of 1.7 *M*. The large peak observed in the chromatogram at about 5–10 min is caused by the breakthrough of a small amount of solvent impurity in the CHAPS (identified by gas chromatography as dimethylformamide). The detector was re-zeroed at about 10 min to keep the entire chromatogram on scale. Breakthrough of CHAPS ocurred at approximately 60 min, followed by the carbonic anhydrase B peak at approximately 70 min, as [CHAPS] in the mobile phase continued ro rise, approaching equilibrium.

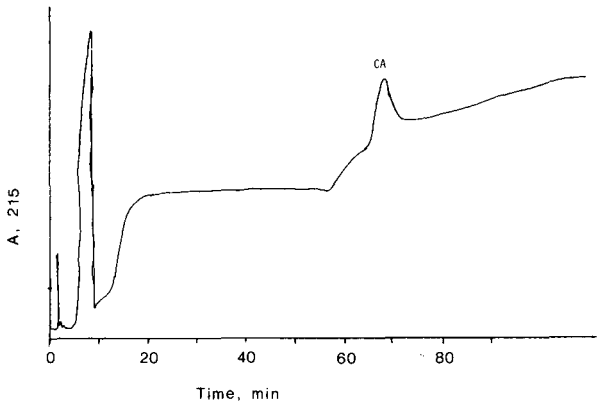

Fig. 3. Type I gradient elution of carbonic anhydrase B (CA). At t_0 a step gradient of 0 to 0.6 m*M* CHAPS in 1.70 *M* ammonium sulfate + 0.02 *M* potassium phosphate was introduced. The apparent peak at 5–10 min is an artifact caused by the breakthrough of a small amount of solvent impurity, followed by re-zeroing the detector at a time corresponding to the apparent peak maximum. Re-zeroing was necessary to keep the entire chromatogram on scale.

The extent of change of retention time for Type III gradient elution is affected by the initial CHAPS concentration. Fig. 4 shows the effect of increasing the initial surfactant concentration from 0.1 to 0.6 m*M* on the retention time of BPTI. As this example shows, the magnitude of the change in retention time increases with the initial CHAPS concentration. The protein BPTI shows a small decrease in retention with an initial mobile phase concentration of 0.1 m*M* CHAPS in Type III gradient elution. When the initial CHAPS concentration is increased to 0.6 m*M*, a significantly

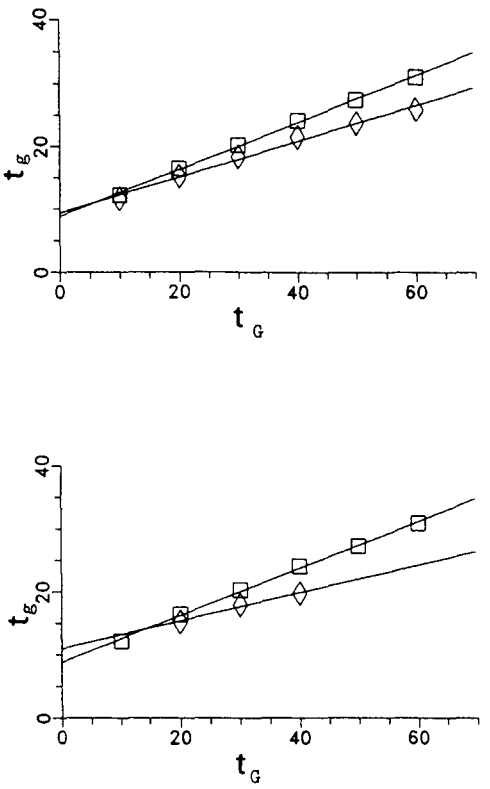

Fig. 4. Effect of initial CHAPS concentration on the retention of the protein BPTI in Type III gradient elution. Type III bilinear gradient elution with CHAPS (◇), 100% 1.7 *M* ammonium sulfate + 0.1 m*M* CHAPS (top) or 0.6 m*M* CHAPS (bottom) to 100% 3 m*M* CHAPS + 0.02 *M* potassium phosphate, pH 6.1. Gradient elution without CHAPS (□), 100% 1.7 *M* ammonium sulfate + 0.02 *M* potassium phosphate, pH 6.1 to 100% 0.02 *M* potassium phosphate, pH 6.1. Retention and gradient times in min.

larger decrease in retention time is seen for BPTI. A similar pattern was observed for lysozyme.

Protein retentions in Type II and Type III gradient elution modes were also compared. Fig. 5 shows the effect of the two gradient modes on α-chymotrypsinogen A. Contrary to our expectation of shorter retention times with Type III gradients (compared to Type II), the data show no significant differences. We believe that this is the result of the appreciable lag time between t_0 and the time required to load the stationary phase with surfactant. Substantial lag times are evident in both Fig. 3 (0–60 min) and Fig. 6 (50–85 min). This is discussed further in the following section.

Equilibration

In order to study equilibration requirements of the HIC column after execution of a surfactant gradient, blank elution profiles were recorded, using a detector wavelength where CHAPS exhibits significant UV absorbance, *i.e.* 215 nm. The resulting blank elution profiles are shown in Fig. 6 (Type II) and Fig. 7 (Type III). For Type II

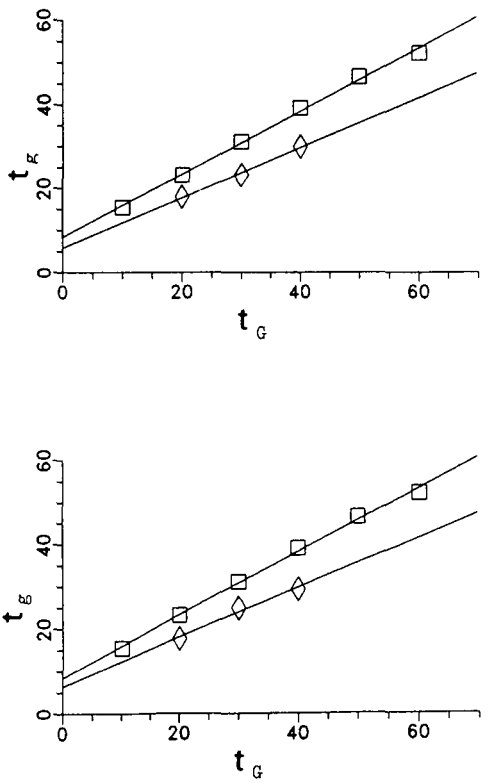

Fig. 5. Type II *vs.* Type III gradient elution for α-chymotrypsinogen A. (Top) Type II linear gradient elution with CHAPS (◇): 100% 1.7 *M* ammonium sulfate + 0.6 m*M* CHAPS + 0.02 *M* potassium phosphate, pH 6.1 to 100% 0.6 m*M* CHAPS + 0.02 *M* potassium phosphate, pH 6.1. (Bottom) Type III bilinear gradient elution with CHAPS (◇): 100% 1.7 *M* ammonium sulfate + 0.6 m*M* CHAPS + 0.02 *M* potassium phosphate, pH 6.1 to 100% 3 m*M* CHAPS + 0.,02 *M* potassium phosphate, pH 6.1. Gradient elution without CHAPS, 100% 1.7 *M* ammonium sulfate + 0.02 *M* potassium phosphate, pH 6.1 to 100% 0.02 *M* potassium phosphate, pH 6.1. □ = Retention times without CHAPS. Retention and gradient times in min.

gradients a number of features are observable. First, at a point near the end of the gradient (approximately 22 min), a large peak is observed. This is believed to be due to the elution of CHAPS from the stationary phase. Shortly after returning to initial conditions at the end of the gradient, a large negative deflection is observed at approximately 48 min. This corresponds to removal of CHAPS from the mobile phase by adsorption onto the stationary phase for reequilibration of the stationary phase surface. This is expected, since with a decrease in mobile phase salt concentration, the equilibrium amount of CHAPS adsorbed on the SynChropak propyl stationary phase surface decreases [20]. Thus, CHAPS adsorbed on the stationary phase at the initially high salt concentration at the start of the gradient would be expected to be eluted from the column as the salt concentration decreases in the gradient. After reequilibration of the stationary phase surface, breakthrough of the CHAPS-containing mobile phase is seen at 80–90 min followed by a return to the original baseline at

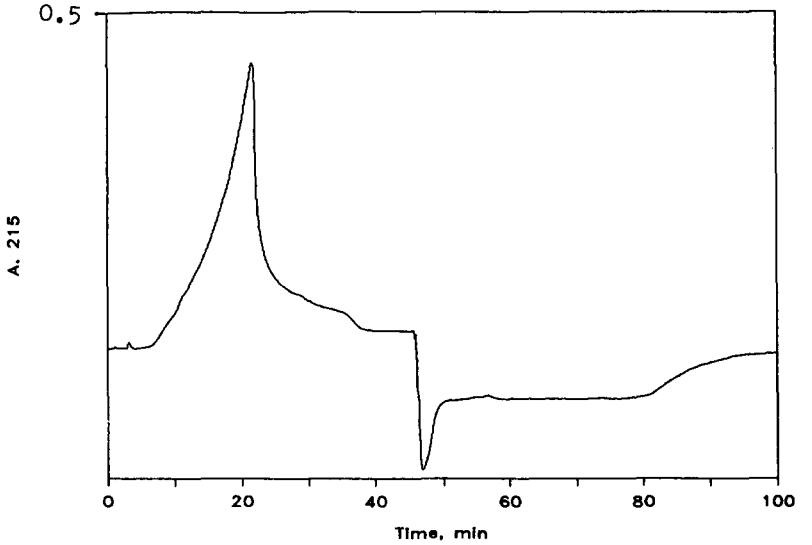

Fig. 6. Type II gradient equilibration with 0.2 m*M* CHAPS. Blank gradient on SynChropak propyl, 10 cm × 4.6 mm I.D., 100% 1.7 *M* ammonium sulfate + 0.2 m*M* CHAPS + 0.02 *M* potassium phosphate, pH 6.1 to 100% 0.2 m*M* CHAPS + 0.02 *M* potassium phosphate, pH 6.1. A.u.f.s. = 0.5.

100 min. In these studies reequilibration times of 60–90 min were employed, depending on column volume and surfactant concentration. Increase in the mobile phase concentrations of CHAPS or ammonium sulfate leads to increased adsorption of CHAPS on the stationary phase and a longer time for equilibration. Longer equili-

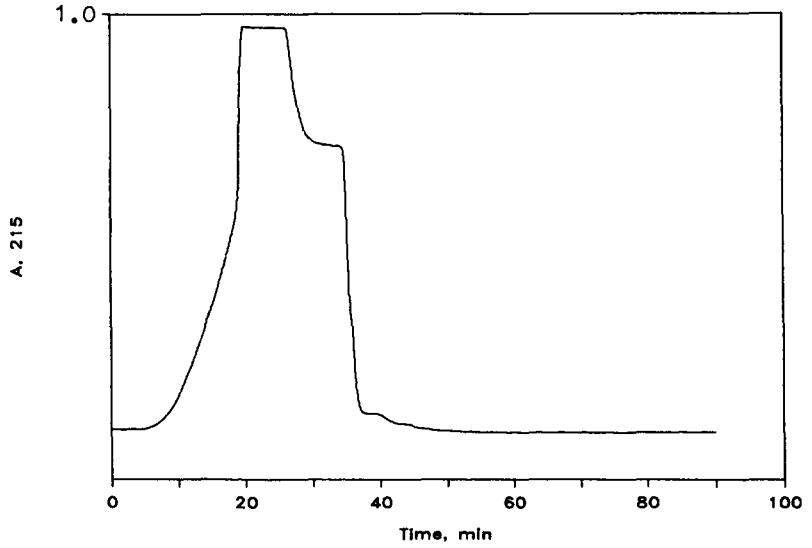

Fig. 7. Type III gradient equilibration. Blank bilinear gradient on SynChropak propyl, 10 cm × 4.6 mm I.D., 100% 1.7 *M* ammonium sulfate + 0.6 m*M* CHAPS + 0.02 *M* potassium phosphate, pH 6.1 to 100% 3 m*M* CHAPS + 0.02 *M* potassium phosphate, pH 6.1. A.u.f.s. = 1.0.

bration times result from atypical adsorption isotherms and the marked depletion of surfactant from the mobile phase [20,31,32] while the stationary phase is being loaded. The effect is seen clearly in the determination of adsorption isotherms by frontal analysis [20,31,32].

Type III gradients (Fig. 7), exhibit some significant differences from Types I and II. (Note: comparison of Figs. 6 and 7 should allow for the difference in absorbance scales.) First, the magnitude of the peak observed near the end of the gradient (*i.e.* the "CHAPS peak") is larger than for Type II. This is probably due to the combined effects of increasing [CHAPS] and decreasing $[(NH_4)_2SO_4]$ in the Type III gradient as compared with only decreasing $[(NH_4)_2SO_4]$ in the Type III gradient. Furthermore, the negative deflection observed in Type II gradient elution is not present in Type III. The breakthrough of CHAPS-containing mobile phase after reequilibration of the column is also missing. No negative peak is observed at the return to initial conditions at 40 min, and the detector signal returns immediately to the original baseline value. Also no breakthrough of CHAPS was noted at the end of the equilibration period. Therefore the required equilibrations for our Type III gradients are much shorter than for Type II gradients. Typically, equilibration times of 15–20 min were used in this study. These equilibration requirements are comparable to those required in conventional high-performance HIC separations without surfactant. Since we have not carried out an extensive survey of different Type III gradients, we cannot be sure that rapid equilibration will always be obtained. Nonetheless it appears likely that Type III gradient will be preferred for repetitive analyses.

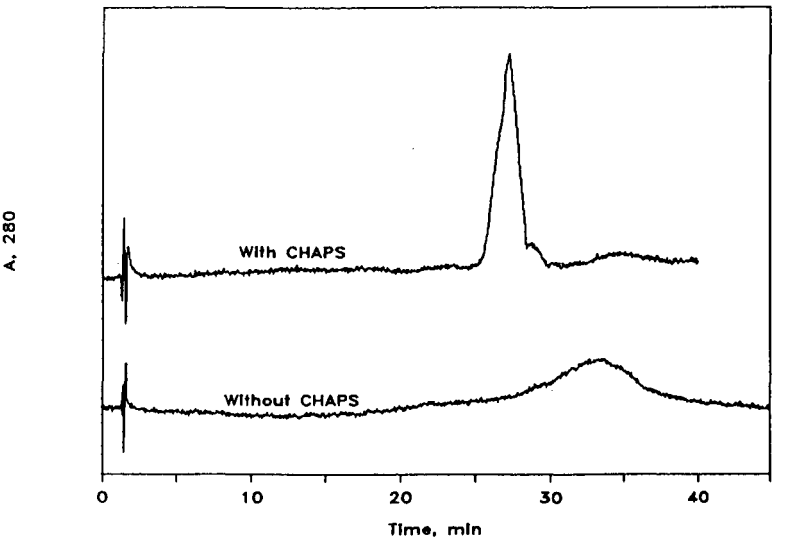

Fig. 8. The effect of CHAPS on the peak shape of bovine serum albumin in gradient elution. Lower curve: 100% 1.7 *M* ammonium sulfate + 0.02 *M* potassium phosphate, pH 6.1 to 100% 0.02 *M* potassium phosphate, pH 6.1. Linear gradient of 30 min with a 15-min hold at final conditions. Gradient elution with CHAPS (upper curve) is Type III: 0.6 m*M* CHAPS linearly increasing to 3.0 m*M* CHAPS at 30 min, superimposed on the salt gradient for the lower curve.

Peak shapes

Almost all the proteins examined in this study produced chromatographic peaks of normal shape with or without the presence of CHAPS. However, the protein bovine serum albumin (BSA) has been reported to yield distorted peak shapes in HIC [4]. We therefore decided to examine the effect of CHAPS on the peak shape of this protein in gradient elution HIC. When BSA is eluted from a SynChropak propyl HIC column it elutes as a broad distorted peak with a much larger bandwidth than the other proteins in this study (Fig. 8). When CHAPS is added to the mobile phase, the retention time is considerably reduced and a narrowed, less distorted peak results. The presence of CHAPS had negligible effects on peak shapes of the eight other proteins in this study. We assume that distortion of the BSA peak in the absence of CHAPS is the result of sluggish conformational equilibria in the protein [27]. On this assumption it appears that CHAPS has the effect of either shifting the equilibrium or of speeding rate-limiting conformation interconversions. Another possibility is binding of BSA to the stationary phase surface followed by a conformational change induced by the stationary phase. This mechanism has been reported for the reversed-phase chromatography of proteins [9]. In the presence of CHAPS we know that BSA is bound less tightly to the stationary phase surface, possibly reducing conformational instability induced by contact with the stationary phase.

ACKNOWLEDGEMENTS

This work was initiated with a grant form Pharmacia-LKB Biotechnology Group and supported in its later stages by NSF grant CHE-8707592. We thank Dr. Richard Brantley for synthesis of the CHAPS, and Dr. Joseph Glajch for the preparation of packed HPLC columns. The SynChropak Propyl packing material was a gift from SynChrom Inc.

REFERENCES

1 J. L. Fausnaugh, E. Pfannkoch and F. E. Regnier, *Anal. Biochem.*, 137 (1984) 464.
2 L. A. Kennedy, W. Kopciewicz and F. E. Regnier, *J. Chromatogr.*, 359 (1986) 464.
3 M. N. Schmuck, M. P. Nowlan and K. M. Gooding, *J. Chromatogr.*, 371 (1986) 55–62.
4 Y. Kato, Y. Kitamura and T. Hashimoto, *J. Chromatogr.*, 360 (1986) 260.
5 S. C. Goheen and S. C. Englehorn, *J. Chromatogr.*, 317 (1984) 55.
6 N. T. Miller, B. Feibush and B. L. Karger, *J. Chromatogr.*, 316 (1984) 519.
7 J. L. Fausnaugh, L. A. Kennedy and F. E. Regnier, *J. Chromatogr.*, 317 (1984) 141.
8 S. A. Cohen, K. Benedek and Y. Taphui, *Anal. Biochem.*, 144 (1985) 275.
9 K. Benedek, S. Dong and B. L. Karger, *J. Chromatogr.*, 317 (1984) 227.
10 X. Lu, K. Benedek and B. L. Karger, *J. Chromatogr.*, 359 (1986) 19.
11 S. A. Cohen, K. P. Benedek, S. Dong, Y. Tapuhi and B. L. Karger, *Anal. Chem.*, 56 (1984) 217.
12 J. Steinhardt, J. R. Scott and K. S. Birdi, *Biochemistry*, 16 (1977) 718.
13 W. G. Tramposch and S. G. Weber, *Anal. Biochem.*, 58 (1986) 3006.
14 A. Berthod, I. Girard and C. Gonnet, *Anal. Chem.*, 58 (1986) 1362.
15 A. Berthod, I. Girard and C. Gonnet, *Anal. Chem.*, 58 (1986) 1359.
16 A. Berthod, I. Girard and C. Gonnet, *Anal. Chem.*, 58 (1986) 1356.
17 J. G. Dorsey, *Chromatography*, 2, No. 4 (1987) 13.
18 J. P. Chang, *J. Chromatogr.*, 317 (1984) 157.
19 D. B. Wetlaufer and M. Koenigbauer, *J. Chromatogr.*, 359 (1986) 55.
20 J. J. Buckley and D. B. Wetlaufer, *J. Chromatogr.*, 464 (1989) 61–71.

21 L. M. Hjelmeland, *Methods Enzymol.*, 124 (1986) 135.
22 L. R. Snyder, in Cs. Horváth (Editor), *High-Performance Liquid Chromatography, Advances and Perspectives,* Vol. 1, Academic Press, New York, 1980 p. 207.
23 L. R. Snyder and M. A. Stadalius, in Cs. Horváth (Editor), *High-Performance Liquid Chromatography, Advances and Perspectives,* Vol. 4, Academic Press, New York, 1986, p. 195.
24 N. T. Miller and B. L. Karger, *J. Chromatogr.*, 326 (1986) 45.
25 M. A. Quarry, R. L. Grob and L. R. Snyder, *Anal. Chem.*, 58 (1986) 97.
26 L. M. Hjelmeland, *Proc. Natl. Acad. Sci. U.S.A.*, 77 (1980) 6368.
27 W. Melander and C. Horvath, *Arch. Biochem. Biophys.*, 183 (1977) 200.
28 J. L. Fausnaugh and F. E. Regnier, *J. Chromatogr.*, 359 (1986) 131.
29 W. Melander, D. Corradini and Cs. Horváth, *J. Chromatogr.*, 317 (1984) 67.
30 E. Parente and D. B. Wetlaufer, *J. Chromatogr.*, 314 (1984) 337.
31 J. J. Buckley, *Ph. D. Thesis,* University of Delaware, Newark, DE, 1989.
32 J. J. Buckley and D. B. Wetlaufer, in preparation.

Journal of Chromatography, 518 (1990) 111–121
Elsevier Science Publishers B.V., Amsterdam

CHROM. 22 569

Water-soluble proteins do not bind octyl glucoside as judged by molecular sieve chromatographic techniques

PER LUNDAHL* and ERIK MASCHER
Department of Biochemistry, Biomedical Centre, University of Uppsala, P.O. Box 576, S-751 23 Uppsala (Sweden)
and
KEIICHI KAMEYAMA and TOSHIO TAKAGI
Institute for Protein Research, Osaka University, 3–2 Yamadaoka, Suita, Osaka 565 (Japan)
(First received January 30th, 1990; revised manuscript received May 14th, 1990)

ABSTRACT

It is well known that the non-ionic detergent octyl glucoside (1-O-*n*-octyl-β-D-glucopyranoside) solubilizes biological membrane components. It forms complexes with membrane-spanning proteins by hydrophobic interactions and it forms mixed micelles with membrane lipids. In contrast, non-ionic detergents usually do not bind to water-soluble proteins. According to a recent report, substantial and cooperative binding of octyl glucoside to several water-soluble proteins does occur near the critical micelle concentration. However, data have been obtained that contradict this report. No decrease was found in the elution volumes of five water-soluble proteins on molecular sieve chromatography on two Superose columns in tandem when 35 m*M* octyl glucoside was included in the eluent. No binding of the detergent to these proteins was observed at 20 or 22.5 m*M* octyl glucoside on molecular sieve chromatography on a TSK SW guard column as determined by differential refractometry and UV spectrophotometry of the proteins in the absence or presence of octyl glucoside. The experiments were done with the same buffer system and with six of the proteins used in the reported study. It is concluded that, as expected, there is no binding of octyl glucoside to water-soluble proteins above the detection limit (0.1 g detergent/g protein) of the refractometric method. The binding of, on average, 1.3 ± 0.2 g of detergent per gram of water-soluble protein that was observed at 20 m*M* octyl glucoside in the reported study is not consistent with the present results.

INTRODUCTION

Octyl glucoside (1-O-*n*-octyl-β-D-glucopyranoside) has a high solubilizing capacity for some membrane proteins [1–7] and does not usually affect the biological acitivity of membrane proteins and water-soluble enzymes [8–11]. However, the reconstituted activity of monosaccharide transporters may decrease if essential lipids are displaced from the protein on solubilization or fractionation [9,10,12]. The relative micellar mass of octyl glucoside at room temperature and near the critical micelle concentration is 21 000–25 000 [13–15]. The value of 8000 reported earlier [16] is an underestimate. The micelle size seems to become heterogeneous as the octyl glucoside concentration is increased [14]. In water, at 22°C, the micellar hydrodynamic radius is 2.35 nm [15]. The high critical micelle concentration of 23–25 m*M* [15–17] makes

0021-9673/90/$03.50

octyl glucoside easy to remove by molecular sieve chromatography or dialysis, for the preparation of proteoliposomes in reconstitution experiments [10,18]. The critical micelle concentration of octyl glucoside decreases with increasing ionic strength [17] and increases as the temperature is decreased from 25°C [15]. Some membrane proteins have been crystallized in the presence of octyl glucoside [13,19–21]. Results from X-ray crystallographic studies of the octyl glucoside–bacteriorhodopsin complex [20] were interpreted as an interaction of the detergent only with the hydrophobic parts of the protein, whereas the hydrophilic ends of the protein molecules bind to each other and thus build up the crystal lattice [21, 22]. Octyl glucoside has also been reported to show effects on the crystallization of water-soluble proteins [23].

A knowledge of the structures of the complexes between amphiphilic proteins and octyl glucoside, in addition to other non-ionic or zwitterionic detergents, is important in membrane biochemistry. Essential aspects are the state of association of the solubilized proteins and the sizes of their monomeric complexes with the detergent, which can be determined by molecular sieve chromatography [10,24]. Quantitative determinations can be made by low-angle laser light-scattering (LALLS) photometry, differential refractometry and UV absorbance photometry of eluates from high-performance gel chromatographic columns [25,26].

Non-ionic detergents do not bind to water-soluble proteins according to the few reports that we have found [27–30]. This is not surprising as the hydrophobic hydrocarbon moieties of the detergent molecules probably do not interact with the mainly hydrophilic surfaces of water-soluble proteins, at moderate ionic strengths. However, results suggesting substantial binding of octyl glucoside to several water-soluble proteins, at low ionic strength, below the critical micelle concentration and in proportion to the molecular weights of the proteins, have recently been reported [11]. Enzymes nevertheless had the same activities in the absence as in the presence of octyl glucoside [11]. The results were interpreted as indicating incorporation of each protein molecule into an octyl glucoside micelle. This seems unlikely as no denaturation occurred and as the protein surfaces are mainly hydrophilic, whereas the interior of an octyl glucoside micelle is hydrophobic.

To verify or disprove these data, we have now studied the effect of octyl glucoside on the elution volumes of some water-soluble proteins on molecular sieve chromatography on Superose columns. If a globular protein binds a large amount of octyl glucoside (as reported by Cordoba *et al.* [11]), the corresponding decrease in elution volume can easily be detected [31]. We have also attempted to detect octyl glucoside binding to some water-soluble proteins by differential refractometry combined with UV spectrophotometry for monitoring the proteins on high-performance molecular sieve chromatography, in the absence and presence of octyl glucoside, on a TSK SW guard column. This procedure allows the determination of binding by use of the ratios between the refractometer and spectrophotometer signals [26]. The results of the above two methods are internally consistent but they contradict the results of Cordoba *et al.* [11]. By use of equilibrium dialysis and infrared spectrometry, about fifteen binding sites for octyl glucoside monomers per bovine serum albumin molecule have also been found [32]. However, this value is below our detection limit of 0.1 g detergent/g protein, or about 20 octyl glucoside monomers per albumin molecule.

EXPERIMENTAL

Materials

For elution volume determinations, octyl glucoside (No. O-8001), ribonuclease A (Type 1-A; No. R 4875), ovalbumin (Grade V; No. A 5503), bovine serum albumin ("essentially fatty acid free"; No. A 7030), fibrinogen from human plasma (Type 1; No. F 3879), bovine catalase (No. C 100) and *Aspergillus niger* catalase (No. C 3515) were bought from Sigma (St. Louis, MO, U.S.A.). All chemicals were of analytical-reagent grade. Solutions were passed through 0.2-μm filters (SM 11107; Sartorius, Göttingen, F.R.G.) and simultaneously degassed.

For binding measurements, octyl glucoside was bought from Dojin Chemicals (Kumamoto, Japan) and bovine serum albumin preparations (No. 001, "fatty acid free" and No. 002, "reagent grade") from Chiba Chikusan Kogyo (Chiba, Japan). Other proteins were from the same source as above. Solutions were filtered through 0.3-μm filters (PHWP 04700; Nihon Millipore Kogyo, Yonezawa, Japan).

Methods

Molecular sieve chromatographic experiments. These experiments, for comparison of protein elution volumes in the absence or presence of octyl glucoside, were done on prepacked 23-ml (28 × 1 cm I.D.) columns of Superose-12 and Superose-6 cross-linked agarose gels connected in tandem, unless stated otherwise. A mixture containing all of the six proteins studied was usually applied. For peak identifications the proteins were also applied separately. In a series of experiments on the possible time dependence of binding of octyl glucoside, only the Superose-6 column was used. In these latter experiments bovine serum albumin and bovine catalase were studied. The proteins were fractionated separately on the Superose-6 column. All experiments were done at room temperature (23 ± 1°C).

The columns were equilibrated with 25 m*M* sodium phosphate buffer (pH 6.4) containing 0.1 *M* NaCl (as used in ref. 11) in the presence or absence of 35 m*M* octyl glucoside, with at least five column volumes of the solution to be used. The sample volume was 500 μl. The flow-rate was 0.3 ml/min. The chromatographic equipment [31] used for the above experiments was provided by Pharmacia LKB Biotechnology (Uppsala, Sweden).

Differential refractometric measurements. The proteins were applied, one by one, to a 3.3-ml (7.5 × 0.75 cm I.D.) TSK SW guard column, at room temperature (25 ± 1°C). The column was connected to a high-speed liquid chromatograph (Type CCPD) equipped with a degasser (ERC-3522). The eluate was monitored by a UV spectrophotometer (UV-8010) and by the LALLS instrument LS-8000, which contains a light-scattering detector and a differential refractometer (RI-8011). All the above pieces of equipment were obtained from Tosoh (Tokyo, Japan), except the degasser, which was from Erma Optical Works (Kawaguchi, Japan).

The solutions used were the same as for molecular sieve chromatography except that 3 m*M* sodium azide and 0, 20 or 22.5 m*M* octylglucoside were included. The sample volume was 100 μl and the flow-rate was 0.2 ml/min.

The TSK SW guard column was chosen as it affords a resolution high enough for the present purpose, and as its small volume gives short run times. The amount of the expensive octyl glucoside consumed is also minimized.

A procedure similar to that described above has recently been developed for the determination of sodium dodecyl sulphate (SDS) binding to proteins above the critical micelle concentration [33]. This procedure is based on the decrease in the refractometer signal from the micelles in samples with known amounts of SDS when part of the micellar detergent binds to protein molecules. It gave higher binding ratios than those obtained by earlier methods.

Sample preparation

Experiments with Superose columns. The proteins were dissolved together in 25 m*M* sodium phosphate buffer, (pH 6.4), prepared from Na_2HPO_4 and NaH_2PO_4, containing 100 m*M* NaCl, unless stated otherwise. The protein concentrations were ribonuclease A 3, ovalbumin 3, bovine serum albumin 3.2, fibrinogen 1.4, bovine catalase 1.6 and *Aspergillus niger* catalase 1.6 mg/ml. The protein solutions were passed through 0.2-μm Acrodisc-13 filters (Gelman, Ann Arbor, MI, U.S.A.).

The protein stability and octyl glucoside binding to bovine catalase and bovine serum albumin during incubations with octyl glucoside for several days were also tested. Separate samples of the proteins (concentrations as above) were incubated at 25°C in the absence or presence of 50 m*M* octyl glucoside in the above solution. This detergent concentration is sufficient to obtain the binding levels reported in ref. 11. After 20, 90 and 120 h, 500-μl aliquots of the samples were applied separately to a Superose-6 column.

Binding measurements. The proteins were dissolved separately at a concentration of 1.0 mg/ml in 25 m*M* sodium phosphate buffer (pH 6.4) containing 100 m*M* NaCl and 3 m*M* NaN_3 or, for experiments in the presence of octyl glucoside, in the above solution containing 22.5 m*M* octyl glucoside. The samples for runs at 20.0 or 22.5 m*M* octyl glucoside were dialysed overnight against buffer solution containing 22.5 m*M* octyl glucoside (the dialysis volume was ten times the sample volume). All samples were filtered through 0.22-μm filters (Type SLGV025LS; Nihon Millipore Kogyo).

Evaluation

Elution volumes. A difference in the elution volume (ΔV_e) of 30 μl can be detected in the Superose chromatographic experiments. According to a graph of V_e *vs.* log M_r for the proteins studied (not shown), $\Delta V_e = 30$ μl corresponds to an increase in molecular weight of 1% and an increase in radius for a globular protein of 0.3%. Massive binding of octyl glucoside, as reported by Cordoba *et al.* [11], can thus easily be detected as a decrease in V_e in the molecular sieve chromatographic experiments.

Binding. The refractometer signal, $(\text{Output})_{RI}$, can be expressed as

$$(\text{Output})_{RI} = k_1(dn/dc)c \quad (1)$$

where k_1 is a constant, dn/dc is the specific refractive index increment and c is the weight concentration of the protein. The UV absorbance signal, $(\text{Output})_{UV}$, can be expressed as

$$(\text{Output})_{UV} = k_2Ac \quad (2)$$

where k_2 is a constant and A is the absorption coefficient, based on weight concentration. This gives

$$dn/dc = k_3\{(\text{Output})_{RI}/[(\text{Output})_{UV}/A]\} \quad (3)$$

where k_3 is a constant.

The refractive index increment for a solution of the complex between detergent (D) and protein (P) with respect to the protein concentration, at constant chemical potential of diffusible components, $(\partial n/\partial c_P)_\mu$, can be expressed as [34]

$$(\partial n/\partial c_P)_\mu = (\partial n/\partial c_P)\{1 + \xi[(\partial n/\partial c_D)_c/(\partial n/\partial c_P)_c]\} \quad (4)$$

where ξ is the binding ratio (w/w), $(\partial c_D/\partial c_P)_\mu$, of detergent to protein, assuming that the system can be regarded as a three-component system (protein, detergent, aqueous solution). Thus,

$$\xi = (R-1)(\partial n/\partial c_P)_c/(\partial n/\partial_D)_c \quad (5)$$

where $R = (\partial n/\partial c_P)_\mu/(\partial n/\partial c_P)_c$, $(\partial n/\partial c_P)_c = 0.187$ ml/g [26] and $(\partial n/\partial c_D)_c = 0.138$ ml/g, as determined for octyl glucoside micelles [15]. According to eqn. 3,

$$R = [(\text{Output})_{RI}/(\text{Output})_{UV}]_{DP} / [(\text{Output})_{RI}/(\text{Output})_{UV}]_P \quad (6)$$

where DP denoting values in the presence of octyl glucoside and P values in the absence of detergent. The peak heights were measured. R was calculated according to eqn. 6 and finally the binding values ξ (g octyl glucoside/g protein) were calculated according to eqn. 5, which, with the above numerical values, can be written as

$$\xi = 1.355(R-1)$$

The limits of error (see Table I) are based on the sums of the standard deviations (σ_{n-1}) for the peak-height ratios in eqn. 6.

For a complete description of this methodology, see ref. 26.

RESULTS

Elution volumes

Fractionation on the tandem Superose-12 and Superose-6 columns (see *Methods*) showed that the presence of 35 mM octyl glucoside (*i.e.*, well above the critical micelle concentration) did not detectably affect the elution volumes of five of the six proteins studied, compared with fractionation in the absence of the detergent. The elution volumes were constant (Fig. 1). The only exception was fibrinogen, which was eluted earlier in the presence of 35 mM octyl glucoside than in the absence of detergent. The decrease in elution volume was small, about 300 μl (*cf.*, Fig. 1). This corresponds to an increase in M_r of *ca.* 17 000 for a globular protein or to about 60 octyl glucoside molecules to one protein molecule. However, as no binding to fibrinogen was detected by the refractometric method (see below), a plausible explanation

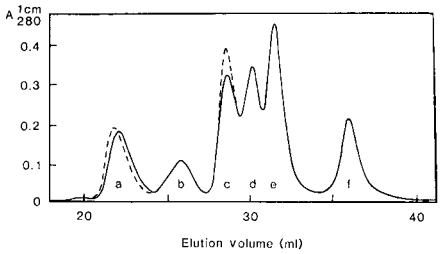

Fig. 1. Fractionation of six water-soluble proteins on a Superose-12 and a Superose-6 column in tandem, equilibrated with 25 m*M* sodium phosphate buffer (pH 6.4), containing 0.1 *M* NaCl, without detergent (solid line) or with 35 m*M* octyl glucoside (dashed line). Flow-rate, 0.3 ml/min; sample volume, 500 μl. The columns were equilibrated with at least five column volumes of the solution to be used. After equilibration in the detergent-free solution, ten 500-μl aliquots of the protein sample were applied one by one. No change in the elution pattern was observed. After equilibration with at least five column volumes of solution containing 35 m*M* octyl glucoside, six 500-μl aliquots of the protein sample were chromatographed as above with about two column volumes of eluent for each run. The elution patterns were identical in all six runs, within the narrow limits set technically by the sample application device, the monitor and the recorder. Finally, the columns were again equilibrated with detergent-free solution and four 500-μl aliquots of the protein sample were fractionated. The elution patterns were identical with the ten previous patterns in the absence of detergent. The studied proteins were (a) fibrinogen, (b) *Aspergillus niger* catalase, (c) bovine catalase, (d) bovine serum albumin, (e) chicken ovalbumin and (f) ribonuclease A. The elution peaks of these proteins are indicated. The decrease in elution volume for fibrinogen (a) with octyl glucoside may reflect decreased retardation rather than detergent binding (*cf.*, Results, *Elution volumes*). The reason for the increase in peak height for bovine catalase (c) in the presence of octyl glucoside is not known.

may be that fibrinogen was slightly retarded, by weak adsorption effects, in the Superose columns, in the absence of octyl glucoside.

Chromatography on Superose-6 of bovine catalase and bovine serum albumin after long incubation times in the presence of 50 m*M* octyl glucoside showed no differences in the elution volumes of these proteins compared with chromatography after incubations in the absence of detergent (not illustrated). The elution volumes were also the same whether the fractionations were done in the presence of octyl glucoside or not.

Binding

A series of high-performance gel chromatographic experiments with differential refractometric and UV spectrophotometric monitoring failed to detect any binding of octyl glucoside to any of the water-soluble proteins studied (Table I). The high resolution of the TSK SW guard column is illustrated in Fig. 2. Only with ribonuclease A was the refractometric peak sometimes slightly disturbed by minor total-volume valleys or peaks. A binding of, on the average, 1.3 g of octyl glucoside per gram of protein at an equilibrium concentration of 20 m*M* octyl glucoside (as calculated from the $\bar{v}$ values in Table I in ref. 11) is more than ten times higher than our detection limit of 0.1 g detergent/g protein.

DISCUSSION

Binding of detergents to proteins can be divided into two main categories, (I)

TABLE I

ATTEMPT TO DETECT OCTYL GLUCOSIDE BINDING TO WATER-SOLUBLE PROTEINS BY HIGH-PERFORMANCE GEL CHROMATOGRAPHY[a] MONITORED BY DIFFERENTIAL REFRACTOMETRY AND UV SPECTROPHOTOMETRY[b]

Protein[c]	Bound octyl glucoside (g/g protein)	
	$C_{OG} = 20$ mM[d]	$C_{OG} = 22.5$ mM[d]
Ribonuclease A	-0.01 ± 0.02	–
Ovalbumin	-0.04 ± 0.02	-0.04 ± 0.02
Bovine serum albumine[e]	0.00 ± 0.02	0.02 ± 0.02
Bovine serum albumin[f]	0.00 ± 0.02	0.00 ± 0.03
Bovine catalase	-0.03 ± 0.02	-0.03 ± 0.01
Fibrinogen[g]	0.00 ± 0.01	0.01 ± 0.02
Average: -0.01 ± 0.02 ($n = 11$)		

[a] Three to five runs for each protein on a TSK SW guard column for each of the octyl glucoside concentrations 0, 20 and 22.5 mM.

[b] Details in *Methods*.

[c] See *Materials*.

[d] Equilibrium concentration in the chromatographic column. For runs in 20 and 22.5 mM octyl glucoside the samples were dialysed against 22.5 mM octyl glucoside (in buffer).

[e] "Fatty-acid free".

[f] "Reagent grade".

[g] Fibrinogen was partly adsorbed on the prefilter or column in the first two runs in the absence of octyl glucoside. Only the two following runs were used for the calculations.

non-denaturing binding of non-ionic or zwitterionic detergents to amphiphilic proteins, by hydrophobic interaction, and (II) denaturing binding of ionic detergents to amphiphilic and hydrophilic proteins.

Examples of the Type-I binding are complexes between octyl glucoside and the human red cell glucose transporter [10,24] and the octaethylene glycol *n*-dodecyl ether complex with canine renal Na^+/K^+-ATPase [35]. Both of these proteins are integral membrane proteins.

Type-II binding is found in SDS complexes of water-soluble and membrane proteins. It is still not clear why SDS and other ionic detergents bind not only hydrophobically to amphiphilic proteins but also to water-soluble proteins. Binding of SDS dramatically affects the protein structure. A hypothesis on the course of events during interactions between SDS and water-soluble proteins is outlined in ref. 31.

Non-ionic detergents, on the other hand, can presumably not generally bind to the surfaces of water-soluble, hydrophilic proteins. The hydrophobic interactions that may occur with some grooves or patches of the surface of a hydrophilic protein are probably insufficient to allow cooperative binding of detergent.

The glucose moiety of octyl glucoside is large ($M_r = 179$) compared with the the alkyl chain ($M_r = 113$). The number of monomers in a micelle is also large (87 according to ref. 15). This indicates a compact structure in the hydrophilic shells of the octyl glucoside micelle, as illustrated in Fig. 3A. In reality the alkyl chains are probably staggered [15]. Octyl glucoside micelles may interact with surfaces of water-soluble proteins, mainly by hydrogen bonding (Fig. 3A). Such interactions can hardly lead to

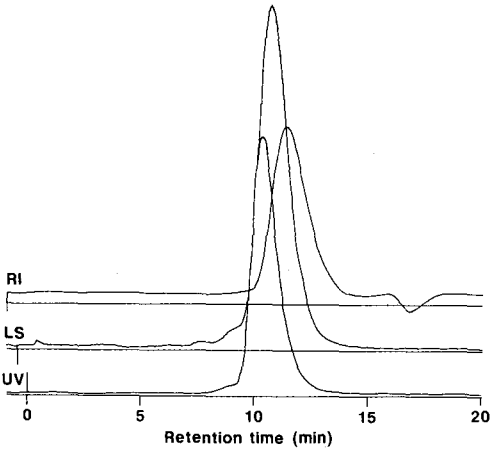

Fig. 2. Chromatography of bovine catalase on a TSK SW guard column (see *Methods*). These elution profiles were obtained at an equilibrium concentration of 22.5 m*M* octyl glucoside in the column. Essentially identical profiles were found at 0 and 20 m*M* octyl glucoside. UV, UV absorption (at 280 nm; 1 cm path length); LS, low-angle laser light-scattering; RI, differential refractive index. The UV curve indicates a high protein purity as regards low-molecular-weight proteins or protein fragments. Small amounts of high-molecular-weight proteins or protein aggregates are separated, as shown by the light-scattering curve. The main refractive index peak is well separated from the small valley approximately at the total volume of the column. The valley derives from a slight deviation of the salt and detergent concentrations of the sample from those of the eluent. The detectors were connected to the column in the order UV, LS and RI. The distances between the horizontal lines is 10% of full-scale. Similar elution profiles as in this example were obtained for the other proteins that were analysed. For a homogenous material (such as, in this instance, a pure protein) the peak positions along the time axis would coincide if the three parameters were monitored in a single cell and if the signals were recorded with a common starting point. Note that the baseline levels for the light-scattering signal and for the differential refractometric signal are the same before as after the peaks. This shows that equilibrium prevails.

the formation of micelles below the critical micelle concentration or to binding of micelles. The micellar structure probably prevents denaturation of proteins by octyl glucoside, as a polypeptide cannot easily distribute its hydrophilic and hydrophobic groups between (a) the aqueous phase outside the micelle or the glucose shell of the micelle and (b) the apolar micelle core, without severely disrupting the micelle structure. The type of octyl glucoside interaction with water-soluble proteins that was suggested in ref. 11 (Fig. 3B) seems to us thermodynamically unstable, as hydrogen bonding to serine or threonine (inward-facing monomers in Fig. 3B) will be weak and as most of the surface of a water-soluble protein is hydrophilic. The latter disfavours an outward-facing mode of binding whether the alkyl chains of octyl glucoside are staggered or not. Hence octyl glucoside can probably neither denature nor bind to non-denatured water-soluble proteins.

The sulphate groups of the ionic detergent SDS are small ($M_r = 96$) and repel each other owing to their negative charge, whereas the alkyl chains of SDS are relatively long ($M_r = 169$). The micelles of SDS allow denaturation, possibly as they give space enough for hydrophilic side-groups of an interacting polypeptide to face the aqueous medium and also space enough for hydrophobic side groups to be inserted

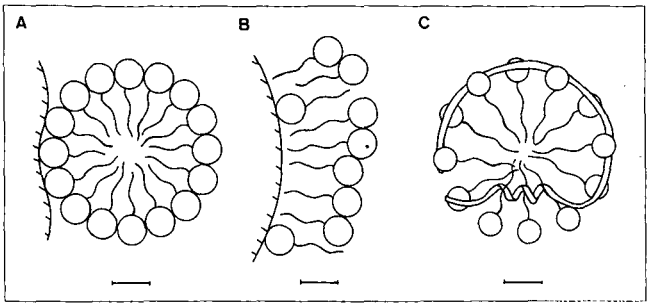

Fig. 3. Detergent–protein complexes. (A) Hypothetical interaction between an octyl glucoside micelle and the surface of a water-soluble protein (see Discussion). (B) Interpretation of the structure proposed tentatively in ref. 11 for monolayers of octyl glucoside on the surfaces of water-soluble proteins below the critical micelle concentration. These types of octyl glucoside binding to water-soluble proteins were not found in our experiments. (C) Model of a complex between SDS and the denatured polypeptide of a water-soluble protein lacking disulphide bonds, partly based on neutron-scattering data [37] (see Discussion). The length of the bars corresponds to 1 nm.

individually or in stretches (probably as α-helices) into the micelle core(s). The backbone of the polypeptide may even be hydrogen bonded to sulphate groups [36]. Most of the polypeptide of a non-disulphide-bonded protein in a complex with SDS is probably situated at the surface of SDS micelles [37]. The repulsion between the sulphate head groups keeps the polypeptide segments apart and prevents refolding. This type of complex is illustrated schematically in Fig. 3C. The properties of SDS contribute to a spacious and stable structure of the micelles in a complex with a polypeptide, a type of structure which cannot be attained by octyl glucoside.

We therefore consider it unlikely that octyl glucoside can bind, at moderate ionic strengths, to water-soluble proteins, except possibly at a few sites where stable binding on the protein surface is possible. Our results show that octyl glucoside does not bind to water-soluble proteins, at least not in amounts exceeding 0.1 g per gram of protein. However, hydrophobic interactions between water-soluble proteins and hydrophobic groups do occur at high concentrations of salts, as evidenced by hydrophobic interaction chromatography, where water-soluble proteins are adsorbed on hydrophobic ligands at 2–5 *M* salt concentrations.

Interestingly, SDS analogues with six or eight oxyethylene ($-CH_2CH_2O-$) groups inserted between the sulphate group and the dodecyl chain do not denature bovine serum albumin [38]. The reason for this is presumably that the hydrophilic moiety becomes much larger ($M_r = 360$ or 448), which leads to steric effects similar to those proposed for octyl glucoside (above). The weight proportion between the hydrophilic and hydrophobic moieties is 0.6 for dodecyl sulphate, 2.1 for the dodecyl sulphate analogue with six oxyethylene groups and 1.6 for octyl glucoside.

We cannot exclude that some subtle differences in conditions cause the discrepancy between our results and those of Cordoba *et al.* [11]. However, as the octyl glucoside concentrations were determined only in the protein-free compartment of the dialysis cell and as we do not find the proposed micellar binding of octyl glucoside around the proteins convincing, there are reasons to suspect that some unknown factor in the experimental procedures used by Cordoba *et al.* [11] may be the cause of

the inconsistency. One possibility is that the binding observed was not to the native proteins but to amphiphilic contaminants such as polypeptide fragments (formed on proteolysis). Even small fragments would remain in the protein compartment if they formed complexes with octyl glucoside and induced formation of micelles, as the relative micellar mass is 21 000–25 000 [13–15] and the exclusion limit of the dialysis membrane used in ref. 11 was 6 000–8 000. Small proteolytic fragments and octyl glucoside binding to such fragments will not easily be detected on molecular sieve chromatography.

A method suitable for studying this aspect further may be small-angle neutron scattering [22,36].

CONCLUSION

The non-ionic detergent octyl glucoside does not bind in micellar form to the water-soluble proteins ribonuclease A, ovalbumin, bovine serum albumin, fibrinogen and bovine catalase or *Aspergillus niger* catalase at an ionic strength of 0.14 *M* and at equilibrium concentrations of 20–35 m*M* octyl glucoside. This is contrary to the model used by Cordoba *et al.* [11] for the analysis of binding data. The binding of octyl glucoside to the studied water-soluble proteins fell below the detection limit of 0.1 g detergent/g protein in refractometrically monitored chromatography at 20 m*M* octyl glucoside. The substantial binding at 20 m*M* octyl glucoside reported by Cordoba *et al.* [11] is thus not consistent with our results.

ACKNOWLEDGEMENTS

P. Lundahl visited the Institute for Protein Research during part of this work and is grateful to Prof. Takagi and Osaka University for this opportunity. This work was supported by the Swedish Natural Science Research Council, the O.E. and Edla Johansson Science Foundation and a grant to P.L. from Osaka University.

REFERENCES

1 C. Baron and T. E. Thompson, *Biochim. Biophys. Acta*, 382 (1975) 276.
2 G. W. Stubbs and B. J. Litman, *Biochemistry*, 17 (1978) 215.
3 P. Rosevear, T. VanAken, J. Baxter and S. Ferguson-Miller, *Biochemistry*, 19 (1980) 4108.
4 R. J. Gould, B. H. Ginsberg and A. A. Spector, *Biochemistry*, 20 (1981) 6776.
5 P. K. Werner and R. A. F. Reithmeier, *Biochemistry*, 24 (1985) 6375.
6 Z. Markovic-Housley and R. M. Garavito, *Biochim. Biophys. Acta*, 869 (1986) 158.
7 L. Corazzi and G. Arienti, *Biochim. Biophys. Acta*, 875 (1986) 362.
8 A. Helenius and J. Kartenbeck, *Eur. J. Biochem.*, 106 (1980) 613.
9 S. A. Baldwin, J. M. Baldwin and G. E. Lienhard, *Biochemistry*, 21 (1982) 3836.
10 E. Mascher and P. Lundahl, *Biochim. Biophys. Acta*, 945 (1988) 350.
11 J. Cordoba, M. D. Reboiras and M. N. Jones, *Int. J. Biol. Macromol.*, 10 (1988) 270.
12 C.-C. Chen and T. H. Wilson, *J. Biol. Chem.*, 259 (1984) 10150.
13 W. Kühlbrandt, *Q. Rev. Biophys.*, 21 (1988) 429.
14 R. W. Roxby and B. P. Mills, *J. Phys. Chem.*, 94 (1990) 456.
15 K. Kameyama and T. Takagi, *J. Colloid Interface Science*, 137 (1990) 1.
16 T. VanAken, S. Foxall-VanAken, S. Castleman and S. Ferguson-Miller, *Methods Enzymol.*, 125 (1986) 27.
17 K. Shinoda, T. Yamaguchi and R. Hori, *Bull. Chem. Soc. Jpn.*, 34 (1961) 237.

18 G. D. Eytan, *Biochim. Biophys. Acta*, 694 (1982) 185.
19 R. M. Garavito and J. P. Rosenbusch, *J. Cell Biol.*, 86 (1980) 327.
20 H. Michel and D. Oesterhelt, *Proc. Natl. Acad. Sci. U.S.A.*, 77 (1980) 1283.
21 H. Michel, *Trends Biochem. Sci.*, 8 (1983) 56.
22 M. Roth, A. Lewit-Bentley, H. Michel, J. Deisenhofer, R. Huber and D. Oesterhelt, *Nature (London)*, 340 (1989) 659.
23 A. McPherson, S. Koszelak, H. Axelrod, J. Day, R. Williams, L. Robinson, M. McGrath and D. Cascio, *J. Biol. Chem.*, 261 (1986) 1969.
24 E. Mascher and P. Lundahl, *J. Chromatogr.*, 397 (1987) 175.
25 S. Makino, S. Maezawa, R. Moriyama and T. Tagaki, *Biochim. Biophys. Acta*, 874 (1986) 216.
26 Y. Hayashi, H. Matsui and T. Takagi, *Methods Enzymol.*, 172 (1989) 514.
27 A. Helenius and K. Simons, *J. Biol. Chem.*, 247 (1972) 3656.
28 S. Makino, J. A. Reynolds and C. Tanford, *J. Biol. Chem.*, 248 (1973) 4926.
29 A. Helenius and K. Simons, *Biochim. Biophys. Acta*, 415 (1975) 29.
30 S. Clarke, *J. Biol. Chem.*, 250 (1975) 5459.
31 E. Mascher and P. Lundahl, *J. Chromatogr.*, 476 (1989) 147.
32 Z. Wasylewski and A. Kozik, *Eur. J. Biochem.*, 95 (1979) 121.
33 P.-F. Rao and T. Takagi, *Anal. Biochem.*, 174 (1988) 251.
34 H. Eisenberg, *Biological Macromolecules and Polyelectrolytes in Solution*, Clarendon Press, Oxford, 1976.
35 Y. Hayashi, K. Mimura, H. Matsùi and T. Takagi, *Biochim. Biophys. Acta*, 983 (1989) 217.
36 P. Lundahl, E. Greijer, M. Sandberg, S. Cardell and K.-O. Eriksson, *Biochim. Biophys. Acta*, 873 (1986) 20.
37 K. Ibel, R. P. May, K. Kirschner, H. Szadkowski, E. Mascher and P. Lundahl, *Eur. J. Biochem.*, 190 (1990) 311.
38 K. Ohbu, J. Jona, N. Mizushima and I. Kashiwa, *Yukagaku*, 29 (1980) 866.

Journal of Chromatography, 518 (1990) 123–134
Elsevier Science Publishers B.V., Amsterdam

CHROM. 22 602

Fractionation of basic nuclear proteins of human sperm by zinc chelate affinity chromatography

FABIEN BIANCHI, ROSELYNE ROUSSEAUX-PREVOST, PIERRE SAUTIÈRE and JEAN ROUSSEAUX*

URA CNRS 409, Institut de Recherches sur le Cancer de Lille, Place de Verdun, 59045 Lille (France)

(First received December 6th, 1989; revised manuscript received April 19th, 1990)

ABSTRACT

Immobilized metal affinity chromatography was investigated for the fractionation of basic nuclear proteins of human sperm. Human sperm nuclei essentially contain two classes of protamines: a protamine of type P1 (HP1), rich in cysteine but with only one histidine, and three protamines of type P2 (HP2, HP3, HP4), rich in cysteine and histidine (nine in protamine HP2), potential ligands for transition metal ions. The critical conditions for metal affinity chromatography were defined: choice of metal, protein material and buffer, type of elution and sample loading. Chromatography of nuclear proteins, without histones and with cysteine residues alkylated by iodoacetamide, was optimum on zinc Chelating Sepharose in a Tris–acetate buffer and elution with an increasing concentration gradient of imidazole. Under these conditions, the two classes of protamines were completely separated. The intermediate basic proteins were further purified by reversed-phase high-performance liquid chromatography. Heterogeneity of binding to zinc of protamine HP1 was demonstrated. The proposed method is simple and reproducible and the recovery of proteins is high. It may be applied to study the expression and function of P1 and P2 protamines, *e.g.*, in the case of infertile men.

INTRODUCTION

Metal chelate affinity chromatography of proteins was first described by Porath *et al.* [1]. This method allows the separation of proteins on the basis of their different affinities to chelated metal ions. The principles of the binding have been presented in detail by Porath's group [1–4]: exposed histidine, cysteine and tryptophan residues coordinate to many transition metals such as zinc, copper, nickel and cobalt etc. Of these amino acids, histidine seems to be the predominant ligand for zinc and copper [4]. The topography of histidine residues at the surface of the molecule is a critical factor for metal chelate affinity chromatography [4–6].

The nucleus of human sperm contains four different protamines, together with a small proportion of histones and of minor intermediate basic proteins [7]. The protamines may be divided into two groups: HP1 (P1 protamine), rich in cysteine but with only one histidine [8], and HP2, HP3 and HP4 (P2 protamines), which are structurally related and very rich in histidine (*e.g.*, nine in HP2 and eight in HP3), and containing also cysteine (five in HP2 and HP3) [9,10]. The intermediate basic proteins HPI1, HPI2, HPS1, HPS2 are now known as precursors of protamines HP2 and HP3 [11], and these proteins are also rich in histidine and cysteine. On the basis of these

0021-9673/90/$03.50

structural differences, metal chelate affinity chromatography could be expected to effect a fractionation of human protamines. In this paper, a procedure using chromatography on zinc Chelating Sepharose is described as a simple and convenient method for the separation of HP1 (a P1 protamine) from HP2, HP3 and HP4 (P2 protamines) together with their precursors.

EXPERIMENTAL

Isolation of nuclei and extraction of basic nuclear proteins

Sperm from human healthy, fertile donors was obtained from the CECOS (Lille, France). Nuclei were purified as described by Ammer *et al.* [10]. Extraction of the basic nuclear proteins was performed according to Gusse *et al.* [7], with slight modifications. Briefly, a pellet of nuclei was incubated for 1 h at 4°C under nitrogen in 0.05 *M* Tris–HCl–0.002 *M* EDTA–0.01 *M* dithiothreitol (pH 8.8). Alkylation of the thiols was effected with iodoacetamide (final concentration 0.03 *M*) for 1 h at 4°C. Reduced and alkylated proteins were extracted with 0.25 *M* hydrochloric acid, then precipitated with 20% trichloroacetic acid, washed with acidified acetone and acetone, dissolved in water and freeze-dried. A variation of this procedure was used in which nuclei were reduced with dithiothreitol as described above, but the alkylation step with iodoacetamide was omitted.

Metal chelate affinity chromatography

Chelating Sepharose 6B (Pharmacia) was thoroughly washed with water and the suspension (in water) was poured in a 3 × 1 cm I.D. column (volume of the gel = 0.5 ml). The gel was charged with 0.6 ml of 3 mg/ml zinc chloride solution, (*i.e.*, *ca.* 13.5 μmol of $ZnCl_2$).

The following buffers were used for equilibration: (A) 0.05 *M* sodium acetate–0.5 *M* NaCl (pH 7.0) and (B) 0.05 *M* Tris–acetate–0.5 *M* NaCl (pH 7.0). The column was equilibrated overnight with either buffer A or buffer B at a flow-rate 6 ml/h.

The elution procedures were as follows: (1) stepwise elution with buffer A or B of pH 7.0, 6.0, 5.0, 4.0 and 3.0 (14 ml of each buffer); (2) washing of the column with buffer A or B (pH 7.0) (14 ml), then stepwise elution with buffer A or B (pH 6.0) containing 0.1 *M* histidine (14 ml), then 0.5 *M* histidine (14 ml); (3) washing with buffer A or B (pH 7.0) (14 ml), then elution with a gradient of imidazole produced by mixing two identical cylindrical chambers containing for the first 40 ml of buffer A or B and for the second 40 ml of buffer A or B containing 0.25 *M* imidazole–HCl. The actual profile of the imidazole gradient was established by monitoring the absorbance at 220 nm (buffer B) or 240 nm (buffer A) of the effluent in several separate runs where no sample was applied to the column. Stepwise elution with imidazole in buffer B was also used as follows: washing with buffer B (14 ml) and elution with 0.05, 0.1 and 0.2 *M* imidazole in buffer B (14 ml of each solution).

In all the experiments, fractions of 2 ml were collected and the protein concentration in each fraction determined by the Coomassie blue method (see below). Fractions containing proteins were precipitated three times with 20% trichloroacetic acid and washed with acidified acetone and acetone. The pellet was stored dried at −20°C or dissolved at a final concentration 1 mg/ml in 0.01 *M* hydrochloric acid–8 *M* urea–0.5 *M* mercaptoethanol prior to polyacrylamide gel electrophoresis.

After chromatography, elution was performed with 0.05 *M* EDTA (pH 8)–0.05 *M* NH_4HCO_3 (pH 10.5)–water (50 ml of each) [12]. Fractions of 2 ml were again collected and the protein contents were determined. The column was then recharged with zinc chloride as described above.

The various elution procedures were also performed with Chelating Sepharose Fast Flow (Pharmacia). The experimental conditions for the preparation of the column and for elution were identical with those described above except that a flow-rate of 30 ml/h was used.

Reversed-phase high-performance liquid chromatography

Fractions containing P2 protamines together with precursors were loaded on a Deltapak C_{18} HPLC column (Millipore–Waters) (300 mm × 3.6 mm I.D.) equilibrated in 0.1% trifluoroacetic acid (TFA)–10% acetonitrile (flow-rate 1.5 ml/min). About 0.1 mg of protein material in 0.1 ml of 0.1% TFA was loaded on the column. A linear gradient from 10 to 35% acetonitrile in 0.1% TFA was developed in 60 min. Fractions of 1 ml were collected.

Protein determination

The protein concentrations in the solution loaded onto the zinc Sepharose column and in the fractions from chromatography were determined by Coomassie Blue protein dye-binding assay according to Read and Northcote [13] with an adaptation to a microtitration plate, and reading on a enzyme immunoassay (EIA) reader. A 10-μl volume of the protein solution was mixed in a well of a microtitration plate (96-well flat bottomed, microtitration plate, Falcon) with 40 μl of distilled water and 150 μl of Coomassie Brilliant Blue solution prepared as described [13]. The mixture was stirred to effect homogenization on a stir plate. The plate was read on an EIA reader (Dynatech MR 610) equipped with an interference filter at 600 nm. A standard of salmon protamine (Sigma, grade IV) was used at concentrations ranging from 5 to 100 μg/ml.

Electrophoretic controls

Proteins were analysed by electrophoresis in 17% acrylamide–6.25 *M* urea (pH 3.2) [14] on slab gels as described previously [7].

RESULTS

Protein material

The first experiments were performed with proteins extracted from human sperm nuclei according to Gusse *et al.* [7]. The material contains histones, together with protamines and intermediate basic proteins. Histones from sperm nuclei could not be resolved from one of the protamines, HP1, on a zinc Sepharose column whatever the procedure used. Further, this separation also could not be achieved on a copper Sepharose column (data not shown). Therefore, the simple preparation procedure of Ammer *et al.* [10] was used. This gives a protein material devoid of histones but containing all the protamines and intermediate basic proteins.

All the experiments reported below were performed with proteins extracted after reduction of nuclei with dithiothreitol and alkylation of the thiols with iodoacetamide. In order to determine the contribution of thiols to interaction with zinc Sepha-

rose, an extraction of nuclear proteins was performed without alkylation of the thiols with iodoacetamide. However, such a protein material, either in sodium acetate buffer (buffer A) or in Tris–acetate buffer (buffer B), yielded a substantial precipitate. The precipitate was analysed by polyacrylamide gel electrophoresis in 6.25 *M* urea–2-mercaptoethanol–0.9 *M* acetic acid (pH 3.2). All the protamines (together with minor intermediate basic proteins) were observed (data not shown). It was concluded that at neutral pH, reduced thiol groups are reoxidized with the formation of intermolecular bridges. Such a material was unsuitable for metal chelate affinity chromatography.

Buffers

Metal chelate affinity chromatography was first expected to be performed in a buffer with no chelating properties and a good buffering capacity at neutral pH, *i.e.*, phosphate buffer. Nevertheless, basic nuclear proteins of human sperm precipitate in 0.05 *M* sodium phosphate–0.5 *M* NaCl buffer (pH 7.0), probably because of the neutralization of guanidinium groups of arginine residues by phosphate ions. Protein determination in the supernatant indicated that less than 10% was soluble in phosphate buffer.

In order to study the effects on zinc affinity chromatography of buffers with or without chelating properties, two buffers were selected: 0.05 *M* sodium acetate–0.5 *M* NaCl buffer (buffer A) with no chelating activity and 0.05 *M* Tris–acetate–0.5 *M* NaCl (buffer B), where Tris is known to have low chelating properties [2,15,16]. The disadvantage of buffer A is its low buffering capacity at pH 7.0. In addition, sperm basic nuclear proteins are poorly soluble in buffer A (about 40–50%), whereas their solubility in buffer B is good (about 80–90%).

Elution by a pH gradient

Fig. 1 shows the elution profile with (a) buffer A and (b) buffer B at pH 7.0, 6.0, 5.0, 4.0 and 3.0. No protein is eluted with equilibration buffer of pH 7.0. With buffer A, two peaks are observed, at pH 5.0 (about 19%) and pH 4.0. The total yield of proteins recovered by chromatography is about 45%, starting with 0.5 mg of material. This low recovery is probably due to the poor solubility of sperm nuclear proteins in sodium acetate buffer (pH 7.0). Elution with buffer B also shows two peaks, one at pH 6.0 (12%) and the other at pH 4.0. The yield of protein is about 90%. With both buffers, no additional material is recovered by sequential treatment of the column with EDTA, ammonium carbonate and water. The first peak (eluted at pH 5.0 with buffer A and pH 6.0 with buffer B) represents protamine HP1 (Fig. 2); HP1a is the monophosphorylated form and HP1b the dephosphorylated protamine [7]. The second peak contains several proteins: the minor intermediate basic proteins, mainly HPS2, and the P2 protamines HP2, HP3 and HP4, but also a significant amount of protamine HP1, fraction HP1b being predominant (Fig. 2).

Elution with competitor ligand

Histidine. Fig. 3 shows the elution profile of a stepwise gradient with 0.1 and 0.5 *M* histidine in buffer B. The same results were obtained with buffer A (not shown). Also a gradient from 0 to 0.5 *M* histidine (2 × 40 ml) gave a similar profile. Protamine HP1 is recovered in the first peak (Fig. 4), and represents 25% of the total

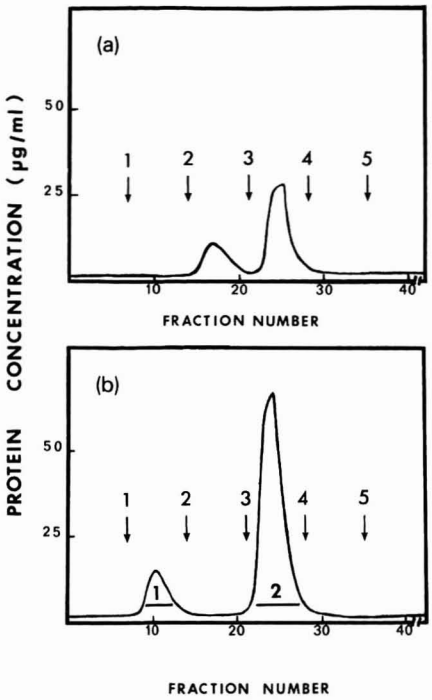

Fig. 1. Elution profile of human sperm basic nuclear proteins (0.5 mg) on a zinc Chelating Sepharose column (3 × 1 cm I.D.), equilibrated either in (a) buffer A (0.05 *M* sodium acetate–0.5 *M* NaCl, pH 7.0) or (b) in buffer B (0.05 *M* Tris–acetate–0.5 *M* NaCl, pH 7.0). Elution with equilibration buffer, then with buffer of pH (1) 6.0, (2) 5.0, (3) 4.0 and (4) 3.0, followed by (5) 0.05 *M* EDTA (pH 8.0) [Elutions with 0.05 *M* NH_4HCO_3 (pH 10.5) and water are not shown]. Volume of gel, 0.5 ml; flow-rate, 6 ml/h; volume of fractions, 2 ml. Protein concentration was determined by the Coomassie Brilliant Blue protein dye assay [13].

protein eluted from the column. The fraction eluted with 0.5 *M* histidine contains P2 protamines together with intermediate basic proteins and a small amount of protamine HP1b (Fig. 4). No protein was eluted either with the washing buffer or, at the end of chromatography, with EDTA, ammonium carbonate and water applied sequentially.

Imidazole. Fig. 5 shows the elution profile obtained with a gradient of imidazole from 0 to 0.25 *M* in buffer B. Two main peaks are obtained, but the second is preceded by a shoulder. It may be noted that the first fraction is eluted in a part of the gradient where the concentration of imidazole in the effluent increases weakly (from 0 to 0.02 *M*). This can be interpreted as binding of imidazole to available zinc ions. In the second part of the gradient, the concentration of imidazole increases sharply, from 0.02 to 0.1 *M*, corresponding to elution of the shoulder (fraction 2); thereafter, the gradient is linear from 0.1 to 0.25 *M* (elution of fraction 3). Electrophoretic controls (Fig. 6) showed that fraction 1 (about 29% of the total) contains HP1a and HP1b, fraction 2 (8% of the total) corresponds to HP1b and fraction 3 (63% of the total) contains P2 protamines, HP2, HP3 and HP4, together with intermediate basic

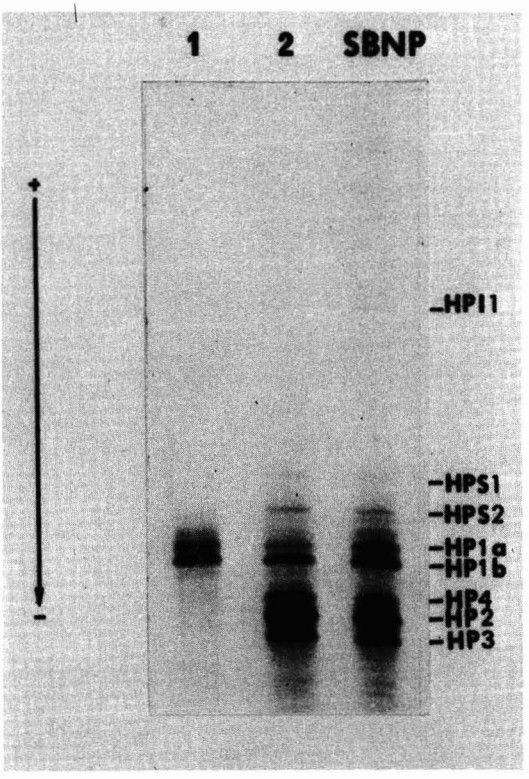

Fig. 2. Controls of fractions 1 and 2 from Fig. 1b by polyacrylamide slab gel electrophoresis (17% acrylamide) in 0.9 *M* acetic acid–6.25 *M* urea (pH 3.2). SBNP = sperm basic nuclear proteins loaded onto to the zinc Chelating Sepharose column.

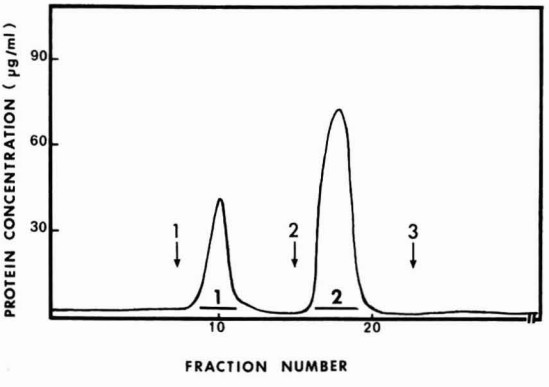

Fig. 3. Elution profile of human sperm basic nuclear proteins (0.4 mg) on zinc Chelating Sepharose (0.5 ml of gel) equilibrated in buffer B (0.05 *M* Tris–acetate–0.5 *M* NaCl, pH 7.0). Elution with (1) 0.1 *M* histidine, (2) 0.5 *M* histidine in buffer B (pH 6.0) followed by (3) 0.05 *M* EDTA (pH 8.0). Flow-rate, volume of fractions and protein determination as in Fig. 1.

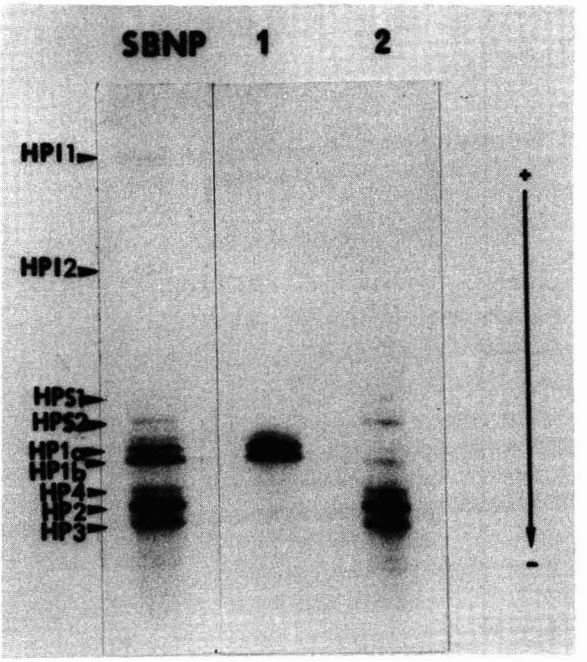

Fig. 4. Polyacrylamide slab gel electrophoresis of fractions 1 and 2 from Fig. 3. Experimental conditions as in Fig. 2. SBNP = Sperm basic nuclear proteins used as starting material.

proteins, mainly HPS2. The P2 protamines and the main minor protein HPS2 were resolved by reversed-phase high-performance liquid chromatography (HPLC) (Fig. 5b) with a linear gradient from 10 to 35% acetonitrile. Fraction 3a corresponds to P2 protamines and fraction 3b to protein HPS2 (Fig. 6). The other minor proteins were present in too small amounts to be detected.

It is important to note that a gradient of imidazole in sodium acetate buffer (buffer A) gave similar results, and that no protein material was detected either by elution with the washing buffer or with subsequent treatments for regeneration of the column. In addition, we observed that stepwise elution with buffer B and buffer B with 0.05, 0.1 and 0.2 *M* imidazole was able to separate P1 protamine (elution with 0.05 *M* imidazole) from P2 protamines and intermediate basic proteins (elution with 0.2 *M* imidazole). In all the experiments, the yield of protein recovered from the column was between 80 and 90%.

Effect of protein load

This effect was only studied in the case of stepwise elution with imidazole in buffer B. A column of 0.5 ml was loaded, in separate runs, with 0.25, 0.5, 1 or 2 mg of protein. The results were reproducible when the loading of the column was from 0.25 to 1 mg of protein (Table I). With 2 mg, part of the protein material was eluted with the washing buffer and corresponded to protamine HP1 (the remaining HP1 was eluted with 0.05 *M* imidazole). P2 protamines together with intermediate basic proteins were eluted with both 0.1 and 0.2 *M* imidazole (Table I).

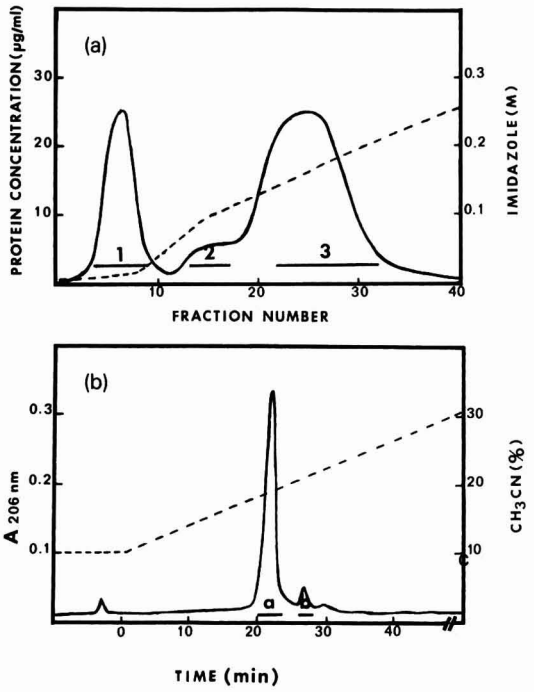

Fig. 5. (a) Fractionation of human sperm basic nuclear proteins (0.5 mg) on zinc Chelating Sepharose (0.5 ml of gel) equilibrated in buffer B (0.05 *M* Tris–acetate–0.5 *M* NaCl, pH 7.0). After washing the column with 15 ml of buffer B (not shown), an increasing concentration gradient of imidazole was applied to the column (0 to 0.25 *M*, produced by mixing two cylindrical chambers containing in the first 40 ml of buffer B and in the second 40 ml of 0.25 *M* imidazole in buffer B). The actual profile of the imidazole gradient was monitored by measuring the absorbance at 220 nm of the effluent in separate runs where no sample was applied to the column. Flow-rate, volume of fractions and protein determination as in Fig. 1. (b) Reversed-phase HPLC separation of fraction 3 from Fig. 5a. Column: Deltapak C_{18} (300 × 3.6 mm I.D.). Elution with 10% acetonitrile in 0.1% trifluoroacetic acid (TFA) for 10 min, followed by a linear gradient from 10 to 35% acetonitrile in 0.1% TFA for 60 min at room temperature and flow-rate 1.5 ml/min. Sample load, 0.12 mg. The elution profile was monitored by determination of the absorbance at 206 nm ($A_{206\ nm}$).

DISCUSSION

The purpose of this work was to evaluate metal chelate affinity chromatography as a method for the separation of human sperm basic nuclear proteins. Sperm chromatin contains essentially two classes of protamines: one P1 protamine (HP1) containing six cysteine residues but only one histidine, and three P2 protamines (HP2, HP3 and HP4) with five cysteine residues, but also very rich in histidine (*e.g.*, nine in HP2). Cysteine residues are present in the nucleus essentially as disulphide bridges. Hence extraction of the protamines (and intermediate basic proteins) requires the reduction of cystine by dithiothreitol and blocking of the thiols by an alkylating agent, such as iodoacetamide. We have tried to evaluate the role of cysteine in metal chelate affinity chromatography by performing a reduction of nuclear proteins with dithiothreitol without alkylation with iodoacetamide. However, the proteins extract-

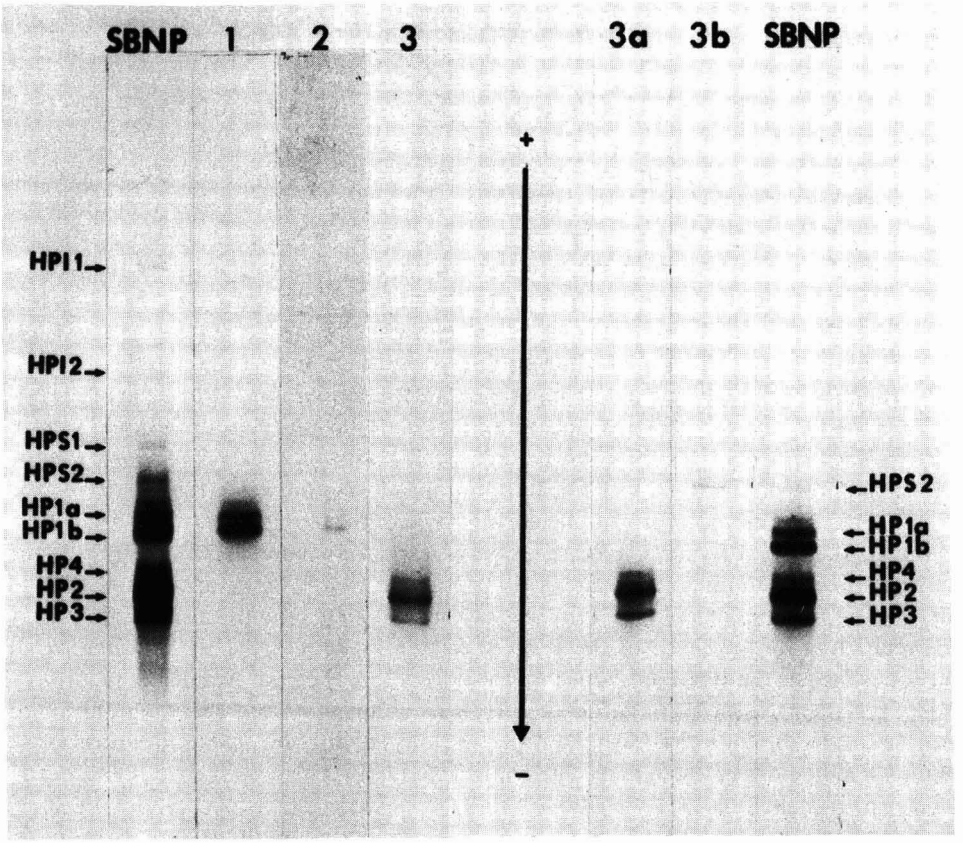

Fig. 6. Electrophoretic controls of fractions 1, 2 and 3 from Fig. 5a and fractions 3a and 3b from Fig. 5b by polyacrylamide gel electrophoresis. Experimental conditions as in Fig. 2. SBNP = sperm basic nuclear proteins used as starting material.

TABLE I

EFFECT OF PROTEIN LOAD ON ZINC CHELATING SEPHAROSE CHROMATOGRAPHY

A column (0.5 ml of gel) equilibrated in 0.05 *M* Tris–acetate–0.5 *M* NaCl (pH 7.0) (buffer B) was used. Results are recoveries of total protein (%).

Eluent	Amount of protein applied (mg)			
	0.25	0.5	1	2
Buffer B	0	0	0	10
Buffer B with 0.05 *M* imidazole	38	37	36	28
Buffer B with 0.1 *M* imidazole	0	2	2	27
Buffer B with 0.2 *M* imidazole	62	61	62	35

ed by 0.25 *M* hydrochloric acid probably make, at neutral pH, intermolecular disulphide bridges. Hence the role of the cysteine of protamines in metal chelate affinity chromatography could not be evaluated.

Zinc ion was chosen as a ligand for the following reasons. First, it has been demonstrated that zinc is abundant in human sperm nuclei and probably plays a role in stabilization of sperm chromatin; a reversible binding to thiols has been suggested by Kvist and co-workers [17,18]. Nevertheless, it is important to note that the preparations of sperm nuclear proteins used in this study are devoid of protein-bound zinc. This is due to the protocol of isolation, which involves several steps, such as reduction with dithiothreitol, alkylation of the thiols, extraction with 0.25 *M* hydrochloric acid and precipitation of proteins with trichloroacetic acid; all these steps clearly remove zinc ions which could be linked to protamines. The second reason for the choice of zinc was that initial experiments with copper ion led to a strong retention of sperm nuclear proteins (including histones), so no separation could be obtained. Experiments with zinc showed that a resolution of nuclear proteins could be possible and the critical factors for an optimum separation were studied.

The first condition for zinc chelate affinity chromatography was to use a protein material depleted of sperm histones. This fraction has a weak affinity to the zinc chelate affinity column and coelutes with protamine HP1. This result was unexpected as somatic histones (such as calf thymus histones) do not bind to the column. It may be related to the presence of the testis specific variant TH2B [19]. Elimination of histones was easily obtained with the procedure described by Ammer *et al.* [10]. A second critical factor was the choice of buffer. Phosphate buffer, commonly used because of its absence of chelating properties, was unsuitable; protamines precipitate almost completely in this buffer. The comparison between sodium acetate buffer (no chelating properties) and Tris–acetate buffer (weak chelating properties) did not show significant differences. More especially, all the protein material was retained on the column at neutral pH. Hence Tris–acetate (buffer B) is to be preferred as protamines are almost completely soluble in this buffer, whereas this is not the case with sodium acetate.

The optimum separation of sperm nuclear proteins was obtained by the use of a competitor ligand. Imidazole gave the best resolution: the two classes of protamines P1 and P2 (the intermediate basic proteins being related to P2 protamines) are well separated, either by a gradient from 0 to 0.25 *M* imidazole or by stepwise elution. The latter method is simpler and is now routinely used in our laboratory.

Chelating Sepharose Fast Flow is preferred to Chelating Sepharose, as the separation is fast (2 h). The weak affinity of protamine HP1 and the high affinity of P2 protamines (together with their precursors HPS1, HPS2, HPI1 and HPI2) seems to be clearly related to their different contents of histidine residues. Nevertheless, two points deserve comment. First, the affinity of P2 protamines is very high (in comparison with other proteins or large peptides previously described). This may be due to the large number of histidine residues and also to the good accessibility of this potential ligand; protamines are small and very hydrophilic molecules. A second point observed in chromatographic elution was unexpected, namely the presence of two fractions related to HP1. The second minor fraction has the electrophoretic mobility of protamine HP1b (dephosphorylated HP1). The origin of such heterogeneity is unknown. It may be due to the existence of protamine variants. Gusse *et al.* [7] also

observed different fractions corresponding to HP1 when purification was achieved by reversed-phase HPLC after chromatography on CM-cellulose.

Zinc chelate affinity chromatography of human sperm nuclear proteins is a simple and efficient method for the purification of P1 and P2 protamines. The minor intermediate basic proteins may be recovered (essentially protein HPS2) by a second step of reversed-phase HPLC. The method is reproducible if the protein loading is correctly adjusted to the size of the column. A ratio of 1 mg of protein to 0.5 ml of gel seems optimum. Larger amounts probably induce a displacement of P1 protamine by P2 protamines, which have higher affinity for zinc ions. Such a result has been reported previously for serum proteins by Porath and Olin [2].

Other procedures for the isolation of human sperm nuclear proteins have been described previously. Reversed-phase HPLC was proposed by Ammer *et al.* [10]. This technique can only be applied to small amounts of material (a few hundred micrograms). Ion-exchange chromatography on CM-cellulose has the advantage of very good resolution [7,9]. All the protamines may be separated by this method [7], but it is difficult to use CM-cellulose chromatography for small amounts of material such as a few milligrams, and the recovery is low (about 30–40%).

Zinc chelate affinity chromatography has the advantage of a very good recovery of protein material (about 80–90%). Hence this method will be very useful for studying the expression and function of P1 and P2 protamines. For example, Balhorn *et al.* [20] have suggested that expression of P2 protamines is reduced in some infertile men. Zinc chelate affinity chromatography could be applied to the isolation of protamines from small amounts of material, such as individual ejaculates from infertile patients. In addition, the procedure may also be applied to study the expression of nuclear proteins during spermatogenesis, or to other species which possess P1 and P2 protamines such as the mouse and hamster [21].

ACKNOWLEDGEMENTS

We thank Professor J. Leonardelli and Dr. P. Saint-Pol (CECOS, Lille) for providing the semen samples. The technical assistance of A. M. Mir and D. Deffrasnes and the secretariat help of T. Ernout are gratefully acknowledged. The work received financial support from the Centre National de la Recherche Scientifique and the Université de Lille II.

REFERENCES

1 J. Porath, J. Carlsson, I. Olsson and G. Belfrage, *Nature (London)*, 258 (1975) 598.
2 J. Porath and B. Olin, *Biochemistry*, 22 (1983) 1621.
3 J. Porath, in H. Tschesche (Editor), *Modern methods in Protein Chemistry*, Vol. 2, Walter de Gruyter, Berlin, 1985, p. 85.
4 J. Porath, *Trends Anal. Chem.*, 7 (1988) 254.
5 E. Sulkowski, *Trends Biotechnol.*, 3 (1985) 1.
6 E. S. Hemdan, Y. J. Zhao, E. Sulkowski and J. Porath, *Proc. Natl. Acad. Sci. U.S.A.*, 86 (1989) 1811.
7 M. Gusse, P. Sautière, D. Bélaïche, A. Martinage, C. Roux, J. P. Dadoune and P. Chevaillier, *Biochim. Biophys. Acta*, 884 (1986) 124.
8 D. J. McKay, B. S. Renaux and G. H. Dixon, *Biosci. Rep.*, 5 (1985) 383.
9 D. J. McKay, B. S. Renaux and G. H. Dixon, *Eur. J. Biochem.*, 156 (1986) 5.
10 H. Ammer, A. Henschen and C. H. Lee, *Biol. Chem. Hoppe Seyler*, 367 (1986) 515.

11 P. Sautière, A. Martinage, D. Bélaïche, A. Arkhis and P. Chevaillier, *J. Biol. Chem.* 263 (1988) 11059.
12 D. C. Rijken and D. Collen, *J. Biol. Chem.*, 256 (1981) 7035.
13 S. M. Read and D. H. Northcote, *Anal. Biochem.*, 116 (1981) 53.
14 S. Panyim and R. Chalkley, *Arch. Biochem. Biophys.*, 130 (1969) 337.
15 M. Belew, T. T. Yip, L. Andersson and R. Ehrnström, *Anal. Biochem.*, 164 (1987) 457.
16 S. A. Margolis, A. J. Fatiadi, L. Alexander and J. J. Edwards, *Anal. Biochem.*, 183 (1989) 108.
17 U. Kvist, B. A. Afzelius and L. Nilsson, *Dev. Growth Differ.*, 22 (1980) 543.
18 G. M. Roomans, E. Lundevall, L. Björndahl and U. Kvist, *Int. J. Androl.*, 5 (1982) 478.
19 N. Tanphaichitr. P. Sohbon, N. Taluppeth and P. Chalermisarachai, *Exp. Cell Res.*, 117 (1978) 347.
20 R. Balhorn, S. Reed and N. Tanphaichitr, *Experientia*, 44 (1988) 52.
21 P. A. Bower, P. C. Yelick and N. B. Hecht, *Biol. Reprod.*, 37 (1987) 479.

Journal of Chromatography, 518 (1990) 135–140
Elsevier Science Publishers B.V., Amsterdam

CHROM. 22 590

Responses of different UV–visible detectors in high-performance liquid chromatographic measurements when the absolute number of moles of an analyte is measured

G. TORSI*, G. CHIAVARI, C. LAGHI and A. M. ASMUDSDOTTIR
Dipartimento di Chimica "G. Giamician", Via Selmi 2, 40126 Bologna (Italy)
(First received January 5th, 1990; revised manuscript received May 18th, 1990)

ABSTRACT

A simple model for the determination of the absolute number of moles of an analyte in high-performance liquid chromatography with UV–VIS detectors was tested on five commercial instruments. The data show that three gave results in agreement with theory and the other two gave systematic errors of *ca.* 18 and 20%. The possibility of presenting the experimental results of a chromatographic analysis directly as the number of moles instead of peak area is briefly discussed.

INTRODUCTION

In a previous paper [1], a simple equation was derived for the absolute measurement of the number of moles of an analyte from peak-area data. The equation applies to measurements with flow-through non-destructive detectors. The experimental validation of the proposed model from which the above-mentioned equation was derived is particularly easy for UV–VIS detectors in high-performance liquid chromatography (HPLC) as all the quantities involved can be obtained in a straightforward way. A test with a Varian 2550 UV–VIS detector showed that there is a positive systematic error in the number of moles measured of *ca.* 18% independent of volume of sample injected, wavelength and type of analyte. The flow-rate had only a neglibible effect in the range investigated (0.5–5 $cm^3\ min^{-1}$).

The error, even if significant, is not very high and, as fairly drastic assumptions were introduced in the model, it is possible that, with different optics and cell design, experimental conditions could be found with which the systematic error encountered is less severe than that obtained with the tested apparatus.

One of the assumptions made was parallelism of the light beam rays. However, it has been demonstrated experimentally that with concentration gradients, which are naturally present when an analyte is eluted, with a UV–VIS chromatographic cell the rays can be deflected out of the light sensor [2], simulating an absorbance in agreement with the positive error found. An attempt to take into account in the model the variation of the refractive index in a specific cell failed, owing to difficulties in deriving mathematical equations describing the concentration gradients in time and space.

0021-9673/90/$03.50

TABLE I

MAIN CHARACTERISTICS OF THE INSTRUMENTS USED

Specification	Varian 2550	Perkin-Elmer LC-95	Hewlett-Packard HP 1090 diode-array	Jasco 875 UV	Waters Assoc. Lambda Max Model 481
Spectral band width (nm)	8	5	4	8	5
Wavelength accuracy (nm)	±2	±1	±1	±2	±2
Wavelength reproducibility (nm)	±0.3	±0.5		±0.3	±0.5
Light source	D_2 lamp	D_2 lamp	D_2 lamp	D_2 lamp	D_2 lamp
Wavelength range (nm)	190–600	190–700	190–600	190–600	190–700
Flow-cell volume (μl)	8	4.5	4.5	8	14
Measured path length (mm)	9.96	9.85	5.9	9.68	10.1
Detector output (V/A.U.)	0.5	1.0	0.5	1.0	1.0
Detector output (measured) (V/A.U.)	0.485	0.912		1.012	
Integrator	Varian 4290	Varian 4290	HP Series 300 computer	Spectra Physics 4270	Model 730 Data Module
Injector	Rheodyne Model 7010	Rheodyne Model 7125	Rheodyne Model 7161	Rheodyne Model 7125	Model U6K Universal Chrom

For these reasons we considered it more convenient to test the simple model proposed previously [1] on different detectors to see if, at least for some of them, the systematic error is eliminated or reduced to such a level that only random errors are detected. This paper presents the experimental results obtained with five commercial UV–VIS detectors.

EXPERIMENTAL

The detectors used and their major characteristics are summarized in Table I. The preparation of the samples, the calibration procedures and the measuring sequence have already been described [1]. It was difficult, however, to follow the same procedure when measuring the numerical factor for transforming the area given by the Hewlett Packard and Waters Assoc. chromatographs to A min (where A is the absorbance) as required in our calculations, because in these instruments there is an integrated data acquisition and treatment system with no direct access to the various steps followed in reaching the final results. Both, however, give A *versus* time diagrams with areas of peaks.

It was therefore possible to integrate a peak manually from the hard copy of a chromatogram and obtain the desired value of A min. By comparison with the numerical value of the area given, the transformation factor was easily calculated. A statistical analysis has shown that the precision of values so obtained was better than 1% at the 95% confidence level.

RESULTS AND DISCUSSION

The experimental results are summarized in Table II, where the slopes and intercepts of the straight lines obtained with three analytes (paranitroaniline (PNA), toluene and chromate) and the detectors reported in Table I are shown. The data at the bottom ("Average") were obtained by using all the points available for all substances. Some data at low wavelength are missing because the experimental points were too scattered to be of any use. A possible explanation may be found an insufficient energy output of the source or in optical components with high UV absorption. The straight lines were obtained by plotting on the abscissa the number of moles injected and on the ordinate the number of moles found according to the equation

$$A(i) = 10^3 \varepsilon b N(0)/F \tag{1}$$

where $A(i)$ (A min) is the area of the peak, F (cm^3 min^{-1}) the mobile phase flow-rate, ε (cm^2) the molar absorptivity of the analyte at the given wavelength, b (cm) the cell thickness and $N(0)$ the total number of moles; 10^3 is a multiplying factor introduced to maintain the numerical value of ε given in the literature.

The ideal behaviour is found when the line has a slope of unity and passes through the origin. Table II indicates that three detectors show nearly ideal behaviour as at the 95% confidence level the slopes and the intercepts cannot be said to be different from the sought values. This implies that, with these instruments and under the specified experimental conditions, the systematic error is lower than the random error at the 95% confidence level. It is evident that a still better agreement is found

TABLE II

a = Intercept; b = slope; r = correlation coefficient.

Substance	Varian 2550	Perkin Elmer LC-95	Hewlett-Packard HP 1090 diode-array	Jasco 875 UV	Waters Assoc. Lambda Max Model 481
Toluene	$a=0.05\pm1.27$			$a=0.07\pm1.56$	$a=0.07\pm0.25$
($\lambda=206$ nm)	$b=1.19\pm0.13$			$b=0.99\pm0.10$	$b=1.17\pm0.05$
	$r=0.9944$			$r=0.9956$	$r=0.9985$
PNA	$a=0.10\pm0.32$		$a=0.14\pm0.44$	$a=0.77\pm1.95$	$a=0.01\pm0.13$
($\lambda=228$ nm)	$b=1.20\pm0.04$		$b=1.01\pm1.01$	$b=0.96\pm0.17$	$b=1.21\pm0.04$
	$r=0.9983$		$r=0.9998$	$r=0.9999$	$r=0.9974$
PNA	$a=0.06\pm0.19$	$a=0.05\pm0.15$	$a=0.05\pm0.27$	$a=0.02\pm0.85$	$a=0.03\pm0.19$
($\lambda=376$ nm)	$b=1.16\pm0.02$	$b=0.96\pm0.04$	$b=0.96\pm0.01$	$b=1.01\pm0.08$	$b=1.20\pm0.05$
	$r=0.9999$	$r=0.9987$	$r=0.9999$	$r=0.9999$	$r=0.9980$
Chromate	$a=0.10\pm0.23$	$a=0.004\pm0.13$	$a=0.08\pm0.024$	$a=0.08\pm0.05$	$a=0.03\pm0.29$
($\lambda=373$ nm)	$b=1.19\pm0.10$	$b=0.98\pm0.01$	$b=0.96\pm0.02$	$b=0.94\pm0.02$	$b=1.22\pm0.06$
	$r=0.9992$	$r=0.9998$	$r=0.9998$	$r=0.9999$	$r=0.9981$
Average	$a=0.001\pm0.18$	$a=0.091\pm0.09$	$a=0.013\pm0.13$	$a=0.13\pm0.48$	$a=0.02\pm0.09$
	$b=1.18\pm0.02$	$b=0.99\pm0.01$	$b=0.98\pm0.01$	$b=0.99\pm0.55$	$b=1.20\pm0.02$
	$r=0.9991$	$r=0.9997$	$r=0.9995$	$r=0.9995$	$r=0.9996$

when all points relevant to all the different substances (bottom entries in Table II) are pooled. This is to be expected because in this way the errors introduced in setting the instruments parameters such wavelength and in preparing the solutions are averaged.

The data relevant to the Varian spectrometer given in Table II were obtained with a different instrument located in a different laboratory. This choice was made on purpose to see if the systematic error was similar to that obtained previously [1]. Even if it is risky to draw conclusions from only two instruments tested, the practical coincidence of the values points toward a physical origin related to the optics and/or cell design.

With the Waters Assoc. instrument there is the problem of the cell form, which is tapered instead of cylindrical, so that one of the assumptions of the model (constant cell cross-section) is not fulfilled. However, the link between this type of cell and the systematic error encountered was not investigated.

Use of molar absorptivity values

From the data presented above, it is clear that it is possible to measure the absolute number of moles of an analyte in a given sample if the appropriate instrument is chosen. If we assume that calibrations such as wavelength and absorbance in such an instrument are made automatically, as in all modern spectrometers, and that the flow-rate is fed to the data-treatment system directly from the pump, then the data can be presented as number of moles instead of peak area if the value of εb for the specific peak is known.

In our calculations we used the product εb derived from calibration graphs (A *vs.* c) measured with the chromatographic system under investigation [1]. In this way, any systematic errors related to ε and b are removed at the cost of a calibration graph

for each analyte. The value of b can be determined in many ways with high accuracy once and for all for a given cell, thus leaving only ε as the last quantity needed. Values of ε can be found in the literature if the mobile phase is not too complex. However, it is well known that ε is constant only if the instrumental spectral band width (SBW) is at least ten times smaller than the natural band width (NBW) of the absorption band of the analyte under investigation [3–5]. Now, for obvious reasons, with a chromatographic microcell it is difficult to have a small SBW (see Table I), and consequently any use of ε values taken from the literature must be carefully considered. Recently a UV–VIS detector has been proposed also for gases or vapours [6]. In this instance an even more cautious approach must be made, as the absorption bands of gases and vapours are very sharp. Of course, fixed-wavelength detectors cannot be used for measurements of the absolute number of moles except when the molar absorptivity of the analyte is constant in the source line wavelength interval.

The experimental values of b given in Table I were obtained from PNA at 376 nm and K_2CrO_4 at 373 nm from the calibration graphs relevant to each instrument and the molar absorptivity given in the literature [7] for the chromate and measured on a Perkin-Elmer Model 554 spectrometer with 0.2 SBW for PNA. It was then possible to calculate a molar absorptivity for each compound on each instrument, which, as already shown [4], should be a function of the SBW/NBW ratio. The results are summarized in Table III. No systematic errors are evident even when the SBW/NBW ratio is fairly large, as with toluene. A possible explanation of the data shown in Table III may be the difficulty in setting the wavelength reproducibly on commercial instruments. It must be noted that this kind of error increases with increase in the SBW/NBW ratio.

TABLE III

ε VALUES (cm^2)

Instrument	Toluene ($\lambda = 206$ nm)	PNA ($\lambda = 228$ nm)	PNA ($\lambda = 376$ nm)	Chromate ($\lambda = 373$ nn
Perkin-Elmer PE 551 UV–VIS spectrophotometer	$7.20 \cdot 10^{3a}$	$5.80 \cdot 10^{3a}$	$1.56 \cdot 10^{4a}$	$4.82 \cdot 10^{3b}$
Varian 2550	$6.90 \cdot 10^3$	$5.81 \cdot 10^3$	$1.56 \cdot 10^4$	$4.81 \cdot 10^3$
Perkin-Elmer LC-95			$1.56 \cdot 10^4$	$4.74 \cdot 10^3$
Hewlett-Packard HP 1090 diode array		$6.03 \cdot 10^3$	$1.56 \cdot 10^4$	$4.84 \cdot 10^3$
Jasco 875 UV	$6.40 \cdot 10^3$	$6.20 \cdot 10^3$	$1.55 \cdot 10^4$	$4.70 \cdot 10^3$
Water Assoc. Lambda Max Model 481	$7.50 \cdot 10^3$	$5.94 \cdot 10^3$	$1.56 \cdot 10^4$	$4.83 \cdot 10^3$

[a] Obtained on PE Model 551 with 0.2-nm slit width.
[b] Ref. 7.

CONCLUSIONS

It is possible with well chosen commercial instruments to measure the absolute number of moles with flow-through detectors. However, one must know the flow-rate, the molar absorptivity of the analyte and the thickness of the cell. All these quantities except the molar absorptivity can be easily obtained and automatically acquired by a data-treatment station. A databank of ε values could be considered as a

first step toward calibrationless analysis in the linear region of the absorption–concentration law.

However, the data presented indicate that a reduction in the random errors is necessary with present-day instruments. We are now trying to assess the origin of these errors and the relevant limits of detection for real samples.

ACKNOWLEDGEMENTS

We thank Prof. G. Barbiroli, G. Cainelli and R. Zironi for allowing us to use their HPLC instruments. Partial support by MPI and CNR (Contract No. 880088) is duly acknowledged.

REFERENCES

1 G. Torsi, G. Chiavari, C. Laghi, A. M. Asmundsdottir, F. Fagioli and R. Vecchietti, *J. Chromatogr.*, 482 (1989) 207.
2 K. Peck and M. D. Morris, *J. Chromatogr.*, 448 (1988) 193.
3 A. Knowles and C. Burgess (Editors), *Practical Absorption Spectrometry*, Chapman and Hall, London, 1964.
4 F. C. Strong, III, *Anal. Chem.*, 48 (1976) 2155.
5 J. R. Edisbury, *Practical Hints on Absorption Spectrometry*, Hilger, London, 1966.
6 V. Lagesson and J. M. Newman, *Anal. Chem.*, 61 (1989) 1249.
7 R. W. Burke, E. R. Deardogg and O. Menis, *J. Res. Natl. Bur. Stand., Sect. A*, 76 (1972) 469.

Journal of Chromatography, 518 (1990) 141–148
Elsevier Science Publishers B.V., Amsterdam

CHROM. 22 591

High-performance liquid chromatographic determination of proteins by post-column fluorescence derivatization with thiamine reagent

TOSHIO YOKOYAMA*
Central Research Laboratory, SS Pharmaceutical Co. Ltd., 1143 Nanpeidai, Narita-shi, Chiba 286 (Japan)
and
TOSHIO KINOSHITA
Pharmaceutical Sciences, Kitasato University, 9-1 Shirokane-5, Minato-ku, Tokyo 108 (Japan)
(First received February 20th, 1990; revised manuscript received May 28th, 1990)

ABSTRACT

A post-column derivatization method for the high-performance liquid chromatography of peptides and proteins giving a fluorescence intensity proportional to the number of peptide bonds is described. Peptide bonds were chlorinated with hypochlorite and the N-chlorite formed was allowed to react with thiamine to give fluorescent thiochrome. This method was applied the determination of membrane-forming proteins of microorganisms.

INTRODUCTION

The determination of proteins and peptides by high-performance liquid chromatography (HPLC) has been extensively investigated in recent years [1–7]. In most of the HPLC methods, the proteins and peptides were usually detected spectrophotometrically because most proteins and peptides absorb at 210 or 280 nm. Although the absorbance at 210 nm reflected the actual content of proteins because it is based on the absorption by the peptide bonds in the protein molecule, it is seriously affected by various UV-absorbing substances in biological samples. On the other hand, the absorbance at 280 nm is subject to interferences by contaminants, but is not proportional to the actual content of proteins because it reflects the amount of aromatic amino acids.

There have also been reports of post-column fluorescence derivatization methods with *o*-phthalaldehyde [8,9] or fluorescamine [9,10] for peptides of low molecular weight, with alkaline ninhydrin [11] or benzoin [12] for arginine-containing peptides and with hydroxylamine–cobalt (II) [13] or a phenol-sensitive electrode [14,15] for tyrosine-containing peptides. However, these methods were also based on the reaction of terminal amino groups or particular side-chains and did not reflect the actual amount of proteins.

Kinoshita *et al.* [16] reported a fluorimetric method in which the peptide bonds of protein were chlorinated and allowed to react with thiamine to give thiochrome.

0021-9673/90/$03.50

We have recently applied this principle to the flow-injection analysis (FIA) of proteins in which the fluorescence intensity was proportional to the number of peptide bonds [17].

In this study, we have devised an HPLC method based on this principle that facilitates the detection of various proteins and peptides at the same level of sensitivity.

EXPERIMENTAL

Chemicals

Bovine serum albumin (BSA), thyroglobulin, γ-globulin, myoglobin, lysozyme, ovalbumin, cytochrome *c*, α-chymotrypsin, α-chymotrypsinogen A, trypsinogen, ribonuclease and jack bean meal were purchased from Sigma (St. Louis, MO, U.S.A.). Sodium hypochlorite solution (Antiformin), sodium nitrite, thiamine hydrochloride, Brij-35, anhydrous sodium sulphate, sodium hydrogenphosphate dodecahydrate, sodium dihydrogenphosphate dihydrate and other chemicals were of analytical-reagent grade from Wako (Osaka, Japan).

Deionized, distilled water was used throughout.

Mobile phase and derivatization reagents

The mobile phase for HPLC was prepared by adding 0.1 *M* sodium sulphate to 0.1 *M* phosphate buffer (pH 7.5). The solution was filtered through a 0.45-μm microfilter (Fuji Photo Film, Tokyo, Japan) and degassed prior to use.

Hypochlorite reagent was prepared by diluting commercial sodium hypochlorite solution (Antiformin) with 0.05 *M* phosphate buffer (pH 7.5), adjusting the pH to 7.5 and the final concentration of available chlorine to 0.8% with 0.05 *M* sodium hydrogenphosphate solution and 0.05 *M* sodium dihydrogenphosphate solution and adding 0.1% Brij-35.

Thiamine reagent was prepared by dissolving 8.0 g of sodium nitrite and 40 mg of thiamine hydrochloride in *ca.* 100 ml of 0.05 *M* phosphate buffer (pH 7.5), adjusting the pH of the solution to 7.5 using 0.05 *M* sodium hydrogenphosphate solution and 0.05 *M* sodium dihydrogenphosphate solution and diluting the resulting mixture to 200 ml with 0.05 *M* phosphate buffer (pH 7.5). The final concentrations of sodium nitrite and thiamine hydrochloride were 4 and 0.02% (w/v), respectively. This reagent was stable for at least 24 h at room temperature and for 1 week in a refrigerator.

The above reagent solutions were filtered to remove suspended material before use.

Chromatographic system

Fig. 1 shows a schematic diagram of the HPLC system. Chromatographic separations were carried out on a 30 cm × 7.5 mm I.D. TSKgel-G3000SW column (Tosoh, Tokyo, Japan), operated at ambient temperature. The mobile phase and fluorescence reagents were delivered using LC-6A high-pressure semi-micro solvent-delivery systems (Shimadzu, Kyoto, Japan). Samples were injected using a KMT-60A HPLC autosampler (Kyowa-Seimitu, Tokyo, Japan) equipped with a 20-μl loop.

The column eluate was first passed through an SPD-6A UV detector (Shimad-

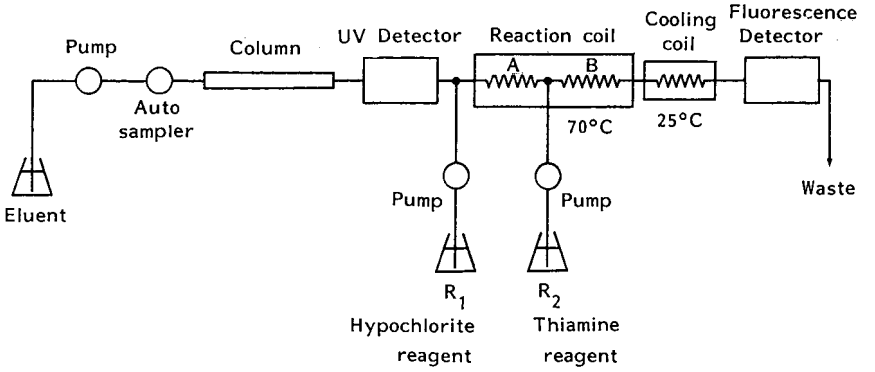

Fig. 1. Schematic diagram of the separation and post-column fluorescence derivatization of proteins.

zu) equipped with a 20-μl flow cell set at 210 or 280 nm, and then it was introduced into a fluorescence reactor system. The hypochlorite reagent was delivered to the eluate stream at a tee-mixer at a flow-rate of 0.2 ml/min, and then the stream passed through PTFE reaction coil A (3 m × 0.5 mm I.D.) immersed in a thermostated water-bath (Thermo-minder, Type Ace-80; Taiyo Service Centre, Tokyo, Japan) maintained at 70°C. After the chlorination reaction, the thiamine reagent was delivered to the reaction steam at a flow-rate of 0.2 ml/min. Then the mixture was passed through PTFE reaction coil B (5 m × 0.5 mm I.D.) immersed in a water-bath at 70°C.

The effluent from coil B was passed through a PTFE cooling coil (1 m × 0.5 mm I.D.). The fluorescence generated was monitored with an RF-535 spectrofluorimeter (Shimadzu) equipped with a xenon lamp and a 20-μl flow cell, with excitation and emission wavelengths of 370 and 440 nm, respectively.

Preparation of microbiological samples

The ammonium sulphate fraction of *Escherichia coli* cell debris was prepared as follows. Cultured bacteria cells were suspended in 1/15 *M* phosphate buffer (pH 6.5) and disrupted ultrasonically, and cell debris was removed by centrifugation and fractionated with 30 and 70% ammonium sulphate solution [18]. The suspension of precipitated crude protein in 70% ammonium sulphate was dissolved in 0.05 *M* phosphate buffer (pH 7.5) and the solution obtained was used as a sample.

RESULTS AND DISCUSSION

Optimization of the post-column reaction conditions

Proteins were separated in the gel-filtration mode in which phosphate buffer (pH 7.5) was used as the mobile phase. The components of the mobile phase were the same as those of the carrier solution in our previous FIA method for proteins [17].

The post-column reaction conditions were examined by varying the concentrations of the reagents. Fig. 2 shows that the fluorescence intensity increases with increase in the concentration of available chlorine and reaches a plateau at 0.8%. It also demonstrates that the fluorescence intensity increases with increase in the concentration of sodium nitrite and the maximum fluorescence intensity was observed at 4%.

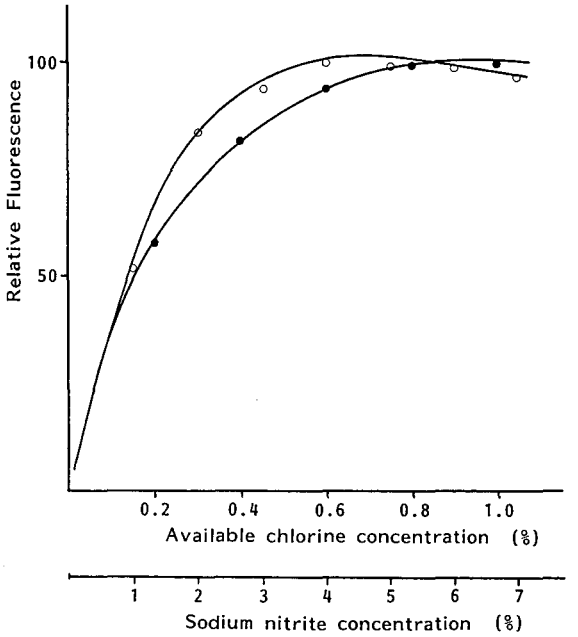

Fig. 2. Effect of the concentrations of available chlorine (●) and nitrite (○) on the fluorescence development of BSA (2 μg per injection). HPLC and post-column reaction conditions as in text, except for reagent concentrations.

The concentration of thiamine in the reagent was adjusted to 0.02% (w/v), where the maximum fluorescence was observed.

System performance

Fig. 3 shows the HPLC profile of the standard proteins which were simultaneously detected utilizing the absorbance at 210 or 280 nm and fluorescence intensity.

The fluorescence intensity hardly fluctuated among the different proteins, whereas the absorbance at 210 nm gave a higher peak for thyroglobulin than for other proteins. Further, considerable differences in the absorbance at 280 nm were observed among the proteins. For example, the peak height of lysozyme was *ca.* five times larger than that of BSA. The peak-height ratio of cytochrome *c* to ovalbumin measured at 210 nm was 1.1 and that measured at 280 nm was 3.2, but that measured by the present method was almost unity.

Fig. 4 shows the calibration graphs for α-chymotrypsin, BSA, trypsinogen, myoglobin and thryroglobulin. Linear relationships between the peak responses and the amounts of the proteins were observed in the range 20 ng–2 μg per injection (20 μl). The limit of detection by the present method for BSA was 10 ng per injection at a signal-to-noise ratio of 2.0; this value was equal to that of the absorbance at 210 nm. The relative standard deviation was 1.9% ($n=10$) for 500 ng in a 20-μl injection.

Fig. 5 shows the relationships between the number of peptide bonds and the peak responses in the present method and the UV 280-nm method. The fluorescence responses in the present method were found to be proportional to the number of

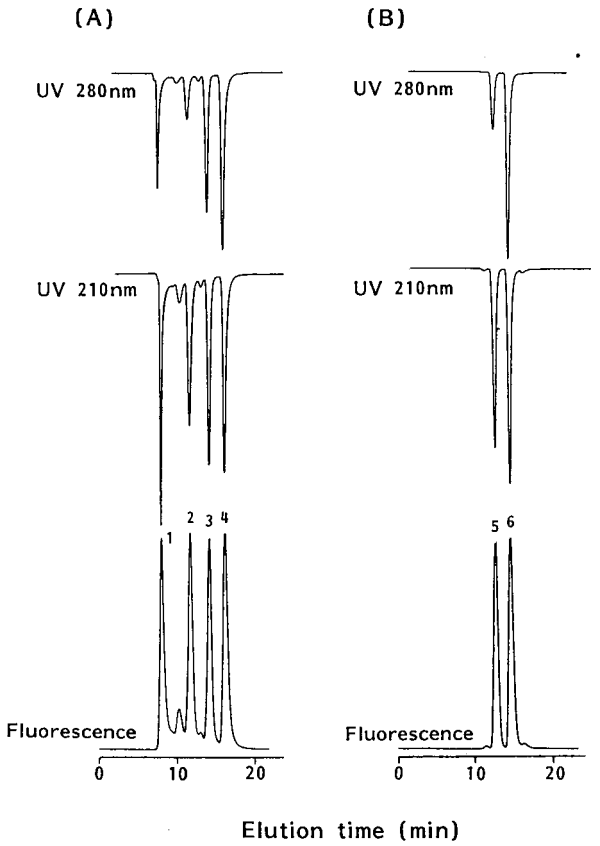

Fig. 3. Chromatograms of a mixture of standard proteins (2 μg each), obtained by dual UV detection at 210 or 280 nm and by the present method. (A) Thyroglobulin, BSA, myoglobin and lysozyme; (B) ovalbumin and cytochrome *c*. Column, TSKgel-G3000SW (30 cm × 7.5 mm I.D.); mobile phase, 0.1 *M* phosphate buffer (pH 7.5) containing 0.1 *M* sodium sulphate; flow-rate, 0.8 ml/min. Peaks: 1 = thyroglobulin; 2 = BSA; 3 = myoglobin; 4 = lysozyme; 5 = ovalbumin; 6 = cytochrome *c*.

peptide bonds, whereas the absorbances at 280 nm deviated substantially from a linear relationship. These results suggest that the present detection method is advantageous for mixtures of proteins having different amino acid compositions.

Fig. 6 shows the chromatograms of jack bean meal and the ammonium sulphate fraction of *E. coli* cell debris. The chromatograms obtained by the present method are similar to those given by the method using the absorption at 210 nm. The large response at a retention time of 26 min shown in Fig. 6A is due to the ammonium sulphate used for the fractionation. However, the peak has a very different retention time to those of the peptides and proteins.

Ionic surfactants, such as sodium dodecyl sulphate (SDS) and Triton X-100, which interfere in protein determinations based on UV absorption at 210 nm, did not affect the present method. Therefore, the present method is also useful for the study

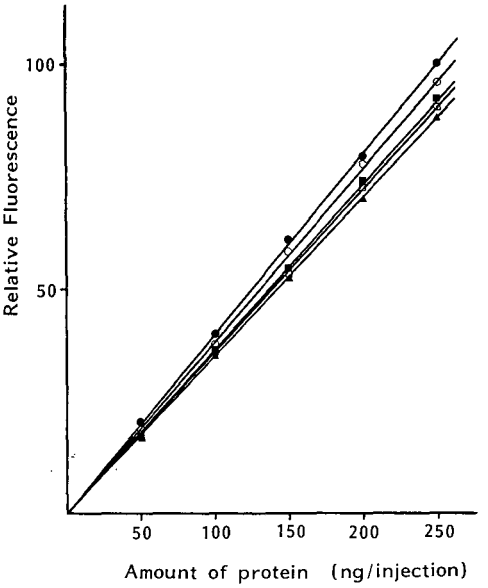

Fig. 4. Calibration graphs for (●) α-chymotrypsin, (○) trypsinogen, (■) myoglobin, (□) BSA and (▲) thyroglobulin obtained by the present method.

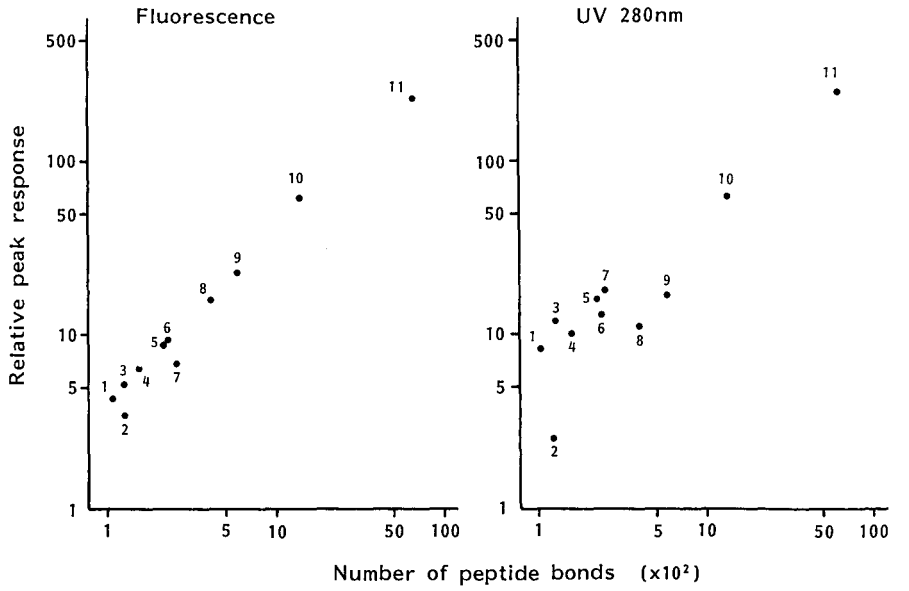

Fig. 5. Relationships between number of peptide bonds and peak responses obtained by the UV 280-nm method and the present method. A 20-μl volume of a sample containing 2 μg of each protein was injected. 1 = Cytochrome *c*; 2 = ribonuclease; 3 = lysozyme; 4 = myoglobin; 5 = α-chymotrypsin; 6 = trypsinogen; 7 = α-chymotrypsinogen A; 8 = ovalbumin; 9 = BSA; 10 = γ-globulin; 11 = thyroglobulin.

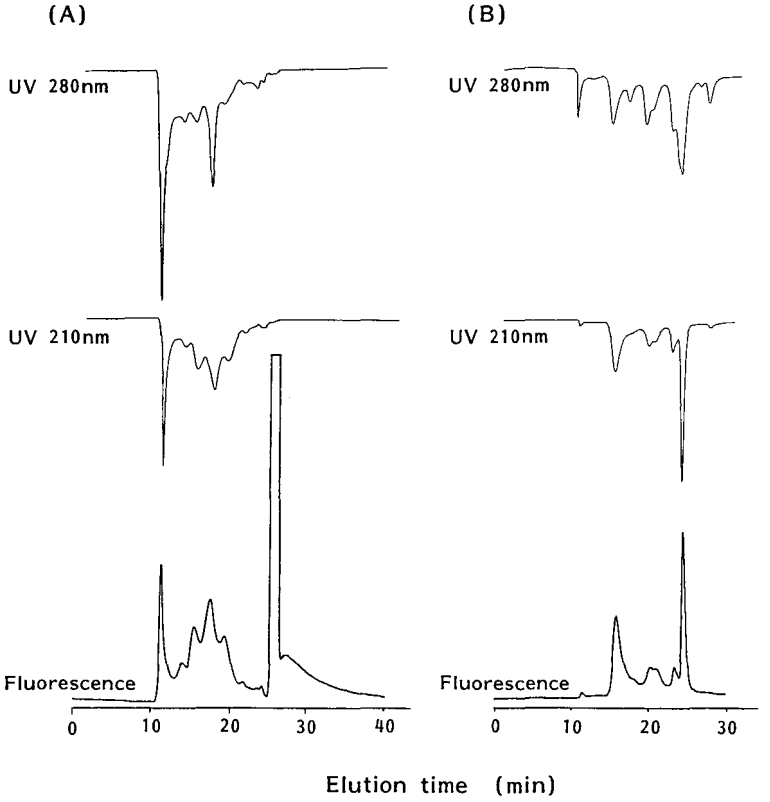

Fig. 6. Chromatograms of the ammonium sulphate fraction of (A) *E. coli* cell debris and (B) jack bean meal obtained by dual detection with the UV 210- or 280-nm method and the present method. Column, TSKgel-G3000SW (30 cm × 7.5 mm I.D.); mobile phase, 0.1 *M* phosphate buffer (pH 7.5) containing 0.1 *M* sodium sulphate; flow-rate, 0.8 ml/min.

of membrane-forming proteins which are usually analysed after eluation with such ionic surfactants.

Detection conditions in HPLC other than gel filtration mode, such as the ion-exchange and reversed-phase modes, are currently under investigation.

REFERENCES

1 T. Sasagawa, T. Okuyama and D. C. Teller, *J. Chromatogr.*, 240 (1982) 329.
2 T. Kadoya, T. Ogawa, H. Kuwahara and T. Okuyama, *J. Liq. Chromatogr.*, 11 (1988) 2951.
3 J. S. Swan, M. Azadpur, A. J. Bharucha and M. A. Krafczyk, *J. Liq. Chromatogr.*, 11 (1988) 3385.
4 B. S. Welinder, H. H. Sorensen and B. Hansen, *J. Chromatogr.*, 462 (1989) 255.
5 K. Fukano, K. Komiya, H. Sasaki and T. Hashimoto, *J. Chromatogr.*, 166 (1978) 47.
6 N. T. Miller, B. Feibush and B. L. Karger, *J. Chromatogr.*, 316 (1985) 519.
7 N. Hirata, M. Kasai, Y. Yanagihara and K. Noguchi, *J. Chromatogr.*, 434 (1988) 71.
8 S. Terabe, A. Tsuchiya and T. Ando, *Bunseki Kagaku*, 33 (1984) 361.
9 T. D. Schlabach, *J. Chromatogr.*, 266 (1983) 427.
10 R. W. Frei, L. Michel and W. Santi, *J. Chromatogr.*, 126 (1976) 665.
11 Y. Hiraga, K. Shirono, S. Ohishi, S. Sakakibara and T. Kinoshita, *Bunseki Kagaku*, 33 (1984) E279.

12 M. Ohno, M. Kai and Y. Ohkura, *J. Chromatogr.*, 392 (1987) 309.
13 M. Ohno, M. Kai and Y. Ohkura, *J. Chromatogr.*, 421 (1987) 245.
14 S. Mousa and D. Couri, *J. Chromatogr.*, 267 (1983) 191.
15 M. W. White, *J. Chromatogr.*, 262 (1983) 420.
16 T. Kinoshita, J. Murayama, K. Murayama and A. Tsuji, *Chem. Pharm. Bull.*, 28 (1980) 641.
17 T. Yokoyama, N. Nakamura and T. Kinoshita, *Anal. Biochem.*, 184 (1990) 184.
18 Y. Kato, K. Komiya, Y. Sawada, H. Sasaki and T. Hashimoto, *J. Chromatogr.*, 190 (1980) 305.

Journal of Chromatography, 518 (1990) 149–156
Elsevier Science Publishers B.V., Amsterdam

CHROM. 22 593

Determination of aromatic amines at trace levels by ion interaction reagent reversed-phase high-performance liquid chromatography

Analysis of hair dyes and other water-soluble dyes

M. C. GENNARO*, P. L. BERTOLO and E. MARENGO
Dipartimento di Chimica Analitica, Università di Torino, Via P. Giuria 5, 10125 Torino (Italy)
(First received February 5th, 1990; revised manuscript received May 29th, 1990)

ABSTRACT

A reversed-phase high-performance liquid chromatographic method, making use of interaction reagents, was developed for the separation and determination of aromatic amines. Different interaction reagents were used and compared. The use of octylammonium salicylate or octylammonium orthophosphate as the interaction reagent and a reversed-phase spherical 5-μm RP-18 as the stationary phase, with spectrophotometric detection at different wavelengths, gave good results. The separation of up to seven aromatic amines (the three isomers of phenylenediamine, benzylamine, 2-phenylethylamine, 3-phenylpropylamine and aniline) was obtained with sensitivity levels ranging between 50 and 100 ppb. The method was applied to the analysis of water-soluble dyes such as fabric dyes, brown and blond hair dyes, black shoe dye and black fountain-pen ink. It was possible to detect and determine 1,4-phenylenediamine in commercial hair dyes. The results indicate that very large amounts of this amine are present in these products, namely 7320 ppm for brown hair and 598 ppm for blond hair.

INTRODUCTION

The need to develop reliable and sensitive methods for the identification and determination of aromatic amines at trace levels continues to increase in fields such as the environment, food and cosmetics.

Only a few methods have been proposed for the determination of aromatic amines, generally using high-performance liquid chromatography (HPLC), through derivatization precolumn reactions [1–5]. Also flow injection voltammetric methods were employed, with diazotization [6] or bromination [7] reactions. Unfortunately, these methods involve tedious and time-consuming procedures for the preparation of the sample. No example has been found in the literature of the use of the interaction reagent reversed-phase HPLC technique for the identification and separation of aromatic amines. This technique, already employed in this laboratory for the separation of anionic species and amines [8,9], is generally characterized by good resolution and sensitivity. Further, it requires no derivatization, clean-up or pretreatment of the sample.

In this paper the optimum conditions for the determination of amounts of aromatic amines are discussed.

0021-9673/90/$03.50

EXPERIMENTAL

Apparatus

Analyses were carried out with a Merck–Hitachi Lichrograph Model L-6200 chromatograph, equipped with a Merck–Hitachi Model D-2500 Chromato-Integrator and an L-4200 UB–VIS detector.

For pH measurements, a Metrohm 654 pH meter equipped with a combined glass–calomel electrode was employed. A Hitachi 150-20 spectrophotometer was employed for absorptivity evaluation.

Chemicals and reagents

Ultra-pure water from a Milli-Q system (Millipore) was used for the preparation of solutions.

Octylamine of analytical-reagent grade was obtained from Fluka and salicylic acid and all other reagents of analytical-reagent grade from Carlo Erba.

Chromatographic conditions

A Merck Hibar LiChrosorb RP-18 (5 μm) column (250 × 4.0 mm I.D.) was used. Although a Merck LiChrosorb RP-18 (10 μm) column (250 × 4.0 mm I.D.) was also tested it was not employed because it gave too long retention times.

The solutions to be used as eluents, namely octylammonium salicylate and octylammonium orthophosphate, were prepared (as elsewhere described [8–10]) by dissolving a weighed amount of octylamine in ultra-pure water and adjusting the pH of the solutions to 6.4 ± 0.4 by addition of salicylic or orthophosphoric acid. At this pH and taking into account the acid formation constant, octylamine is present in the protonated octylammonium form and the composition of the eluents so prepared is not completely stoichiometric. For the sake of simplicity, however, the eluents used as the mobile phase are referred to henceforth as octylamonium salicylate and octylammonium orthophosphate.

In order to condition the chromatographic system properly, the eluent was allowed to flow through the column until a stable baseline signal was obtained (a minimum of 1 h was necessary). The eluent solutions were freshly prepared every third day.

The reproducibility of measurements was very good for sequential measurements under the same conditions of eluent preparation and column conditioning but slightly lower for different eluent preparations. For the sake of general validity, the average data and reproducibilities listed in Table I were calculated for different preparations.

Between uses, the column was regenerated by passing water–methanol (1:1, v/v) through it. This treatment maintained the column lifetime comparable to that in other chromatographic techniques.

Preparation of samples

The samples of the water-soluble dyes tested for the presence of aromatic amines (namely fabric dye, brown and blond hair dyes, black shoe dye and black fountain-pen ink) were prepared simply by dissolving the samples in ultra-pure water, filtering through a 0.45-μm filter and diluting when necessary with ultra-pure water.

RESULTS AND DISCUSSION

Previous work [8–11] indicated the versatility of ion interaction reagent reversed-phase HPLC. The mechanisms that govern retention were discussed and it was pointed out that the mechanism of interaction through which amines are retained involves the formation of ammonium salts (or ions pairs) between the amine injected and the anion of the flowing interaction reagent. The investigated amines are then released and eluted in the same form in which they were retained, a result which can be demonstrated when octylammonium salicylate is used as the mobile phase. Under these conditions, aliphatic amines can be easily detected at 254 nm, even if their absorptivities are almost zero at this wavelength. The observed absorbance is due to the accompanying salicylate anions.

In order to establish the optimum conditions for the trace determination of aromatic amines, a preliminary comparative study was carried out by employing different stationary phase packings and different interaction reagents.

The choice and the comparative use of octylammonium salicylate and octylammonium orthophosphate as the interaction reagents, together with a spherical 5-μm RP-18 as the stationary phase, proved to be of particular interest.

Spectrophotometric detection at different wavelengths was employed; Table I lists the absorptivity values obtained for the investigated amines at 210, 230 and 254 nm.

Good results were obtained in the separation of aromatic amines with the above eluents. Fig. 1 shows the chromatogram obtained by using octylammonium salicylate as the interaction reagent in the separation of a mixture of six aromatic amines, namely 1,4-phenylenediamine (0.50 ppm), 1,3-phenylenediamine (1.50 ppm), 2-phenylethylamine (10.00 ppm), 1,2-phenylenediamine (2.00 ppm), 3-phenylpropylamine (10.00 ppm) and aniline (5.00 ppm) with UV detection at 254 nm. It is worth remembering that at this wavelength both aromatic amines and salicylate anions are characterized by non-zero absorptivities (see Table I).

Fig. 2 shows the chromatogram obtained by using octylammonium orthophosphate as the mobile phase in the separation of a mixture of benzylamine, 2-phenylethylamine, 3-phenylpropylamine and aniline at concentrations of 1.00 ppm each and employing spectrophotometric detection at 210 nm.

TABLE I

ADSORPTIVITY VALUES, ε (l mol^{-1} cm^{-1}), FOR THE INVESTIGATED AMINES AND FOR SALICYLATE EVALUATED AT DIFFERENT WAVELENGTHS

Compound	λ = 210 nm	λ = 230 nm	λ = 254 nm
Aniline	$(4.1 \pm 0.1) \cdot 10^3$		$(2.9 \pm 0.1) \cdot 10^2$
Benzylamine	$(8.4 \pm 0.3) \cdot 10^3$	$(1.1 \pm 0.1) \cdot 10^2$	$(1.7 \pm 0.1) \cdot 10^1$
1,2-Phenylenediamine	$(3.59 \pm 0.09) \cdot 10^4$	$(8.4 \pm 0.1) \cdot 10^3$	$(2.0 \pm 0.1) \cdot 10^3$
1,3-Phenylenediamine	$(3.47 \pm 0.08) \cdot 10^4$	$(1.03 \pm 0.06) \cdot 10^4$	$(2.0 \pm 0.1) \cdot 10^3$
1,4-Phenylenediamine	$(6.5 \pm 0.1) \cdot 10^3$	$(7.0 \pm 0.1) \cdot 10^3$	$(4.4 \pm 0.2) \cdot 10^3$
2-Phenylethylamine	$(5.5 \pm 0.9) \cdot 10^3$		$(2.3 \pm 0.1) \cdot 10^2$
3-Phenylpropylamine	$(7.7 \pm 0.1) \cdot 10^3$		$(2.0 \pm 0.1) \cdot 10^2$
Salicylate			$(3.1 \pm 0.1) \cdot 10^2$

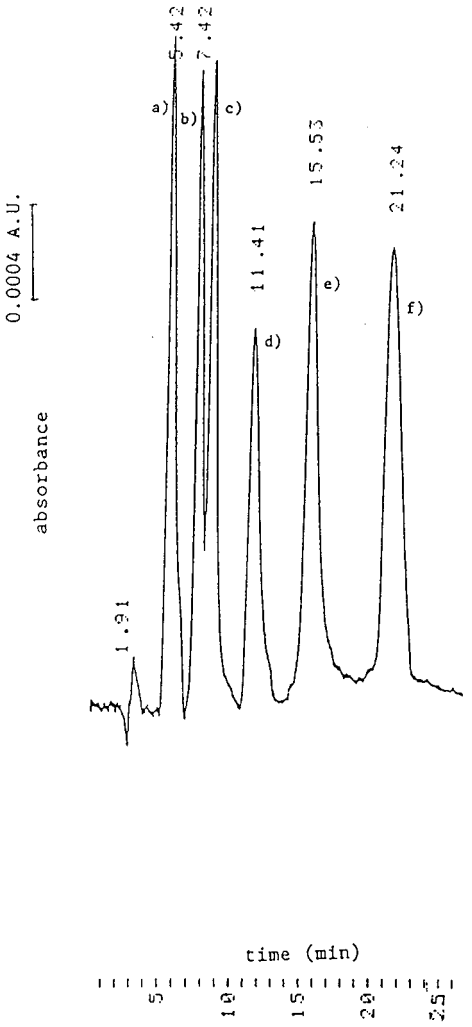

Fig. 1. Separation of a mixture of (a) 1,4-phenylenediamine, (b) 1,3-phenylenediamine, (c) 2-phenylethylamine, (d) 1,2-phenylenediamine, (e) 3-phenylpropylamine and (f) aniline. Stationary phase, Merck Hibar LiChrosorb RP-18, 5 μm; ion interaction reagent, 0.0050 *M* octylammonium salicylate; flow-rate, 0.7 ml/min; injection, 100 μl; detection, UV (254 nm).

Because orthophosphate anions are characterized by zero absorptivity at this wavelength, it follows that the observed absorbance is due entirely to the aromatic amines themselves. Therefore, the detection sensitivity varies as a function of the detection wavelength, which can therefore be chosen as a function of the analyte to be evaluated.

A typical example is shown by the comparison of the three chromatograms in Fig. 3, all concerning the separation of the three isomeric forms of phenylenediamine in a mixture containing 1.00 ppm of each. The three chromatograms were recorded

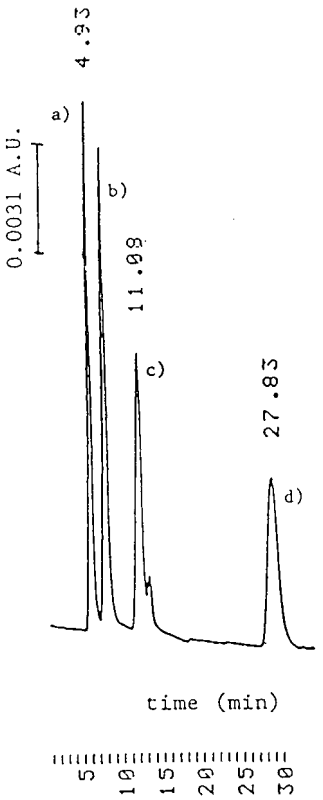

Fig. 2. Separation of a mixture of (a) benzylamine, (b) 2-phenylethylamine, (c) 3-phenylpropylamine and (d) aniline, 1.00 ppm each. Stationary phase, Merck Hibar LiChrosorb RP-18, 5 μm; ion interaction reagent, 0.0050 *M* octylammonium orthophosphate; flow-rate, 0.7 ml/min; injection, 100 μl; detection, UV (210 nm).

under different conditions. In Fig. 3a, octylammonium salicylate was used as the interaction reagent with UV detection at 254 nm. The three amines show comparable detection sensitivities, peak a having a larger area than the others. The observed absorbance is due to the additive contributions of both the salicylate anion and the aromatic ammonium ion. As the contribution from the salicylate anion remains the same, the highest peak area in Fig. 3a is due to 1,4-phenylenediamine, in agreement with the highest absorptivity shown at 254 nm by this analyte (see Table I).

Fig. 3b and c refer to the use octylammonium orthophosphate as the eluent at wavelengths of 210 and 230 nm, respectively. Provided that at these wavelengths no contribution to the absorbance derives from orthophosphate, it can be observed that the sensitivity responses follow the expected absorptivity order (see Table I), namely 1,2- = 1,3- > 1,4-phenylenediamine at 210 nm and 1,3- > 1,2- > 1,4-phenylenediamine at 230 nm.

As regards sensitivity, levels of the order of 50 ppb can be achieved. Fig. 4 shows as an example the chromatogram obtained for the injection of 91 pmol of

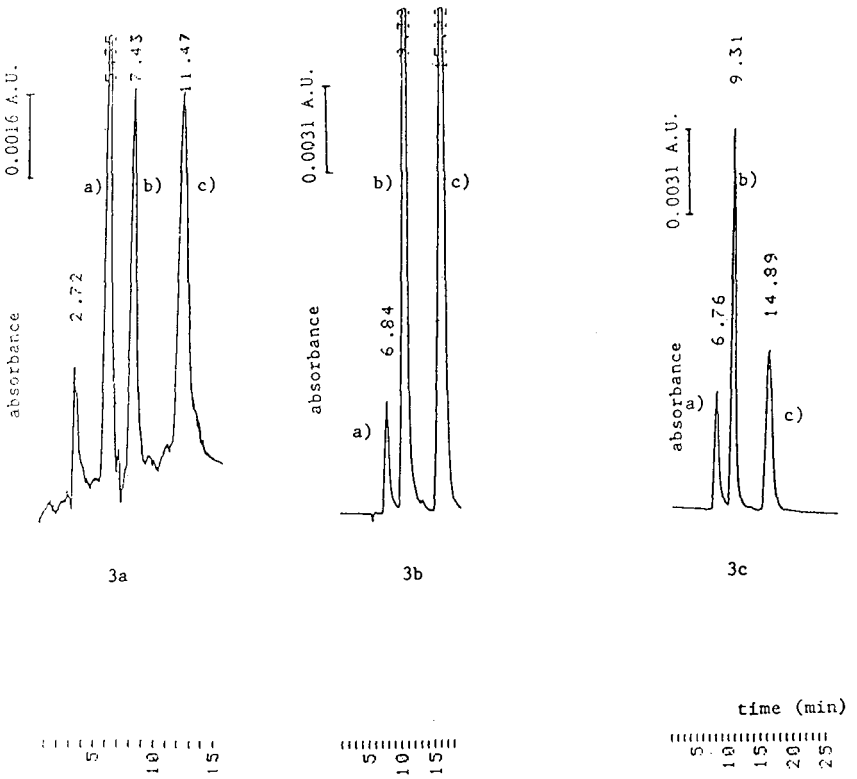

Fig. 3. Separation of a mixture of peak (a) 1,4-phenylenediamine, (b) 1,3-phenylenediamine and (c) 1,2-phenylenediamine, 1.00 ppm each. Stationary phase, Merck Hibar LiChrosorb RP-18, 5 μm; injection, 100 μl. Part (a), ion interaction reagent, 0.0050 *M* octylammonium salicylate; flow-rate, 0.7 ml/min; detection, UV (254 nm). Part (b), ion interaction reagent, 0.0050 *M* octylammonium orthophosphate; flow-rate, 0.7 ml/min; detection, UV (210 nm). Part (c), ion interaction reagent, 0.0050 *M* octylammonium orthophosphate; flow-rate, 0.7 ml/min; detection, UV (230 nm).

1,3-phenylenediamine using octylammonium salicylate as the eluent with UV detection at 210 nm.

The methods described were applied to the analysis of some commercial water-soluble dyes: brown and blond hair dyes, black shoe dye, green fabric dye and black fountain-pen ink.

Whereas the presence of the investigated aromatic amines at concentrations greater than 0.5 ppm can be excluded in shoe and fabric dyes and in ink, significant amounts of 1,4-phenylenediamine were found in the hair dyes. Fig. 5 shows the result of the analysis of a commercial brown hair dye for a sample diluted 1:100 (v/v) and then filtered through 0.45-μm filters. The results obtained for the same sample both with octylammonium salicylate as eluent at 254 nm (Fig. 5a) and with octylammonium orthophosphate at 210 nm (Fig. 5b) are shown. Both clearly indicate the presence of 1,4-phenylenediamine.

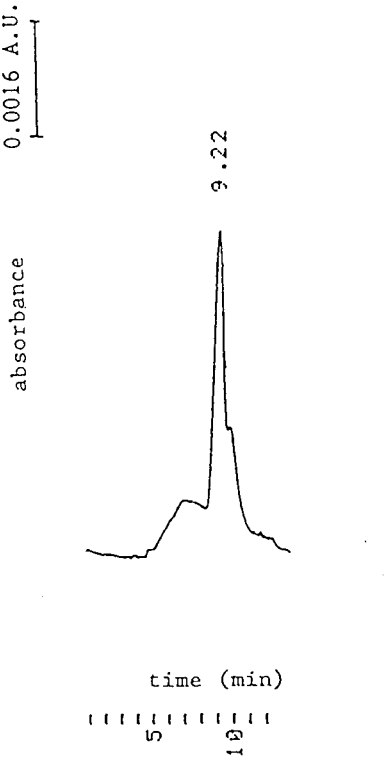

Fig. 4. Injection of 100 μl of a 0.10 mg l^{-1} solution of 1,3-phenylenediamine. Stationary phase, Merck Hibar LiChrosorb RP-18, 5 μm; ion interaction reagent, 0.0050 *M* octylammonium orthophosphate; flow-rate, 0.7 ml/min; detection, UV (210 nm).

Owing to the good linearity of the plot of peak area *versus* standard concentration, it was possible to carry out a quantitative evaluation by employing the standard additions method. Amounts of 7320 ± 8 ppm of 1,4-phenylenediamine were determined for a brown hair dye and about 598 ± 7 ppm for blond hair dye.

1,4-Phenylenediamine is widely used as an ingredient in oxidative hair-dyeing formulations. It is not included in the list of carcinogenic amines, but recent papers have reported its toxic effects [4] and percutaneous absorption during hair-dyeing procedures employing a commercial product [12].

In conclusion, the proposed method permits the reliable, sensitive and rapid determination of aromatic amines in real samples and does not require any sample derivatization or work-up procedures.

ACKNOWLEDGEMENTS

This investigation was supported by the Italian National Research Council and the Ministero della Pubblica Istruzione.

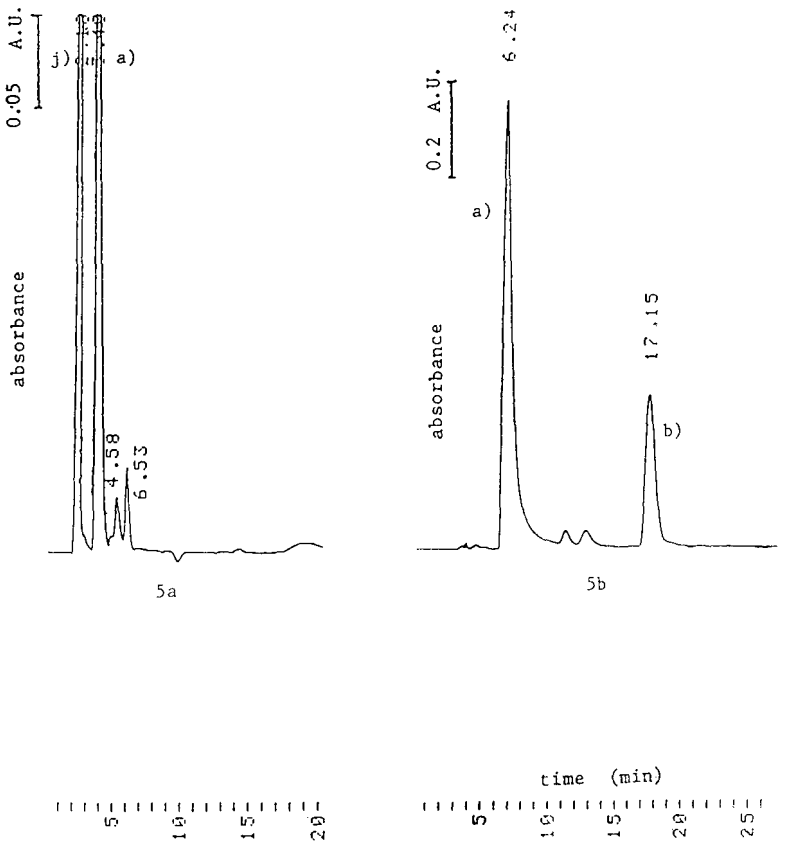

Fig. 5. Analysis of brown hair dye. Stationary phase, Merck Hibar LiChrosorb RP-18, 5 μm; injection, 100 μl. Part (a), ion interaction reagent, 0.0050 *M* octylammonium salicylate; flow-rate, 1.00 ml/min; detection, UV (254 nm). Part (b), ion interaction reagent, 0.0050 *M* octylammonium orthophosphate; flow-rate, 0.7 ml/min; detection, UV (210 nm). Peaks: (j) injection peak; (a) 1,4-phenylenediamine; (b) unidentified.

REFERENCES

1 C. R. Nony and M. C. Bowman, *J. Chromatogr. Sci.*, 18 (1980) 64–74.
2 N. Richfield-Fratz, J. E. Bailey and C. J. Bailey, *J. Chromatogr.*, 331 (1985) 109–123.
3 R. B. Geerdink, *J. Chromatogr.*, 445 (1988) 273–281.
4 M. J. Avery, *J. Chromatogr.*, 488 (1989) 470–475.
5 P. J. Rennie, *J. Chromatogr.*, 461 (1989) 277–280.
6 A. G. Fogg, N. K. Bsebsu and M. A. Abdulla, *Analyst (London)*, 107 (1982) 1462–1465.
7 A. G. Fogg, M. S. Ali and M. A. Abdulla, *Analyst (London)*, 108 (1983) 840–846.
8 M. C. Gennaro and E. Marengo, *Chromatographia*, 25 (1988) 603–608.
9 M. C. Gennaro and P. L. Bertolo, *J. Chromatogr.*, 472 (1989) 433–440.
10 M. C. Gennaro and P. L. Bertolo, *Ann. Chim. (Rome)*, 80 (1990) 13–25.
11 M. C. Gennaro and P. L. Bertolo, *J. Chromatogr.*, 509 (1990) 147–156.
12 N. Goetz, P. Lasserre, P. Bore and G. Kalopissis, *Int. J. Cosmet. Sci.*, 10 (1988) 63–73.

Journal of Chromatography, 518 (1990) 157–165
Elsevier Science Publishers B.V., Amsterdam

CHROM. 22 605

Sensitive analysis of phospholipid molecular species by high-performance liquid chromatography using fluorescent naproxen derivatives of diacylglycerols

A. RASTEGAR and A. PELLETIER
Centre de Neurochimie du CNRS, Antenne de Cronenbourg, BP20CR, 67073 Strasbourg Cedex (France)
G. DUPORTAIL
Laboratoire de Physique, Faculté de Pharmacie, CNRS UA491, BP24, 67401 Illkirch Cedex (France)
and
L. FREYSZ and C. LERAY
Centre de Neurochimie du CNRS, Antenne de Cronenbourg, BP20CR, 67037 Strasbourg Cedex (France)
(First received December 13th, 1989; revised manuscript received May 16th, 1990)

ABSTRACT

A sensitive high-performance liquid chromatographic (HPLC) method for the separation and determination of diacylglycerophospholipid and diacylglycerol (DAG) molecular species has been developed. Phospholipids are hydrolysed with phospholipase C and the resulting DAGs are reacted with naproxen chloride in the presence of 4-dimethylaminopyridine. The naproxen–DAGs were purified by thin-layer chromatography on silica gel G plates. Molecular species were separated using reversed-phase HPLC with isocratic elution and determined by measuring the absorbance at 230 nm or fluorescence at 352 nm (excitation at 332 nm). The method was applied to the determination of diacylglycerophosphoethanolamine in rat cerebrum and cerebellum. The molar absorption coefficient of the naproxen derivatives was 53 000 $lmol^{-1}$ cm^{-1} at 230 nm, permitting the generation of linear concentration-dependent determinations down to less than 10 pmol. A ten-fold increase in sensitivity was obtained with a fluorescence detection system owing to the fluorescent properties of the proposed adduct.

INTRODUCTION

The accurate separation and determination of molecular species of glycerophospholipids and diacylglycerols (DAGs) is difficult owing to the lack of chromogenic moieties in such molecules. The separation of intact phospholipid molecular species has been proposed [1–4], but without sufficient resolution and sensitivity. Further, the determination of the eluted molecular species is complex owing to the absorption properties which depend on the unsaturation of the individual molecules. The use of post-column fluorescence detection is attractive because it allows the determination of intact phospholipid species in the nanomole range [5]. Unfortunately, none of these techniques permits the resolution of phospholipid subclasses (alk-1-enylacyl, alkylacyl and diacyl types).

Several studies have been reported in which UV-absorbing derivatives of dira-

0021-9673/90/$03.50

dylglycerols[a] prepared from phospholipids after phospholipase C hydrolysis were used [6–9]. Recent improvements in the detection sensitivity have been reported in coupling diacylglycerol moieties with fluorescent compounds [10,11].

This paper describes a method for the determination of the diacylglycerol moieties by high-performance liquid chromatography (HPLC) in the picomole range after their derivatization with naproxen chloride. The technique has been utilized for the analysis of the diacylglycerophosphoethanolamine (PE) composition of rat brain cerebrum.

EXPERIMENTAL

Chemicals

Naproxen (6-methoxy-α-methyl-2-naphthaleneacetic acid) and 4-dimethylaminopyridine were obtained from Aldrich. Oxalyl chloride was obtained from Janssen Chimica and methanol, chloroform, acetonitrile (HPLC grade), 2-propanol (HPLC grade), diethyl ether, light petroleum (b.p. 35–60°C) and hexane were obtained from SDS (Peypin, France). Phospholipase C type XIII (from *Bacillus cereus*), 1,2-dipalmitoyl-*sn*-glycerol, 1,2-dioleoyl-*sn*-glycerol, 1-stearoyl 2-arachidonoyl-*sn*-glycerol were obtained from Sigma (St. Louis, MO, U.S.A.) and pyridine and silica gel 60 thin-layer chromatographic (TLC) plates from Merck (Darmstadt, F.R.G.).

Synthesis of naproxen chloride

Naproxen (500 mg) was dissolved in 50 ml chloroform, 0.3 ml of oxalyl chloride was slowly added and the resulting solution was refluxed for 1 h. The solvent was evaporated to dryness in a rotary evaporator under reduced pressure at 40°C and the residue was kept overnight over potassium hydroxide under vacuum. The powdered naproxen chloride was used without further purification. All the procedures were carried out under reduced light.

Preparation of diacylglycerols from phospholipids

Rat brain cerebrum and cerebellum from adult animals were extracted according to Folch *et al.* [12]. The phospholipids were purified by silicic acid column chromatography [13], spotted on boric acid-impregnated silica gel plates (LK5; Whatman, Clifton, NJ, U.S.A.) and separated using chloroform–ethanol–water–triethanolamine (30:35:7:35, v/v) as solvent [13]. The PE-containing spot was made visible by spraying the TLC plates with 0.01% primuline dye in acetone–water (4:1, v/v) and viewing under UV light. The phospholipid was eluted with 2 × 2 ml of chloroform–methanol–water (5:5:1, v/v/v) and, after evaporation of the solvent, PE was dissolved in chloroform–methanol (2:1, v/v). An aliquot was sonicated in a sonic water-bath (Branson) for 10 s in 1 ml of sodium phosphate buffer (50 m*M*, pH 7.4) containing 30 m*M* sodium borate. After addition of 1.5 ml of diethyl ether and 30 U of phospholipase C, the capped tubes were shaken vigorously for 45 min at room temperature. The ether phase and one wash with diethyl ether were combined and the solution was evaporated to dryness under a stream of nitrogen at room temperature and rapidly derivatized.

---

[a] The term "radyl" is used to denote an acyl, alkyl or alkenyl group.

Derivatization of diglycerides

Up to 1 mg of dried diradylglycerols prepared from phospholipids as described above, 5 mg of naproxen chloride and 10 mg of 4-dimethylaminopyridine were kept under vacuum for 20 min at room temperature. The mixture was dissolved in 1 ml of dry pyridine and heated in a sealed vial at 80°C for 15 min. A 2-ml volume of 0.1% $NaHCO_3$ was added and the derivatized diradylglycerols were extracted twice with 2 ml of hexane. After evaporation of the solvent, the residue was dissolved in a convenient volume of dichloromethane.

Chromatographic analyses

Derivatized diradylglycerols were separated by TLC on silica gel 60 plates developed with light petroleum–diethyl ether (75:25, v/v). The alk-1-enylacyl, alkylacyl and diacyl subclasses were made visible under UV light as brillant spots after spraying with primuline. The naproxen derivates migrated with $R_F \approx 0.82$, 0,75, 0.67 for the alk-1-enylacyl, alkylacyl and diacyl subclasses, respectively, as determined with appropriate standards. The silica gel band containing the diacyl derivatives was scraped off and extracted twice with 2 ml of acetonitrile.

The molecular species were separated by HPLC using a Waters Model 510 pump and either a C_{18} reversed-phase column (150 × 4 mm I.D.) (Resolve, 5 μm; Waters Assoc.) or a 125 × 4 mm I.D. LiChroCART (Lichrospher 100RP-18, 5 μm; Merck–Clevenot, France) at room temperature. The solvent was acetonitrile–2-propanol (95:5, v/v) pumped at a flow-rate of 2 ml min^{-1}. The separated components were measured either with a UV spectrophotometer (Uvidec-100-V; Spectra-Physics) at 230 nm or a scanning fluorescence detector (Waters Model 470, excitation at 332 nm, emission at 352 nm). Peak-area percentages and retention times were obtained with a Spectra-Physics SP4290 recorder–integrator.

The identification of individual molecular species was obtained by gas chromatographic analysis of methyl esters prepared from resolved peaks, by calibration with various diacylglycerol species from commercial sources and by developing a relative retention time–carbon number plot as described previously [14,15]. The fatty acids were analysed from the collected peaks containing not less than 1 nmol of each species.

Fatty acid methyl esters were prepared [16] and analysed with a Perkin-Elmer Sigma 1 instrument fitted with a capillary column (bonded fused silica, 50 m × 0.32 mm I.D., Superox; Alltech), a flame ionization detector and a Sigma 10 data system. The separation was carried out at 190°C with helium as carrier gas. Aliquots of 2 μl of sample were injected in the splitless mode and the methyl esters were identified using appropriate standards.

Spectroscopic analyses

UV spectra were obtained using a Kontron recording spectrophotometer (Uvikon 820) and the fluorescence spectra with an SLM 48000 spectrofluorimeter. Fluorescence lifetimes were determined with a laboratory-built instrument (Ortec components), which is based on the single photoelectron technique.

RESULTS AND DISCUSSION

Naproxen chloride has recently been proposed as a fluorescent reagent for the chiral derivatization of optically active amines and alcohols [17]. This substituted naphthylacetic acid showing a strong intrinsic fluorescence and ultraviolet absorbance seems well suited for the determination of diglycerides after its coupling with the alcohol function.

In order to determine the optimum conditions for the derivatization reaction with 0.1–0.5 mg of diradylglycerols, the effects of excess of reagent, catalyst, reaction time and temperature were determined. A diradylglycerol:reagent:catalyst ratio of 1:5:10 (w/w) was found to be optimum when the reaction proceeded for 15 min at 80°C. Under these conditions, 75 ± 3% of diacylglycerols were converted (deter-

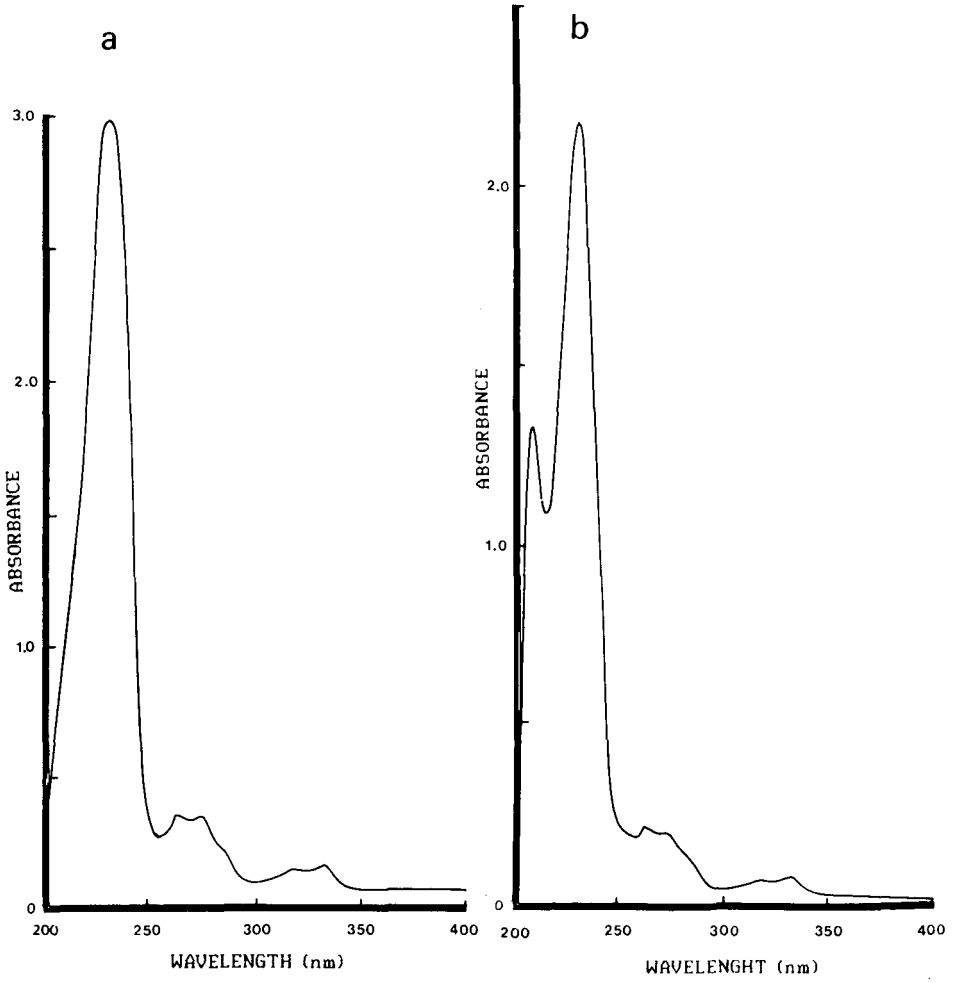

Fig. 1. Absorption spectra of (a) a methanolic solution (50 μM) of naproxen chloride and (b) a methanolic solution (40 μM) of naproxen–diacylglycerols derived from rat cerebrum phosphatidylethanolamine.

mined by fatty acid analysis) and no acyl migration occurred. With UV detection a high sensitivity was observed as the molar absorption coefficient of naproxen–dioleoylglycerol was *ca.* 53 000 l mol^{-1} cm^{-1} at 230 nm, the detection limit being about 10 pmol. Naproxen chloride had an absorption spectrum (Fig. 1a) similar to the lipid derivatives (Fig. 1b) but with a higher molar absorption coefficient at 230 nm (*ca.* 57 000 l mol^{-1} cm^{-1}). Further, HPLC separations of the naproxen diacylglycerols obtained from rat cerebrum diacylphosphatidylethanolamine (Table I) gave similar patterns with detection at 230 and 240 nm, indicating that the quantification is not affected by the degree of fatty acid unsaturation and is directly related to the amount of each molecular species present in the mixture.

In contrast to unsubstituted naphthalene, the absorption spectrum of naproxen chloride displays an additional band near 330 nm, allowing the excitation of the derivatized molecules in this region. This characterization avoids interferences from several fluorescent impurities. The spectral properties of naproxen chloride and the naproxen–diacylglycerol complex displayed the same exitation maximum (in methanol) at 332 nm and the same fluorescence maximum at 352 nm (Fig. 2), without any effect of the degree of acyl chain unsaturation. This was confirmed using various diacylglycerol molecular species with different degrees of unsaturation either collected at the HPLC column outlet or derivatized from diacylglycerol from commercial sources (namely 1,2-dipalmitoylglycerol, 1,2-dioleoylglycerol and 1-stearoyl-2-arachidonoylglycerol). The determined fluorescence quantum yield was 0.35 ± 0.02 in methanol for naproxen chloride and for the three derivatives from the above commercial diacylglycerols. This determination was performed using β-naphthol in cyclohex-

TABLE I

DISTRIBUTION OF MOLECULAR SPECIES IN DIACYLPHOSPHATIDYLETHANOLAMINE FROM RAT CEREBRUM

Peak No.[a]	Molecular species[b]	Composition (%)
1	16:1/20:4*n*6	0.14
2	16:1/22:5*n*6	0.19
3	18:1/22:6*n*3	1.43
4	16:0/22:6*n*3	5.30
5	18:1/20:4*n*6	5.12
6	16:0/20:4*n*6	5.15
7	18:1/18:2*n*6	1.70
8	18:0/22:6*n*3	8.77
9	16:0/22:4*n*6	1.91
10	18:0/22:5*n*3	1.03
11	18:0/20:4*n*6	32.56
12	18:1/18:1*n*9	7.65
13	16:0/18:1*n*9	9.86
14	18:0/20:3*n*6	0.41
15	16:0/16:0	6.47
16	16:0/20:1*n*9	0.30
17	18:0/18:1*n*9	12.40

[a] Peak numbers correspond to those shown in Fig. 3a.

[b] The molecular species are identified by the fatty acid at the 1-position (left) and the fatty acid at the 2-position (right) of the glycerol moiety. The fatty acids are identified by the number of carbon atoms and double bonds.

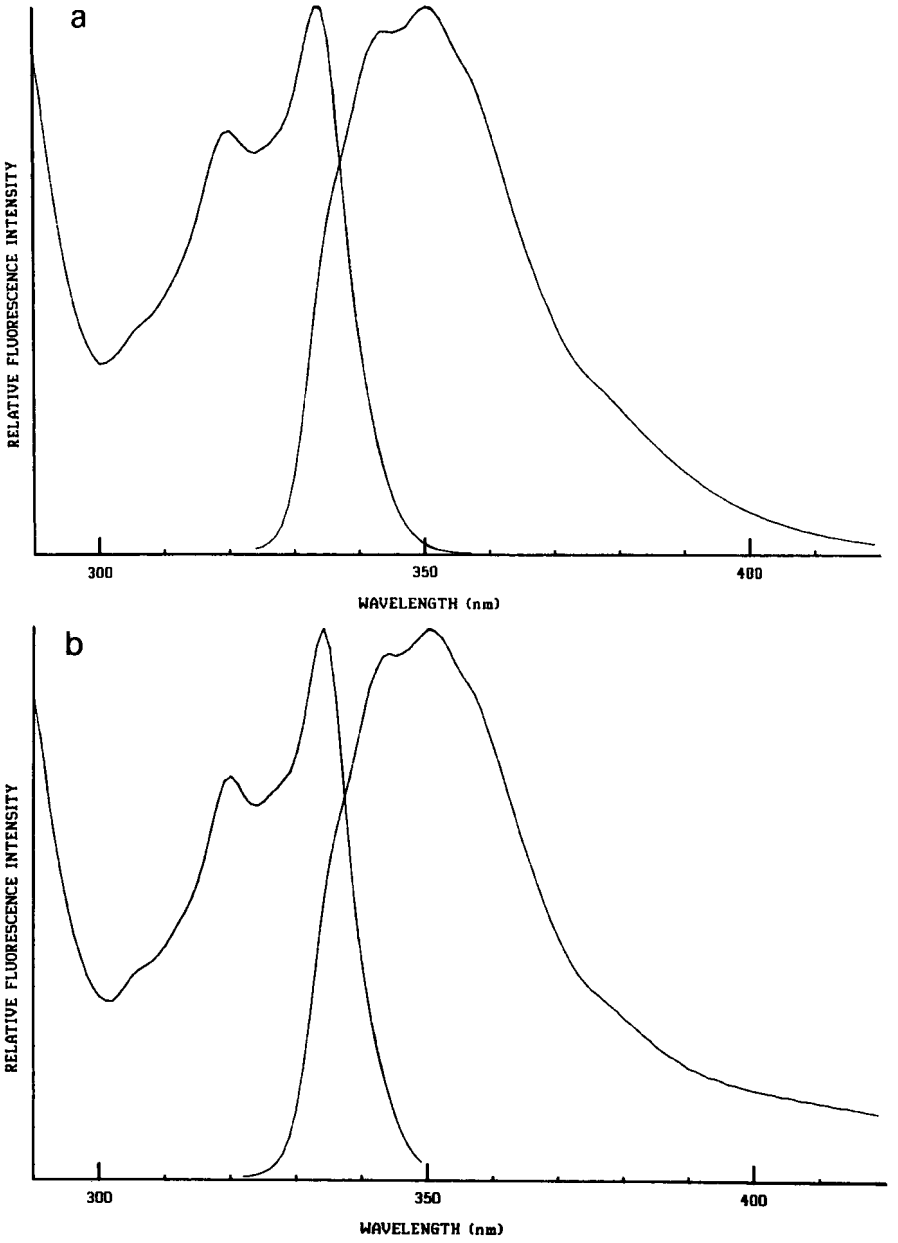

Fig. 2. Excitation spectra (left, $\lambda_{em.}$ = 360 nm) and emission spectra (right, $\lambda_{exc.}$ = 320 nm) of (a) a methanolic solution (50 μM) of naproxen chloride and (b) a methanolic solution (40 μM) of naproxen–diacylglycerols derived from rat cerebrum phosphatidylethanolamine.

Fig. 3. High-performance liquid chromatograms of (a) an acetonitrile solution (32 μM) and (b) acetonitrile → solution (2 μM) of naproxen–diacylglycerols derived from rat cerebrum phosphatidylethanolamine. Operating conditions: column, 12.5 cm LiChrospher 100 RP-18 (5 μm); mobile phase, acetonitrile–2-propanol (95:5); flow-rate, 2 ml min^{-1} at room temperature. The sample [(a) 1.6 nmol and (b) 100 pmol of diacylglycerols] was injected with a 50-μl loop. Fluorescence detector: excitation at 332 nm, emission at 352 nm. For identity of peaks in (a) see Table I. Peaks in (b): (1) 2.3 pmol 18:1/22:6; (2) 8.6 pmol 16:0/22:6; (3) 3.0 pmol 18:1/20:4; (4) 3.0 pmol 16:0/20:4; (5) 31.3 pmol 18:0/22:6; (6) 24.6 pmol 18:0/20:4; (7) 5.0 pmol 18:1/18:1; (8) 5.5 pmol 16:0/18:1; (9) 5.0 pmol 16:0/16:0; (10) 8.6 pmol 18:0/18:1.

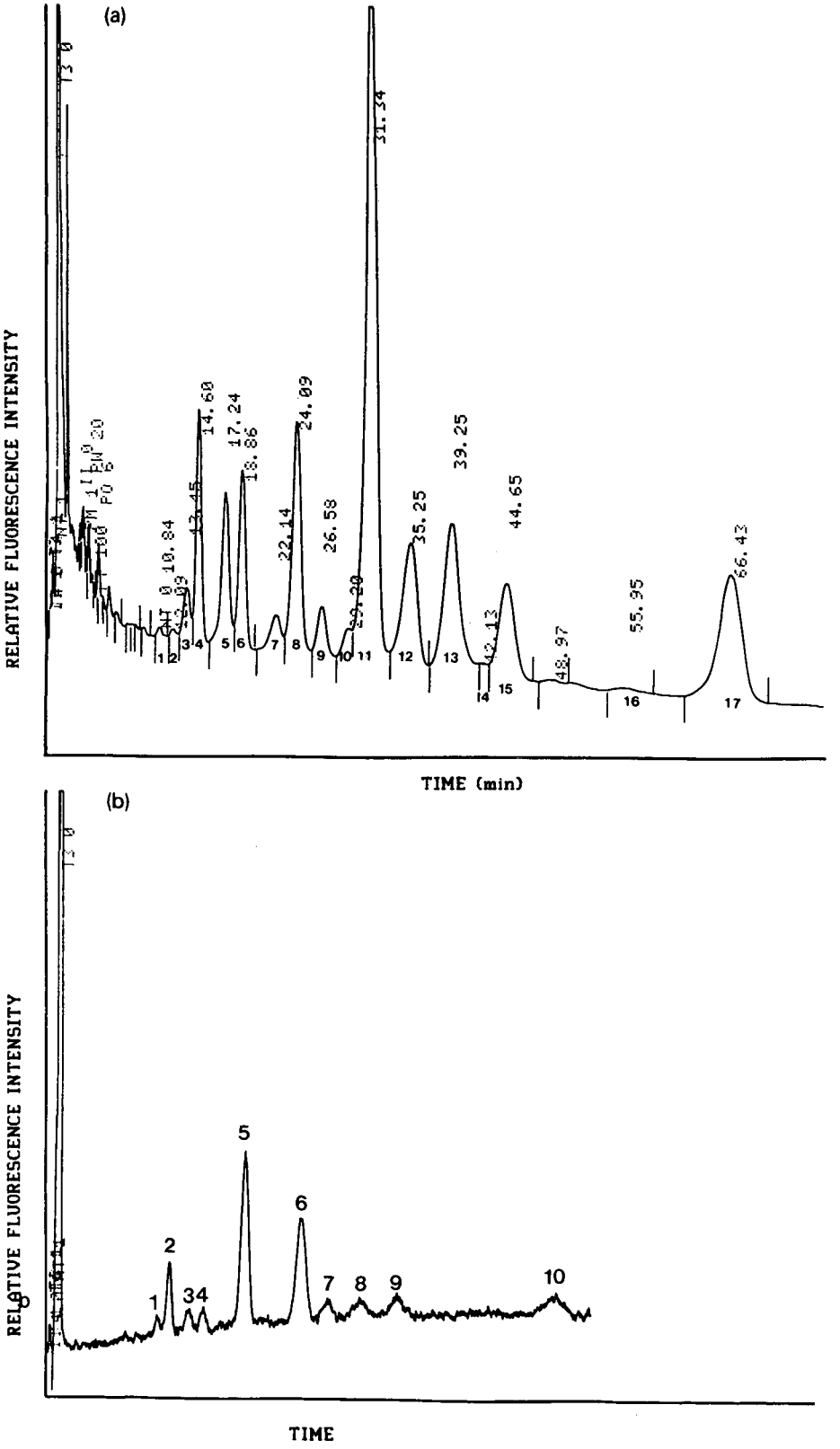
(a)
RELATIVE FLUORESCENCE INTENSITY
TIME (min)
10.84
14.60
17.24
18.86
22.14
24.09
26.58
31.34
35.25
39.25
44.65
55.95
66.43
(b)
RELATIVE FLUORESCENCE INTENSITY
TIME
1
2
34
5
6
7
8
9
10

ane (fluorescence quantum yield $\varphi = 0.32$) as a standard [18]. The constancy of the fluorescence quantum yield was confirmed by that of the fluorescence lifetime ($\tau = 7.6 \pm 0.1$ ns) for each molecular species. With such a quantum yield, the fluorescence efficiency can be considered to be good and allows quantitative determinations, as it does not depend on the degree of unsaturation of the fatty acids.

Fig. 3a depicts a chromatogram of naproxen–diacylglycerols synthesized from rat cortex diacyl glycerophosphoethanolamine and the distribution of the main species is listed in Table I. Identical molecular species distributions were obtained after dinitrobenzoyl derivatization and UV detection [19], but with a ten times lower sensitivity. No differences were detected in the species distribution and yield when widely different amounts of DAGs (from 10 to 1000 μg) were processed. The linearity of the response was verified with fluorescence detection and ranged from 15 pmol to 10 nmol of a single molecular species, the detection limit being at least 1 pmol (Fig. 3b). The achievement of a greater sensitivity is dependent on the reduction of the background noise by using purer and hence more expensive solvents.

In conclusion, these studies have shown that naproxen is a useful reagent for the determination of DAG molecular species. The proposed method is very sensitive to picomole levels of these lipids and can be extended as for other derivatization procedures to all diradylglycerols. The formation of stable fluorescent derivatives is facile, using a readily available compound whose activation to the acyl chloride is easy to perform. When compared with other chromophores or fluorophores, the naproxen adduct is at least ten times more sensitive and allows the excellent resolution of molecular species on C_{18} columns with very simple isocratic HPLC equipment. Preliminary experiments have indicated that the procedure is sufficiently sensitive for the determination of the molecular species distribution of diacyl PE and diacylglycerophosphocholine purified from cultured neurons by our TLC procedure [13]. It may also be possible to elucidate the changes occurring in the distribution of molecular species of free diacylglycerols and the different phospholipids in small biological samples such as biopsies, cultured cells and membrane preparations.

ACKNOWLEDGEMENTS

The authors thank Mrs. G. Gutbier for skilful technical assistance. This work was supported by grant 0080/87 from NATO.

REFERENCES

1 M. Smith and F. B. Jungalwala, *J. Lipid Res.*, 22 (1981) 697–704.
2 G. M. Patton, J. M. Fasulo and S. J. Robins, *J. Lipid Res.*, 23 (1982) 190–196.
3 N. A. Porter, R. A. Wolf and J. R. Nixon, *Lipids*, 14 (1979) 20–24.
4 B. J. Compton and W. C. Purdy, *J. Liq. Chromatogr.*, 3 (1980) 1183–1194.
5 A. D. Postle, *J. Chromatogr.*, 415 (1987) 241–251.
6 M. Kito, H. Takamura and H. Narita, *J. Biochem.*, 98 (1985) 327–331.
7 M. Batley, N. H. Packer and J. W. Redmond, *J. Chromatogr.*, 198 (1980) 520–525.
8 M. Batley, N. H. Packer and J. W. Redmond, *Biochim. Biophys. Acta*, 710 (1982) 400–405.
9 M. L. Blank, M. Robinson, V. Fitzgerald and F. Snyder, *J. Chromatogr.*, 298 (1984) 473–482.
10 J. Kruger, H. Rabe, G. Reichmann and B. Rustow, *J. Chromatogr.*, 307 (1984) 387–392.
11 P. J. Ryan and T. W. Honeyman, *J. Chromatogr.*, 331 (1985) 177–182.

12 J. Folch, M. Lees and G. H. Sloane-Stanley, *J. Biol. Chem.*, 226 (1957) 497–509.
13 C. Leray, X. Pelletier, S. Hemmendinger and J. P. Cazenave, *J. Chromatogr.*, 420 (1987) 411–416.
14 G. M. Patton, J. M. Fasulo and S. J. Robins, *J. Lipid Res.*, 23 (1982) 190–196.
15 Y. Nakagawa, L. A. Horrocks, *J. Lipid Res.*, 24 (1983) 1268–1275.
16 W. R. Morrison and L. M. Smith, *J. Lipid Res.*, 5 (1964) 600–608.
17 H. Spahn, *Arch. Pharm.*, 321 (1988) 847–850.
18 I. R. Berlman, *Handbook of Fluorescence Spectra of Aromatic Molecules*, Academic Press, New York, 2nd ed. 1971.
19 C. Leray, A. Pelletier, R. Massarelli, H. Dreyfus and L. Freysz, *J. Neurochem.*, 54 (1990) 1677–1681.

Journal of Chromatography, 518 (1990) 167–177
Elsevier Science Publishers B.V., Amsterdam

CHROM. 22 635

Electrochemical enhancement of high-performance liquid chromatography–UV detection for determination of phenylpropanolamine

J. H. MIKE*, B. L. RAMOS and T. A. ZUPP
Department of Chemistry, Youngstown State University, Youngstown, OH 44555-0001 (U.S.A.)
(First received February 13th, 1990; revised manuscript received June 14th, 1990)

ABSTRACT

A common difficulty for many high-performance liquid chromatographic (HPLC) analyses is the inadequate detectability of analytes in the chromatographic eluent. One of the most common detection modes for HPLC, UV absorption, is also among the most problematic in this regard. A fast, simple and inexpensive solution to this problem is accomplished through an application of spectroelectrochemistry. A post-column electrochemical reactor placed before the UV detector was used to oxidize phenylpropanolamine (PPA), a common drug with a very low UV absorptivity, to species the UV absorptivities of which were significantly higher. The net effect of the oxidation was a significant enhancement of detector sensitivity for PPA. Electrochemical and spectroelectrochemical data, reactor design characteristics and application of the system to the analysis of PPA in dosage forms are presented.

INTRODUCTION

Inadequate sensitivity of detection when using high-performance liquid chromatography (HPLC) with ultraviolet (UV) detection is a commonly encountered problem. The problem arises because UV detection has two conditions that must be met to give good, sensitive detection and reliable quantitation: (1) a suitably strong chromophore must be present in the analyte(s), and (2) the chromophore must absorb within a useful wavelength range of the detector. If these conditions are not met other modes of detection, such as fluorescence, if the analyte(s) can be derivatized to fluorescent compounds, or electrochemistry, if the analyte(s) are accommodating to amperometric detection, may be used.

Other modes of detection also require the availability of suitable detection equipment. If the equipment is unavailable, or budgetary limitations preclude such costly purchases, it may be possible to derivatize the analyte(s) to enhance their UV absorption properties using dansylating agents [1] or 3,5-dinitrobenzoyl chloride [2,3]. However, such reagents inevitably require additional manipulations that are often time consuming and complex and may represent a significant investment of labor and cost.

Phenylpropanolamine (PPA), a widely analyzed drug, represents this type of problem. The molecule has a low molar absorptivity at the wavelengths commonly

0021-9673/90/$03.50

used for UV detection (*i.e.*, >230 nm). Additionally, it has been reported that PPA is an unsuitable analyte for electrochemical detection for HPLC analysis [4] nor is it inherently fluorescent. PPA can be oxidized, however, to the highly UV-absorbing compound benzaldehyde using sodium periodate. This is the basis for an analytical determination of PPA in pharmaceutical mixtures using UV spectrophotometry [5]. This process has found analytical use as a pre-column derivatization for HPLC analysis of PPA as well [6]. Electrochemical oxidation has not been reported however.

We demonstrate here a fast, simple and economical method that is useful for enhancement of the absorption properties of PPA in liquid chromatographic eluents. In addition, the method may be generally useful for enhancing the absorption properties of other molecules.

A post-column electrochemical reactor has been developed using common and readily available off-the-shelf hardware. Electrochemical oxidation of PPA generates products that are significantly more UV absorbing than PPA at wavelengths greater than 230 nm. This enhancement markedly improves the detectability of PPA using UV absorption. The method is simple and no additional pumps or reagents are required nor is pre-column derivatization. Time is saved and additional sample manipulations beyond normal sample preparation are unnecessary. The method is presented for the analysis of PPA in pharmaceutical mixtures.

MATERIALS AND METHODS

Reagents and supplies

Phenylpropanolamine · HCl was obtained from Sigma (St. Louis, MO, U.S.A.). Anhydrous sodium perchlorate, ACS reagent grade, was obtained from GFS (Columbus, OH, U.S.A.). Powdered nickel, platinum and copper (all Aldrich Gold Label grade, −100 mesh) and Darco G-60 powdered (100–325 mesh), high-purity, activated carbon, were obtained from Aldrich (Milwaukee, WI, U.S.A.). HPLC-grade acetonitrile and water were manufactured by J. T. Baker (Phillipsburg, NJ, U.S.A.). The male 316 stainless-steel connectors and Flexon tubing (0.25 m I.D.) were obtained from Alltech (Deerfield, IL, U.S.A.). The optical quartz split cell and holder used for spectroelectrochemical studies were obtained from NSG Precision Cells (Farmingdale, NY, U.S.A.). The gold-grid (4 wires/cm) electrode for the spectroelectrochemical cell was obtained from Buckbee-Mears St. Paul, MN, U.S.A.). Generic drug samples were obtained from a local drug store.

Electrochemical studies

A Model CV-27 potentiostat (Bioanalytical Systems, W. Lafayette, IN, U.S.A.) was used for both cyclic voltammetric and spectroelectrochemical experiments. Cyclic voltammetry was performed in stirred solution using a working electrode of either gold, platinum or glassy carbon and auxiliary and reference electrodes of platinum and Ag/AgCl, respectively.

A spectroelectrochemical cell was constructed from a demountable, split quartz spectrophotometer cell with a path length of 1.0 mm. A gold-grid working electrode (4 wires/cm) was sandwiched between PTFE spacers and placed to cover approximately the lower two-thirds of the cell, which was glued together. A portion of the grid protruded from the cell to allow connection of the potentiostat. A reference electrode

(Ag/AgCl) was a length of narrow glass tubing fused to fritted glass that was suspended in the test solution above the light beam. The platinum auxiliary electrode was suspended at the same level as the reference. A Model 8452A diode array spectrophotometer (Hewlett-Packard, Palo Alto, CA, U.S.A.) was used for data collection.

Chromatographic studies

Chromatographic experiments were performed using a Model LC/9533 high-performance liquid chromatograph (IBM, Danbury, CT, U.S.A.). The system consisted of a ternary gradient pump, a Model 7120 injector (Rheodyne, Cotati, CA, U.S.A.) fitted with a 20-μl loop, and an IBM Model LC/9523 variable-wavelength UV–VIS detector equipped with a high-pressure flow cell. To eliminate excessive bubbling in the flow cell, a backpressure regulator was packed after the detector to maintain a pressure of 1.4 MPa on the flow cell. All separations were done using an Econosphere, silica-based, octadecylsilane column (Alltech). The column was 250 × 4.6 mm I.D. and was packed with 5-μm particles. The mobile phase was water–acetonitrile–acetic acid (64.5:34.5:1) containing 0.2 mol/l sodium perchlorate at a flow-rate of 1.00 ml/min. All experiments were performed at ambient temperature.

The electrochemical cell was made from two 316 stainless-steel male connectors, serially placed and connected by a 2.54-cm length of 0.25 mm I.D. Flexon tubing. Flexon was chosen over PTFE because of its durability.

Potentials for the electrochemical cell were applied using a Heath–Schlumberg Model 17a (Heath, St. Joseph, MI, U.S.A.) constant-voltage electrophoresis-type power supply. It had a potental range of 0–400 V at up to 100 mA current. Current was monitored with a digital voltmeter. Electrical connections to the electrodes were shielded for safety.

Electrode preparation

The stainless-steel male connectors used for the reactor were not of the zero-dead-volume type. Inside the connectors there was a gap that measured approximately 1.0 × 5.0 mm into which the electrode material was packed. A plug of glass fiber was held in place in the bottom of the fitting by short tube and ferrule. Small portions of the electrode materials were tapped gently into the cell until the gap was filled. Packing the materials very tightly resulted in excessive backpressures that ruptured the Flexon lines. When using metal electrodes, the oxidation potentials were such that the electrodes had a limited lifetime due to solubilization. To insure an adequate amount of electrode material the electrodes were repacked every 2–3 days. A schematic representation of the electrochemical cell is shown in Fig. 1.

Sample preparation

Cold syrup samples were prepared for analysis by pipetting 5.00 ml of sample into a 50-ml volumetric flask and diluting to the mark using deionized water. Diet aid tablet samples were prepared by weighing ten tablets to obtain a weight per tablet. The ten tablets were crushed using a mortar and pestle and an amount of powder approximately equivalent to one tablet was weighed and dissolved in 25 ml of deionized water in a 100-ml volumetric flask. A volume of 35 ml of acetonitrile was added and the flask shaken for at least 2 h on a mechanical shaker. Deionized water

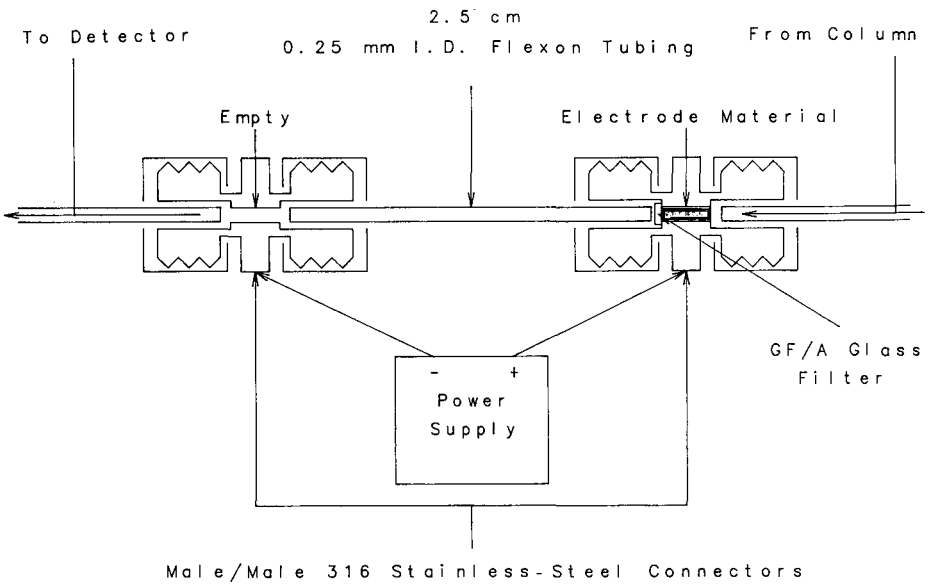

Fig. 1. Schematic representation of flow-through electrochemical cell.

was added up to the mark in the flask and the contents were thoroughly mixed. All solutions were filtered using a 0.45-μm nylon filter before injection.

RESULTS AND DISCUSSION

Oxidation of PPA

For this study it was shown, using techniques such as cyclic voltammetry, spectroelectrochemistry and chromatographic peak collection, that PPA could be oxidized electrochemically. For cyclic voltammetry, scans were performed in the positive direction from 0 to 2.00 V and showed a distinct wave with a peak at +1.89 V. There was no reduction peak observed on the reverse scans. The oxidation peak was virtually identical with respect to peak voltage and shape for all electrodes tested, although later experiments demonstrated that the choice of electrode material as well as the reaction conditions were important factors to consider for optimization of the electrochemical reaction for maximum UV absorption.

In the reaction scheme shown below, it appeared that two possible products could result from the oxidation of PPA: benzoic acid or benzaldehyde, dependent upon the degree of oxidation.

Both benzaldehyde and benzoic acid are very strong UV absorbers above 230 nm while PPA is not. In ethanol, benzaldehyde has an absorption maximum at 250 nm (ε = 15 000 l mol^{-1} cm^{-1}) and benzoic acid at 230 nm (ε = 10 000 l mol^{-1} cm^{-1}) [7]. PPA was determined to have an absorption maximum at 258 nm (ε = 190 l mol^{-1} cm^{-1}) in the chromatographic solvent.

Investigations of the anodic oxidation reactions for evidence of formation of either benzaldehyde or benzoic acid were performed by spectroelectrochemistry.

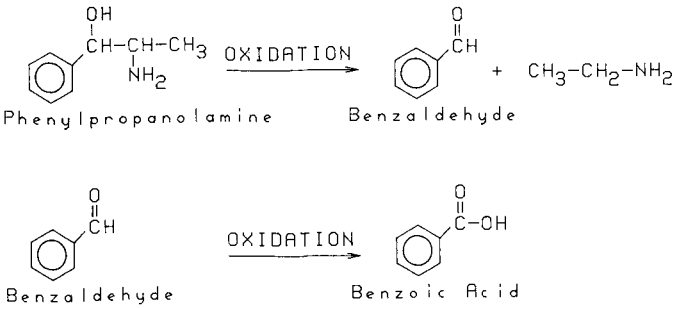

Initially, the studies were done using a spectroelectrochemical photometer cell. Later studies involved collection of chromatographic peaks obtaind at various applied potentials, followed by spectrophotometry. In each case, as the potential was increased it was possible to see spectral changes occur that appeared consistent with the formation of the two products. The observed data are outlined below.

Initial efforts using the spectroelectrochemical cell appeared to point to formation of benzoic acid as the major anodic oxidation product. The spectra, shown in Fig. 2, exhibited a large peak at 230 nm that was attributed to benzoic acid formation. Some benzaldehyde appeared to be present and was detected as a barely discernible shoulder at around 252 nm on the much larger benzoic acid peak. Initial chromatographic studies, using a nickel electrode, were consequently performed by monitoring the chromatographic eluent at 230 nm. This resulted in only minor enhancement of the PPA chromatographic peak and a very high background absorbance. Monitoring at 252 nm gave a significantly greater enhancement, as well as a much lower background absorbance.

To examine this further, HPLC peak collection after on-line oxidation with the nickel electrode in the reactor cell was performed. Under these conditions, the major

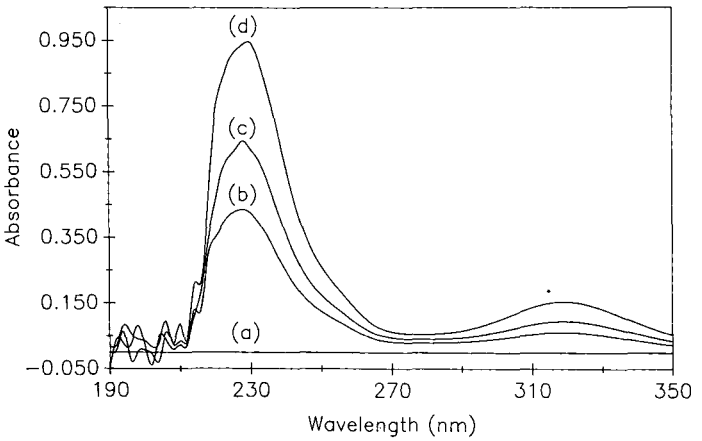

Fig. 2. Spectra obtained at: (a) = 0 s; (b) = 60 s; (c) = 120 s; (d) 180 s; electrochemical oxidation of PPA, 1 mg/ml, in chromatographic mobile phase using spectroelectrochemical photometer cell. Potential, 1,89 volts; gold-grid working electrode, Pt auxiliary electrode, Ag/AgCl reference electrode.

oxidation product appeared to be benzaldehyde, since an absorption maximum was observed at 252 nm. From these spectra there appeared to be little formation of benzoic acid, since as the potential was increased there was only a small increase in absorbance at 230 nm. This was difficult to confirm, however, since the mobile phase absorbed very strongly in this spectral region, with a cut-off close to 230 nm.

These results appeared to be at odds with one another. Oxidation at different electrodes may proceed by different mechanisms, however. It has been pointed out by other investigators [8] and observed in later experiments that gold, and noble metal electrodes in general, behaves much differently than do certain transition metal electrodes such as nickel. These experiments plausibly demonstrated that both benzaldehyde and benzoic acid may be formed as products of the electrochemical oxidation of PPA, but it was apparent from these and later data that both the solvent and the electrode played an important role in the electrochemical reaction. The results indicated clearly, however, that the chromatographic solvent system, with the reactor cell set up with a nickel electrode, would be an excellent choice for optimization of the electrode reaction for maximal yield of benzaldehyde, since benzaldehyde appeared to be the only major oxidation product in that system. Further studies are presently underway to elucidate the mechanisms for electrochemical oxidation of PPA at different electrodes and under different solvent conditions.

Electrochemical cell design

In the design of the flow-through electrochemical cell, a simple two-electrode system was adopted. Simplicity was a major consideration in the design of the cell since many laboratories may not have sophisticated machine-shop facilities or complex instrumentation. A two-electrode system was less expensive, easier to build and easier to maintain than a three-electrode system and required a simple power supply rather than a potentiostat. In addition, bulk oxidation of solutes without precise monitoring of the current was the only purpose for the cell and two-electrode cells have been used for such purposes [8,9].

The mobile phase was in large proportion non-aqueous resulting in a substantial resistance between the working and auxiliary electrodes. High potentials were required to obtain a sufficiently positive oxidation potential at the working-electrode surface. Such high potentials were beyond the limits of the potentiostats available in our laboratories. To produce these potentials it was necessary to use an electrophoresis-type power supply

The stainless-steel fittings did not contribute to the oxidation reaction. Potential applied to an empty electrode gave no detectable enhancement of absorption. In conjunction with this, the electrodes were inspected frequently. After approximately 8 months of using a single pair of fittings as the working and auxiliary electrodes, no observations of pitting or malformation were made in either fitting. The fittings were thus considered inert, serving as simple electrical conductors.

The order of placement of the working and auxiliary electrodes in the flow stream was important. Oxidation of PPA was observed with either orientation of the electrodes in the flow stream. However, the yield of product absorbing strongly at 252 nm was significantly greater when the working electrode was placed first, followed by the auxiliary electrode. The reason for this has not yet been determined but all subsequent experiments were done with the working electrode placed first.

With respect to the effects of the electrochemical reactor cell on chromatographic performance, as seen in Fig. 3, addition of the cell to the flowing system contributed very little to the total band broadening observed on the chromatograms. The major advantages of the chosen reactor design were thus the simplicity of the system as a whole and the null effects of the cell on chromatographic performance.

Optimization of the electrode reaction

Electrochemical oxidation of PPA under the chromatographic conditions presumably gave benzaldehyde as the primary product detected by monitoring absorbance at 252 nm. For optimization of the reaction, changes in absorbance at 252 nm were monitored as the electrode conditions were changed. The type of electrode material, the applied potential and the concentration of sodium perchlorate (supporting electrolyte) were all important variables for obtaining a maximal yield of benzaldehyde.

The electrode materials examined were powdered carbon, copper, platinum and nickel, all chosen primarily to represent a range of electrode types. As seen in Fig. 4, the yield of product formed at 252 nm increased with increasing applied potential. This

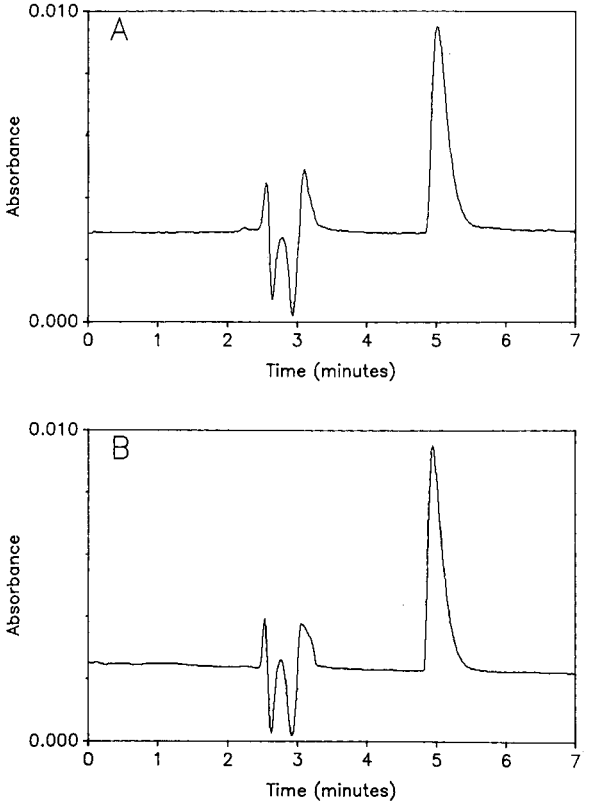

Fig. 3. Demonstration of the effect of addition of the electrochemical reactor to the HPLC system, 20 μg PPA injected. (A) Reactor in place, 258 nm; peak width at half height ($w_{\frac{1}{2}}$) = 0.23 min; (B) no reactor, 258 nm; $w_{\frac{1}{2}}$ = 0.22 min.

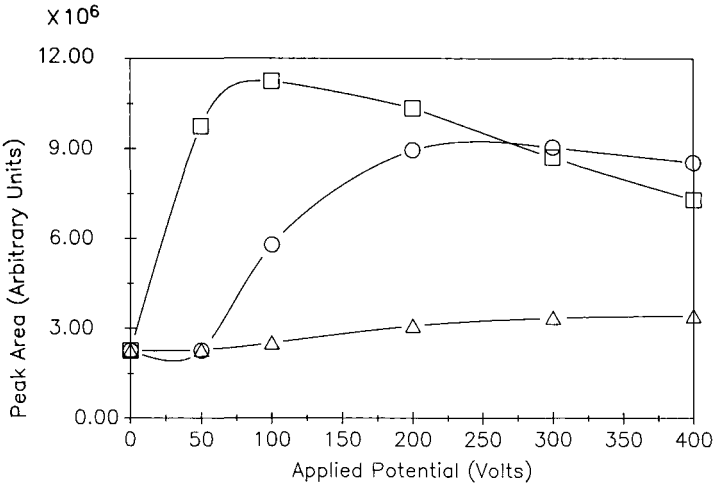

Fig. 4. Oxidation profiles for different electrode material in the electrochemical reactor, 20 μg PPA per 20 μl injection, 252 nm. ○ = Ni electrode; △ = C; □ = Pt.

was noted with all electrode materials except copper, but in differing degrees with each material. Copper was not suitable at any potential due to extremely high background absorbance from oxidized copper.

With a powdered carbon electrode, little increase in absorption at 252 nm was evident up to the 400-V limit of the power supply. This could have been due either to non-oxidation of PPA at the carbon electrode, or to almost exclusive formation of benzoic acid during the oxidation, which would have had shifted the absorption maximum.

When using a platinum electrode, oxidation to benzaldehyde occured at a relatively low potential. But, the absorbance maximum showed a fairly sharp peak that decreased significantly as the applied potential was increased. The decrease in absorption at higher potential was attributed to more complete oxidation of the analyte to benzoic acid with subsequent shifting of the absorbance maximum from 252 nm to 230 nm.

In this application, nickel electrodes appeared to perform the best. The absorbance enhancement climbed to a maximum and stayed there over nearly the entire range of potentials investigated. This behavior was attributed to the general manner in which certain metal electrodes, such as nickel or silver, function. Unlike noble metal or carbon electrodes, oxidation at these electrodes proceeds by an indirect electron transfer process. The electrode surface first becomes oxidized and this oxide subsequently passes electrons to the substrate. This mechanism has been observed in anodic oxidations of alcohols and amines using transition metal electrodes [8]. It has also been observed when using these electrodes, that oxidations of compounds from the same class all appear to occur at the same potential, that of the formation of the metal oxide. In the oxidation of PPA at the nickel electrode this was the presumable reason that the oxidation did not readily proceed past the benzaldehyde stage, but was nearly constant for the range of potentials investigated.

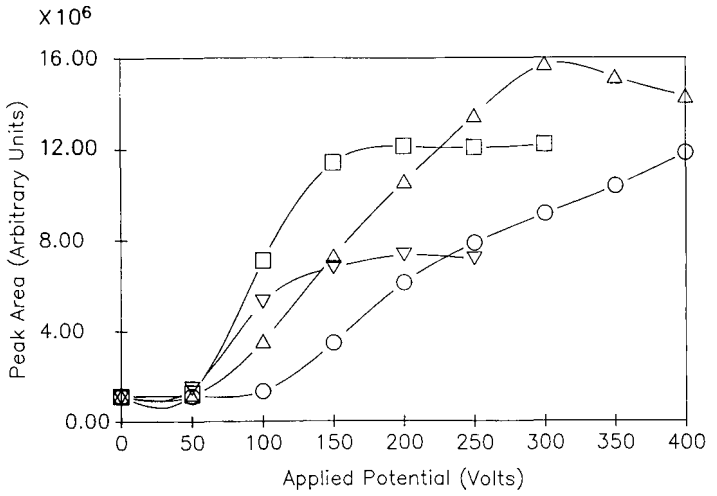

Fig. 5. Variation of oxidation profile with concentration of sodium perchlorate, 20 μg PPA per 20 μl injection, Ni electrode. ○ = 0.1 mol/l; △ = 0.2 mol/l; □ = 0.3 mol/l; ▽ = 0.5 mol/l.

Fig. 5 shows the dependence of the oxidation reaction on the concentration of the supporting electrolyte when monitoring at 252 nm for yield of benzaldehyde. At a given applied potential, the yield of benzaldehyde at first increased and then decreased as the electrolyte concentration was increased. The initial increase in peak areas was attributed to increased formation of benzaldehyde from more efficient charge transfer through the solution. Above 0.2 mol/l sodium perchlorate concentration, it appeared that product formation began to shift from benzaldehyde to benzoic acid. This shifted the absorbance maximum and decreased the peak areas observed at 252 nm.

Quantitative analysis

Reproducibility of injections when using the electrochemical cell was very good. A coefficient of variation of $\pm 3.302\%$ was determined for 9 replicate injections. To achieve this level of reproducibility required conditioning of the new electrode by the application of potential for approximately 15 to 30 min. Repeated injections performed prior to this equilibration period showed peaks heights 5–10% over the observed equilibrium enhancement, which gradually decreased to the equilibrium height. Presumably, formation of a stable oxide coat on the nickel surface was required to insure a reproducible oxidation mechnism. After the initial equilibration period, the electrode functioned reproducibly throughout its usable lifetime of 2–3 days.

For quantitative analysis of PPA, linearity was observed over the range of the calibration curve. A comparison of slopes from sensitivity curves, using identical standards for PPA and oxidized PPA demonstrated that the sensitivity of analysis was enhanced by addition of the electrochemical reactor. The line slope for unoxidized PPA was $1.07 \cdot 10^6$/(ng/ml) while that for oxidized PPA was $9.84 \cdot 10^6$/(ng/ml). Approximately a 10-fold improvement in sensitivity was observed.

In a comparison of the linearity of PPA and oxidized PPA over a much wider

TABLE I

QUANTITATIVE ANALYSIS OF PHARMACEUTICALS

Each point represents duplicate analyses; 252 nm; applied potential, 275 V; current, 2.60 mA.

	Multicomponent liquid		Diet aid	
	mg/5 ml	% of label claim	mg/tablet	% of label claim
	24.8	99.2	74.8	99.7
	25.5	102.0	74.8	99.7
	24.9	99.6	75.4	100,5
Mean	25.1	100.3	75.0	100.0
S.D.	0.38	1.5	0.35	0.46
Coefficient of variation (%)	1.5	1.5	0.46	0.46

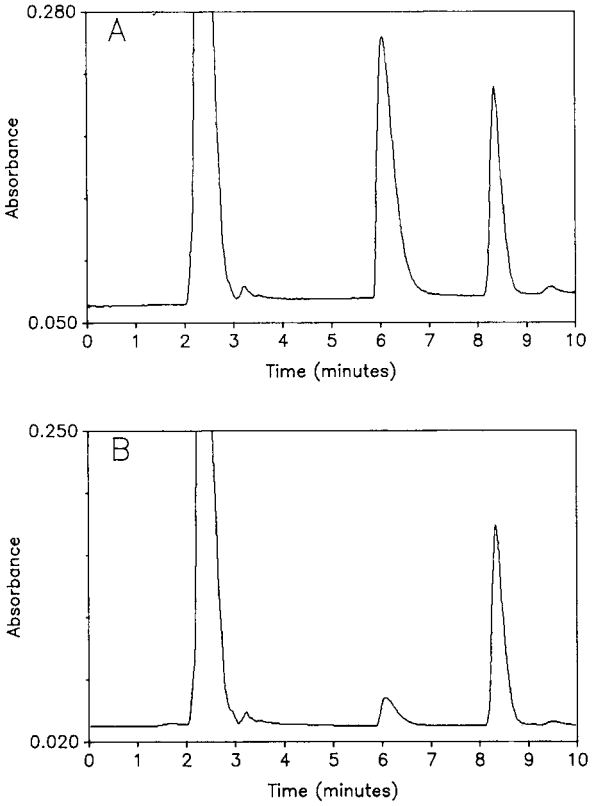

Fig. 6. Chromatograms from analysis of multicomponent cold liquid. (A) = 275 V applied potential, 2.52 mA, 252 nm; (B) = 0 V applied potential, 258 nm.

range of concentrations and under identical chromatographic conditions, neither PPA nor oxidized PPA displayed a large range of linearity with the IBM 9523 UV–VIS detector. Generally, if a detector exhibits a linear response, a logarithmic plot of response *vs.* concentration should have a slope of 1.00 [10]. In an experimental logarithmic plot of the detector response in each case, parallel lines with nearly equal slopes of 0.8907 and 0.9021, for oxidized and native PPA respectively, were obtained. Considering this, it is likely that the detector, not the electrochemical reactor, was the limiting factor for linearity.

Analysis of pharmaceutical samples displayed excellent agreement with labelled quantities (Table I). As an illustration of the enhancement, typical chromatograms are shown in Fig. 6, for an over-the-counter multicomponent liquid cold preparation, with the reactor off and with potential applied. From a comparison of peak areas, the enhancement obtained for this sample was 10-fold. Given this enhancement, application of this system to the analysis of PPA in biological systems, where detection much nearer to the detection limit is typical should thus prove advantageous.

CONCLUSIONS

On-line electrochemical oxidation for enhancement of UV detectability represents an inexpensive and easy-to-construct system that has been applied to the analysis of PPA in pharmaceutical samples. The degree of detection enhancement in this instance was significant and no reagents, extraneous pumping systems or temperature control was required. The simplicity of the system was such that it should be readily and easily available to almost every laboratory.

Many compounds are oxidizable. The system should consequently be broadly applicable to many other compounds, pharmaceutical and non-pharmaceutical alike, even those that are already UV absorbers, to enhance their detectability. The potential exists, likewise, for use of such a system for enhancement of other modes of detection (*e.g.*, fluorescence, visible or electrochemical) in many applications.

ACKNOWLEDGEMENT

This work was supported, in part, by a grant from the Youngstown State University Research Council, Grant 708.

REFERENCES

1 R. W. Frei and J. F. Lawrence, *J. Chromatogr.*, 83 (1973) 321.
2 M. A. Carey and H. E. Perisinger, *J. Chrom. Sci.*, 10 (1972) 537.
3 J. F. Lawrence and R. W. Frei, *Chemical Derivatization in Liquid Chromatography*, Elsevier, Amsterdam, 1976.
4 I. Jane, A. McKinnon and R. J. Flanagan, *J. Chromatogr.*, 323 (1985) 191.
5 A. C. Nonzioli, *SAFYBI*, 15 (1975) 865; *C.A.*, 83 (1975) 209460h.
6 H. S. I. Tan and G. C. Salvador, *J. Chromatogr.*, 261 (1983) 111.
7 R. M. Silverstein, G. C. Bassler and T. C. Morrill, *Spectrometric Identification of Organic Compounds*, Wiley, New York, 3rd ed., 1974, p. 250.
8 S. D. Ross, M. Finkelstein and E. J. Rudd, *Anodic Oxidation*, Academic Press, New York, 1975.
9 D. K. Kyriacou, *Basics of Electroorgaic Synthesis*, Wiley, New York, 1981.
10 I. A. Fowliss and R. P. W. Scott, *J. Chromatogr.*, 11 (1963) 1.

Journal of Chromatography, 518 (1990) 179–188
Elsevier Science Publishers B.V., Amsterdam

CHROM. 22 618

High-performance liquid chromatographic analysis of Romet-30® in salmon following administration of medicated feed

JACQUELINE A. WALISSER, HELEN M. BURT and TERESA A. VALG
Faculty of Pharmaceutical Sciences, University of British Columbia, Vancouver, BC V6T 1W5 (Canada)
DAVID D. KITTS
Department of Food Sciences, University of British Columbia, Vancouver, BC V6T 1W5 (Canada)
and
KEITH M. McERLANE*
Faculty of Pharmaceutical Sciences, University of British Columbia, Vancouver, BC V6T 1W5 (Canada)
(First received March 14th, 1990; revised manuscript received June 8th, 1990)

ABSTRACT

A sensitive and selective high-performance liquid chromatographic assay was developed for the simultaneous quantitation of sulphadimethoxine (SDM) and ormetoprim (OMP) in chinook salmon muscle tissue. SDM and OMP were extracted from tissue samples using a solid-phase extraction technique. Resolution of both drugs was accomplished using an Ultrasphere ion-pair column (250 × 4.6 mm I.D.) and a mobile phase of acetonitrile–methanol–0.1 *M* phosphate buffer, pH 4 (17:10:73) with ultraviolet detection at 280 nm. The calibration curve in salmon muscle tissue was linear over the concentration range 0.2–20 ppm for both SDM (r^2 = 0.9974) and OMP (r^2 = 0.9956). The minimum detectable quantity of SDM and OMP in salmon muscle tissue was 0.2 ppm at a signal-to-noise ratio of 5:1. An *in vivo* feeding experiment was undertaken where chinook salmon were administered Romet-30®-medicated feed for a 10-day period, followed by a 42-day wash-out period. The rate of tissue uptake and decline of SDM and OMP was shown to differ.

INTRODUCTION

The use of antibiotics in the aquaculture industry for the control of bacterial infections in salmon, has led to public concern over antibiotic residues in salmon tissue and the potential health risk to humans. To address these concerns, quality assurance procedures are required for the control of antibiotic residues in farmed salmon. Therefore, there is a need for the development of sensitive, specific assays for the detection and quantitation of antibiotics in salmon tissue and the determination of wash-out times of antibiotics from the tissue.

Romet-30®, an antibiotic approved for use in the aquaculture industry, is a potentiated sulphonamide containing sulphadimethoxine and ormetoprim in a 5:1 ratio. This antibiotic is effective against a wide range of bacterial pathogens including

0021-9673/90/$03.50

Vibrio ordali and *Vibrio anguillarum*, the causal agents of Vibriosis, a disease common to farmed salmon.

Various methods for the analysis of antibiotics in fish tissue have been reported. Microbiological assays are frequently used as screening methods for antibiotics in animal tissues. Two bioassays have been reported for the determination of trimethoprim, an antibiotic potentiator similar to ormetoprim, in the tissues of rainbow trout [1,2]. Microbiological methods often lack the sensitivity required to accurately quantitate antibiotics in fish tissue and are characteristically non-specific and therefore would fail to differentiate between similar drugs in the two products, Romet-30 and Tribissen® (sulphadiazine and trimethoprim).

The Bratton–Marshall colourimetric assay has been used extensively to measure sulphadimethoxine and other sulphonamide levels in the blood and tissues of different trout species [1,3–6]. However, such analyses are also relatively non-specific.

Radio-isotope methods involving liquid scintillation counting have been used to quantitate sulphadimethoxine residue levels. This procedure, when combined with high-performance liquid chromatographic (HPLC) or thin-layer chromatographic analyses of metabolites, has provided information on tissue distribution, pharmacokinetics and metabolism of sulphadimethoxine in rainbow trout (*Salmo gairdneri*) [7] and channel catfish (*Ictalurus punctatus*) [8]. However, these methods are not applicable for the routine analysis of fish treated with non-radioactively labelled drug.

Chromatographic methods offer the advantages of selectivity and increased sensitivity over many other analytical procedures. Trimethoprim concentrations in skin, muscle and blood of rainbow trout, following administration of medicated feed, have been measured by HPLC [9]. One method has been reported for the simultaneous determination of sulphadimethoxine and ormetoprim in catfish tissue [10]. To date, there have not been any methods reported for the simultaneous analysis of sulphadimethoxine and ormetoprim in salmon tissue.

The kinetics of absoprtion, distribution, metabolism and excretion of various sulphonamides, including sulphadimethoxine, following both a single oral dose to rainbow trout [1,3,4,7] and multiple doses to trout [7] and catfish [8] have been investigated. The tissue levels of a number of orally administered sulphonamides in trout, including sulphamerazine [5,6], sulphaguanidine, sulphadiazine, sulphamethazine, sulphanilamide and sulphathiazole [5] and trimethoprim [2] have also been investigated. However, these studies failed to address possible differences in the clearance of the two antibiotics in combination products such as Romet-30.

In the present study, a sensitive and selective HPLC assay for the simultaneous quantitation of sulphadimethoxine and ormetoprim in salmon tissue was developed for determining withdrawal periods for Romet-30 in chinook salmon (*Oncorhynchus tshawytscha*) following medicated feed administration.

EXPERIMENTAL

Materials

Sulphadimethoxine (SDM) and ormetoprim (OMP) were obtained from Hoffmann-La Roche (Etobicoke, Canada). The internal standard, carbamazepine-diol (*trans*-10,11-dihydroxy-10,11-dihydrocarbamazepine), was obtained from Ciba-Geigy (Mississauga, Canada). HPLC-grade methanol, acetonitrile and disodium hydro-

gen orthophosphate heptahydrate ($Na_2HPO_4 \cdot 7H_2O$) were obtained from BDH (Vancouver, Canada). Purified water was produced using a Milli-Q water purification system (Millipore, Mississauga, Canada). Phosphoric acid (H_3PO_4) 85% was obtained from Mallinckrodt (KY, U.S.A.) and trichloroacetic acid (TCA) from Sigma (St. Louis, MO, U.S.A.).

Apparatus

The HPLC system consisted of a Beckman Model 110A solvent metering system, a Model 210 sample injection valve equipped with a 20-μl loop, a Hitachi Model 155 variable-wavelength detector with a Shimadzu C-R1A Chromatopac data processor (Beckman, Fullerton, CA, U.S.A.). Ultraviolet detection was at 280 nm for all analyses. The HPLC column was an Ultrasphere ion-pair 5-μm column (250 × 4.6 mm I.D.) (Beckman). A NewGuard holder equipped with an RP-18 cartridge (15 × 3.2 mm I.D.) (Brownlee, Santa Clara, CA, U.S.A.) was used as a guard column. A direct-connect column prefilter containing a 0.5-μm filter element (Alltech, Deerfield, IL, U.S.A.) placed between the injector and the guard column was used as an inline filter. The mobile phase, acetonitrile–methanol–0.1 *M* phosphate buffer, pH 4.0 (17:10:73), was delivered isocratically at 1.0 ml/min. Filtration of the mobile phase prior to use was done using a HPLC solvent clean-up assembly (Kontes, Vineland, NJ, U.S.A.) and FP Vericel 47 mm, 0.45-μm membrane filters (Gelman, Ann Arbor, MI, U.S.A.).

Preparation of standard solutions and reagents

Stock solutions of SDM and OMP were prepared by dissolving 10 mg of each compound in 100 ml of acetonitrile to give a final concentration of 100 μg/ml for both SDM and OMP. Serial dilutions of the stock solution were made to give final working concentrations of 50, 30, 10, 5, 3.5, 2.5, 2.0 and 1.0 μg/ml for each antibiotic.

Carbamazepine-diol was used as an internal standard for calibration curve samples, treated fish samples and as an external standard in the recovery study. A stock solution of carbamazepine-diol (100 μg/ml) was prepared in methanol. Each tissue sample, weighing 5 g, was spiked with 1 ml of the internal standard solution to yield a final concentration of 20 μg/g tissue.

Extraction procedure

To each 5-g sample of salmon muscle tissue were added 1 ml of the internal standard solution, 15 ml acetonitrile and 0.5 ml 50% (w/v) TCA. Each sample was homogenized in a 50-ml plastic centrifuge tube for 30 s at medium speed using a Brinkmann Polytron homogenizer Model PT 10/35 (Brinkmann, Rexdale, Canada). The samples were centrifuged for 25 min at 7800 *g* and 4°C (JA-20 rotor) in a Beckman Model J2-21 centrifuge. The supernatant was transferred to a 50-ml tube, and evaporated under nitrogen in a 40°C water bath. The residue was reconstituted in 5 ml of purified water and vortex-mixed for 30 s. The extracts were then filtered in a filtration unit consisting of a Membra-Fil membrane filter disc (8 μm, 13 mm diameter) (Nucleopore , Toronto, Canada) in a Swinnex 13 Millipore filter holder attached to a 5-ml Luer-Lok Multifit B-D glass syringe (Becton Dickenson, Mississauga, Ont., Canada). Following filtration, the extracts were passed directly into a second 5-ml Luer-Lok Multifit B-D glass syringe with an activated Sep-Pak C_{18} cartridge (Wa-

ters, Milford, MA, U.S.A.) attached. Activation of the Sep-Pak cartridge prior to loading the sample was accomplished by passing 5 ml of methanol followed by 5 ml of water. The extracts were then passed through the Sep-Pak cartridge and the eluent discarded. SDM, OMP and the internal standard were subsequently eluted from the cartridge into a 15-ml culture tube with 5 ml of methanol. Samples were dried under nitrogen in a water bath at 40°C and stored at −20°C until required for analyses. Just prior to analysis each sample was reconstituted with 1 ml of the mobile phase and vortex-mixed for 30 s. A 20-μl aliquot was injected onto the HPLC column. Each extract was analyzed in duplicate. The injection valve was flushed with 1 ml mobile phase between each analysis.

Calibration curve, assay precision and recovery

A calibration curve was prepared from salmon tissue samples (5 g) spiked with 1 ml of the internal standard solution (20 μg/g tissue) and 1 ml of the appropriate SDM/OMP standard solutions to give final concentrations of 0.2, 0.4, 0.5, 0.7, 1, 2, 6, 10 and 20 μg/g tissue. Calibration curves were constructed by plotting the area ratios of SDM and OMP to that of internal standard against the known concentration ratios of SDM and OMP to that of internal standard.

Intra-assay variability was determined by performing multiple injections (n = 7) of a single extracted tissue sample spiked with SDM and OMP at a concentration of 2 μg/g tissue. Inter-assay variability was determined by the duplicate analysis of independent spiked tissue samples (2 μg/g tissue, $n=4$) over a 59-day time period.

The recovery of SDM and OMP from salmon muscle tissue was determined by the addition of 1 ml of each of the prepared standard solutions containing 2.5, 5, 10 and 30 μg each of SDM and OMP to 5-g samples of control salmon tissue. The samples were extracted and analyzed as described above, except that the internal standard was added just prior to the final evaporation. Recovery was determined by calculating the area ratios of SDM and OMP to that of internal standard for extracted tissue samples and comparing these to the area ratios obtained from unextracted standard solutions of identical quantities.

Feeding study

Approximately 80 chinook salmon varying in weight from 141 to 976 g were maintained in a circular (1.2 m deep × 2.3 m diameter) flowing seawater tank at the West Vancouver Laboratory of the Department of Fisheries and Oceans (West Vancouver, Canada). During the 52-day study period the water temperature varied from a minimum of 7.8°C to a maximum of 10.3 °C. Three fish were taken prior to the start of the feeding study and analyzed to confirm the absence of SDM and OMP. These fish also served as control samples for all calibration curve, assay precision and recovery studies. A medicated diet, Extruded New Age Salmon Feed, 3.5 mm pellets (Moore–Clarke, Vancouver, Canada) containing Romet-30 at a concentration of 16.7 kg per tonne of feed was used. Medicated feed was administered twice daily at a rate of 135 mg per kg fish per day for 10 days. After the medication period, the fish were transferred to a non-medicated feed formulation (Moore–Clark). Four fish were removed from the tank prior to the morning feeding on days 2, 4, 6, 8, 11, 12, 14, 17, 20, 24, 27, 31, 34, 38, 41, 45 and 52. The fish were killed immediately by a blow to the head, tagged and stored at −20°C. For analysis three 5-g samples were taken from each fish at evenly spaced sites along the length of the fish.

RESULTS AND DISCUSSION

Representative chromatograms of a blank salmon extract and a salmon extract containing SDM, OMP and internal standard are shown in Fig. 1. Carbamazepine-diol was selected as an internal standard because of its appropriate elution volume

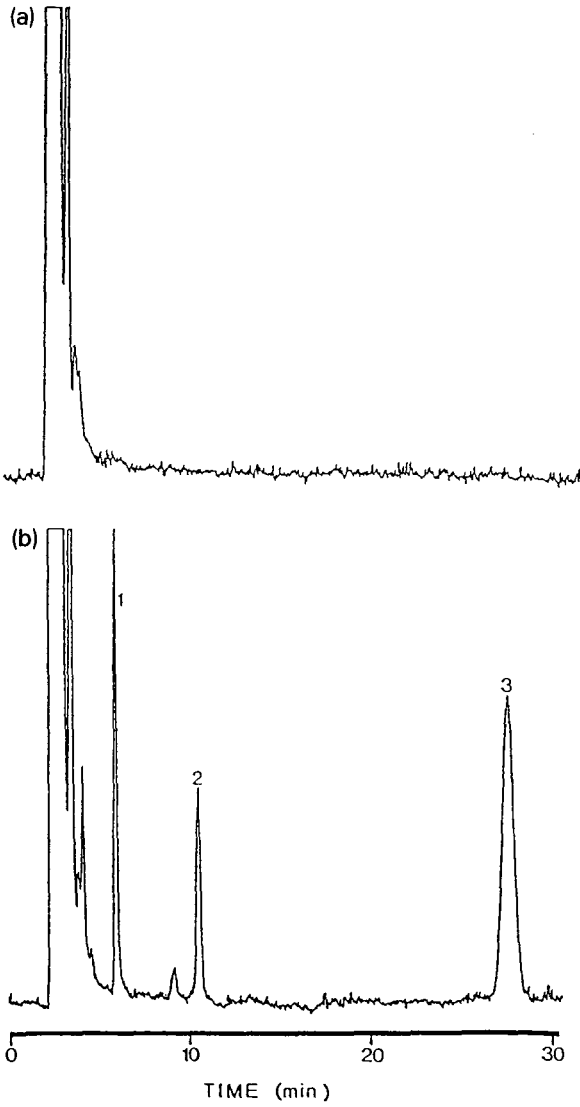

Fig. 1. Chromatogram of (a) a control salmon muscle tissue extract and (b) a salmon muscle tissue extract spiked with 2.0 ppm of ormetoprim and 2.0 ppm of sulphadimethoxine. Chromatographic conditions: column: Ultrasphere I.P. 5 μm (25 cm × 4.6 mm I.D.); mobile phase: acetonitrile–methanol–0.1 *M* phosphate buffer pH 4.0 (17:10:73); HPLC flow-rate: 1.0 ml/min; ultraviolet detection wavelength: 280 nm. Peaks: 1 = ormetoprim; 2 = carbamazepine diol; 3 = sulphadimethoxine.

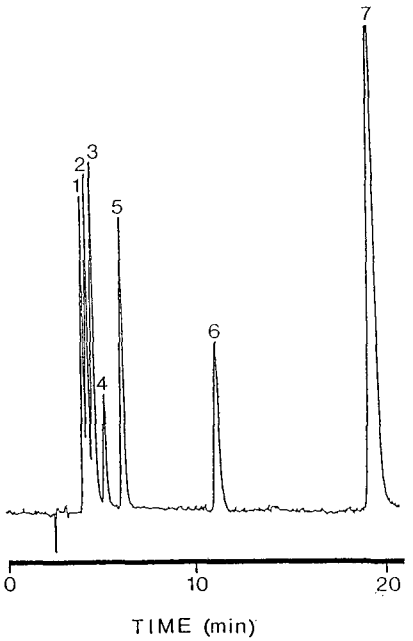

Fig. 2. Chromatogram of various sulphonamides and ormetoprim. Chromatographic conditions as for Fig. 1 except mobile phase: acetonitrile–methanol–0.1 *M* phosphate buffer pH 4.0 (20:10:70). Peaks: 1 = sulphacetamide; 2 = sulphadiazine; 3 = ormetoprim; 4 = sulphamerazine; 5 = sulphamethazine; 6 = sulphisoxazole; 7 = sulphadimethoxine.

and ultraviolet absorption characteristics. The assay developed in the present study has the capacity to separate other sulphonamides in addition to SDM and OMP (Fig. 2). However, their potential use as antimicrobial agents in the aquaculture industry negated their use as internal standards.

Calibration curves for SDM and OMP from extracted salmon muscle tissue are presented in Fig. 3. The area ratio measurements showed a linear relationship between SDM and the internal standard ($r^2 = 0.9974$) and OMP with the internal standard ($r^2 = 0.9956$) over the concentration range 0.2–20 μg/g tissue.

The intra-assay coefficient of variation was 4.8% for SDM and 4.3% for OMP (Table I). The precision of the extraction procedure was determined over a 59-day period and the resultant inter-assay coeffient of variation was found to be 4.6% and 4.4% for SDM and OMP respectively (Table II).

A solid phase extraction method was developed to simultaneously recover SDM and OMP from salmon muscle tissue. The percent recovery of SDM and OMP over the concentration range 0.5–6.0 ppm is presented in Table III. A mean recovery of 54.6% for SDM and 67.1% for OMP was computed from the various levels of antibiotic-spiked salmon tissue. The combination of acetonitrile and TCA as the chosen extraction solvent was found to provide the most efficient recovery for SDM and OMP. Repeated extractions were not found to significantly enhance recovery of either antibiotic. The extraction efficiencies for both SDM and OMP were lower in this study using salmon muscle tissue, than previous reports with other domestic

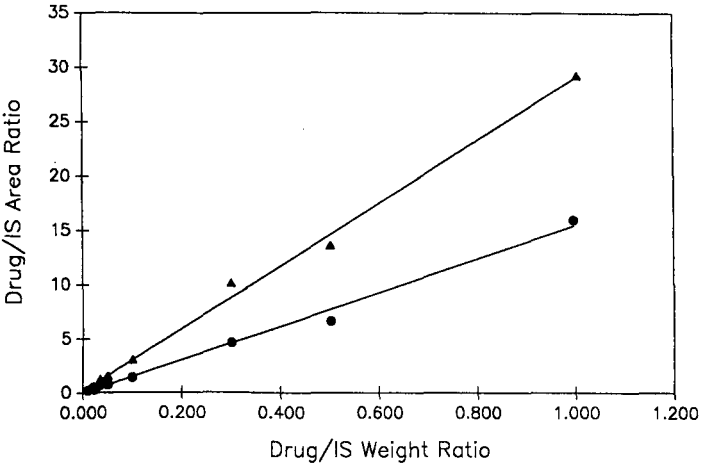

Fig. 3. Calibration curve for sulphadimethoxine (▲) and ormetoprim (●) from extracted salmon tissue over the concentration range 0.2–20 ppm. Sulphadimethoxine: $r^2 = 0.9974$; y intercept = 0.1027; slope = 28.8409. Ormetoprim: $r^2 = 0.9956$; y intercept = −0.0748; slope = 15.4948. IS = internal standard.

animal species including catfish, cattle and chicken [10]. This difference may be due to the presence of relatively high cholesterol levels in salmon muscle tissue. Sheridan [11] has reported that coho salmon (*Oncorhynchus kisutch*) have cholesterol levels in dark muscle tissue that are approximately twice that of other salmonids such as rainbow trout. The high cholesterol level, in addition to the carotenoid content of salmon muscle, may increase the total lipid content of the tissue and may adversely affect antibiotic extraction efficiencies. Despite the relatively low recoveries, the minimum quantifiable amount of both SDM and OMP detected in salmon muscle tissue was 0.2

TABLE I

INTRA-ASSAY VARIABILITY OF SULPHADIMETHOXINE AND ORMETOPRIM IN CHINOOK SALMON MUSCLE TISSUE

Injection No.	SDM/IS Area ratio	OMP/IS Area ratio
1	1.723	0.823
2	1.596	0.777
3	1.504	0.836
4	1.555	0.818
5	1.640	0.737
6	1.588	0.799
7	1.700	0.788
Mean area ratio	1.615	0.797
S.D.[a]	0.078	0.033
C.V.[b]	4.8%	4.2%

[a] Standard deviation.
[b] Coefficient of variation.

TABLE II

INTER-ASSAY VARIABILITY OF SULPHADIMETHOXINE AND ORMETOPRIM IN CHINOOK SALMON MUSCLE TISSUE

Sample Concentration (ppm)	SDM/IS Area ratio	OMP/IS area ratio	Analysis day
2.0	2.720	1.280	1
2.0	2.506	1.277	45
2.0	2.453	1.278	45
2.0	2.599	1.393	59
Mean area ratio	2.570	1.307	
S.D.[a]	0.117	0.057	
C.V.[b]	4.6%	4.4%	

[a] Standard deviation.
[b] Coefficient of variation.

ppm, when taken at a signal-to-noise ratio of 5:1. In addition, this method is advantageous in that it allows a single extraction and analysis for both drugs. The sensitivity of this assay could be improved by increasing the amount of fish tissue extracted and/or by increasing the amount of sample injected onto the HPLC column; however, this would increase the quantity of endogenous substances injected and shorten column lifetime.

The *in vivo* feeding experiment was intended to evaluate the applicability of our HPLC method and to establish a wash-out period for Romet-30 in salmon muscle tissue. The feeding study was designed to model the situation on a fish farm with respect to method and time course of treatment. The data in Fig. 4 show the tissue uptake for SDM and OMP during the first 10 days of treatment followed by the decline of tissue levels from days 11 to 52 after cessation of medicated feed administration. It is apparent from these graphs that there is a large variation in tissue antibiotic concentration between the fish sampled on a given day; however, there was no observable difference in tissue antibiotic concentration between sites sampled on

TABLE III

RECOVERY OF SULPHADIMETHOXINE AND ORMETOPRIM FROM CHINOOK MUSCLE TISSUE

Sample concentration (ppm)	Sulphadimethoxine recovery (%)[a]	Ormetoprim recovery (%)[a]
0.5	54.4	57.1
1.0	68.8	76.4
2.0	46.0	66.7
6.0	49.3	68.3
Mean recovery	54.6	67.1

[a] Each value represents a single determination at each sample concentration.

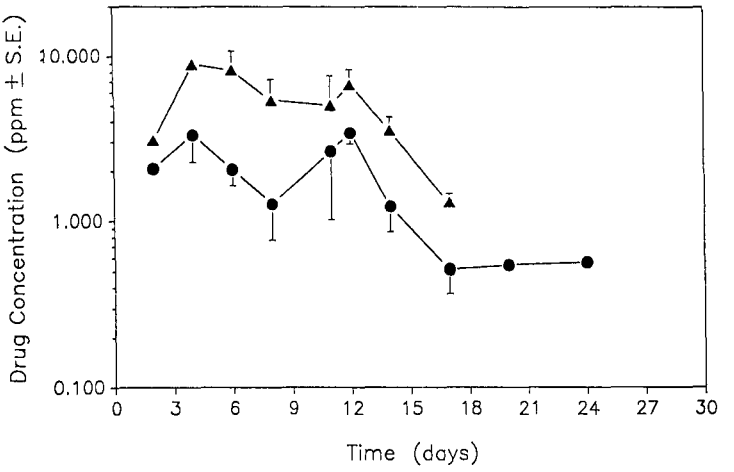

Fig. 4. Tissue uptake (day 1–10) and decline of sulphadimethoxine (▲) and ormetoprim (●) in muscle tissue samples from chinook salmon administered medicated feed. Each point represents an average of four individuals sampled on each day ± standard error.

the same fish. The variation between individual fish is likely the consequence of the hierarchical feeding dominance which results in certain individuals feeding more aggressively than others. In the present study, the fish size varied considerably from 141 to 976 g which may have exacerbated this feeding pattern contributing significantly to the large range of tissue antibiotic concentrations at a given sampling time.

During the 10-day medicated feed administration period, the tissue antibiotic concentration in individual fish varied from below quantifiable limits to a peak concentration of 13.86 ppm for SDM on day 6 and 4.28 ppm for OMP on day 11. The ratios of tissue levels of SDM to OMP found in the present study were not the same as the 5:1 SDM to OMP ratio in Romet-30 and suggests a difference in the rate of maximal uptake or excretion of these two drugs in salmon tissue. Moreover, SDM was detectable in salmon tissue for up to 7 days, while OMP could be detected for as much as 14 days after cessation of treatment. These results show that there are differences in the rate of tissue uptake and decline of SDM and OMP in salmon. Due to the variability in individual fish antibiotic concentrations, a wash-out period could not accurately be determined; however, in this study OMP residues appeared to remain in the tissues approximately twice a long as SDM residues.

In summary, the HPLC method developed herein allows for the simultaneous quantitation of SDM and OMP in farmed chinook salmon treated with Romet-30. This assay has the advantage of requiring only a single extraction for the determination of both SDM and OMP. The HPLC analysis of SDM and OMP reported in this study was reliable and allowed for the detection of the antibiotics contained in Romet-30 at levels down to 0.2 ppm. The *in vivo* feeding experiment illustrated the differences in the muscle tissue antibiotic concentration between individual fish after administration of medicated feed. In addition, the rate of tissue uptake and decline of SDM and OMP was shown to differ pointing to the necessity for measuring residues of both SDM and OMP in salmon treated with Romet-30.

ACKNOWLEDGEMENTS

This work was supported by the Science Council of British Columbia, the Department of Fisheries and Oceans, Canada, the Ministry of Agriculture, B. C. and Hoffmann-La Roche, Canada. The authors would like to acknowledge Mr. Andy Lamb for his technical assistance during the feeding study.

REFERENCES

1 D. H. McCarthy, J. P. Stevenson and A. W. Salsbury, *Aquaculture*, 4 (1974) 299.
2 A. McCracken, S. Fidgeon, J. J. O'Brien and D. Anderson, *J. Appl. Bact.*, 40 (1976) 61.
3 T. Hara and S. Inoue, *Bull. Jpn. Soc. Sci. Fish.*, 33 (1967) 618.
4 T. Hara, S. Inoue and N. Saito, *Bull. Jpn. Soc. Sci. Fish.*, 33 (1967) 624.
5 S. F. Snieszko and S. B. Friddle, *Trans. Am. Fish. Soc.*, 80 (1950) 240.
6 S. F. Snieszko and S. B. Friddle, *Trans. Am. Fish. Soc.*, 81 (1951) 101.
7 K. M. Kleinow and J. J. Lech, *Vet. Human Toxicol.*, 30, Suppl. 1 (1988) 26.
8 R. S. Squibb, C. M. F. Michel, J. T. Zelikoff and J. M. O'Connor, *Vet Human Toxicol.*, 30, Suppl. 1 (1988) 31.
9 M. D. Jacobsen, *J. Fish Dis.*, 12 (1989) 29.
10 G. Weiss, P. D. Duke and L. Gonzales, *J. Agric. Food Chem.*, 35 (1987) 905.
11 M. A. Sheridan, *Comp. Biochem. Physiol.*, 90B (1988) 679.

Journal of Chromatography, 518 (1990) 189–198
Elsevier Science Publishers B.V., Amsterdam

CHROM. 22 571

Use of cyclodextrins in the isotachophoretic determination of various inorganic anions

KEIICHI FUKUSHI*
Kobe University of Mercantile Marine, Fukae, Higashinada, Kobe 658 (Japan)
and
KAZUO HIIRO
Department of Industrial Chemistry, Ube Technical College, Tokiwadai, Ube 755 (Japan)
(First received March 6th, 1990; revised manuscript received May 16th, 1990)

ABSTRACT

The effects of α-, β- and γ-cyclodextrins on the effective mobilities of various inorganic anions in capillary isotachophoresis were studied. The effective mobilities of several anions decreased when the concentration of cyclodextrins in an ordinary leading electrolyte was increased up to 50 m*M*, whereas the effective mobilities of a few anions remained almost constant. Hence by use of α-cyclodextrin, nitrite and nitrate ions, cyanate, thiocyanate and selenocyanate ions and chlorate and perchlorate ions were completely separated and could be determined. The effective mobilities of iodide, periodate and tetrathionate ions also decreased with increasing concentration of α-, β- or γ-cyclodextrin.

INTRODUCTION

The most important task in isotachophoresis is to control or adjust the effective mobilities of analyte ions. The mutual separation of analyte ions having approximately equal mobilities is essential in order to expand its analytical applications [1].

Recently, cyclodextrins (CDs) have been used for this purpose. The effective mobilities of analyte ions are altered by the formation of complexes of the ions with CD added to a leading electrolyte. So far most of these analyte ions have been organic [1–12]. Tazaki *et al.* [13] used α-CD for the separation of iodide ion in chloride–bromide mixtures and for the detemination of perchlorate ion in the presence of hexacyanoferrate(III) and -(II) ions. There has been no report concerning the isotachophoretic separation of inorganic ions with the use of CD apart from the one above.

It is difficult to separate nitrite and nitrate ions, cyanate, thiocyanate and selenocyanate ions, chlorate and perchlorate ions and chloride, bromide and iodide ions with ordinary leading electrolytes by capillary isotachophoresis, because their ionic mobilities are approximately equal in aqueous solutions [14]. Therefore, we have studied the effects of α-, β- and γ-CDs on the effective mobilities of nitrite, nitrate, cyanate, thiocyanate, selenocyanate, chlorate, perchlorate, fluoride, bromide, iodide,

0021-9673/90/$03.50

iodate, periodate and tetrathionate ions. The results of these experiments were applied to the simultaneous determination of nitrite and nitrate ions, cyanate, thiocyanate and selenocyanate ions and chlorate and perchlorate ions by capillary isotachophoresis with ordinary leading electrolytes containing α-CD.

EXPERIMENTAL

Apparatus

A Shimadzu Model IP-2A isotachophoretic analyser was used with a potential-gradient detector. The main column was a fluorinated ethylene–propylene (FEP) copolymer tube (15 cm × 0.5 mm I.D.), and the precolumn was a PTFE tube (15 or 20 cm × 1.0 mm I.D.). A Hamilton Model 1701-N microsyringe was used for the injection of samples into the isotachophoretic analyser. Distilled and demineralized water was obtained from a Yamato-Kagaku Model WG-25 automatic still and a Nihon Millipore Milli-QII system.

Reagents

All reagents were of analytical-reagent grade and used without further purification. Distilled and demineralized water was used throughout. α-, β- and γ-CDs were obtained from the Nacalai Tesque. Standard solutions of various anions were prepared by dissolving their sodium or potassium salts in water; those of periodate ion were prepared immediately before use because periodate is considerably hydrolysed.

Procedures

Volumes of 5-μl of solutions containing 1.0 m*M* of each anion are injected into the isotachophoretic analyser. The migration current is maintained at 150 μA for the first 14 min and then reduced to 50 μA. The leading electrolyte is an aqueous solution containing 5 m*M* histidine hydrochloride, 0.01 wt.-% Triton X-100 and an appropriate amount of CD, and the terminating electrolyte is 10 m*M* sodium acetate solution. The concentration of α- or γ-CD in the leading electrolyte is increased to 50 m*M* and that of β-CD to 15 m*M* owing to the poor solubility of β-CD compared with that of α- and γ-CD in water [15].

The potential unit (*PU*) value [16] (relative step height [7]) which is generally used as a parameter of identification of the analyte ions, and is defined by the equation

$$PU = (PG_A - PG_L)/(PG_T - PG_L) \quad (1)$$

where *PG* is the potential gradient and the subscripts denote quantities relating to analyte (A), leading (L) and terminating (T) ions, respectively, is calculated. The relationship between the *PU* value and the effective mobility of the analyte ion ($\bar{m}_A$) [16] is given by

$$PU = (a - 1)^{-1}\, \bar{m}_L/\bar{m}_A - (a - 1)^{-1} \quad (2)$$

where $\bar{m}$ is the effective mobility and $a = \bar{m}_L/\bar{m}_T$. Eqn. 2 indicates that the *PU* value becomes larger when the effective mobility of the analyte ion ($\bar{m}_A$) becomes smaller, and the former becomes smaller when the latter becomes larger. That is the change in

the effective mobility of the analyte ion can be indirectly determined in terms of the *PU* values.

RESULTS AND DISCUSSION

Effective mobilities of analyte ions [1]

The effective mobilities of analyte ions A and B ($\bar{m}_A$ and $\bar{m}_B$, respectively) in the presence of an electrically neutral ligand N are expressed as follows:

$$\bar{m}_A = (m_A + m_{AN}K_{AN}[N]_A)/(1 + K_{AN}[N]_A) \quad (3)$$

$$\bar{m}_B = (m_B + m_{BN}K_{BN}[N]_B)/(1 + K_{BN}[N]_B) \quad (4)$$

where m_A, m_B, m_{AN} and m_{BN} are the ionic mobilities of the free analyte ions A and B and the complexed analyte ions AN and BN, respectively, K_{AN} and K_{BN} the complex-formation constants of A and B, respectively, with the ligand N and $[N]_A$ and $[N]_B$ the ligand concentrations in each zone. Eqns. 3 and 4 indicate that A and B can be separated from each other even when they have the same ionic mobilities ($m_A = m_B$) if the complex-formation constants with N are appreciably different ($K_{AN} \neq K_{BN}$): if $K_{AN} > K_{BN}$, $\bar{m}_A < \bar{m}_B$ and if $K_{AN} < K_{BN}$, $\bar{m}_A > \bar{m}_B$. In addition, $\bar{m}_A$ and $\bar{m}_B$ decrease with increasing $[N]_A$ and $[N]_B$, respectively.

In this study, N corresponds to CDs. The stability of the inclusion complex of the analyte ion with CD depends on the hydrophobicity, size and geometric arrangement of the analyte ion [1,7,17].

Determination of nitrite and nitrate ions

The limiting molar conductivity of nitrite ion is approximately equal to that of nitrate ion, as shown in Table I. Therefore, it is difficult to separate these ions from each other with ordinary leading electrolytes. These ions have been separated with an

TABLE I

LIMITING MOLAR CONDUCTIVITIES (λ^{∞}_{-}) OF VARIOUS ANIONS IN AQUEOUS SOLUTION (25°C) [14]

Anion	λ^{∞}_{-} (S cm^2 mol^{-1})
NO_2^-	71.8
NO_3^-	71.5
OCN^-	64.6
NCS^-	66.5
$NCSe^-$	64.7
ClO_3^-	64.6
ClO_4^-	67.4
F^-	55.4
Cl^-	76.3
Br^-	78.1
I^-	76.8

aqueous leading electrolyte containing inorganic or organic co-counter ions [18,19] and with non-aqueous leading electrolytes [20,21].

Fig. 1 shows the effect of α-CD concentration on the *PU* values of various anions. The *PU* value of nitrate ion slightly increased linearly with increasing concentration of α-CD up to 50 m*M*. On the other hand, the *PU* value of nitrite ion remained almost constant. This indicated that the nitrate ion formed a weak inclusion complex with α-CD, whereas the nitrite ion did not. The separation of the nitrate ion from the leading ion (chloride ion) was insufficient when the α-CD concentration was relatively low, and the difference between the *PU* values of nitrite and nitrate ions decreased when the α-CD concentration increased. Therefore, 25 m*M* α-CD was selected as the optimum concentration in the leading electrolyte for the simultaneous determination of nitrite and nitrate ions.

Linear calibration graphs were obtained for nitrite and nitrate ions up to 3.0 m*M* by using a leading electrolyte containing 25 m*M* α-CD. The regression equations of these graphs for nitrite and nitrate ions were $y = 9.5x + 0.4$ ($0 \leqslant x \leqslant 3.0$, $0 \leqslant y \leqslant 28.8$) and $y = 12.7x + 0.1$ ($0 \leqslant x \leqslant 3.0$, $0 \leqslant y \leqslant 37.0$), respectively. The correlation coefficients were 1.000 and 0.998, respectively. In these equations x is the concentration of the ion in m*M* and y the zone length in mm when the recording speed is adjusted to 40 mm/min. The relative standard deviations were obtained by calculating the zone length per 1.0 m*M* at each point on the calibration graphs. They were 0.040 and 0.045 ($n = 6$), respectively. The limits of determination for nitrite and nitrate ions were $1.1 \cdot 10^{-2}$ and $7.9 \cdot 10^{-3}$ m*M*, respectively, corresponding to a 0.1-mm zone lengh.

When 5-μl volumes of mixed solutions containing various concentrations of nitrite and nitrate ions were injected and analysed by use of the calibration graphs, the

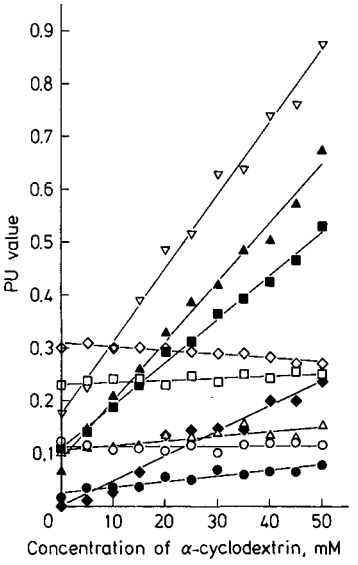

Fig. 1. Effect of α-cyclodextrin concentration on the *PU* values of various anions. ○, NO_2^-; ●, NO_3^-; □, OCN^-; ■, NCS^-; ▽, $NCSe^-$; △, ClO_3^-; ▲, ClO_4^-; ◇, F^-; ◆, I^-.

error in the determination of these ions was less than ± 11%, as shown in Table II. The isotachopherogram of mixture 2 in Table II is shown in Fig. 2. Completely separated zones with sharp boundaries for the nitrite and nitrate ions were obtained with the leading electrolyte containing 25 m*M* α-CD, whereas a completely separated zone for nitrate ion was not obtained without α-CD.

Determination of cyanate, thiocyanate and selenocyanate ions

The limiting molar conductivities of cyanate, thiocyanate and selenocyanate ions are approximately equal, as shown in Table I. Therefore, their separation is difficult with ordinary leading electrolytes. There is no report concerning the simultaneous determination of these ions by capillary isotachophoresis.

The *PU* values of thiocyanate and selenocyanate ions increased linearly with increasing concentration of α-CD, whereas that of cyanate ion remained almost constant, as shown in Fig. 1. The slope of the regression line of *PU* value *vs.* α-CD concentration for the selenocyanate ion was larger than that for the thiocyanate ion. This result suggests that the complex-formation constant of selenocyanate ion with α-CD is larger than that of thiocyanate ion. It can be presumed that the α-CD concentration of 30 m*M* or above is sufficient for the mutual separation of cyanate, thiocyanate and selenocyanate ions. However, the reproducibility of separation of these ions was not sufficient in the concentration range 30–40 m*M*. Therefore, 45 m*M* was adopted as the optimum concentration of α-CD for the simultaneous determination of cyanate, thiocyanate and selenocyanate ions.

Linear calibration graphs were obtained for cyanate, thiocyanate and selenocyanate ions by using a leading electrolyte containing 45 m*M* α-CD. The regression equations for cyanate, thiocyanate and selenocyanate ions were $y = 6.7x - 0.1$ ($0 \leqslant x \leqslant 3.0$, $0 \leqslant y \leqslant 20.7$) and $y = 12.3x + 0.7$ ($0 \leqslant x \leqslant 3.0$, $0 \leqslant y \leqslant 36.9$) and $y = 15.8x + 0.4$ ($0 \leqslant x \leqslant 3.0$, $0 \leqslant y \leqslant 47.6$), the correlation coefficients were 0.998, 0.999 and 1.000 and the relative standard deviations were 0.049, 0.053 and 0.028, respectively. The limits of determination for cyanate, thiocyanate and selenocyanate ions were $1.5 \cdot 10^{-2}$, $8.1 \cdot 10^{-3}$ and $6.3 \cdot 10^{-3}$ m*M*, respectively. The error in the simultaneous determination of these ions was less than ± 14%, as shown in Table III. The isotachopherogram of mixture 2 in Table III is shown in Fig. 3. Completely

TABLE II

ANALYTICAL RESULTS FOR NITRITE AND NITRATE IONS

Mixture	Added (m*M*)		Found (m*M*)		Error (%)	
	NO_2^-	NO_3^-	NO_2^-	NO_3^-	NO_2^-	NO_3^-
1	0.50	3.0	0.47	2.9	−6.0	− 3.3
2	1.0	1.0	0.99	0.89	−1.0	−11
3	1.0	2.5	1.0	2.3	0.0	− 8.0
4	1.5	2.0	1.5	2.1	0.0	+ 5.0
5	2.0	1.5	1.9	1.4	−5.0	− 6.7
6	2.5	1.0	2.4	0.92	−4.0	− 8.0
7	3.0	0.50	2.9	0.48	−3.3	− 4.0

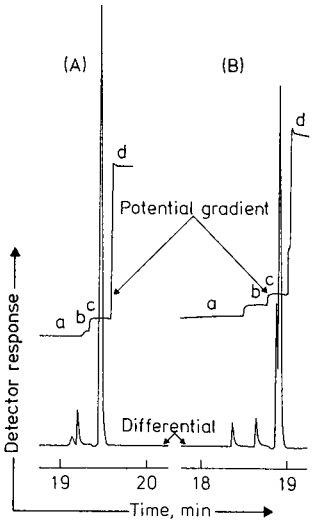

Fig. 2. Isotachopherograms for the separation of nitrite and nitrate ions. (A) Without α-cyclodextrin; (B) 25 m*M* α-cyclodextrin. (a) Cl^- (leading ion); (b) NO_3^-; (c) NO_2^-; (d) CH_3COO^- (terminating ion).

separated and stable zones with sharp boundaries for these ions were obtained by use of a leading electrolyte containing 45 m*M* α-CD, whereas thiocyanate and selenocyanate ions were not completely separated without α-CD.

Determination of chlorate and perchlorate ions

The limiting molar conductivity of chlorate ion is approximately equal to that of perchlorate ion in aqueous solution, as shown in Table I, whereas those of chlorate and perchlorate ions differ from each other in methanol (61,4 and 70.1 S cm^2 mol^{-1} at 25°C, respectively [21]). Therefore, it is difficult to separate these ions by use of ordinary leading electrolytes, whereas it is possible by use of methanolic leading electrolytes.

TABLE III

ANALYTICAL RESULTS FOR CYANATE, THIOCYANATE AND SELENOCYANATE IONS

Mixture	Added (m*M*)			Found (m*M*)			Error (%)		
	OCN^-	NCS^-	$NCSe^-$	OCN^-	NCS^-	$NCSe^-$	OCN^-	NCS^-	$NCSe^-$
1	0.50	2.5	2.0	0.43	2.4	2.0	−14	− 4.0	0.0
2	1.0	1.0	1.0	0.94	1.1	0.99	− 6.0	+10	−1.0
3	1.0	1.5	2.5	0.88	1.5	2.5	−12	0.0	0.0
4	1.5	0.50	3.0	1.4	0.57	2.9	− 6.7	+14	−3.3
5	1.5	3.0	0.50	1.3	2.9	0.52	−13	− 3.3	+4.0
6	2.0	2.0	1.0	1.8	2.0	1.0	−10	0.0	0.0
7	2.5	1.0	1.5	2.3	1.1	1.4	− 8.0	+10	−6.7
8	3.0	1.0	1.0	2.8	1.0	0.98	− 6.7	0.0	−2.0

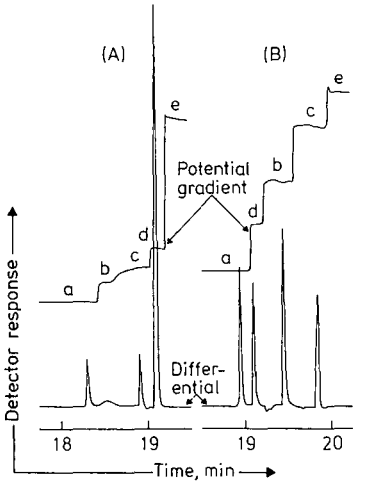

Fig. 3. Isotachopherograms for the separation of cyanate, thiocyanate and selenocyanate ions. (A) Without α-cyclodextrin; (B) 45 m*M* α-cyclodextrin. (a) Cl^-; (b) NCS^-; (c) $NCSe^-$; (d) OCN^-; (e) CH_3COO^-.

The *PU* value of perchlorate ion increased linearly with an increase in α-CD concentration, whereas that of chlorate ion remained almost constant, as shown in Fig. 1.

Linear calibration graphs were obtained for chlorate and perchlorate ions by using a leading electrolyte containing 10 m*M* α-CD. The regression equations for chlorate and perchlorate ions were $y = 10.7x + 0.4$ ($0 \leqslant x \leqslant 3.0$, $0 \leqslant y \leqslant 32.6$) and $y = 11.2x$ ($0 \leqslant x \leqslant 3.0$, $0 \leqslant y \leqslant 33.7$), respectively (correlation coefficients both 1.000). The relative standard deviations were 0.047 and 0.0074, respectively. The limits of determination for chlorate and perchlorate ions were $9.3 \cdot 10^{-3}$ and $8.9 \cdot 10^{-3}$ m*M*, respectively. The error in the simultaneous determination of these ions was less than ±14%, as shown in Table IV. The isotachopherogram of mixture 2 in Table IV is shown in Fig. 4. These ions were completely separated with a leading electrolyte containing 10 m*M* α-CD.

TABLE IV

ANALYTICAL RESULTS FOR CHLORATE AND PERCHLORATE IONS

Mixture	Added (m*M*)		Found (m*M*)		Error (%)	
	ClO_3^-	ClO_4^-	ClO_3^-	ClO_4^-	ClO_3^-	ClO_4^-
1	0.50	3.0	0.43	3.0	−14	0.0
2	1.0	1.0	0.98	1.0	− 2.0	0.0
3	1.0	2.5	0.91	2.6	− 9.0	+ 4.0
4	1.5	2.0	1.4	2.0	− 6.7	0.0
5	2.0	1.5	1.9	1.5	− 5.0	0.0
6	2.5	1.0	2.5	1.0	0.0	0.0
7	3.0	0.50	3.0	0.55	0.0	+10

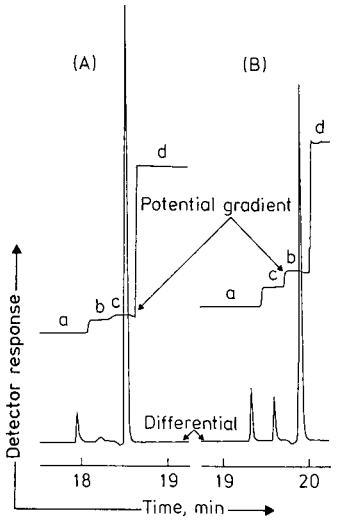

Fig. 4. Isotachopherograms for the separation of chlorate and perchlorate ions. (A) Without α-cyclodextrin; (B) 10 m*M* α-cyclodextrin. (a) Cl^-; (b) ClO_4^-; (c) ClO_3^-; (d) CH_3COO^-.

Separation of halide ions

The limiting molar conductivities of chloride, bromide and iodide ions are approximately equal, as shown in Table I. Therefore, their separation is difficult with ordinary leading electrolytes. These ions have been separated by complex formation with cadmium ion [22] or by use of a methanolic leading electrolytes [21,23,24].

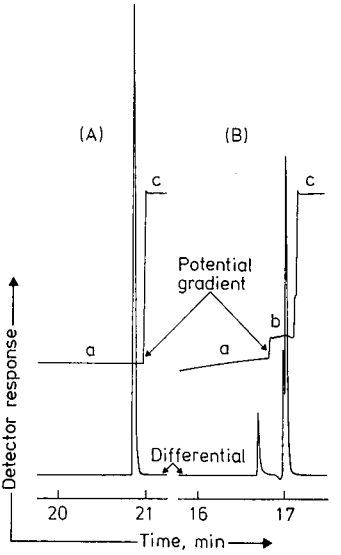

Fig. 5. Isotachopherograms for the separation of iodide ion. (A) Without α-cyclodextrin; (B) 20 m*M* α-cyclodextrin. (a) Cl^-; (b) I^-; (c) CH_3COO^-.

The *PU* value of iodide ion increased linearly with increasing concentration of α-CD, as shown in Fig. 1. Bromide ion was not separated from chloride ion (leading ion).

A linear calibration graph was obtained for iodide ion by use of a leading electrolyte containing 20 m*M* α-CD. The regression equation was $y = 11.6x + 0.1$ ($0 \leqslant x \leqslant 3.0$, $0 \leqslant y \leqslant 35.0$) and the correlation coefficient was 0.999. The relative standard deviation was 0.047. The limit of determination was $8.6 \cdot 10^{-3}$ m*M*. Iodide ion (1.0 m*M*) was completely separated from chloride ion (leading ion) with a leading electrolyte containing 20 m*M* α-CD, as shown in Fig. 5.

Further, the effect of β-CD concentration on the PU values of the above anions was examined by increasing the β-CD concentration up to 15 m*M*. This effect was smaller than that of α-CD.

Applications to other anions

The effect of α-, β- and γ-CD concentration on the *PU* values of iodate, periodate and tetrathionate ions was investigated. The results are shown in Fig. 6. The *PU* value of periodate ion increased linearly with increasing concentration of α- or β-CD. The slope of the regression line for β-CD was larger than that for α-CD. The *PU* value of tetrathionate ion increased linearly when the β- or γ-CD concentration increased. The slope of the regression line for β-CD was larger than that for γ-CD. These results indicate that the complex-formation constant of periodate ion with β-CD is larger than that with α-CD, and that of tetrathionate ion with β-CD is larger than that with γ-CD. The *PU* value of iodate ion remained almost constant when the α- or β-CD concentration increased.

It can be concluded that almost all the anions studied can be separated from each

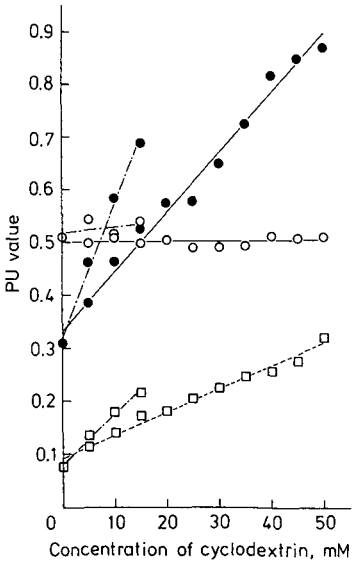

Fig. 6. Effect of cyclodextrin concentration on the *PU* values of some anions. ○, IO_3^-; ●, IO_4^-; □, $S_4O_6^{2-}$. ———, α-CD; —·—, β-CD; ....., γ-CD.

other by use of a leading electrolyte containing 45 m*M* α-CD, although the separation of nitrite and chlorate ions may be insufficient. It is concluded from the slopes of the regression lines which represent the increase in *PU* values that the complex-formation constant of anions with α-CD increases in the order nitrate, iodide, thiocyanate, perchlorate, periodate and selenocyanate ions.

ACKNOWLEDGEMENTS

The authors are grateful to Dr. M. Tazaki (Department of Industrial Chemistry, Kumamoto Institute of Technology, Kumamoto, Japan) for useful suggestions for this research.

REFERENCES

1 M. Tazaki, T. Hayashita, Y. Fujino and M. Takagi, *Bull. Chem. Soc. Jpn.*, 59 (1986) 3459.
2 T. Kamimura, Y. Fujino, T. Hayashita, M. Takagi, M. Tazaki, S. Tsutsui and S. Nagahama, *Proceedings of the 3rd Isotachophoresis Symposium, Osaka, December 14, 1983*, Japan Discussion Group of Electrophoretic Analysis, Japan Society for Analytical Chemistry, Tokyo, 1983, p. 7.
3 N. Kuramoto and K. Asao, *Proceedings of the 5th Isotachophoresis Symposium, Kyoto, December 11–12, 1985*, Japan Discussion Group of Electrophoretic Analysis, Japan Society for Analytical Chemistry, Tokyo, 1985, p. 17.
4 N. Kuramoto and K. Asao, *Osaka Furitsu Kogyo Gijutsu Kenkyusho Hokoku*, 88 (1986) 18.
5 N. Kuramoto, *Proceedings of the 6th Isotachophoresis Symposium, Nagoya, December 11–12, 1986*, Japan Discussion Group of Electrophoretic Analysis, Japan Society for Analytical Chemistry, Tokyo, 1986, p. 21.
6 I. Jelínek, J. Snopek and E. Smolková-Keulemansová, *J. Chromatogr.*, 405 (1987) 379.
7 J. Snopek, I. Jelínek and E. Smolková-Keulemansová, *J. Chromatogr.*, 411 (1987) 153.
8 N. Kuramoto and K. Asao, *Osaka Furitsu Sangyo Gijutsu Sogo Kenkyusho Hokoku*, 1 (1988) 45.
9 I. Jelínek, J. Dohnal, J. Snopek and E. Smolková-Keulemansová, *J. Chromatogr.*, 435 (1988) 496.
10 J. Snopek, I. Jelínek and E. Smolková-Keulemansová, *J. Chromatogr.*, 438 (1988) 211.
11 I. Jelínek, J. Snopek and E. Smolková-Keulemansová, *J. Chromatogr.*, 439 (1988) 386.
12 J. Snopek, E. Smolková-Keulemansová, I. Jelínek, J. Dohnal, J. Klinot and E. Klinotová, *J. Chromatogr.*, 450 (1988) 373.
13 M. Tazaki, M. Takagi and K. Ueno, *Chem. Lett.*, (1982) 639.
14 Chemical Society of Japan, *Kagaku Binran*, Maruzen, Tokyo, 3rd ed., 1984, p. II-460.
15 M. L. Bender and M. Komiyama, *Cyclodextrin Chemistry*, Springer, Berlin, 1978; translated by H. Hirai and M. Komiyama, *Cyclodextrin no Kagaku*, Gakkai-Shuppan-Center, Tokyo, 183, p. 8.
16 H. Miyazaki and K. Kato, *Tosoku-Denki-Eido-Ho(Isotachophoresis*, in Japanese), Kodansha Scientific, Tokyo, 1980, p. 30.
17 I. Tabushi, T. Nishiya, E. Kimura, K. Hattori, K. Odashima, K. Koga and F. Tota, *Host–Guest no Kagaku (Host–Guest Chemistry*, in Japanese), Kyoritsu-Shuppan, Tokyo, 1980, p. 15.
18 I. Matejovič and J. Polonský, *J. Chromatogr.*, 438 (1988) 454.
19 I. Matejovič and M. Bieliková, *Collect. Czech. Chem. Commun.*, 53 (1988) 3067.
20 *Shimadzu Application News*, CA 198-010, 1977.
21 *Shimadzu Application News*, CA 198-096, 1983.
22 P. Boček, I. Miedziak, M. Deml and J. Janák, *J. Chromatogr.*, 137 (1977) 83.
23 J. L. Beckers and F. M. Everaerts, *J. Chromatogr.*, 51 (1970) 339.
24 P. Boček and F. Foret, *J. Chromatogr.*, 313 (1984) 189.

Journal of Chromatography, 518 (1990) 199–206
Elsevier Science Publishers B.V., Amsterdam

CHROM. 22 639

Note

Continuous monitoring of a changing sample by multiplex gas chromatography

JOSE R. VALENTIN*
Solar System Exploration Branch, NASA Ames Research Center, Moffet Field, CA 94035 (U.S.A.)
and
KIRSTEN W. HALL and JOSEPH F. BECKER
Department of Physics, San Jose State University, San Jose, CA 95192 (U.S.A.)
(First received January 9th, 1990; revised manuscript received June 19th, 1990)

Multiplex gas chromatography (MGC) is a technique in which multiple samples may be introduced into a chromatographic system regardless of the elution time of the individual components [1]. Although the output obtained from a MGC experiment is not directly interpretable, computational techniques can be used to obtain the chromatogram from the detector output data. This is done by calculating the impulse response function from the multiplexed output data.

The impulse response function is defined as the response of a system to an applied impulse input signal. The impulse response function is related to the output and input modulation signal by the following equation [2]:

$$h(\tau) = FT^{-1} [FT(Output)/FT(Input)] \quad (1)$$

where FT is the Fourier transform, "Output" is the detector output signal, "Input" is the modulation or injection signal, and $h(\tau)$ is the system impulse response function. For a single injection or pulse, $h(\tau)$ is the chromatogram of the sample that is directly obtained from the output data. For a long modulated signal composed of multiple sample injections, eqn. 1 is used to calculate the chromatogram. This technique is well summarized by Phillips [1].

Some of the most promising applications of this technique are either in areas where more data are needed to improve the detection limits of a detector or where continuous monitoring of a sample stream is required. Specifically, for NASA, this technique is being investigated as a way of conducting GC analyses from a descending spacecraft through a planetary atmosphere [3]. Under such a scenario the time available to complete a gas chromatographic analysis will be very limited. If conventional gas chromatography (*i.e.*, one single injection for each sample) is used, then, there will only be time for analysis of just a few samples before the spacecraft reaches the surface of a planet. Under such scenario, no information will be obtained from altitudes the spacecraft passes while it is involved in GC analysis.

0021-9673/90/$03.50

One of the most important restrictions for using MGC on a descending spacecraft is that the data collected will be representative of a sample whose composition varies as a function of altitude. The concentration of any given component of the atmosphere may increase or decrease as a function of altitude. In addition, a given component may appear unexpectedly during the sampling period. These changes in composition can deteriorate the signal-to-noise ratio (S/N) of the final calculated chromatogram due to variations in the baseline. These variations will contribute noise to the final calculated chromatogram. This type of noise as been defined as correlation noise by Annino and Bullock [4]. The degree of correlation noise is proportional to the rate of change in the sample. If a change occurs rapidly then the calculated signal will be completely incomprehensible [1,4,5].

In this work, the technique of exponential dilution (ED) [6] was used to change the composition and concentration of a gaseous mixture to emulate the changes in the atmospheric composition that a descending spacecraft will sample. The sample was introduced using MGC and the chromatogram computed using eqn. 1. The ED technique has previously been used by Koel *et al.* [5] to calibrate a GC system with a flame ionization detector using a sample containing methane as the only component which was determined.

In the ED technique, a flask of known volume is filled with a gas sample. Then a diluent is introduced into the flask at a constant rate. The diluted sample mixture then flows from the flask into the GC injection valve. The sample inside the flask is diluted exponentially as a function of time. At any time the concentration of the sample inside the flask can be calculated using the following equation [6]:

$$C_t = C_0 e^{-ft/v} \tag{2}$$

where C_t is the concentration of the sample at time t, C_0 is the initial concentration, f is the diluent flow-rate and v is the volume of the flask. The ED technique can also be used to make changes in sample composition by introducing a new sample in the flask instead of a diluent. After an experiment is completed, the collected data are divided into equal time segments.

It is the purpose of this paper to report results obtained while applying MGC to an environment of changing sample composition. Also the errors that resulted with various degrees of change in the sample concentration were determined by performing a calibration of the MGC system with four different rates of sample dilution.

EXPERIMENTAL

The GC system used in this work is shown in Fig. 1. The GC detector was a Model PI-52 02 photoionization detector (HNU Systems, Newton, MA, U.S.A.) with a 11.70-eV lamp. The column was a 1.5 m × 1.1 mm I.D. stainless-steel tube packed with *tert.*-butyl isocyanate bound to Porasil C (100–150 mesh). The column temperature was 25°C. The GC injection assembly was composed of an 8-port Valco valve with two 100-μl sample loops and a Valco electric actuator (Alltech, Deerfield, IL, U.S.A.) for computer control of the valve. A Datametrics Type 1511 Controller and three Model 825 Datametrics mass flow controllers (MANCO, Santa Clara, CA, U.S.A.) with orifices for 10.0, 20.0 and 100.0 ml/min were used to regulate and measure the flow of all the gases used.

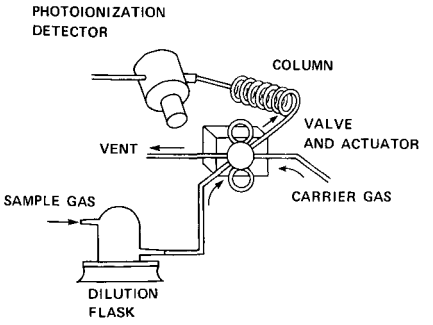

Fig. 1. Schematic diagram showing the major components of the multiplex exponential dilution flask gas chromatographic system.

Testing of the multiplex ED system was conducted with three different gas mixtures. One of them contained methane, ethane, propane and butane at 100.00 ppm in helium (Matheson). Another mixture contained those same components but at 1000.00 ppm (Matheson). A third mixture prepared manometrically contained ten hydrocarbons at the following concentrations: methane and ethane at 71.1 ppm, propane and butane at 142.3 ppm, isobutane and ethylene at 213.4 ppm, acetylene and propene at 227.6 ppm, propyne and propadiene at 355.7 ppm, all in helium. The carrier gas was 99.999% helium (Matheson). The flow-rate through the column was 16.0 ml/min.

In order to emulate the variations in sample concentration, the 100.00 ppm gas mixture was used. An ED flask of known volume was connected upstream of the sample valve. This flask is a glass vessel of accurately determined volume (239.6 ml) equipped with openings to permit continuous gas flow. It contains a magnetically-driven stirring vane to guarantee complete mixing. This flask was fabricated following the same specifications used for the ED flasks made by Varian during the early 1970s. Similar ED flasks were used during the late 1970s to calibrate the GC system that was used on board the Pioneer Venus probe for determining the gaseous components in Venus' atmosphere [7]. These flasks are still in use in our Branch and are very reliable for calibration of newer GC's being developed for use in other missions. Before starting each experiment, the flask was filled with the sample to be used at a rate of 10.0 ml/min for a period of 2 h. To ensure that the flask was completely filled with the sample, a few test injections of the sample entering the sample loop were made and no change in intensity of the GC signal was detected. Four dilution experiments were performed using the following diluent flow-rates: (1) 12.0 ml/min, (2) 18.2 ml/min, (3) 32.2 ml/min and (4) 61.6 ml/min. Before starting with the dilution, the multiplex experiment was run for an 18.0 min period to determine the intensities of the GC peaks for the 100.00-ppm concentration mixture. That peak intensity was used as reference to calculate the concentrations that were used for the exponential dilution plots. The data obtained from the experiments were used to calculate the impulse response functions using eqn. 1 followed by generation of the exponential dilution curves of concentration with respect to time for both propane and butane. To monitor this concentration as a function of time, the time corresponding to the aver-

age concentration was calculated by integrating over the interval of each data segment and using eqn. 1. The four dilution experiments were run for approximately 40, 75, 40 and 18 min, respectively. Four theoretical dilution curves using those same diluent flow-rates were also generated. The natural log of the concentrations of each experiment was plotted *vs.* Time followed by calculation of the relative error between these curves and the theoretical ones. An additional plot of % relative error with respect to diluent flow-rate in ml/min was also generated.

A study was also conducted to test the multiplex ED technique while changing the sample mixture as a function of time. In this experiment, the flask was filled with the ten hydrocarbon mixture described previously. This was followed by the introduction of a mixture containing methane, ethane, propane, and butane, all at 1000.00 ppm in helium. The four hydrocarbon mixture was introduced at a constant rate of 9.0 ml/min for a period of 140 min. A total of 1272 injections were generated during that period.

The multiplex ED system was operated using a System 1800-Model B high-speed microcomputer (Integrated Image Systems, Santa Clara, CA, U.S.A.) through an IEEE 488 interface attached to a Nelson Analytical 900 Series analog-to-digital interface (Cupertino, CA, U.S.A.) both providing the modulation signal and acquiring the detector signal. The software used for modulating the frequency of injections and acquiring the output data was supplied by Nelson Analytical and it is written in Basic. This program will only work for single-injection chromatograms. We added a random generator program to perform the multiplex ED experiments. The probability of injection was 14%. The data acquisition rate was one point per second. After all the experimental data were collected, it was transferred to a MicroVax II (Digital Equipment Corporation, Santa Clara, CA, U.S.A.) to calculate the impulse response function using eqn. 1. All the data collected in each experiment were divided in segments of 15.0-min lengths (900 data points) to monitor the dilution of the sample as a function of time for each second of the experiment. Each 15.0-min segment had the same injection sequence. That sequence was chosen from preliminary MGC experiments in which the injection or input sequence changed as a function of probability of injection. The sequence that resulted in a chromatogram with the highest S/N was the one chosen for this work.

RESULTS AND DISCUSSION

Fig. 2a and b illustrates exponential dilution plots of concentration with respect to time for the theoretical case, and for propane and butane at the starting concentrations of 100.00 ppm for the experiment with a diluent flow-rate of 18.2 ml/min. The sample used also contains methane and ethane at 100.00 ppm but these two components are not detectable by the photoionization detector used. The differences between the experimental values and the ones calculated using eqn. 1 are higher during the first 16.0 min of the dilution due to the faster change in concentration from 100.00 ppm to 30.00 ppm for both propane and butane. After that period of time the experimental values gradually becomes much closer to those predicted by eqn. 2.

Fig. 3a and b shows the plots of % of relative error between the experimental and theoretical curves as a function of diluent flow-rate for propane and butane for four separate experiments. For both propane and butane the relative error is directly

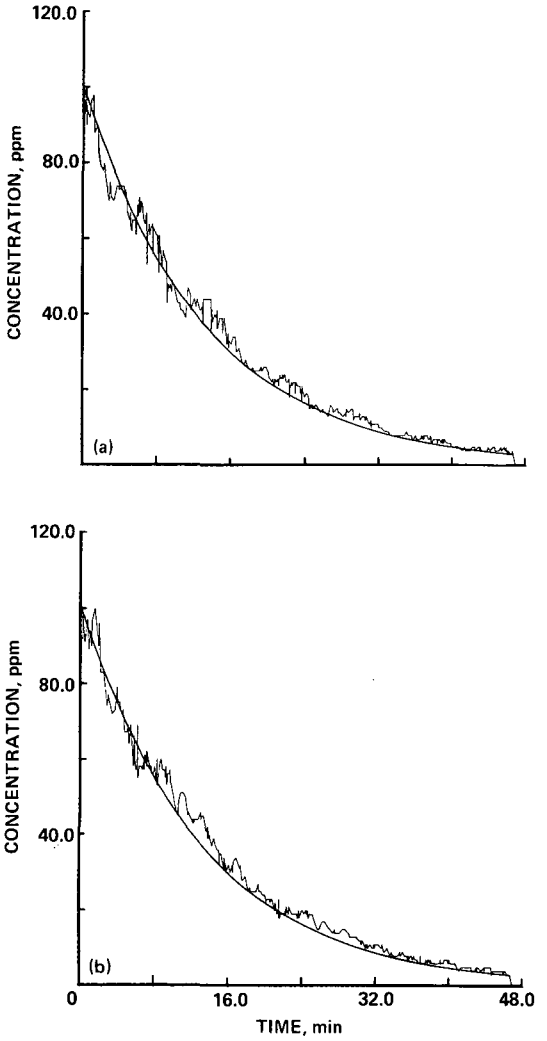

Fig. 2. Exponential curves showing an exponential decrease in concentration for (a) propane and (b) butane both at an initial concentration of 100.00 ppm, and a theoretical curve calculated using eqn. 2 for comparison with the experimental ones using a diluent flow-rate of 18.2 ml/min for a period of 75 min. A total of 670 injections were generated during that period. Each experimental point for both propane and butane represents 15.0 min. of data determined by computation of the impulse response function using eqn. 1. Volume of dilution flask = 239.6 ml.

proportional to the rate of dilution. for propane, the lowest relative error was 5.5% for a diluent flow-rate of 12.0 ml/min corresponding to a dilution time of 64.3 min from 100.00 ppm to 0.35 ppm. The highest relative error was 19.8% for a diluent flow-rate of 61.6 ml/min corresponding to a dilution time of 18.0 min from 100.00 ppm to 0.35 ppm. For butane the lowest relative error was 6.0%, and the highest

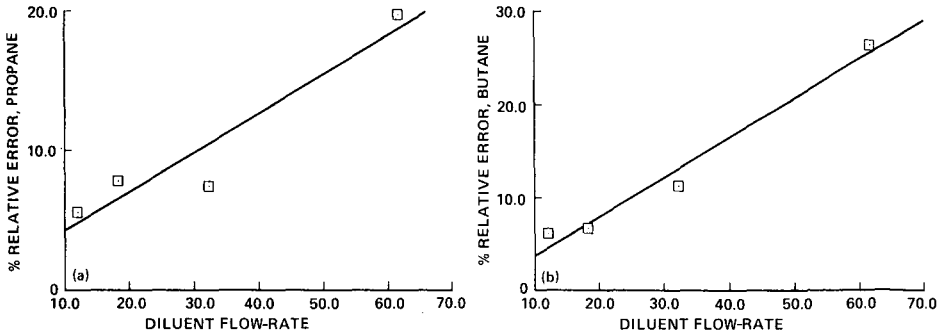

Fig. 3. Plots of % of relative error between the experimental and theoretical curves as a function of the four diluent flow-rates (in ml/min) used for (a) propane and (b) butane. For propane the slope was 0.28 ± 0.07, intercept = 1.4 ± 0.4, and coefficient of determination = 0.90. For butane the slope was 0.42 ± 0.05, intercept = 0.6 ± 1.7, and coefficient of determination = 0.98.

26.3%. The differences between the experimental values and the theoretical ones are due to (1) variations in the gas flow-rate when the injection valve is switched to introduce the sample, (2) non-linear chromatographic effects that contribute more to baseline instabilities if the dilution rate is faster and (3) the fact that Fourier transforms can be used only for stationary systems or slow changing systems. All these effects will result in baseline variations in the calculated chromatogram defined as correlation noise (discussed briefly in the introduction).

Fig. 4 shows the chromatograms obtained for the study in which one mixture containing methane, ethane, propane, and butane, all at 1000.00 ppm, was used to change a mixture of different composition (methane, ethane, ethylene, propane, acetylene, isobutane, butane, propene, propadiene and propyne) by the multiplex ED technique. All the chromatograms were obtained by calculating the impulse response function as defined in eqn. 1. Fig. 4a is the chromatogram of the mixture containing 10 components before the beginning of the dilution. Methane and ethane are not detectable by the photoionization detector used. Propyne is strongly retained in the column and appears as a very low, broad peak beyond the end of the chromatogram. Propene and propadiene elute at the retention time represented by peak 6 in Fig. 4a. In addition, a negative pressure peak, sporadically present in the data (Fig. 4b and c), originated from a change in pressure when the valve turns at the time of injection. Fig. 4b is a chromatogram obtained by calculating the impulse response function after 20.5 min of the dilution experiment. After that period of time, propane and butane increased in concentration to 602.3 ppm, while all other components had decreased. Finally, 116.5 minutes after the experiment began the only detectable components were propane and butane at concentrations close to 1000.0 ppm (Fig. 4c).

This study shows that a multiplex ED technique can be used to simulate environments where a sample is changing with time as long as the composition changes slowly with time. As discussed above, the errors calculated are a combination of uncertainties due to correlation noise. At present, additional data analysis techniques

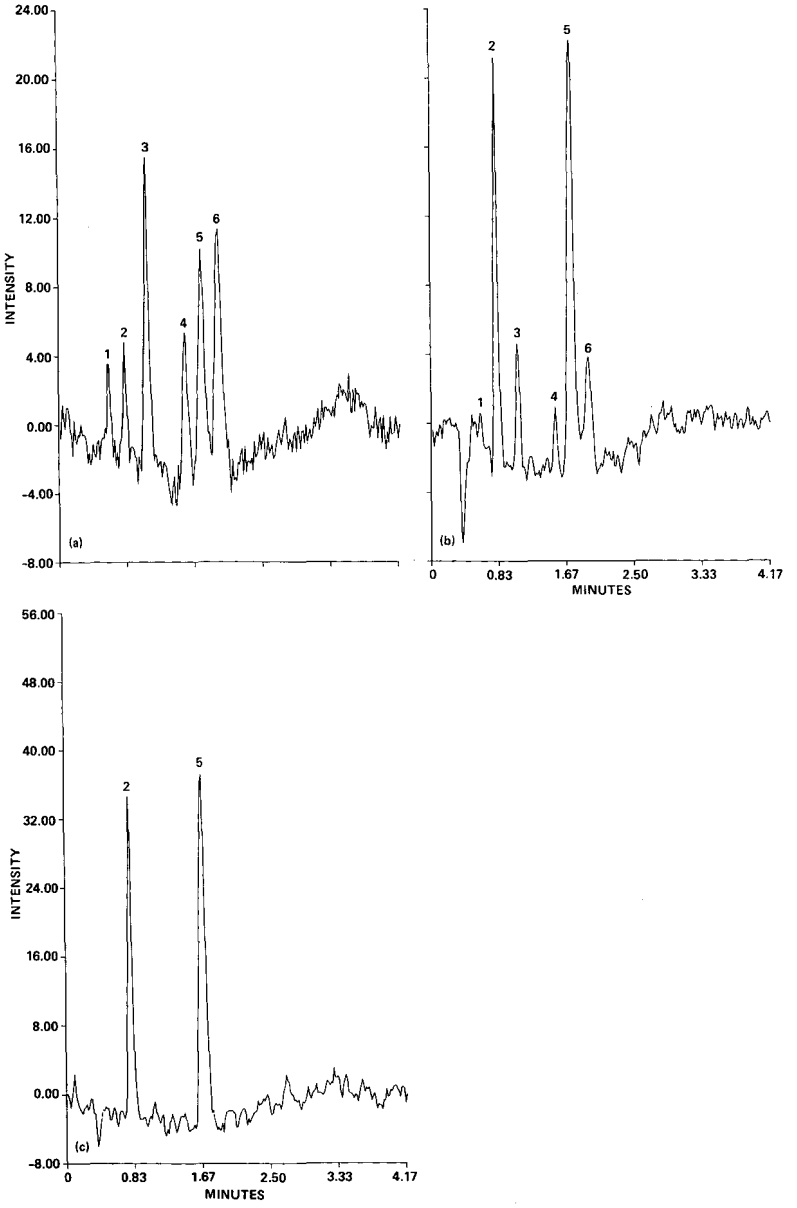

Fig. 4. Chromatograms obtained from the calculation of the impulse response function at three stages during the change in sample composition. The column temperature was 25°C and the flow-rate was 9.0 ml/min. Intensity is in arbitrary units. (a) First 15.0 min of the experiment where no change in sample composition occurred (dilution time = 0.0 min). The six peaks correspond to 1 = ethylene (213.4 ppm), 2 = propane (142.3 ppm), 3 = acetylene (227.6 ppm), 4 = isobutane (213.4 ppm), 5 = butane (142.3 ppm), and 6 = propene (227.6 ppm) and propadiene (355.7 ppm). Not detected: methane, ethane and propyne. (b) Chromatogram obtained from the calculation of the impulse response function 20.5 min after the multiplex ED experiment started. The six peaks correspond to 1 = ethylene (66.0 ppm), 2 = propane (602.3 ppm), 3 = acetylene (105.5 ppm), 4 = isobutane (99.0 ppm), 5 = butane (602.3 ppm), and 6 = propene (105.5 ppm) and propadiene (164.9 ppm). (c) Chromatogram obtained from the calculation of the impulse response 116.5 min after the multiplex ED experiment started. The two peaks correspond to 2 = propane and 5 = butane, each component present at a final concentration of 989.2 ppm.

are being developed to monitor an environment where a sample analyzed changes more rapidly than the one reported in this paper.

REFERENCES

1 J. B. Phillips, *Anal. Chem.*, 52 (1980) 468A–478A.
2 D. C. Champeney (Editor), *Fourier Transforms and Their Physical Applications*, Academic Press, New York, 1973.
3 J. R. Valentin, *LC · GC*, 7 (1989) 248–257.
4 R. Annino and L. E. Bullock, *Anal. Chem.*, 45 (1973) 1221–1227.
5 M. Koel, M. Kaljurand and E. Küllik, *Eesti NSV TA Toimitised, Keemia*, 32 (1983) 125–133.
6 J. J. Ritter and N. K. Adams, *Anal. Chem.*, 48 (1976) 612–619.
7 V. I. Oyama, G. C. Carle, F. Woeller, S. Rocklin, J. Vogrin, W. Potter, G. Rosiak and C. Reichwein, *IEEE Trans. Geosci. Remote Sens.*, GE-18 (1980) 85–93.

Journal of Chromatography, 518 (1990) 207–214
Elsevier Science Publishers B.V., Amsterdam

CHROM. 22 553

Note

Sample introduction in gas chromatography: simple method for the solventless introduction of crude samples of biological origin

B. V. BURGER*, ZENDA MUNRO and DENICE SMIT
Laboratory for Ecological Chemistry, University of Stellenbosch, Stellenbosch 7600 (South Africa)
U. SCHMIDT
Zoologisches Institut der Universität Bonn, Poppelsdorfer Schloss, D-5300 Bonn 1 (F.R.G.)
and
CHIA-LI WU and FENG-CHANG TIEN
Department of Chemistry, Tamkang University, Tamsui 25137 (Taiwan)
(First received February 26th, 1990; revised manuscript received May 8th, 1990)

The preparation of samples of biological origin normally involves extraction of the organic volatiles with a suitable solvent. This step in the work-up procedure has the advantage that it can be employed as a concentration step by extracting a sufficiently large amount of material with a relatively large volume of solvent and concentrating the extract to a suitable volume before injecting it into the gas chromatograph. The efficiency with which organic compounds are extracted from biological matter depends on factors such as the physical state of the sample and the polarity of the organic compounds and of the solvent used for extraction. If known compounds have to be determined, incomplete extraction is not such a serious problem, as quantification can be carried out relative to one or more internal standards which have properties similar to those of the analytes and are added to the biological sample before extraction.

However, if complex mixtures of unknown organic compounds with divergent physical and chemical properties have to be extracted from samples which might, for instance, contain considerable amounts of water and might further be relatively viscous or difficult to mix with the organic solvent, simple extraction techniques offer little hope of obtaining an accurate quantitative picture of the composition of the volatile organic fraction. The determination of the volatile organic constituents of the preorbital gland secretion of the small antelope *Raphicerus melanotis*, which contains water, mucous, water-soluble solid material and a complex mixture of organic compounds ranging from formic acid to long-chain alcohols and formates [1], is an example of the formidable analytical problems posed by such samples. One possible approach to the analysis of such complex samples is the direct solventless introduction of the crude sample into the injector of the gas chromatograph, provided that the

0021-9673/90/$03.50

analytes are present in high enough concentrations to afford reliable quantitative data with amounts of material that can be handled by such direct solventless introduction techniques. Although it is not common practice, the comparison of the results obtained by conventional injection of an extract of the material and those provided by solventless injection of the crude material could provide invaluable information on the reliability of the extraction and work-up procedure and on whether volatiles are lost during the solvent removal step or are obscured by the solvent peak.

Solid sample introduction systems developed by the manufacturers of gas chromatographic equipment or by workers in specific fields of research, such as the system recently elaborated by Attygalle and Morgan [2], can be used for this purpose. However, as most laboratories are only occasionally required to analyse samples that might be amenable to solid sample introduction, these systems are unfortunately not in general use in most laboratories.

In our own research on semiochemical communication in the animal world, results obtained with extracts of the exocrine secretions of insects and mammals are routinely compared with those obtained when the crude untreated secretions, or even the glands producing these secretions, are introduced into the injector of a gas chromatograph. For the past 8 years we have been using an extremely simple solventless sample introducing technique with excellent results. However, this method, which was first mentioned in a paper on the characterization of the defensive larval secretion of the citrus swallowtail butterfly *Papilio demodocus* [3] does not appear to have gained any recognition beyond a reference to it in the paper by Attygalle and Morgan [2]. This has prompted us to describe the method in more detail than in the paper in which it was first mentioned and to illustrate its application to the analysis of a number of different sample types. For this purpose we have selected a few examples from our own research and from work carried out in collaboration with other laboratories.

EXPERIMENTAL

Gas chromatographic (GC) analyses were carried out with Carlo Erba (Milan, Italy) Model 4160 and 5300 gas chromatographs and a Hewlett-Packard (Palo Alto, CA, U.S.A.) Model 5890A gas chromatograph equipped with flame ionization detectors, using helium as carrier gas. GC–mass spectrometric (GC–MS) analysis was done with a Carlo Erba QMD 1000 system. With the exception of the column employed for the analysis of the pheromone glands of the smaller tea tortrix, all columns were coated using either published methods [4] or procedures developed in the Laboratory for Ecological Chemistry.

A hole was made through the centre of a septum with a syringe needle (No. 18, 1.2 mm) with a sharpened 90° point. By rotating the needle slowly and forcing it through the septum, it was possible to produce a tapered hole through the septum. However, any septum which had been pierced a few times during normal use in a gas chromatograph could be used equally successfully without additional widening of the hole. The septum was then installed in the gas chromatograph. By tightening the septum cap sufficiently the hole through the septum can be closed and samples can be injected with a syringe in the normal manner. An empty sample introduction probe or a thin flame-polished glass rod can also be used to close the hole in the septum, which tends to widen if the solventless sample introduction technique is used repeatedly.

Sample introduction probes were made from capillary tubing (0.7 mm I.D. × 1.2 mm O.D.) drawn from soft glass tubing on a capillary drawing machine (Hewlett-Packard 1045A, Hupe & Busch or Carlo Erba GCM60). Ordinary melting point capillaries with similar dimensions can, however, also be used for this purpose. To manufacture a sample introduction probe, a 100-mm length of capillary is sealed off about 20 mm from one end by holding the capillary in the side of the flame from a small bunsen burner until a bead of glass has been formed at this point (Fig. 1A). The capillary is then removed from the flame, rotated to keep it straight and drawn out just enough to decrease the diameter of the soft glass bead to approximately that of the capillary itself. Using a glass-cutting tool or preferably the sharp edge of a fragment of silicon wafer, the shorter section of the capillary is scored a few millimetres from this position and about 15 mm of the capillary is broken off and discarded. The tip of the remaining capillary is flame polished to ensure smooth and unobstructed movement through the septum and to avoid fragments of the septum from being transported into the injector by the sharp edges of the capillary. The other end of the capillary is sealed off or flame polished to avoid hand injuries when the probe is inserted into the injector. To facilitate rapid and quantitative evaporation of volatiles from a sample, the probe is constructed with the shortest possible sample cavity which can still accommodate the sample without losing material when the probe is inserted through the septum. With some experience a sample probe can be made in a few minutes and, instead of cleaning used ones in an ultrasonic bath or muffle furnace, we prefer to use a new probe for each sample.

The sample probe is loaded with a sample by placing an appropriate amount of the material to be analysed in the sample cavity. Care is taken not to obstruct the free movement of the carrier gas into and the transportation of desorbed volatiles out of the sample cavity by blocking it with, for example, a large amount of viscous material.

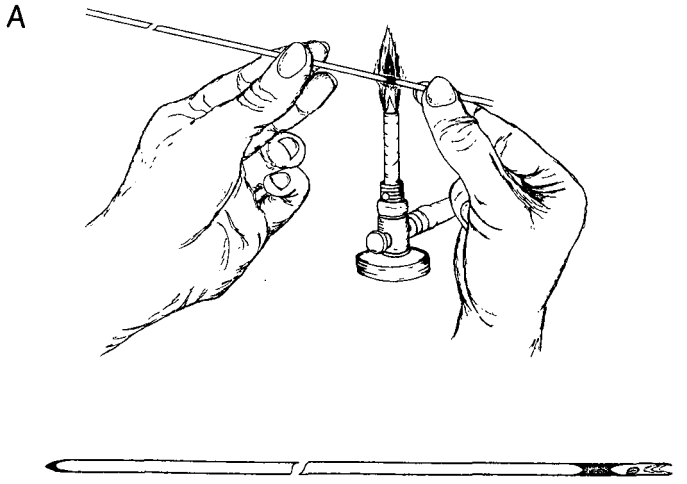

Fig. 1. Preparation and loading of a sample introduction probe. (A) Glass capillary tubing is sealed off about 20 mm from one end in the flame from a small bunsen burner; (B) sample probe trimmed to the required size and sample cavity depth, and loaded with a sample which is retained by a few glass fibres.

Such a sample is preferably spread out as a thin film on the inner surface of the sample cavity. In the case of solid material which might drop out of the sample cavity when the probe is brought into a vertical position, a few fibres of silanized glass-wool are inserted into the cavity to hold the sample in place as shown in Fig. 1B. This is best done under a stereo microscope with a thin glass rod. Fibres protruding from the cavity are removed with a pair of ophthalmic scissors or are cut off against a microscope slide with a razor blade or the sharp edge of a piece of silicon wafer.

To introduce the sample into the injector, the sample probe is pushed firmly down into and through the septum. The sample cavity is sealed gas-tight while it is passing through the septum, preventing any carrier gas or volatile components from escaping. Introduction of highly volatile samples can be done with the injector in the split mode. With solid or highly viscous samples, it is advisable to keep the split valve closed until all the volatiles have evaporated from the sample. It is also possible to use temperature-programmed sample evaporation if thermally labile compounds are expected to be present in the sample. Especially under conditions where volatiles are transported relatively slowly to the capillary column, cold or stationary phase focusing should be employed.

A section through an injector with a sample probe in place is shown in Fig. 2. In most gas chromatographs the needle-guiding holes through the septum cap and septum-supporting insert have to be enlarged to *ca.* 1.5 mm to accommodate the sample introduction probe, which is much thicker than a normal syringe needle.

RESULTS AND DISCUSSION

The application of this solventless introduction of samples into the injector of a gas chromatograph is illustrated in Figs. 3–6.

Larvae of the citrus swallowtail butterfly (*Papilio demodocus*) possess a defensive gland, the osmeterium, situated mid-dorsally behind the head. The gland is normally invisible, but can be extruded as a prong- or fork-like structure. A defensive secretion consisting almost entirely of water is produced by the osmeterium and was found to contain small amounts of terpenoid compounds in the pre-final instars. To collect the defensive secretion a larva was irritated by tapping it on the head with a sample probe. As the larva gradually extended its osmeterium, the two prongs were guided into the sample cavities of two probes. In this experiment sample cavities with a depth of about 5 mm were employed. Slow withdrawal of the osmeterium from the sample probes left a little opaque material in the sample cavities. Using this method, it was found that in some larvae one prong of the osmeterium produces high concentrations of a number of monoterpenes, while these compounds are almost entirely absent from the secretion collected from the other prong. Examples of the gas chromatograms obtained in such an experiment are given in Fig. 3.

In contrast to the defensive secretion of the citrus swallowtail, Lepidoptera mostly produce their sex pheromones in extremely small amounts. The first sex attractants to be identified were therefore isolated by extraction of many thousands of insects. Using modern analytical techniques it is possible, however, to identify the constituents of an insect pheromone by using the pheromone-producing glands of a single insect, preferably employing a direct solventless sample-introduction device [2]. This can be accomplished successfully and simply by using the technique described

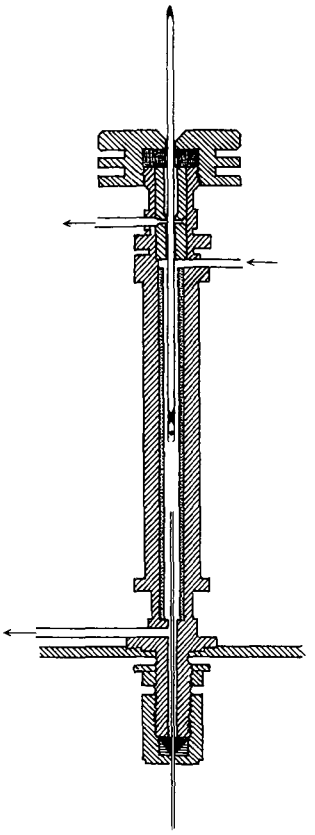

Fig. 2. GC injector with inserted sample probe.

in this paper. The clean profile of the constituents of the sex pheromone gland of the smaller tea tortrix (Taiwanese *Adoxophyes* sp.) shown in Fig. 4 was, for example, obtained by using two excized glands of the female moth.

An advantage of the technique described in this paper that is not offered by most of the other solid-sampling techniques is that the sample can be removed from the injector at any time after the volatiles have been desorbed. The formation of artefacts from the less volatile constituents in a sample at high injector temperatures and the transportation onto the column of heavy lipids which might adversely affect the performance of a column can thus be restricted by timely removal of the sample from the injector. It is essential, however, to carry out a few trial runs to determine the lowest temperature and the shortest time required for quantitative transportation of the volatiles of interest onto the column. This can be done, for example, by subjecting a sample to a second desorption in order to determine whether all the volatiles of interest had been removed from the sample during the first desorption. Gas chromatograms obtained in such an experiment are shown in Fig. 5.

Finally, the technique can also be used for sample introduction in GC–MS analysis. The total ion chromatogram shown in Fig. 6 was, for example, obtained with a trace amount of the waxy buccal secretion of the bat *Nyctalus noctula*.

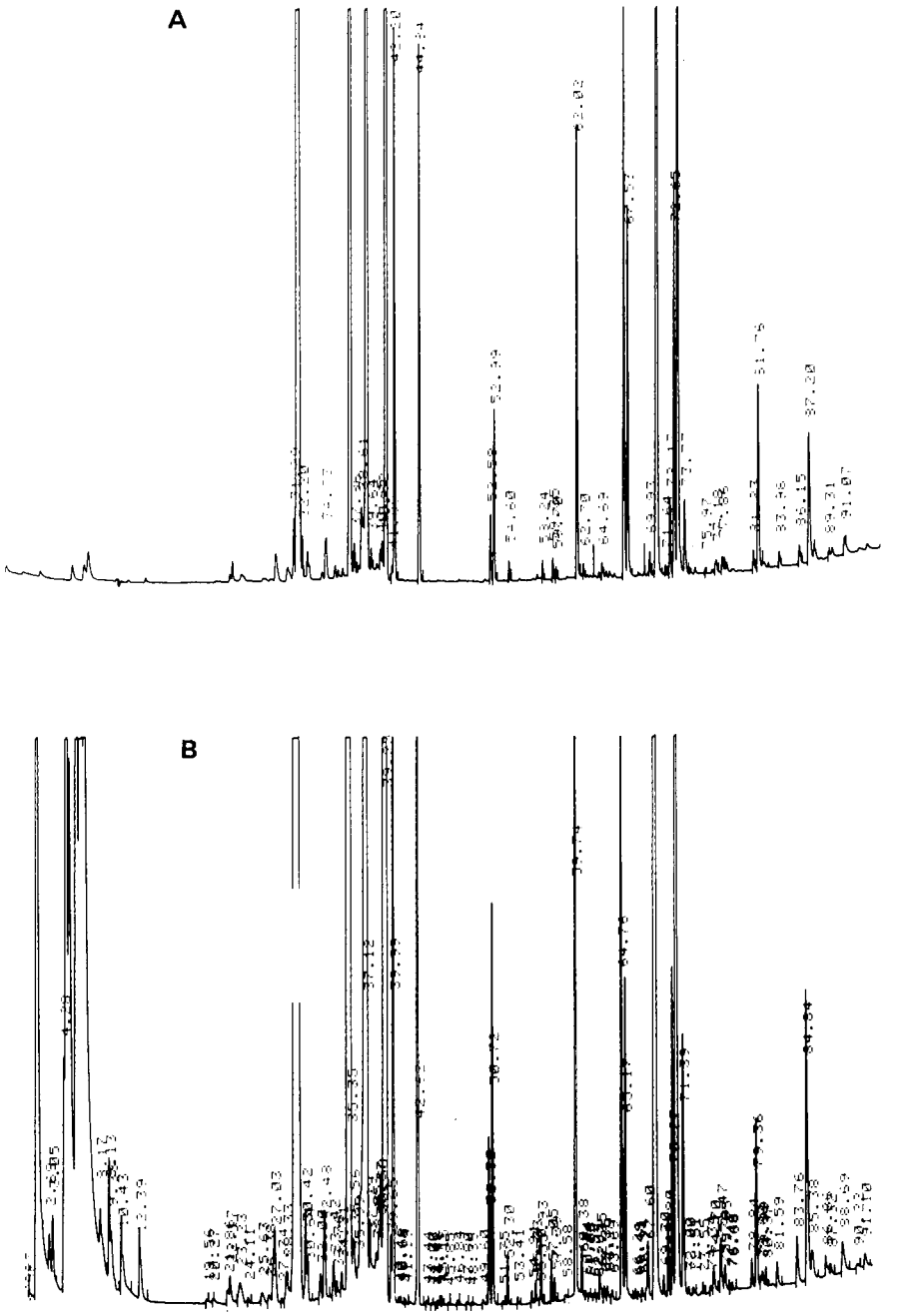

Fig. 3. GC comparison of the defensive secretions (A and B) collected separately from the two prongs of the osmeterium of a *Papilio demodocus* larva. The injector at 220°C was operated in the splitless mode for 2 min and the volatiles were trapped on the column at 30°C. Glass capillary column coated with Carbowax 20M (40 m × 0.3 mm I.D., film thickness 0.3 μm); temperature programmed from 40 to 220°C at 2°C/min.

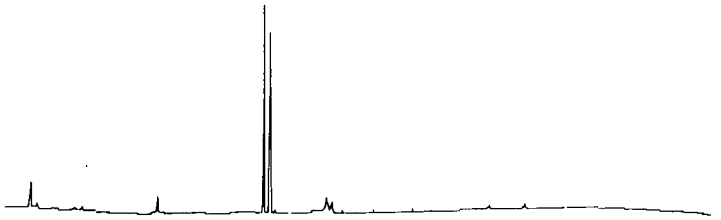

Fig. 4. Gas chromatogram of the organic volatiles desorbed from two excized sex pheromone glands of the smaller tea tortrix (Taiwanese *Adoxophyes* sp.). The injector at 220°C was operated in the splitless mode for 5 min and the volatiles were trapped on the column at 50°C. Fused-silica column (Supelco) coated with SP 2250 (60 m × 0.25 mm I.D., film thickness 0.2 μm); temperature programme, 50°C for 30 s, increased to 150°C at 4°C/min and from 150 to 260°C at 2°C/min, held isothermally at 230°C for 1 h.

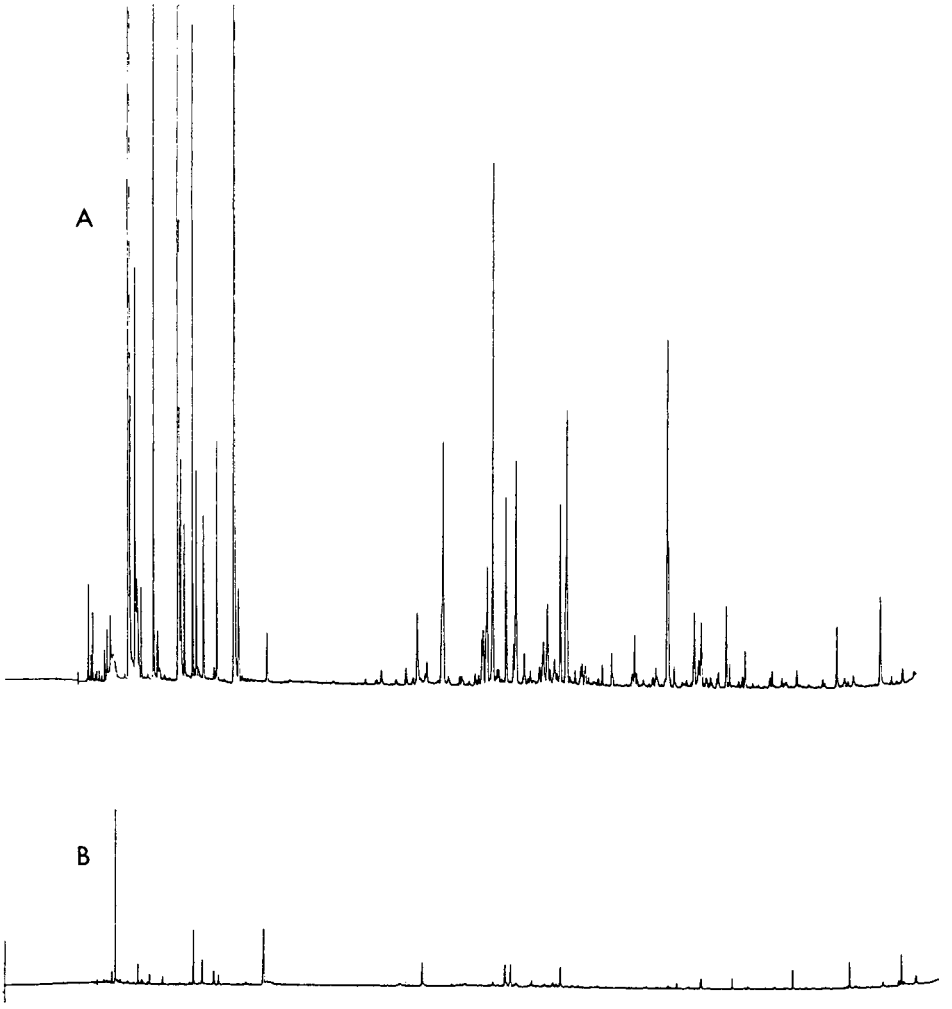

Fig. 5. Gas chromatograms obtained by consecutive desorptions of the volatiles from a 0.3-mg sliver of a *Eucalyptus linearis* leaf. The injector was programmed from 100 to 260°C at 30°C/min and held at 260°C for 15 min and the volatiles were trapped on the column with solid carbon dioxide. Fused-silica capillary column coated with Superox 4 (25 m × 0.25 mm I.D., film thickness 0.25 μm); temperature programmed from 40 to 80°C at 2°C/min and from 80 to 230°C at 4°C/min. (A) First desorption; (B) second desorption.

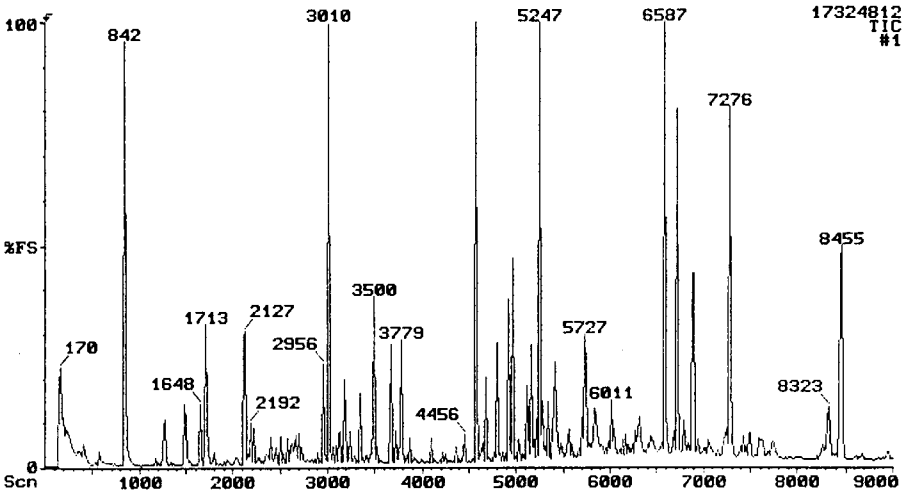

Fig. 6. GC–MS of the buccal gland secretion of a male bat, *Nyctalus noctula*. The injector at 220°C was operated in the splitless mode for 4 min and the volatiles were trapped on the column at 30°C. Glass capillary column coated with OV-1701-OH (40 m × 0.3 mm I.D., film thickness 0.5 μm); temperature programme, 30°C for 3 min, increased to 40°C at 25°C/min and from 40 to 250°C at 2°C/min.

When solventless injection techniques are used, the reproducibility of retention times depends on, *i.a.*, the degree of sophistication of the carrier gas pressure-regulating system, *i.e.*, whether the regulator will reset to exactly the same pressure after the pressure has been released to remove sample residues or glass fragments from the injector. If the injection technique described here is used with a relatively thick silicone-rubber septum and a properly tightened septum cap, it is possible to insert and slowly withdraw the sample introduction probe without losing carrier gas from the injector. In a study of the seasonal changes in the composition of the buccal gland secretion of *Nyctalus noctula* in which almost 100 samples of this secretion have been analysed over a period of more than 2 years, the retention time reproducibility obtained with this technique was found to be fairly good. It must be stressed, though, that cold or stationary phase trapping has to be employed in most instances in order to obtain sharp peaks and reproducible retention times.

ACKNOWLEDGEMENTS

Support of this research by the respective universities, the Foundation for Research Development (South Africa) and the National Science Council (Taiwan) is gratefully acknowledged.

REFERENCES

1 B. V. Burger, M. le Roux, H. S. C. Spies, V. Truter, R. C. Bigalke and P. A. Novellie, *Z. Naturforsch., Teil C*, 36 (1981) 344.
2 A. B. Attygalle and E. D. Morgan, *Angew. Chem., Int. Ed. Engl.*, 27 (1988) 460, and references cited therein.
3 B. V. Burger, Z. Munro, M. Röth, H. S. C. Spies, V. Truter, H. Geertsema and A. Habich, *J. Chem. Ecol.*, 11 (1985) 1093.
4 W. Blum, *J. High Resolut. Chromatogr. Chromatogr. Commun.*, 8 (1985) 718.

Journal of Chromatography, 518 (1990) 215–220
Elsevier Science Publishers B.V., Amsterdam

CHROM. 22 632

Note

Identification using solid phase extraction and gas chromatography–mass spectrometry of timolol in equine urine after intravenous administration

A. M. DUFFIELD*, S. WISE, J. KELEDJIAN and C. J. SUANN
Australian Jockey Club Laboratory, P.O. Box 3, Randwick, N.S.W. 2031 (Australia)
(Received May 15th, 1990)

Drugs belonging to the β-blocker group have the potential to curtail cardiac output in the horse and their possible use as "go-slow" drugs is a continuous concern of the racing industry [1]. Timolol, *S*-1-*tert*-butylamino-3[(4-morpholino-1,2,5-thiadiazol-3-yl)oxy]-2-propanol is a β-blocker used in the treatment of hypertension and angina [2] and to reduce intra-ocular pressure experienced in glaucoma [3].

Methods for the detection and identification of timolol (available as Blocadren) has been described using capillary gas chromatography (GC)–flame ionization detection (FID) and GC–mass spectrometry (MS) [4]. Solid-phase extraction has proved useful in the screening of many other β-blocker drugs [5,6]. We now describe a solid-phase extraction procedure for the isolation of timolol from equine urine and its identification by GC–MS. This methodology was responsible for the identification of timolol in separate post race urine samples taken at Sydney racecourses from three beaten favourites whose individual performances were far below expectation. A procedure is also described for the routine post race screening of timolol in equine urine using a liquid–liquid extraction procedure.

EXPERIMENTAL

Instrumentation

A Finnigan-MAT Incos 50 GC–MS system was utilised in this study. Electron impact (EI) ionisation operating with 70-eV electrons and a trap current of 750 μA was used with the ion source temperature maintained at 190°C and the GC transfer line at 270°C. The GC column (J & W Scientific, Davis, CA, U.S.A., DB-5, 15 m × 0.3 mm I.D.), operated with helium as carrier gas (flow is 1 ml min^{-1}). The initial GC oven temperature of 100°C was programmed to 300°C at 30°C min^{-1} commencing 2 min after sample injection. The mass spectrometer was repetitively scanned from *m/z* 50 to *m/z* 450 in 0.6 s.

0021-9673/90/$03.50

Chemicals

Timolol was supplied by Merck Sharp and Dohme Australia. Solvents were of nanograde quality and were purchased from Mallinckrodt, Meadowbank, Australia. Bond Elut Certify columns were produced by Analytichem and purchased from F.S.E., Homebush, Australia.

Drug administration

Timolol (30 mg) in sterile water (30 ml) was administered intravenously (i.v.) to a healthy Thoroughbred mare and urine samples collected after 2, 4, 6, 8 and 12 h. These samples were stored frozen until analysed.

Solid-phase extraction procedure

Equine urine (50 ml, 2 h administration) was adjusted to pH 6.1 with hydrochloric acid and filtered through a Whatman No. 1 filter paper. Four Bond Elut Certify cartridges were each primed with methanol (2 ml) followed by deionised water (2 ml). Filtered urine (5 ml) was passed through each of the four cartridges which were successively rinsed with water (2 ml), sodium acetate buffer (0.1 *M*, pH 4, 1 ml) and methanol (2 ml). Freshly prepared dichloromethane–isopropanol–conc. NH_4OH (8:2:0.2; 2 ml) was used to elute each cartridge. The combined eluents (8 ml) were

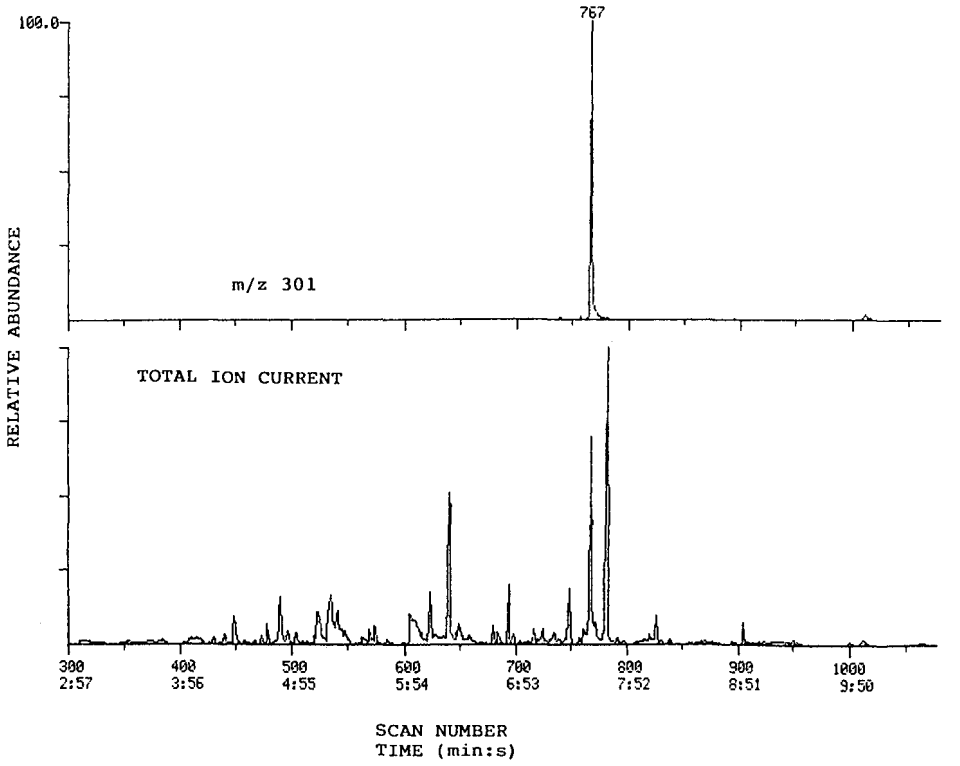

Fig. 1. Total ion current (TIC) trace of an equine urine (2 h administration) extract (lower) and profile for *m/z* 301 indicating the elution of timolol at scan number 767.

concentrated at 70°C under nitrogen gas. The residue was dissolved in methanol (20 μl) and aliquots (2 μl) used for GC–MS analysis.

Screening procedure for timolol in urine

Post-race urines were composited (5 × 2 ml), their pH adjusted to 5.0 and hydrolysed overnight at 37°C with the mixed β-glucuronidase-arylsulphatase enzyme from *Helix pomatia* (Boehringer Mannheim, F.R.G.). The urine composite was adjusted to pH 2–3 with hydrochloric acid and two drops of 10% sodium metabisulphite added and the sample extracted on a rotorack with ethyl acetate (5 ml) for 5 min. After centrifugation the organic layer is aspirated and discarded.

The composite urine sample was then adjusted to pH 9.0–9.5 with concentrated NH_4OH and extracted with a mixture of dichloromethane–isopropanol (4:1; 3 ml). After centrifugation the aqueous layer was aspirated and discarded. Acetic anhydride (one drop) was added and the solvent evaporated at 70°C under nitrogen. The residue was then reacted with acetic anhydride (one drop) in pyridine (two drops) at 80°C for 20 min. Sulphuric acid (0.1 *M*, 1 ml) and dichloromethane (2 ml) were added and the tube thoroughly vortexed. The aqueous layer was transferred to a Kimble Tube, $NaHCO_3$ (50 mg) added, followed by 10% NH_4OH (one drop). Dichloromethane (5 ml) was added, the two phases thoroughly vortexed, and after separation, the aque-

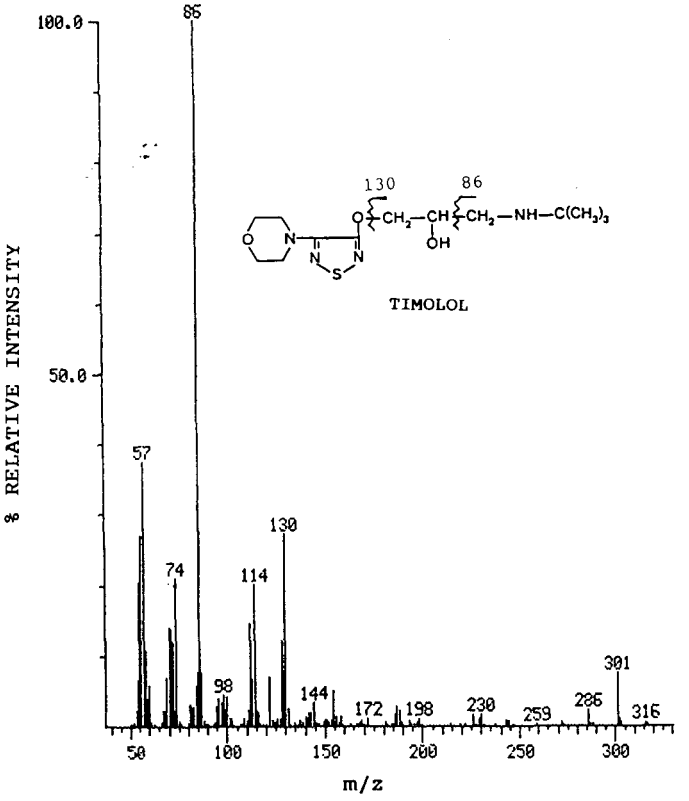

Fig. 2. EI mass spectrum of timolol corresponding to scan number 767 in Fig. 1.

ous phase discarded. The organic phase was dried (Na_2SO_4) and, following the addition of acetic anhydride (one drop), blown to dryness at 70°C under nitrogen.

The residue was reconstituted in isopropanol (30 μl) and an aliquot (2 μl) injected into a Hewlett-Packard MSD Model 5970 GC–MS system equipped with an Autosampler (Ryde, Australia). The GC column was an Ultra 1 plus methyl silicone (Hewlett-Packard; 12 m, 0.23 mm I.D., coating thickness 0.33 μm). GC analysis was accomplished using an initial oven temperature of 130°C, which was maintained for 1 min after sample injection, programmed at 30°C min^{-1} to 280°C and held at this temperature for 1 min. Methyl stearate served as an internal standard for retention time (4 min 58 s) and timolol acetate eluted at 5 min 40 s.

This procedure could readily detect timolol acetate after processing urine from the 2- and 4-h i.v. drug administration samples which were used as positive controls for each batch analysis (20 composited samples representing 100 urines).

RESULTS AND DISCUSSION

Fig. 1 records the GC–MS response obtained from the extract of a urine sample collected 2 h after i.v. administration of timolol (30 mg). The drug eluted from the GC–MS system (Incos 50) as a sharp peak and its mass spectrum is recorded in Fig. 2.

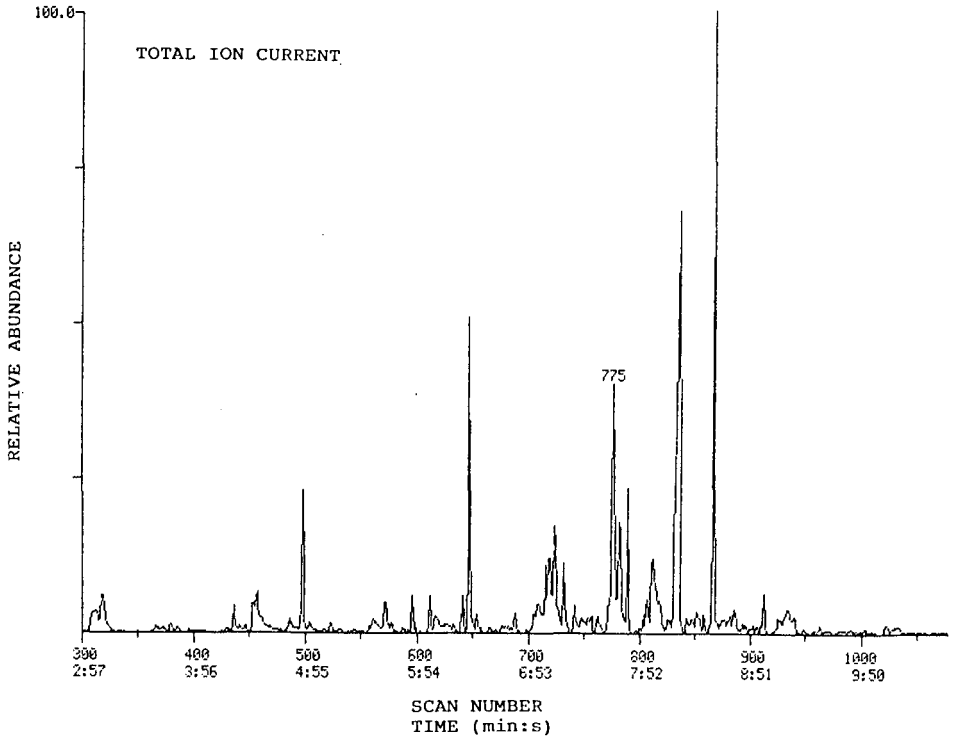

Fig. 3. TIC trace of an acetylated extract of equine urine after i.v. timolol administration. Timolol acetate elutes at scan number 775.

An identical GC retention time (7 min 38 s, scan 767) and mass spectrum was obtained after the analysis of a standard timolol solution.

When the urine extract from solid-phase extraction was acetylated (acetic anhydride in pyridine at room temperature overnight) timolol acetate could be identified (TIC reproduced as Fig. 3) and its mass spectrum is reproduced in Fig. 4. The acetate had a retention time of 7 min 43 s (scan 775 in Fig. 3) (Incos 50 GC–MS system) and its mass spectrum [7] was identical with an authentic standard prepared from timolol.

Following i.v. administration of timolol (30 mg) this methodology could detect the drug in equine urine up to 4 h. If timolol (50 mg) was administered orally (stomach tube) no free drug was detected in urine after either 2 or 4 h. Hydrolysis of urine after i.v. administration with the mixed β-glucuronidase-arylsulphatase enzyme from *Helix pomatia* resulted in approximately a two-fold increase in the amount of timolol detected as compared to non-hydrolysed urine.

Subsequent to the identification of timolol in the urine of three horses, who competed and failed badly at Sydney racecourses as short priced favourites, this laboratory instituted a GC–MS screen for timolol derivatised as its acetate. This

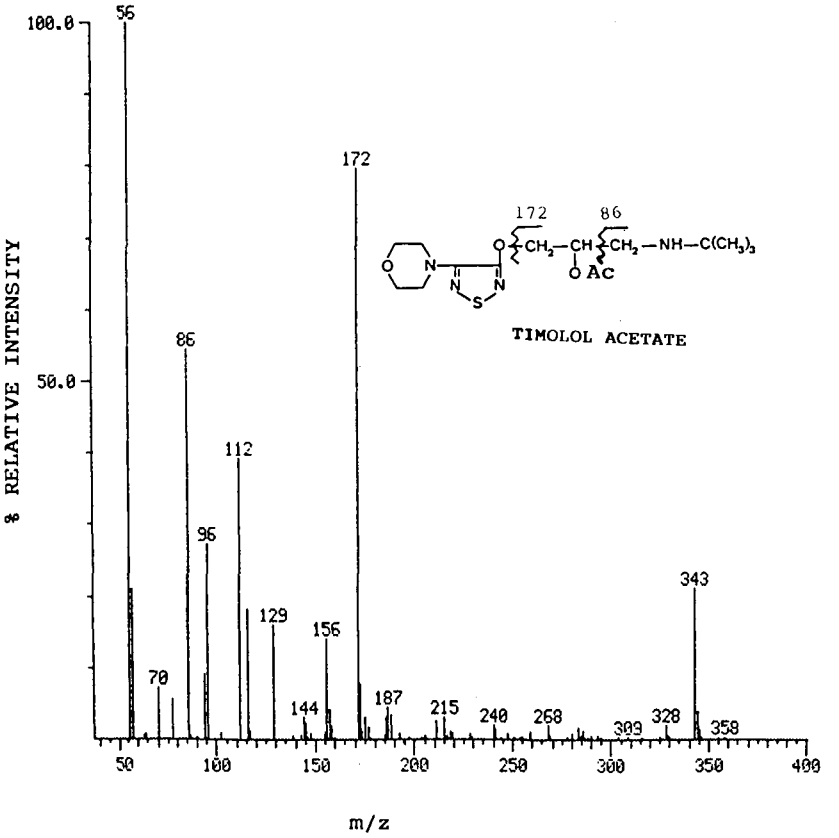

Fig. 4. EI mass spectrum of timolol acetate corresponding to scan number 775 in Fig. 3.

method used selected ion monitoring (SIM) of *m/z* 172 in the mass spectrum of timolol acetate (Fig. 4) isolated from five composite urine samples by liquid–liquid extraction with dichloromethane–isopropanol (4:1). Solvent extraction was used rather than solid phase extraction for the screening of routine samples because of the increased sample throughput and cost savings.

The base peak in the mass spectrum of timolol (Fig. 2), and a prominent ion in its acetate derivative (Fig. 4), occurs at *m/z* 86 and its origin is consistent with α-cleavage to the aliphatic nitrogen atom in both compounds. The ion of mass 130 in the mass spectrum of timolol is located at *m/z* 172 in the mass spectrum of its acetate derivative (Fig. 4) and would result from the indicated bond fissions. Low intensity molecular ions were observed in the mass spectra of timolol and its acetate at *m/z* 316 and *m/z* 358, respectively. A more abundant ion species occurs from the loss of a methyl radical from each molecular ion (see *m/z* 301 and *m/z* 358 in Figs. 2 and 4, respectively).

ACKNOWLEDGEMENTS

Timolol was a generous gift from Merck Sharp and Dohme Australia. We thank the Racecourse Development Committee of New South Wales for the purchase of the GC–MS systems and for laboratory facilities.

REFERENCES

1 M. C. Dumasia and E. G. Houghton, *Biomed. Environ. Mass. Spectrom.*, 18 (1989) 1030.
2 N. Weiner, in A. Goodman Gilman, L. S. Goodman, T. W. Rall and F. Murad (Editors), *The Pharmacological Basis of Therapeutics*, 7th Ed., MacMillan, New York, 1985, p. 200.
3 H. Bundgaard, A. Burr and V. H. L. Lee, *Acta Pharm. Suec.*, 25 (1988) 293.
4 R. D. Rofi and G. E. Aldoma, *J. High Resolut. Chromatogr.*, 12 (1989) 428.
5 P. M. Harrison, A. M. Tonkin and A. J. MacLean, *J. Chromatogr.*, 339, (1985) 429.
6 M. S. Leloux, E. G. de Jong and R. A. A. Maes, *J. Chromatogr.*, 488 (1989) 357.
7 K. Pfleger, H. Maurer and A. Weber, *Mass Spectra and GC Data of Drugs, Poisons and their Metabolites, Part II, Mass Spectra and Indexes*, VCH, Deerfield Beach, FL, 1985, p. 614.

Journal of Chromatography, 518 (1990) 221–229
Elsevier Science Publishers B.V., Amsterdam

CHROM. 22 586

Note

Characterization of volatile components in apricot purées by gas chromatography–mass spectrometry

LUCIANA BOLZONI and MARIA CARERI
Stazione Sperimentale per l'Industria delle Conserve Alimentari, Viale Tanara 31, 43100 Parma (Italy)
and
ALESSANDRO MANGIA*
Istituto di Chimica Generale ed Inorganica, Università di Parma, Viale delle Scienze, 43100 Parma (Italy)
(First received January 25th, 1990; revised manuscript received May 22nd, 1990)

The characterization of the volatile components in apricot purée has been carried out as part of a study dealing with the definition of the quality level of foods on the basis of analytical data. Volatile substances are the main factors responsible for aroma, which, together with other factors such as taste and physical and psychological factors, contributes to the "flavour".

Apricot purées are semi-manufactured products from the industrial production of fruit juices. Some studies dealing with the characterization of apricot aroma have been reported and different procedures for the sampling of the volatiles have been proposed. In one of the earliest studies, Tang and Jennings [1,2] used absorption on charcoal and gas chromatographic (GC) separation for their identification on fruits belonging to the Blenheim variety Terpenic hydrocarbons, terpenic alcohols, lactones and organic acids were identified. Rodriguez *et al.* [3] studied the volatile compounds of the Rouge de Rousillon cultivar, starting both from fresh fruits and from industrially manufactured purées. In their work two different extraction procedures were used. By means of GC–mass spectrometry (GC–MS), terpenes, terpenic alcohols, lactones and methyl and ethyl esters of fatty acids were identified. Chairote *et al.* [4] studied the volatile components of apricot purées of the same variety using two different isolation techniques: a trapping technique, using a Chromosorb 105 trap for the enrichment of the samples, and a vacuum steam distillation followed by fractionation on a silica column. Several compounds were identified for the first time in these products including 3-nonen-2-one, *p*-hydroxybenzaldehyde, damascenone, *β*-ionone, dihydroactinidiolide and 2-phenylethanol.

More recently, Guichard and Souty [5] determined the relative amounts of aroma compounds in fresh fruits of six different varieties having different organoleptic properties. The most abundant substances were found to be terpenic alcohols, lactones, phenolic aldehydes and sesquiterpenic ketones. The volatile components were isolated by vacuum distillation at room temperature, extraction of the distillate with dichloromethane and fractionation of the extracts on a silica column.

0021-9673/90/$03.50

The results of the quantification of twelve volatile components of apricot, obtained by adding known amounts of the single components before the extraction, were compared by Guichard [6] with those obtained with the internal standard method. Considerable differences were observed using the two methods. A selection and classification of 56 volatile components of apricot were achieved by Schlich and Guichard [7] using statistical methods; the components were grouped according to their chemical class.

In this work, the aroma components of apricot purées, industrially manufactured, were characterized using the purge and trap technique for the extraction of the volatile substances with the aim of obtaining a GC profile of the volatile fraction of the different samples and identifying new compounds in this fraction. Using capillary GC–MS 105 compounds were identified.

EXPERIMENTAL

Samples

Twenty purée samples derived from different batches supplied by fruit-juice producers (Eckes, Trento and Zipperle, Merano, Italy) were examined. These purées were obtained from fruits of different varieties and origin, cultivated in Italy. The apricot purées were heated at 115–120°C for 1 min and then frozen and maintained at −18°C until the analysis.

Extraction procedure for volatile substances

The volatile components of the apricot purées were isolated by means of the purge and trap technique, using Tenax as adsorbing material.

To 40 g of purée, 40 g of water were added, followed by 4.5 μg of methyl salicylate, to be used as internal standard to check the reproducibility of the sampling procedure for the different samples. The sample, thermostated at 50°C, was purged with purified helium for 10 min at a flow-rate of 50 ml/min, then the aroma components were stripped out with the same flow of helium and adsorbed on a Tenax trap. To eliminate the adsorbed water, which could interfere in the GC analysis, the trap was flushed with helium for 10 min.

The substances trapped on Tenax were thermally desorbed and injected into the gas chromatograph using a Chrompack TCT thermal desorption cold trap; the Tenax trap was heated at 240°C for 10 min under a helium flow (flow-rate 10 ml/min). The desorbed compounds were cryofocused in a silica capillary, cooled at −108°C; the capillary was then quickly heated to 200°C for injection into the column. The traps for adsorption, purchased from Chrompack, consisted of glass tubes (16 cm × 4 mm I.D.) filled with Tenax (90 mg, 20–35 mesh).

Gas chromatography and mass spectrometry

For GC analysis a Dani 3865 chromatograph, equipped with a flame ionization detector was used with injector and detector temperatures of 250°C.

GC–MS analysis was carried out using a Finnigan system consisting of a Hewlett-Packard Model 5890 gas chromatograph, an Incos 50 quadrupole mass spectrometer and a Data General computer. Ionization was effected by electron impact (70 eV). The gas chromatograms were recorded by monitoring the total ion

current in the 35–350 u range; below these values it was not possible, with the sampling device used, to avoid interferences from peaks derived from air. The temperatures of the interface and of the ion source were 240 and 140°C, respectively.

Using both flame ionization and mass detection, chromatographic separations were carried out on a DB-WAX bonded-phase column (J. & W. Scientific) (30 m × 0.25 mm I.D., film thickness 0.25 μm. The column temperature was held at 40°C for 6 min, then increased from 40 to 60°C at 2.5°C/min and from 60 to 220°C at 7.5°C/min, holding this temperature for 6 min.

The compounds used as reference substances in the GC analysis were obtained from Aldrich.

RESULTS AND DISCUSSION

Table I lists the substances identified in the apricot purées by means of GC/MS following the described procedure. The third column lists the literature sources which report the corresponding substances among the volatile components of apricot and the fourth column indicates the number of samples out of 20 in which the substances were found in this work. The identifications were obtained by mass spectrometry and, where possible, were confirmed by comparison with authentic substances used as references. Fig. 1 shows the chromatograms obtained with flame ionization detection for two samples having considerably different aromatic profiles and Fig. 2 shows a chromatogram obtained by GC–MS; the peaks are numbered according to Table I.

Using the purge and trap technique, more than 150 compounds were isolated; among these, 105 were identified, 44 of which have not been reported previously. The identified compounds are 14 hydrocarbons, 33 carbonyl derivatives, 30 alcohols, 1 phenol, 4 carboxylic acids, 17 esters, 3 lactones, 2 furans and 1 pyran. Among these are substances that are considered to be typical components of apricot aroma [4] such as benzaldehyde, linalol, α-terpineol, geraniol, linalol oxides, γ-octalactone and γ-decalactone.

Nerol, geraniol and oxides of terpenic alcohols are known to be formed via thermal decomposition of hydroxylic derivatives of linalol [9]. These compounds were found in all the samples and their presence may be due to the blanching undergone by these apricot purées during industrial production, or to the effects of heating in the extraction steps.

Among the compounds identified for the first time as volatile constituents of the apricot purées are methyl acetate, ethyl butanoate, α-phellandrene, α-terpinene, (*E*)-ocimene, acetyl methyl carbinol acetoin, α-farnesene, geranylacetone, phenol, nerolidol I and II and isopropyl myristate and palmitate. With regard to the last two compounds, in a previous study [3] the methyl and ethyl esters of fatty acids were identified as volatile components in frozen apricot fruits.

In addition to the cited compounds, 1,1,6-trimethyl-1,2-dihydronaphthalene and 1,5,8-trimethyl-1,2-dihydronaphthalene were identified; these compounds have structures related to that of β-ionone. The first has been found in peaches, strawberries and in red wine and is probably formed by oxidation of (6-*trans*-2′-*trans*)-6-(but-2′-enylidene)-1,5,5-trimethylcyclohex-1-ene by the following mechanism [10]:

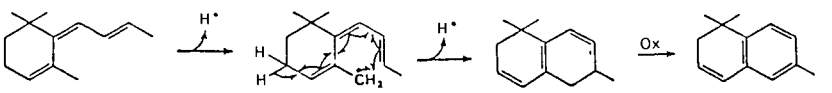

TABLE I

VOLATILE COMPOUNDS IDENTIFIED IN APRICOT PURÉES

No.	Aroma compound	Ref.	Occurrence	Method of identification[a]
1	Acetone	3	20	MS
2	Methyl acetate		19	MS
3	2-Methylfuran		15	MS
4	Butanal	5	12	RT, MS
5	Ethyl acetate	5	20	RT, MS
6	2-Butanone	5	16	MS
7	2-Methylbutanal	5	19	MS
8	Ethanol	5	5	RT, MS
9	Ethyl propanoate	5,8	10	MS
10	Pentanal	3,5	18	MS
11	2-Pentanone	5	4	MS
12	Isobutyl acetate	5	20	MS
13	3-Methyl-2-pentanone		5	MS
14	Toluene	5	20	MS
15	Ethyl butanoate		18	MS
16	1-Propanol	8	14	MS
17	2-Methyl-3-buten-2-ol		20	MS
18	Butyl acetate	5	20	MS
19	Hexanal	3,5	20	RT, MS
20	2-Methyl-2-butenal		2	MS
21	2,6,6-Trimethyl-2-vinyltetrahydro-2*H*-pyran		20	MS
22	2-Methyl-1-propanol	8	18	RT, MS
23	2,4-(8-*p*-Menthadiene)	3	10	MS
24	3-Methylbutyl acetate	5	10	MS
25	α-Phellandrene		4	MS
26	β-Myrcene	1,3,4	20	RT, MS
27	α-Terpinene		20	RT, MS
28	Isobutyl butanoate		1	MS
29	Limonene	1,3,4	20	RT, MS
30	Amyl acetate	5	6	RT, MS
31	1-Butanol	5,8	20	RT, MS
32	Heptanal	5	17	RT, MS
33	1-Penten-3-ol		13	RT, MS
34	2-Heptanone	5	12	MS
35	Eucalyptol	5	18	RT, MS
36	2-Pentylfuran		12	MS
37	(*E*)-Ocimene		7	MS
38	(*E*)-2-Hexenal	3	5	RT, MS
39	γ-Terpinene	3,4	11	RT, MS
40	2-Methyl-1-butanol		15	MS
41	3-Methyl-1-butanol	8	11	RT, MS
42	Ethyl hexanoate	5,8	1	MS
43	*p*-Cymene	3,4	20	MS
44	3-Octanone		5	MS
45	3,7,7-Trimethylbicyclohept-2-ene		20	MS
46	1-Pentanol	3,5,8	19	RT, MS
47	Hexyl acetate	5,8	20	MS
48	Octanal	5	14	MS
49	Acetyl methyl carbinol acetoin		16	MS
50	2,6,6-Trimethylcyclohexanone		20	MS
51	(*Z*)-4-Hexenyl acetate		17	MS
52	(*Z*)-2-Heptenal		17	MS
53	2,3-Octanedione		20	MS

TABLE I *(continued)*

No.	Aroma compound	Ref.	Occurrence	Method of identification[a]
54	(*E*)-2-Hexenyl acetate		17	MS
55	6-Methyl-5-hepten-2-one	3,5	20	RT, MS
56	1-Hexanol	3,4,5,8	20	RT, MS
57	(*E*)-3-Hexen-1-ol		6	RT, MS
58	Nonanal	5	18	RT, MS
59	3,5,5-Trimethyl-2-cyclohexen-1-one		10	MS
60	(*Z*)-3-Hexen-1-ol	3,5	20	RT, MS
61	Buthyl hexanoate		5	MS
62	(*Z*)-2-Hexen-1-ol		18	MS
63	(*E*)-2-Decenal		3	MS
64	Epoxydihydrolinalol I	1,2,3,4	19	MS
65	1-Hepten-3-ol		11	MS
66	Furfural	8	20	MS
67	6-Methyl-5-hepten-2-ol		2	MS
68	Epoxydihydrolinalol II	1,2,3,4	20	MS
69	(*E,E*)-2,4-Heptadienal	5	2	MS
70	Decanal	5	6	MS
71	Benzaldehyde	3,4,5	20	MS
72	3-Nonen-2-one	4	1	MS
73	Linalol	1,2,3,4,5,8	20	RT, MS
74	1-Octanol	8	18	RT, MS
75	Terpinen-4-ol	3,4,5	6	RT, MS
76	2,6,6-Trimethyltetrahydrobenzaldehyde		20	MS
77	Butanoic acid		3	MS
78	2,6,6-Trimethyldihydrobenzaldehyde		20	MS
79	α-Terpineol	1,2,3,4,5	20	RT, MS
80	Ethyl benzoate	5,8	2	MS
81	1,1,6-Trimethyl-1,2-dihydronaphthalene		20	MS
82	1,5,8-Trimethyl-1,2-dihydronaphthalene		1	MS
83	α-Farnesene		14	MS
84	Geranial	1,3	7	MS
85	1-Decanol	8	3	MS
86	Nerol	3,4	20	MS
87	Damascenone	4	8	RT, MS
88	Hexanoic acid	2	4	MS
89	Geraniol	3,4,8	20	RT, MS
90	Geranyl acetone		19	RT, MS
91	2-Phenylethanol	4,5,8	3	RT, MS
92	γ-Octalactone	1,2,3,4,5	3	RT, MS
93	β-Ionone	4,5	20	RT, MS
94	1-Dodecanol		7	MS
95	2,4,4-Trimethyl-3-(2-butenyl-2-cyclohexen-1-one)		9	MS
96	Phenol		19	MS
97	Isopropyl myristate		20	MS
98	Nerolidol I		5	MS
99	γ-Decalactone	1,2,3,4,5	20	RT, MS
100	Isopropyl palmitate		6	MS
101	Nerolidol II		2	MS
102	γ-Dodecalactone	2,4	6	RT, MS
103	Myristic acid		7	MS
104	Palmitic acid		8	MS
105	Farnesol	3,4	3	RT, MS

[a] MS = Identified by means of mass spectrometry. RT = identified by comparison with retention time of authentic reference compounds.

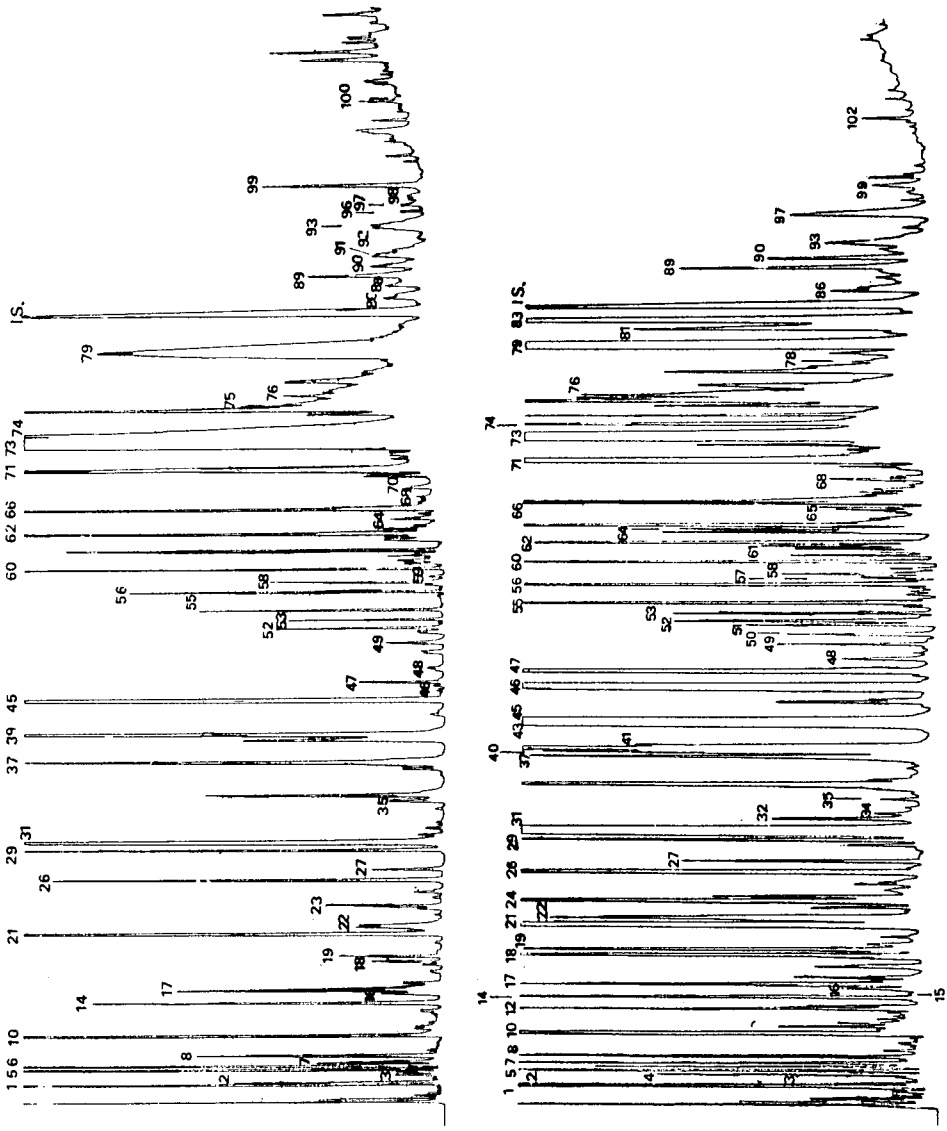

Fig. 1. Gas chromatograms of volatile compounds of two apricot purée samples obtained by means of flame ionization detection. For peak numbers, see Table I.

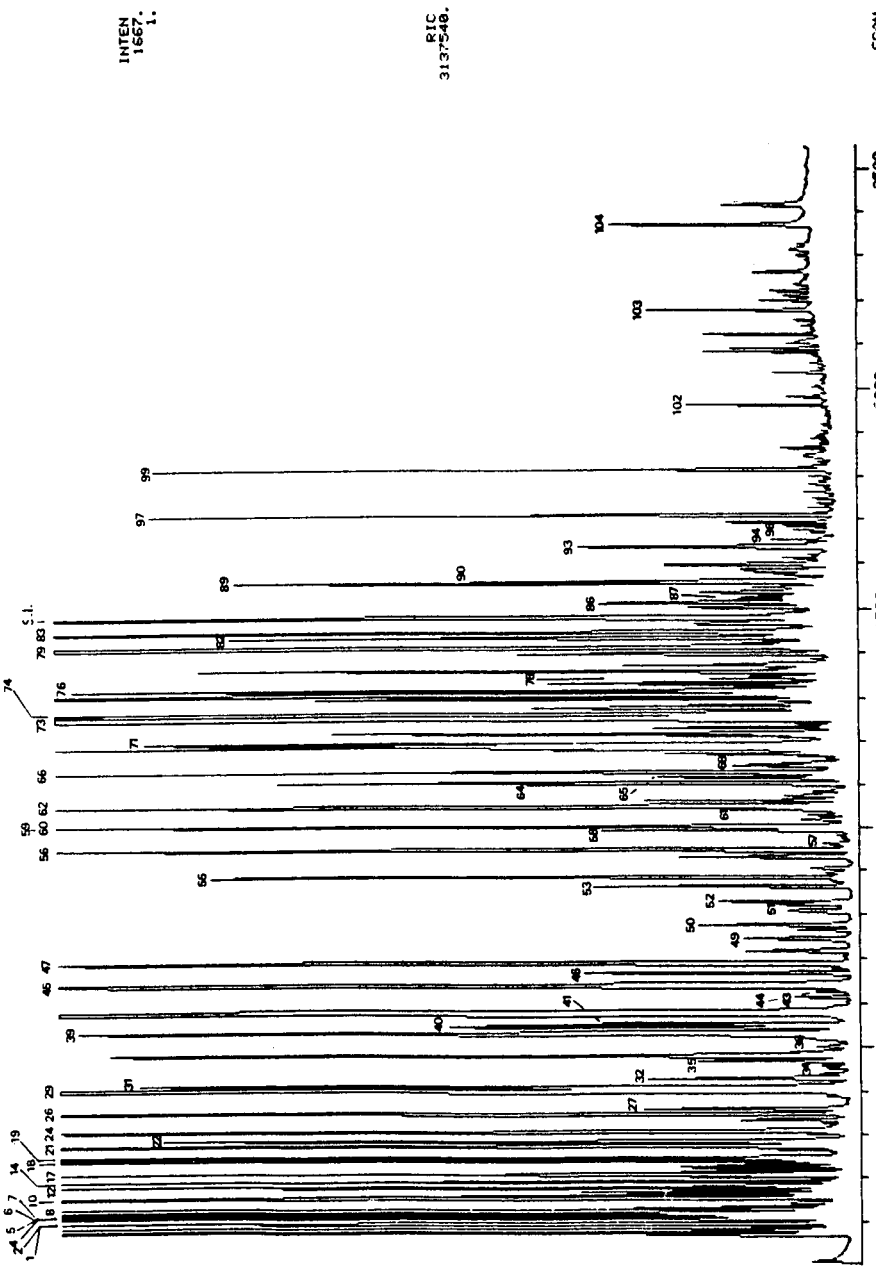

Fig. 2. Gas chromatogram of volatile compounds of a purée sample obtained by means of GC–MS; the signal was obtained by monitoring the total ion current in the range 35–350 u. For peak numbers, see Table I.

Moreover, the mass spectra indicate the presence of a series of compounds which are positional isomers of *x,y,z*-trimethyl-1,2,3,4-tetrahydronaphthalene (TTN), having a structure related to that of α- or β-ionone. These compounds have similar mass spectra, with the parent peak at *m/z* 159 and the molecular peak M^+ = 174, relative abundance 30–40%; Fig. 3 shows the mass spectrum of a trimethyltetrahydronaphthalene. Some of these substances have been found in some varieties of ruhm [11,12] and could be derived from the thermal degradation of β-carotene [13,14].

The two unsaturated ketones, 6-methyl-5-hepten-2-one and 6,10-dimethyl-5,9-undecadien-2-one, known as geranylacetone, may be derived from the oxidation of carotenoids, both having licopene as aroma precursor [10]. Other identified degradation products of carotenoids are β-ionone and damascenone; these compounds have already been found in several products such as tea [15], tobacco [16] and grape [17]. Damascenone, together with linalol oxides, is considered to be responsible for the overcooked note of the aroma and can form in the industrial manufacture of apricot purées [4].

A series of substances were extracted and separated, but it was not possible to give them a definite attribution; however, because of the presence in the mass spectra of fragments at *m/z* 136, 121, 93 and 68, a monoterpenic structure can be attributed to these substances.

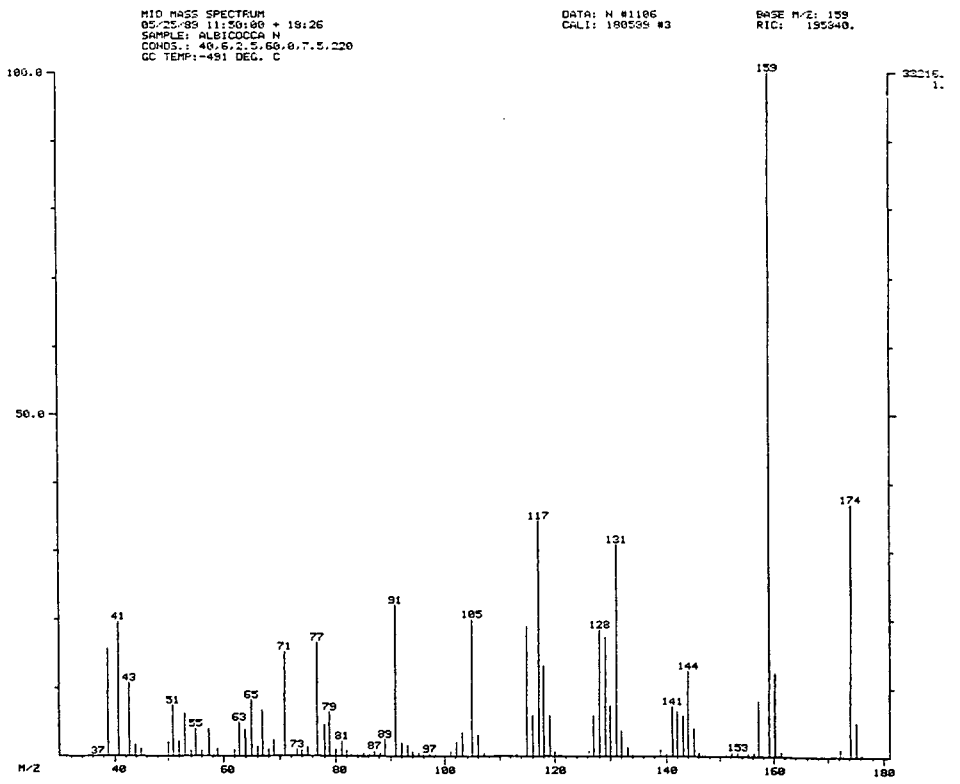

Fig. 3. Mass spectrum of a trimethyltetrahydronaphthalene.

As shown by the list of compounds in Table I, with purge and trap sampling it was possible to extract both very volatile compounds such as methyl and ethyl acetate and poorly volatile compounds such as the lactones; these compounds determine the fruity note of the apricot aroma [5], but cannot be detected with static and dynamic headspace techniques [18,19]. Moreover, the use of cryoconcentration permits fast injection of the sample into the column and contributes to the high efficiency of the chromatographic separation.

REFERENCES

1 C. S. Tang and W. G. Jennings, *J. Agric. Food Chem.*, 15 (1967) 24.
2 C. S. Tang and W. G. Jennings, *J. Agric. Food Chem.*, 16 (1968) 252.
3 F. Rodriguez, S. Seck and J. Crouzet, *Lebensm. Wiss. Technol.*, 13 (1980) 152.
4 G. Chairote F. Rodriguez and J. Crouzet, *J. Food Sci.*, 46 (1981) 1898.
5 E. Guichard and M. Souty, *Z. Lebensm.-Unters.-Forsch.*, 186 (1988) 301.
6 E. Guichard, *J. Food Sci.*, 53 (1988) 1902.
7 P. Schlich and E. Guichard, *J. Agric. Food Chem.*, 37 (1989) 142.
8 F. Yung, *Konservn. Ovoshchesush. Promst.*, 2 (1976) 34.
9 P. J. Williams, C. R. Strauss and B. Wilson, *J. Agric. Food Chem.*, 28 (1980) 766.
10 D. H. Belitz and W. Grosch, *Food Chemistry*, Springer, Berlin, 1987, pp. 196, 197 and 259.
11 P. De Smedt and P. Liddle, *Ann. Technol. Agric.*, 24 (1975) 269.
12 P. De Smedt, P. Liddle and G. Gavazza, *Ann. Falsif. Expect. Chim.*, 73 (1980) 385.
13 J. D. Malik and J. G. Erdman, *Science*, 141 (1963) 806.
14 W. C. Day and J. G. Erdman, *Science*, 141 (1963) 808.
15 J. Bricout, R. Viani, J. P. Marion, F. Muggler-Chavan, D. Reymond and R. H. Egli, *Helv. Chim. Acta*, 50 (1967) 1517.
16 T. Fujimori, R. Kasuga, H. Matsushita, H. Kneko and M. Noguchi, *Agric. Biol. Chem.*, 40 (1976) 303.
17 P. Schreier, F. Drawert and A. Junker, *J. Agric. Food Chem.*, 24 (1976) 331.
18 R. Teranishi, R. A. Flath and H. Sugisawa, *Flavor Research–Recent Advances*, Marcel Dekker, New York, 1981, pp. 205 and 208.
19 W. G. Jennings and M. Filsoof, *J. Agric. Food. Chem.*, 25 (1977) 440.

Journal of Chromatography, 518 (1990) 230–233
Elsevier Science Publishers B.V., Amsterdam

CHROM. 22 570

Note

Essential oil from *Thymus borgiae*, a new Iberian species of the *Hyphodromi* section

M. AMPARO BLAZQUEZ, ANA BONO and M. CARMEN ZAFRA-POLO*
Departament de Farmacologia i Farmacotècnia (Farmacognosia y Farmacodinamia), Facultat de Farmacia, Avda. Blasco Ibáñez 13, 46010 Valencia (Spain)
(First received March 12th, 1990; revised manuscript received May 16th, 1990)

The genus *Thymus* includes a wide range of species, many of which are used in folk medicine for their antimicrobial, antitussive and spasmolytic properties [1]. The taxonomic classification of this genus, however, is very complex and continuous efforts have been made to distribute its species correctly among the eight sections into which it is divided. From a taxonomic point of view, studies on the essential oils and flavonoids of the *Thymus* species can be useful as an aid in defining the species, in detecting hybridization in natural populations, in confirming the presence of geographical races and in confirming section limits.

Along these lines, and as a continuation of our studies on species from the *Hyphodromi* section [2,3], we report the qualitative and quantitative composition of the essential oil of *Thymus borgiae*, a new plant species recently described as an endemic population of thyme growing in Spain and included in the *Hyphodromi* section [4].

EXPERIMENTAL

Plant material

Aerial parts of *Thymus borgiae* growing in Guadalaviar (Teruel, Spain) were collected in July 1989 at the flowering stage. Voucher specimens were authenticated by Prof. B. Peris of the Department of Botany, Faculty of Pharmacy. The fresh plant material was submitted to hydrodistillation (3 x 100 g) in a modified Clevenger apparatus for 2.5 h, yielding 0.41 ± 0.03% (v/w) of a yellowish essential oil. The physical constants of the oil were $n_D^{20} = 1.569$, $[\alpha]_D^{20} = -2.78$ and $d_{20}^{20} = 0.936$.

Column chromatography (CC)

The oil (1 ml) was fractionated on a silica gel column using hexane in order to obtain the hydrocarbon fraction. The oxygenated compounds were then eluted with hexane–dichloromethane mixtures and dichloromethane. A total of ten fractions were obtained.

0021-9673/90/$03.50

Gas chromatography (GC)

GC was performed with a Konic 2000-C gas chromatograph equipped with a 25 m x 0.25 mm I.D. SE-52 (5% phenylmethylsilicone) high-performance capillary column. The column temperature was 60°C for 6 min, then increased at 5°C min to 150°C which was maintained for 10 min. The carrier gas was nitrogen at a flow-rate of 2 ml/min. The injector temperature was 225°C and the detector (flame ionization) temperature was 250°C. Splitless injection was used.

The whole oil and fractions obtained from column chromatography were analysed. The percentage of each component was determined by the peak area measured with a Spectra Physics 4290 electronic integrator.

Gas chromatography–mass spectrometry (GC–MS)

GC–MS analysis was carried out with a Hewlett-Packard 5995 B gas chromatograph–mass spectrometer with a membrane separator coupled to a Hewlett-Packard 9825 B data system. The chromatographic separations were done by a 12 m x 0.25 mm I.D. OV-1 (methylsilicone) high-performance capillary column. The same working conditions as used for GC were employed except that the carrier gas was helium at a flow-rate of 2 ml/min (splitless technique). Mass spectra were taken over the range m/z 28–400 with an ionizing voltage of 70 eV.

Identification of components

The individual compounds were identified by comparing their mass spectra with those of authentic samples or with data already available in the literature [5–7]. A number of components were also identified by GC with co-injection of authentic samples with the essential oil.

^1H NMR analysis

The 60 MHz ^1H NMR spectrum was recorded on a Hitachi Perkin-Elmer Model R-24 B instrument in $CDCl_3$ with tetramethylsilane as internal standard.

IR analysis

Spectra were recorded in carbon tetrachloride solution with a Perkin-Elmer Model 843 infrared spectrophotometer.

RESULTS AND DISCUSSION

The qualitative and quantitative composition of the essential oil from *Thymus borgiae* Rivas-Martinez, Molina & Navarro was determined by CC, GC and GC–MS (see Table I). The gas chromatogram shows the presence of 46 components, one of which represents about 60% of the total oil. GC and GC–MS analysis of the two fractions eluted from CC with hexane yielded the hydrocarbon fraction in which fourteen monoterpenes and twelve sesquiterpenes, which constitute 18.8% of the essential oil, were identified. Longifolene (0.5%), a sesquiterpene hydrocarbon, identified by comparison of its retention time and mass spectral data with those of pure standard, is reported here for the first time as a component of the essential oils from thyme.

Fractions 3–10 eluted with hexane–dichloromethane mixtures yielded the ox-

TABLE I

COMPONENTS IDENTIFIED IN THE ESSENTIAL OIL OF *THYMUS BORGIAE*

Peak	Compound	Retention time on SE-52 (min)	Peak area (%)[a]	Identified by
1	α-Thujene	3.56	0.2	GC; GC–MS
2	α-Pinene	3.61	0.2	GC; GC–MS
3	Camphene	3.73	1.6	GC; GC–MS
4	Δ^3-Carene	3.97	0.1	GC–MS
5	Sabinene	4.09	0.1	GC–MS
6	β-Pinene	4.41	0.2	GC; GC–MS
7	Myrcene	4.69	1.1	GC; GC–MS
8	α-Phellandrene	4.79	0.4	GC–MS
9	α-Terpinene	4.90	0.6	GC; GC–MS
10	*p*-Cymene	5.42	0.1	GC; GC–MS
11	Limonene	5.53	0.4	GC; GC–MS
12	1,8-Cineol	5.94	1.7	GC; GC–MS
13	*cis*-β-Ocimene	6.40	0.1	GC–MS
14	γ-Terpinene	7.20	0.2	GC; GC–MS
15	Terpinolene	7.87	1.2	GC; GC–MS
16	Linalol	9.32	1.0	GC; GC–MS
17	Camphor	10.32	3.9	GC; GC–MS
18	Pulegone	10.56	t	GC–MS
19	Borneol	10.76	1.1	GC; GC–MS
20	Terpinen-4-ol	11.33	0.1	GC; GC–MS
21	α-Terpineol	11.79	0.1	GC; GC–MS
22	Bornyl acetate	12.22	0.2	GC; GC–MS
23	Thymol	15.26	0.5	GC; GC–MS
24	Carvacrol	15.93	59.7	GC; GC–MS IR; ^{1}H NMR
25	α-Copaene	17.63	0.3	GC; GC–MS
26	β-Bourbonene	17.97	t	GC–MS
27	Longifolene	18.18	0.5	GC; GC–MS
28	Caryophyllene	18.68	3.9	GC; GC–MS
29	Unidentified	19.23	0.3	—
30	*allo*-Aromadendrene	19.60	0.1	GC; GC–MS
31	α-Humulene	19.79	0.2	GC; GC–MS
32	α-Cubebene	20.37	0.2	GC–MS
33	Sesquiterpene alcohol	20.45	2.7	GC–MS
34	Unidentified	20.58	0.1	—
35	Germacrene B	20.86	2.6	GC; GC–MS
36	Germacrene D	20.91	3.8	GC; GC–MS
37	Calamenene	21.13	0.1	GC; GC–MS
38	Unidentified	21.63	0.3	—
39	δ-Cadinene	21.75	0.5	GC; GC–MS
40	Calacorene	22.07	t	GC; GC–MS
41	Caryophyllene epoxide	23.03	2.0	GC–MS
42	Aromadendrene epoxide	23.10	1.2	GC–MS
43	Sesquiterpene alcohol	23.21	0.3	GC–MS
44	Sesquiterpene alcohol	23.45	0.9	GC–MS
45	Eudesmol	23.61	0.2	GC–MS
46	Cadinol	24.98	0.4	GC; GC–MS

[a] t = Traces (<0.1%).

ygenated fraction, with carvacrol as the main constituent (59.7%). The isolation of this compound was possible by preparative thin-layer chromatography on silica gel from fraction 8 [solvent, toluene–ethyl acetate (93:7); $R_F = 0.55$ with a red reaction to vanillin–sulphuric acid reagent]. Its IR, ^{1}H NMR and mass spectral data were similar to those obtained for an authentic sample.

In conclusion, the essential oil of *Thymus borgiae* can be considered, for other species of this genus, to be a typical phenolic essential oil. Another phenolic compound (thymol, 0.5%) and its phenolic precursors *p*-cymene (0.1%) and γ-terpinene (0.2%) are also present in this essential oil.

Although traditionally the *Thymus* essences belonging to the *Hyphodromi* section are not considered as phenolic essential oils, when these species grow at altitudes of 1600–1700 m, such as occurs with *Th. borgiae*, a strong increase in carvacrol is observed. Thus, the essential oils from *Th. bracteatus* and *Th. godayanus*, two species with great botanical affinities with one another and with *Th. borgiae*, have percentages of carvacrol ranging from 16.9% [8] to 17.3% [3], respectively. However, when these plants are collected at lower altitudes, this oxygenated monoterpene only appears in trace amounts in *Th. bracteatus* and 4.4% in *Th. godayanus*. This can explain the high percentage of carvacrol found in the essential oil of *Th. borgiae* and its inclusion in the *Hyphodromi* section. Studies on the flavonic content of this taxon are in progress to establish a definitive taxonomic confirmation.

REFERENCES

1 C. O. Van den Broucke, *Fitoterapia*, 54 (1983) 171.
2 M. A. Blázquez, M. C. Zafra-Polo and A. Villar, *Planta Med.*, 55 (1989) 198.
3 M. A. Blázquez and M. C. Zafra-Polo, *Pharmazie*, 44 (1989) 651.
4 S. Rivas-Martinez, A. Molina and G. Navarro, *Opusc. Bot. Pharm. Complutensis*, 4 (1988) 107.
5 A. Cornu and R. Massot, *Compilation of Mass Spectral Data*, Heyden, London, 1975.
6 H. C. Noever de Brauw, J. Bouwman, A. C. Tas and G. La Vos, *Compilation of Mass Spectra of Volatile Compounds in Food*, TNO Zeist, Utrecht, 1979.
7 E. Stenhagen, S. Abrahamsson and F. W. McLafferty, *Registry of Mass Spectral Data*, Wiley, New York, 1974.
8 R. Morales, *Taxonomía de los Géneros Thymus (Excluida la Sección Serpyllum) y Thymbra en la Península Ibérica, Ruizia*, Vol. III, Serv. Public. del C.S.I.C., Madrid, 1986.

Journal of Chromatography, 518 (1990) 234–237
Elsevier Science Publishers B.V., Amsterdam

CHROM. 22 599

Note

Sorption of primary *n*-alkanols on Tenax

JIŘÍ VEJROSTA*, MILENA MIKEŠOVÁ and PAVEL FILIP
Institute of Analytical Chemistry, Czechoslovak Academy of Sciences, Kounicova 82, 611 42 Brno (Czechoslovakia)

(First received January 10th, 1990; revised manuscript received May 28th, 1990)

In a previous paper [1], an empirically modified Langmuir isotherm equation [2]:

$$\log V_g = a + b/T + c \log (1 + ec_s) + (d/T) \log (1 + ec_s) \quad (1)$$

where V_g (ml/g) is the solute specific retention volume, c_s (mol/g) is the solute sorbent-phase concentration, T is the absolute temperature and a, b, c, d and e are adjustable parameters, was successfully used for the description of *n*-alkane sorption in an *n*-alkane–nitrogen–Tenax system. The assumption of a linear dependence of the thermodynamic functions of sorption on the number of methylene groups in the solute molecule [3] leads to

$$\log V_g = c_1 + c_2 n + c_3/T + c_4 n/T + (c_5 + c_6 n)Y + (c_7 + c_8 n)Y/T \quad (2)$$

where n is the number of methylene groups in the *n*-alkane chain, which describes the sorption properties of the whole homologous series. The function Y reflects the extent of the deviation from linearity of the sorption isotherm:

$$Y = \log[1 + (c_9 + c_{10} n)c_s] \quad (3)$$

An average relative deviation of 8.5% was found between the calculated and the experimental values of the specific retention volume (C_5–C_8 *n*-alkanes in the temperature range 19.9–50.3°C and at gas-phase concentrations of $6 \cdot 10^{-12}$–$7.5 \cdot 10^{-7}$ mol/ml) with use of eqn. 2. This was partly due to the systematic deviations at low gas-phase concentration [1]. When the individual sorption isotherm are correlated by eqn. 1, the values of the average relative deviations decrease to 3–4%.

The aim of this work was to demonstrate the correlation capabilities of eqns. 1 and 2 for the description of the sorption isotherms of the homologous series of primary *n*-alkanols in mixture with nitrogen on Tenax.

EXPERIMENTAL

The preparation of standard gaseous mixtures, the measurements and the

0021-9673/90/$03.50

calculation of the partition coefficients were described previously [4,5]. The purity of the *n*-alkanols (C_2–C_5) (Fluka, Buchs, Switzerland) was better than 99.5% and they were used without further purification. *n*-Alkanol partition coefficients (208 values) were measured at temperatures in the range 13.5–41.7°C and at gas-phase concentrations of $2.1 \cdot 10^{-12}$–$2.7 \cdot 10^{-7}$ mol/ml.

RESULTS AND DISCUSSION

First, eqn. 1 was used to correlate the sets of sorption isotherms of the individual primary *n*-alkanols. The results of the optimization are summarized in Table I.

The values of the average deviations increase with increasing carbon number and the average value of 4.65% corresponds with the estimated experimental error of 4–5%. The increased values in comparison with those for non-polar compounds (benzene, *n*-alkanes) are obviously connected with the experimental method used. As already found with acetone [6], the experimental reproducibility of the data is worse for polar than for non-polar compounds.

The linear dependence of the parameters of eqn. 1 on the number of methylene groups is the basic condition for successful application of the additivity principle[3]. Table I shows a very good linear dependence of the parameters *a*, *b* and *d* on the methylene number and the lack of a dependence for *c* and *e*. In spite of this, the whole homologous series of *n*-alkanols was correlated by eqn. 2 and the resulting parameters are given in Table II. An average relative deviation of 18.3% was found, double that for *n*-alkanes, as expected. The results are illustrated graphically in Fig. 1 for *n*-propanol. Marquardt's algorithm was used for the calculation of non-linear parameters [7].

CONCLUSION

The modified Langmuir isotherm equation (eqn. 1) was successfully applied for the description of sorption isotherms of primary *n*-alkanols. The description of the whole homologous series of *n*-alkanols by eqn. 2, which follows from the application of the additivity principle, results in an average relative deviation of *ca.* 18%. This is still

TABLE I

SUMMARY OF OPTIMIZED PARAMETERS OF EQN. 1 FOR PRIMARY *n*-ALKANOLS

n is the number of methylene groups between two carbon atoms in the molecule of primary *n*-alkanols $CH_3(CH_2)_nCH_2OH$; *a*, *b*, *c*, *d* and *e* are the parameters in eqn. 1; $\Delta_i(\%) = 100V_{g,calc} - V_{g,exp}/V_{g,exp}$; the average relative error is defined as $\bar{\Delta}_i\ (\%) = \sum_i \Delta_i/i$, where *i* is the number of experimental points.

n	a	b	c	d	e	i	$\bar{\Delta}_i$ (%)
0	−6.5859	2850.1	2.1225	− 799.90	24986.6	56	2.69
1	−7.0647	3249.89	1.8636	−1000.02	20012.7	50	3.28
2	−7.4331	3600.13	1.9747	−1199.95	20965.5	47	5.17
3	−8.0081	3945.26	1.6426	−1397.40	20020.0	55	7.44

TABLE II

SUMMARY OF OPTIMIZED PARAMETERS OF EQNS. 2 AND 3

Parameter	Value	Parameter	Value
c_1	−6.3427	c_6	−0.2069
c_2	−0.5703	c_7	−798.95
c_3	2795.27	c_8	−187.18
c_4	395.33	c_9	23501.06
c_5	2.1276	c_{10}	−1390.41

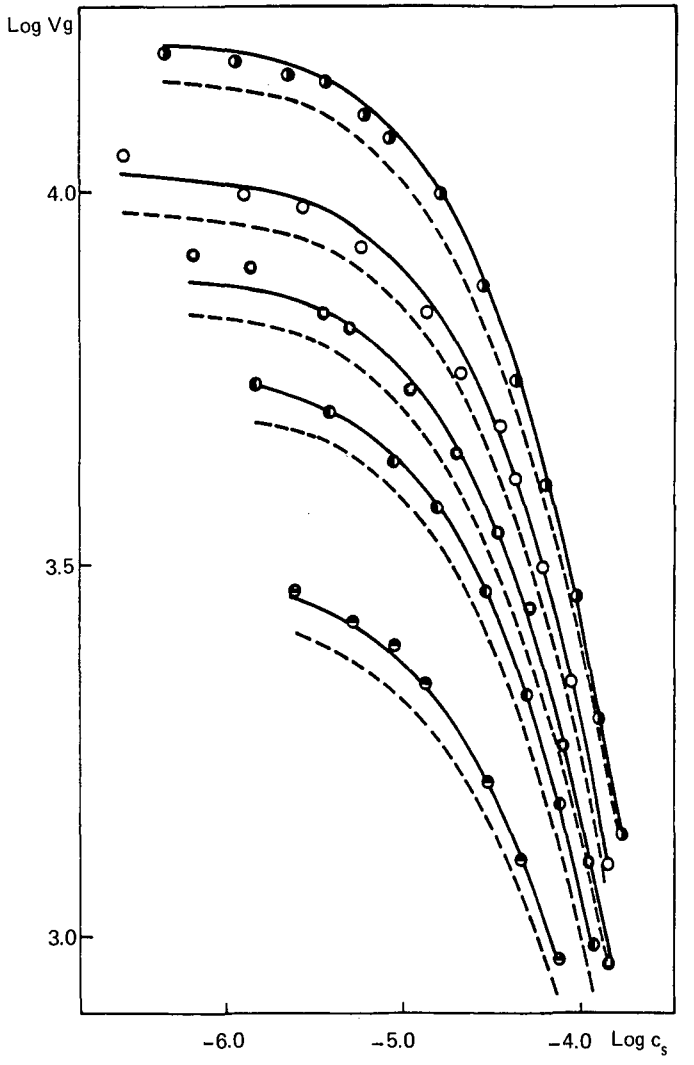

Fig. 1. Relationship between log V_g and log c_s *for n*-propanol on Tenax calculated with eqn. 1 (solid lines) and with eqns. 2 and 3 (dashed lines), and experimental points (◑ = 15.2; ○ = 19.9; ● = 23.5; ◐ = 27.1; ◓ = 35.0°C).

acceptable for the calculation of retention characteristics for trace analysis utilizing preconcentration on Tenax.

REFERENCES

1 J. Vejrosta, M. Mikešová and J. Drozd, *J. Chromatogr.*, 464 (1989) 394.
2 J. Vejrosta, M. Mikešová, A. Ansorgová and J. Drozd, *J. Chromatogr.*, 447 (1988) 170.
3 J. Novák, J. Vejrosta, M. Roth and J. Janák, *J. Chromatogr.*, 199 (1980) 209.
4 J. Vejrosta, M. Roth and J. Novák, *J. Chromatogr.*, 217 (1981) 167.
5 J. Vejrosta and J. Novák, *J. Chromatogr.*, 175 (1979) 261.
6 J. Vejrosta, M. Roth and J. Novák, *J. Chromatogr.*, 219 (1981) 37.
7 D. W. Marquardt, *J. Soc. Ind. Appl. Math.*, 11 (1963) 431.

Journal of Chromatography, 518 (1990) 238–241
Elsevier Science Publishers B.V., Amsterdam

CHROM. 22 600

Note

High-performance vacancy gel permeation chromatography

MEILING YE*, YOUKANG DING, JIANWEN MAO and LIANGHE SHI
Institute of Chemistry, Academia Sinica, Beijing (China)
(Received March 27th, 1990)

Gel permeation chromatography (GPC) is widely used for characterizing the molecular weight distribution of polymers [1]. When a polymer solution is injected into a GPC column with a solvent as the mobile phase, a regular GPC curve is obtained. If a polymer solution is used as the mobile phase and the pure solvent is injected as a sample, the chromatogram obtained will be a mirror image of the regular GPC curve of the polymer sample. This is called vacancy chromatography. Otocka and Hellman [2] reported vacancy chromatography with a conventional GPC column. Their results indicated a difference (Δv) in elution volumes between the regular GPC mode and the vacancy mode, and Δv increases with increase in molecular weight and flow-rate. As a result, the calibration graphs obtained for regular GPC and vacancy chromatography were not identical. It has been suggested that this discrepancy could be minimized by using a high-performance GPC column. In this paper, vacancy chromatography was studied in high performance GPC and the concentration dependences in the regular GPC mode and the vacancy mode were examined.

EXPERIMENTAL

The instrument employed was a Waters Assoc. Model ALC/GPC 244 chromatograph with UV and refractive index detectors. A single μBondagel column was used at a flow-rate of 1 ml/min. The polystyrene (PS) samples used were Waters Assoc. narrow-distribution standards and laboratory-made anionic polymerized PS samples (molecular weight 6000–1 800 000). Tetrahydrofuran (THF) was used as a solvent.

RESULTS AND DISCUSSION

A calibration graph was obtained using the regular GPC mode, the above PS samples at a concentration of $0.3 \cdot 10^{-2}$ g/ml being injected into the column. Another calibration graph was obtained using the vacancy technique in which the column was eluted separately with PS solutions of different molecular weight at the same concentration of $0.3 \cdot 10^{-2}$ g/ml while pure THF solvent was injected as a sample into the column.

The results showed that the two calibration graphs are not identical, and the differences increase with increasing molecular weight, as shown in Fig. 1. However, by

0021-9673/90/$03.50

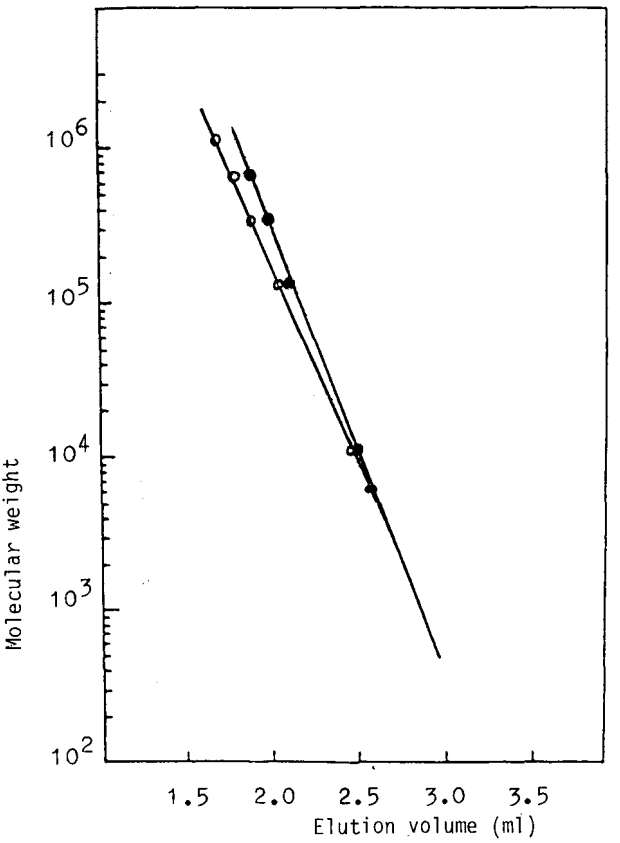

Fig. 1. Comparison of calibration graphs for the regular (○) and vacancy (●) mode on a μBondagel column. PS concentration = $0.3 \cdot 10^{-2}$ g/ml.

lowering the concentration we obtained a vacancy chromatogram that is exactly the mirror image of the regular GPC trace as shown in Fig. 2. The calibration graphs obtained for vacancy and regular GPC for PS–THF at a concentration of $0.03 \cdot 10^{-2}$ g/ml are identical. These results indicate that the discrepancy in the elution volumes between two modes should be attributed to a concentration dependence rather than to the column performance.

Fig. 3 gives an example of the difference in elution volumes for a PS solution at a concentration of 0.6%. The initial slope of the peak elution volume *vs.* concentration plot of PS (mol.wt. $6.9 \cdot 10^5$) in the vacancy mode is much larger than that in the regular mode, as shown in Fig. 4. This is due to a macromolecular crowding effect. When the concentration of the polymer solution is increased, the dimensions of the individual macromolecular chains begin to contract as compared with the size at infinite dilution. In the regular GPC mode there is no polymer in the pores of the column packing, whereas in the vacancy mode the solute polymer is present in the pores of the packing. Hence in the latter instance the macromolecular crowding effect

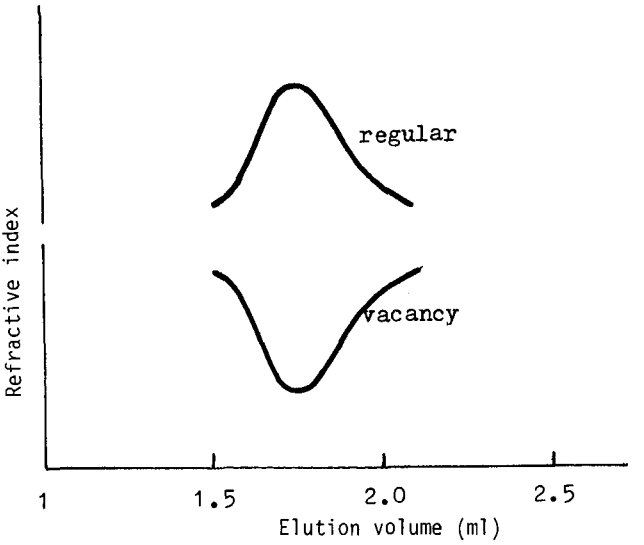

Fig. 2. Comparison of regular chromatogram with 0.03% PS–THF injected in THF and vacancy chromatogram with THF injected in 0.03% PS–THF.

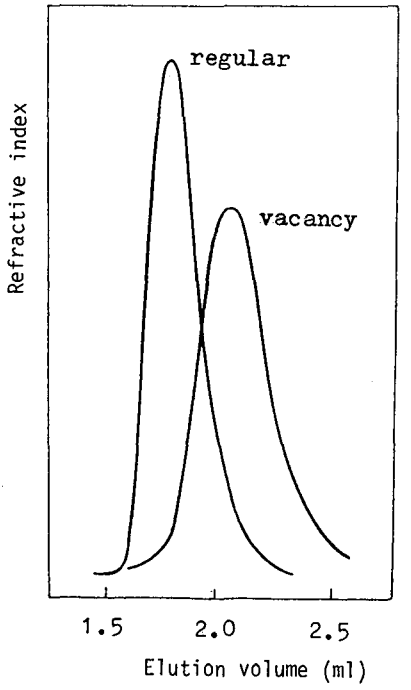

Fig. 3. Comparison of vacancy and regular GPC chromatograms for PS of molecular weight $6.9 \cdot 10^5$. PS concentration = 0.6×10^{-2} g/ml.

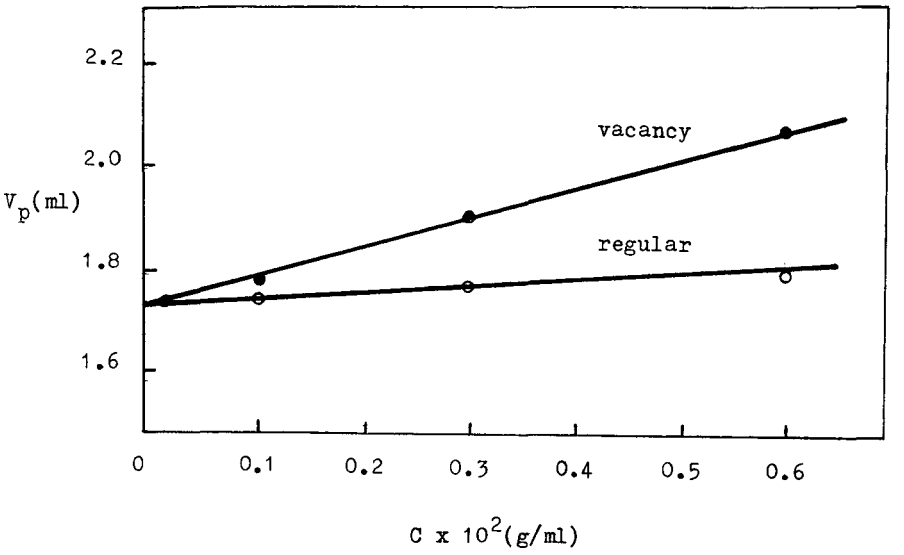

Fig. 4. Comparison of concentration (C) dependences in vacancy and regular GPC for PS of molecular weight $6.9 \cdot 10^5$. V_p = peak elution volume.

would be expected to be more pronounced. This explains the greater concentration dependence in the vacancy mode than in the regular mode.

REFERENCES

1 W. W. Yau, J. J. Kirkland and D. D. Bly, *Modern Size Exclusion Liquid Chromatography*, Wiley, New York, 1979.
2 E. P. Otocka and M. Y. Hellman, *J. Polym. Sci., Polym. Lett. Ed.*, 12 (1974) 439.

Journal of Chromatography, 518 (1990) 242–249
Elsevier Science Publishers B.V., Amsterdam

CHROM. 22 638

Note

Simultaneous determination of trace concentrations of benomyl, carbendazim (MBC) and nine other pesticides in water using an automated on-line pre-concentration high-performance liquid chromatographic method

CHRIS H. MARVIN, IAN D. BRINDLE and RAJ P. SINGH[a]
Department of Chemistry, Brock University, St. Catharines, Ontario L2S 3A1 (Canada)
C. DAVID HALL
Ontario Ministry of the Environment, Rexdale, Ontario M9W 5L1 (Canada)
and
MIKIO CHIBA*
Research Station, Agriculture Canada, Vineland Station, Ontario L0R 2E0 (Canada)
(First received February 27th, 1990; revised manuscript received June 18th, 1990)

Methyl 1-(butylcarbamoyl)-2-benzimidazolecarbamate (benomyl) is used worldwide as a systemic fungicide for disease control in crops. The analysis of benomyl residues in water is made difficult by the varying instability of the compound in different organic solvents [1–3] and its low solubility in water [4]. Benomyl also decomposes in water, but at a rate slower than that in organic solvent [5,6].

High-performance liquid chromatographic (HPLC) methods are most popular for the analysis of benomyl but most employ the determination of the degradation product methyl 2-benzimidazolecarbamate (carbendazim or MBC) after quantitative conversion of the parent compound [7–9]. These techniques are lacking in that the MBC that is produced from the parent benomyl during the sample preparation procedure cannot be distinguished from MBC that was present in the sample as a natural degradation product of benomyl. This methodology, which is not acceptable in principle, has been widely used in the past, however, for the following two reasons. The main reason is that the determination of intact benomyl residues is exceptionally difficult. Another reason is that MBC is also fungitoxic, and the fungitoxicity of benomyl is, in fact, thought to be due to the presence of MBC [10].

An HPLC method for the simultaneous determination of benomyl and MBC in aqueous media has been described [11]. Benomyl is quantitatively converted by treatment with base to 3-butyl-2,4-dioxo-*s*-triazino[1,2-*a*]benzimidazole (STB), while

[a] Present address: Central Analytical and Materials Characterization Laboratories, and Metrology, Standards and Maerial Division, The Research Institute, King Fahd University of Petroleum and Minerals, Dhahran 31261, Saudi Arabia.

0021-9673/90/$03.50

MBC present in the sample matrix is unaffected and is determined as MBC. This technique is suitable for the analysis of benomyl and MBC at the low ppm level.

In this paper, we present an automated method for the simultaneous determination of benomyl, MBC (carbendazim) and nine other presticides at the ppb[a] level. Benomyl is determined as the intact parent compound and any MBC in the sample can be determined exclusively as the natural degradation product.

For reasons discussed above, it would be advantageous to minimize exposure of the sample to any organic solvent during the sample preparation procedure. On-line pre-concentration (or trace enrichment) offers the possibility of isolating intact analytes directly from an aqueous sample matrix by retaining them on a solid sorbent contained in a short pre-column. A subsequent valve switching allows mobile phase to flush analytes from the pre-column to the HPLC analytical column without further sample manipulation. Marvin *et al.* [12] have described an automated on-line preconcentration method for the determination of pesticide residues in drinking water in conjunction with HPLC and UV detection. With the inclusion of a buffered mobile phase, the technique has been modified to include benomyl, MBC and aminocarb, as well as the eight pesticides included in the original study. These include propoxur, carbofuran, carbaryl, propham, captan, chloropropham, barban and butylate. All of the aforementioned pesticides are of concern in Ontario environmental samples.

MATERIALS AND METHODS

Solvents

Acetonitrile was of HPLC grade from Fisher Scientific (Fairlawn, NJ, U.S.A.), and Caledon Labs. (Georgetown, Canada). Water used for preparation of standards was distilled in glass in the laboratory.

Preparation of buffer solutions

Solutions of Na_2HPO_4 and KH_2PO_4 were prepared individually at 0.067 *M*. The two resulting solutions were mixed at 3:2 (v/v) and the pH adjusted to 6.8. This solution was diluted to 5% in water.

Pesticides

Solid pesticide standards were obtained from the United States Environmental Protection Agency, Research Triangle Park, NC, U.S.A. Purities of the individual standards ranged from 97.5 to 100%. Benomyl was purchased commercially as Benlate wettable powder (Wilson Labs., Laval, Canada, 50% active ingredient). The pesticides, listed in the order in which they appear in the chromatograms, are (1) MBC, (2) aminocarb, (3) propoxur, (4) carbofuran, (5) carbaryl, (6) propham, (7) captan, (8) chloropropham, (9) barban, (10) benomyl and (11) butylate.

Preparation of stock standard solutions

Solid standards (with the exception of benomyl and MBC) were dissolved in acetonitrile and diluted in acetonitrile. MBC was dissolved in methanol and diluted in

[a] Throughout this article, the American billion (10^9) is meant.

methanol while benomyl was prepared as a suspension in distilled water.

As benomyl decomposes at room temperature [13], benomyl standard solutions should be refigerated. Benomyl standard suspensions containing benomyl, at greater concentrations than its solubility in water, must be thoroughly stirred before dilution to ensure an even distribution of particulate matter in any aliquot removed.

The individual stock standard solutions were combined at different concentrations because of their varying sensitivities to UV detection. The combined standard solution thus prepared was diluted with water to make standard water samples as below.

Water samples

Standard water samples were prepared by diluting 1 ml of the combined standard solution (prepared as above) to 1000 ml with distilled water from the laboratory unless otherwise noted.

HPLC apparatus

The HPLC system consisted of a Waters (Milford, MA, U.S.A.) Model 600 Powerline solvent delivery system, a Waters WISP Model 710B sample processor, a Waters Model 484 tunable absorbance UV detector, a Fisher Recordall series 5000 strip-chart recorder, and an NEC (Boxborough, MA, U.S.A.) Powermate 2 computer system incorporating Waters 810 chromatography software.

Pre-columns were 5-μm Spherisorb C_{18} and C_8 3 cm $\times$ 4.6 mm I.D. cartridges from Brownlee Labs. (Santa Clara, CA, U.S.A.). Analytical columns were a Supelcosil LC-8 5-μm 25 cm $\times$ 4.6 mm I.D. (Supelco, Bellefonte, PA, U.S.A.), and a Phenomenex Spherisorb C_{18} 5-μm 15 cm $\times$ 4.6 mm I.D. (Phenomenex, Torrance, CA, U.S.A.).

The on-line pre-concentration apparatus (Fig. 1) in corporated two high-pressure in-line filters with 0.5-μm frits from Mandel Scientific (Guelph, Ontario, Canada), and three Rheodyne Model 7000 2 position 6-port switching valves, one of which was equipped with a Rheodyne Model 5701 air actuator controlled by a Rheodyne Model 7163 solenoid valve kit (Rheodyne, Cotati, CA, U.S.A.).

Unidirectional elution from a C_{18} pre-column onto a C_{18} analytical column was used as a standard procedure.

HPLC operating conditions

Wavelength, 220 nm; flow-rate, 1.5 ml/min; chart speed, 0.5 cm/min; detector sensitivity, 0.075 A.U.F.S. (1 mV = $1 \cdot 10^{-3}$ A.U.); recorder range, 10 mV F.S.; column temperature, ambient.

On-line pre-concentration

A 100-ml volume of water sample was passed through the pre-column while the apparatus was in the "load" position unless otherwise noted.

SAMPLE LOAD

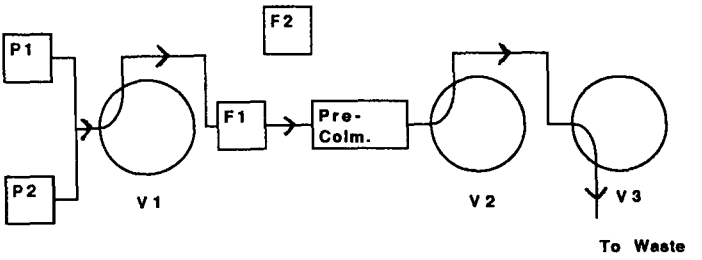

UNIDIRECTIONAL ELUTION

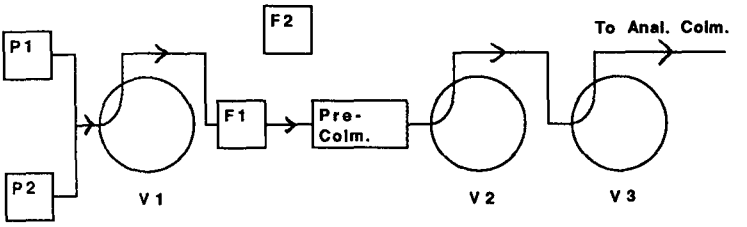

BACKFLUSH ELUTION

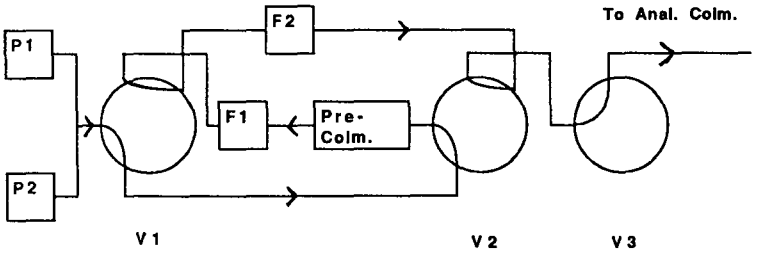

Fig. 1. Schematic of the valve-switching system. V, P, and F denote valves, pumps and filters, respectively. During the sample loading step, P1 dispenses sample. During the elution steps, P1 dispenses water, and P2 acetonitrile as part of the mobile phase. Pre-Colm. = Pre-column; Anal. Colm. = analytical column.

Elution

The following gradient program was run after switching the valves to the "elute" position from the 'load' position:

Elapsed time (min)	*Composition of mobile phase: acetonitrile–buffer–water*
Inital	30:70:0
5	30:70:0
15	60:30:10
25	60:30:10
30	30:50:20
35	30:70:0

Changes in the percentage of organic solvent in the mobile phase throughout the gradient program occurred linearly. The final 10 min of the gradient program serve to return the system to the initial conditions to enable another analysis run.

The inclusion of water in the mobile phase, resulting in a ternary gradient system, was essential in order to maintain a flat baseline profile throughout the gradient program. Decreasing the buffer strength in the aqueous phase during increases in the percentage of acetonitrile, results in an optimum baseline profile. If water was not included in the mobile phase, thereby resulting in a binary gradient system, a marked disturbance in the baseline (a huge bump) was unavoidable. Most analyte peaks appeared on the up and down slopes, as well as at the top of the raised baseline. The baseline disturbance can, however, be negated through the use of gradient correction (baseline subtraction).

RESULTS AND DISCUSSION

Fig. 2 shows a chromatogram resulting from the analysis of a distilled water sample containing the eleven pesticides of concern in the study using unidirectional

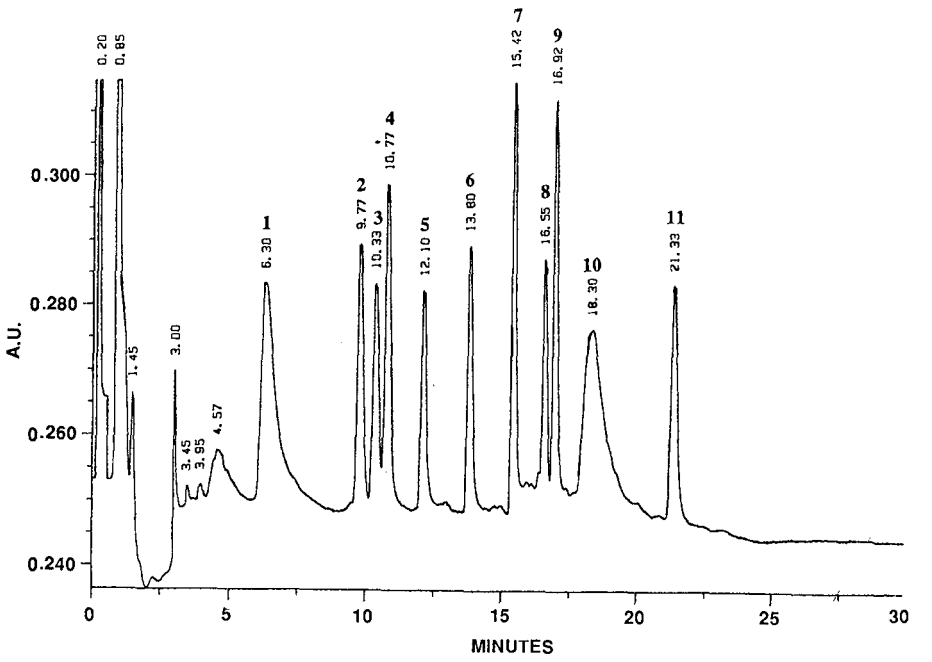

Fig. 2. Chromatogram resulting from the analysis of a 100-ml sample by the described method. The concentrations of the individual pesticides are the same as those listed in Table I.

elution and a C_{18} stationary phase in both the pre-column and the analytical column. Table I lists the pesticides, their retention times, sample concentrations, and minimum detectable concentrations. The minimum detectable concentrations were calculated using a 3:1 signal-to-noise ratio with the exception of benomyl and MBC. The minimum detectable concentrations for benomyl and MBC were calculated using a 6:1 signal-to-noise ratio due to the broadness of the peak profiles. It was essentially impossible to obtain a chromatogram of benomyl without the presence of MBC. Even freshly prepared benomyl analytical standards, prepared in water, were observed to contain a trace amount of MBC.

TABLE I

SELECTED PESTICIDES, THEIR RETENTION TIMES, SAMPLE CONCENTRATIONS AND MINIMUM DETECTABLE CONCENTRATIONS FOR A 100-ml SAMPLE

The pesticides are numbered to coincide with those in the figures.

Compound	Retention time (min)	Sample concentration (μg/l)	Minimum detectable concentration (ng/l)
(1) MBC (carbendazim)	6.30	2.5	100
(2) Aminocarb	9.77	4.0	65
(3) Propoxur	10.33	4.0	65
(4) Carbofuran	10.77	4.5	70
(5) Carbaryl	12.10	0.5	10
(6) Propham	13.80	2.5	50
(7) Captan	15.42	20.0	460
(8) Cl-Propham	16.55	2.0	30
(9) Barban	16.92	3.0	40
(10) Benomyl	18.30	8.0	500
(11) Butylate	21.33	5.0	150

A buffered mobile phase is necessary for the gradient elution program. Otherwise, the peak profile of MBC is unacceptably broad for quantitation. A ternary gradient of acetonitrile, buffer, and water, was found to produce an optimum gradient profile allowing for accurate quantitation of the analytes. A binary gradient of acetonitrile and buffer can be used if the option of gradient correction is available to the analyst. Even with the buffered mobile phase, peak profiles for benomyl and MBC were much broader than the other compounds. These peak profiles were not improved even when other experimental conditions were investigated. Experiments with a more polar pre-column stationary phase (C_8), backflush and unidirectional elution, and a different analytical column stationary phase (C_8), failed to improve peak profiles for MBC and benomyl. The use of a C_8 analytical column improves separation of the three earlier eluting pesticides (aminocarb, propoxur, and carbofuran) but the peak profile for benomyl is poor and co-elutes with butylate. Unidirectional elution from a C_{18} pre-column onto a C_{18} analytical column was found to be the best combination of experimental conditions.

As shown in Fig. 2, peak widths of MBC and benomyl are substantially broader

than those of the other compounds when using unidirectional elution. As concentrations and volumes of water sample (and accordingly, sample loading time) are increased, peak widths increased. In contrast, peak widths of MBC and benomyl are substantially better if streight injections of 100-μl 8.0-ppm benomyl standard suspensions are made directly onto the analytical column without passing through the pre-column. It appears that the band broadening, apparent in the pre-concentration chromatograms, is a results of a large volume of sample loading.

Results obtained with backflush elution were substantially different from those obtained with unidirectional elution. As shown in Fig. 3, four peaks were observed with a sample that contained only MBC and benomyl. It is clear that both the MBC and the benomyl displayed two peaks each. Of the two benomyl peaks, the first peak represents benomyl eluted from particulate matter retained on the inlet side of the pre-column [either on the 0.50-μm filter (F1) or at the head of the pre-column in Fig. 1]. The second peak represents benomyl which is present as solute in water and adsorbed on the pre-column. This presents the possibility of a method for the quantitation of benomyl and MBC both as solute and in the solid state in water samples. It is interesting to note that the peak shape of the first benomyl peak is substantially sharper than the second. Similar results were observed with MBC.

In the above example, benomyl was analysed at 0.136 ppm (Fig. 3). MBC was present in the sample as the degradation product of benomyl. The solubilities of MBC and benomyl are reported to be approximately 3 ppm in water [4]; thus the concentrations of benomyl and MBC were well within the solubilities of the analytes in water.

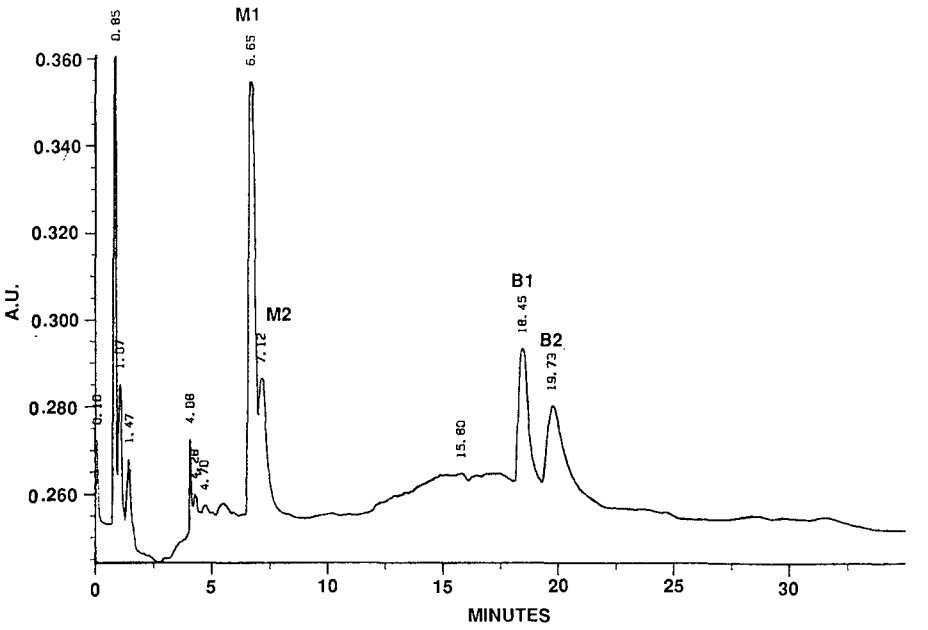

Fig. 3. Chromatogram resulting from the analysis of a 10-ml 0.136-ppm benomyl suspension. Peaks (M1, B1) correspond to MBC and benomyl eluted from particulate matter. Peaks (M2, B2) correspond to MBC and benomyl present as solutes. The sample was analysed by the described method, except that backflush elution was used.

The sample analysis still yielded four peaks, indicating that the analytes were present in the particulate phase, as well as being present as solutes. This may be because the sample was prepared by a 100:1 dilution of a 13.6-ppm stock solution of benomyl and analysed immediately. It appears, therefore, that a period of time is needed for the benomyl to fully dissolve in the water matrix. Further evidence to support this was the observation of a substantial decrease in the area of the first peak, and an increase in the area of the second peak, when the same sample was analysed 45 min later. The sum of the areas of the first and second benomyl peaks were equal for both sample runs. Unidirectional elution yielded a large single peak with a peak area equal to that of the sum of the two peaks obtained from backflush elution.

These findings reveal that consideration must be given to the basic handling procedures of water samples regarding the need for filtration. Depending on the pore size of the filters, regardless of whether they are used on-line or not, analytical results may be substantially different. This is important when analysing samples for compounds which have very low solubilities in water. Benomyl is one of the compounds which merits this consideration, as it is used at the 250–1000-ppm range in agriculture.

The peak profiles of MBC and benomyl can be much improved by elution with a higher percentage of organic solvent in the mobile phase but this results in poor resolution of the other analytes. If benomyl and MBC are the only compounds to be analysed, both compounds can be eluted as sharp peaks by using a gradient program in which the mobile phase contains a higher initial percentage of acetonitrile. Accordingly, the minimum detectable concentrations can be lowered substantially.

CONCLUSION

The method presented in this paper is accurate, sensitive and reproducible. Benomyl in its intact form and MBC, the degradation compound, can be quantitated simultaneously at the low ppb level. Both MBC and benomyl which are present as particulate matter in water can also be quantitated separately if desired.

ACKNOWLEDGEMENTS

The authors would like to thank the Research and Technology Branch of the Ontario Ministry of the Environment for financial support.

REFERENCES

1 M. Chiba, *J. Agric. Food Chem.*, 25 (1977) 368.
2 M. Chiba and E. C. Cherniak, *J. Agric. Food Chem.*, 26 (1978) 573.
3 M. Chiba and F. Doornbos, *Bull. Environ. Contam. Toxicol.*, 11 (1974) 273.
4 R. P. Singh and M. Chiba, *J. Agric. Food Chem.*, 33 (1985) 63.
5 M. Chiba, *Abstracts of Papers, 170th National Meeting of the American Chemical Society, Chicago, IL, 1975*, American Chemical Society, Washington, DC, 1975, Pest 127.
6 F. J. Baude, J. A. Gardiner and J. C. Y. Han, *J. Agric. Food Chem.*, 21 (1973) 1084.
7 J. J. Kirkland, *J.Agric. Food Chem.*, 21 (1973) 171.
8 J. J. Kirkland, R. F. Holt and H. L. Pease, *J. Agric. Food Chem.*, 21 (1973) 368.
9 G. Zweig and R. Y. Gao, *Anal. Chem.*, 55 (1983) 1448.
10 G. P. Clemons and H. D. Sisler, *Pestic. Biochem. Physiol.*, 1 (1971) 32.
11 M. Chiba and R. P. Singh, *J. Agric. Food Chem.*, 34 (1986) 108.
12 C. H. Marvin, I. D. Brindle, C. D. Hall and M. Chiba, *J. Chromatogr.*, 503 (1990) 167.
13 R. P. Singh, I. D. Brindle, C. D. Hall and M. Chiba, *J. Agric. Food Chem.*, (1990) in press.

Journal of Chromatography, 518 (1990) 250–253
Elsevier Science Publishers B.V., Amsterdam

CHROM. 22 543

Note

High-performance liquid chromatographic method for the direct determination of the volatile anaesthetics halothane, isoflurane and enflurane in water and in physiological buffer solutions

P. K. JANICKI*, W. A. R. ERSKINE and M. F. M. JAMES
Anglo American Anaesthetic Research Laboratory, Department of Anaesthetics, Medical School, University of Cape Town, Observatory 7925 (South Africa)
(First received February 13th, 1990; revised manuscript received May 8th, 1990)

The effects of anaesthetic agents on *in vitro* cell preparations and isolated perfused organ preparations have been widely studied. The determination of the concentration of dissolved anaesthetic agents is critical when observations of the effects of these agents on cells or organs are to be made. Several methods have been utilized to administer these volatile agents to the *in vitro* preparations, *e.g.*, bubbling of the agents in the gaseous phase through the solutions or the addition of a saturated aqueous solution of the anaesthetic agents to the preparation [1,2]. It is also important to monitor the concentrations of the anaesthetics at various stages in the experiments because of the relatively rapid evaporation of these volatile substances from the warm (37°C) experimental solutions. Gas chromatography (GC) is widely utilized for the determination of the concentrations of anaesthetics [3,4]. However, it requires the extraction of the samples into an organic solvent, which is both time consuming and expensive.

We describe here a simple high-performance liquid chromatographic (HPLC) method for the direct determination of the commonly used volatile anaesthetics halothane, isoflurane and enflurane. The method makes use of the fact that halothane and to a lesser extent isoflurane and enflurane, in addition to the possession of an absorbtion band in the infrared spectrum, also absorb ultraviolet radiation [1,5,6].

EXPERIMENTAL

Chemicals

Halothane (2-bromo-2-chloro-1,1,1,-trifluoroethane) was obtained from Maybaker (Johannesburg, South Africa). Isoflurane (Forane, 1-chloro-2,2,2-trifluoroethyldifluoromethyl ether) and enflurane (Enthrane, 2-chloro-1,1,2-trifluoroethyldifluoromethyl ether) were obtained from Abott Laboratories (Johannesburg, South Africa). Toluene of analytical-reagent grade was purchased from BDH (Poole, U.K.)

0021-9673/90/$03.50

and methanol of HPLC grade from Merck (Darmstadt, F.R.G.). The water used was glass distilled.

Apparatus

The chromatographic system consisted of Waters M45 HPLC pump with a variable-wavelenght Pye Unicam PU4020 UV detector (Philips). The UV detector was operated at 0.005 a.u.f.s. The samples were injected (injection volume 20 μl) using a Rheodyne 7125 loop injector onto the column (Nova-Pak C_{18}, Radial Compression Module, 10 cm × 8 mm I.D., 4 μm spherical particles (Waters Assoc., Milford, MA, U.S.A.) equipped with an RCSS Guard-Pak μBondapak C_{18} precolumn cartridge (Waters Assoc.). The chromatograms were recorded and processed by a Spectra-Physics Chrom Jet SP 4400 recording integrator. The UV spectra of the investigated volatile anaesthetics dissolved in the mobile phase were measured using a Pye Unicam PU 8800 UV–VIS scanning spectrophotometer (Philips).

Chromatographic conditions

The eluent was methanol–water (50:50, v/v). The flow-rate was 3.5 ml/min. The temperature was ambient and the detector wavelength was set at 210 nm for halothane and 203 nm for isoflurane and enflurane determinations. The mobile phase was degassed and filtered under vacuum through 0.5-μm Millipore FH filters before use.

Procedure

For the preparation of the calibration graph various amounts of volatile anaesthetics were dissolved in methanol and spiked with phosphate buffer in order to obtain the desired final concentrations in buffer (1 μmol/l–1 mmol/l of halothane and 0.2–20 mmol/l of isoflurane and enflurane). After mixing in a tightly closed glass tube, 50 μl of spiked buffer were added to 50 μl of internal standard mixture (0.05 mmol/l toluene in methanol). A 20-μl volume of the final sample was injected onto the column.

RESULTS AND DISCUSSION

The UV spectra (Fig. 1A) show that the anaesthetic agents dissolved in methanol–water (50:50, v/v) as the mobile phase exhibited maximum absorbance of halothane at 210 nm and of both isoflurane and enflurane at 203 nm. It must be stressed, however, that when the absorptions of all three anaesthetics were compared at the same molar concentrations in the mobile phase, the absorption of halothane was at least 200 times greater than that of either enflurane and isoflurane. Under the chosen chromatographic conditions we were able to separate and detect at 203 nm all three anaesthetics in one sample (Fig. 1 B and C). In an experimental situation, for which the proposed method is intended, all three agents would not be present in the same sample. We therefore used toluene as an internal standard for the three different anaesthetics.

The calibration graph was prepared with phosphate buffer spiked with the anaesthetics diluted with methanol in the ranges 1 μmol/l–1 mmol/l of halothane and 0.2–20 mmol/l of isoflurane and enflurane. Over these wide ranges the assay showed a

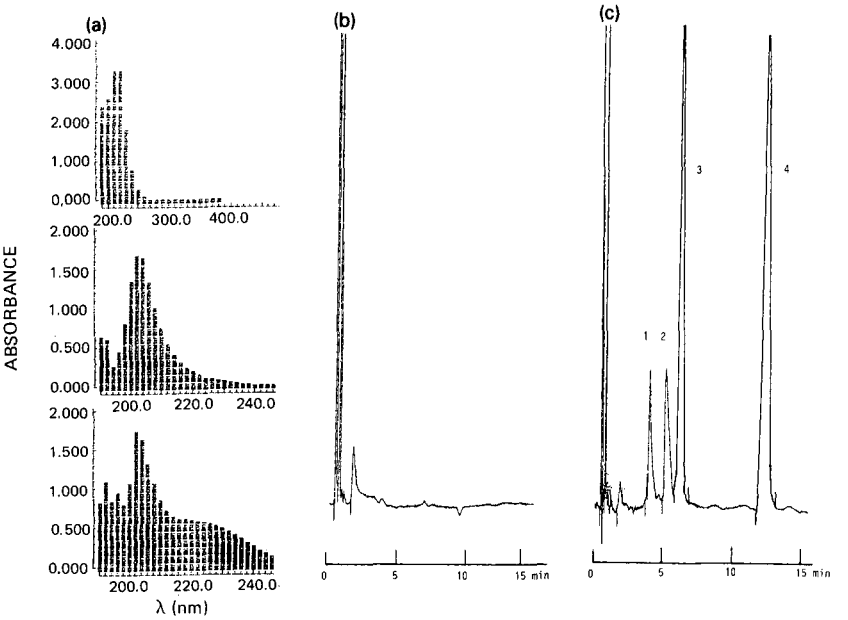

Fig. 1. (A) UV spectra for halothane, isoflurane and enflurane dissolved in mobile phase. The concentration of halothane in mobile phase was 200 times lower than those of isoflurane and enflurane. Chromatograms from injection of (B) blank phosphate buffer and (C) sample of phosphate buffer spiked with 0.1 mmol/l of halothane and 10 mmol/l of isoflurane and enflurane. UV detection at 203 nm. Peaks: 1 = enflurane; 2 = isoflurane; 3 = halothane; 4 = toluene (internal standard).

high degree of linearity on a line forced through the origin and the intra- and inter-assay relative standard deviations (R.S.D) were low (Table I). The sensitivity of the method is adequate for monitoring the concentrations of the anaesthetics in buffers through which the compounds are bubbled at levels as low as 0.5%. It was also found

TABLE I

CHARACTERISTIC PARAMETERS OF THE HPLC ASSAY OF VOLATILE ANAESTHETICS

Limit of detection = sample concentration when compound signal-to-noise ratio = 3, Correlation coefficient refers to the linear fitted calibration graph. Intra-assay R.S.D.: on each of three different days three samples each containing 0.1 mmol/l of halothane or 10 mmol/l of either isoflurane or enflurane were analysed; the R.S.D. of the three samples for each of the three days was calculated, the average of these R.S.D.s was taken and is reported as the intra-assay R.S.D. Inter-assay R.S.D. = the R.S.D. calculated collectively for all nine samples for each compound. Accuracy = the deviation of the average of the nine samples for each compound from the expected value of the concentration of the anaesthetic.

Parameter	Halothane	Isoflurane	Enflurane
Limit of detection (mmol/l)	0.001	0.2	0.2
Correlation coefficient	0.981	0.966	0.958
Intra-assay R.S.D. (%)	4.6	6.1	8.5
Inter-assay R.S.D. (%)	4.9	7.4	8.9
Accuracy (%)	5	6.5	10

that the anaesthetics could be determined directly in various types of buffers (phosphate-buffered saline, Krebs, Hanks) without disturbing the chromatographic conditions after direct injection of a buffer sample onto the column (not shown).

Many experiments of the effects of anaesthetic agents on isolated systems are performed in buffer solutions. The direct determination of an anaesthetic of interest in the buffer solution can be easily carried out without the use of an additional extraction procedure such as would be required with the use of a more sophisticated GC extraction technique.

REFERENCES

1 W. M. Mushin and P. L. Jones (Editors), *MacIntosh, Muschin & Epstein's Physics for the Anaesthesists*, Blackwell, Oxford, 4th ed., 1987, Ch. 5.
2 N. P. Franks and W. R. Lieb, *Nature (London)*, 316 (1985) 349.
3 B. R. Fink and K. Morikawa, *Anaesthesiology*, 32 (1970) 32.
4 D. J. Wartley, *Br. J. Anaesth.*, 40 (1968) 624.
5 D. D. Koblin and E. I. Eger, in R. D. Miller (Editor), *Anaesthesia*, Churchill Livingstone, New York, 2nd ed., 1986, Ch. 18, p. 581.
6 H. Wollman and R. D. Dripps, in A. G. Gilman, L. S. Goodman, T. W. Rall and F. Murad (Editors), *The Pharmacological Basis of Therapeutics*, Macmillan, New York, 7th ed., 1985, Ch. 5, p. 61.

Journal of Chromatography, 518 (1990) 254–257
Elsevier Science Publishers B.V., Amsterdam

CHROM. 22 584

Note

Analytical and preparative high-performance liquid chromatographic systems for the separation of an anomeric mixture of 4-O-(D-glucopyranosyl)gallic acid

WOLFRAM MEIER-AUGENSTEIN[a] and HERMANN SCHILDKNECHT*

Organisch-Chemisches Institut der Universität, Universität Heidelberg, Im Neuenheimer Feld 270, D-6900 Heidelberg (F.R.G.)

(First received March 20th, 1990; revised manuscript received May 23rd, 1990)

Phenolic compounds are widespread in nature and, although they mostly occur as glycosides, the physiological activity is normally released by the aglyca as in the case of juglone [1]. In contrast to this common rule, the turgormediated leaf movement of *Mimosa pudica* L. is controlled by a sulphated glucoside of gallic acid, 4-O-β-D-glucopyranosyl-6-sulphate)gallic acid, which we named PLMF 1 (periodic leaf movement factor) [2]. This compound has been isolated from fourteen higher plants which exhibit nyctinastic movements [3].

For our investigations of the structure–activity relationship of PLMF 1, for leaf-closing activity on leaves of *Mimosa pudica* L., we had to synthesize the PLMF 1 anomeric compound, *i.e.*, 4-O-α-D-glucopyranosyl-6-sulphate)gallic acid [4]. As it was not possible to obtain the pure compound by stereoselective glucosidation, the problem was to separate an anomeric mixture containing the α- and β-anomers in a ratio of 1:1.

Separation of anomers is usually performed by fractional crystallization, but unfortunately this method failed in this instance. With the medium-pressure liquid chromatographic (MPLC) systems developed for the purification of synthesized PLMF 1 and the free glucosides [5], the anomers could not be separated even on different stationary phases and using several different mobile phases.

In this paper we report the high-performance liquid chromatographic (HPLC) systems with which we finally succeeded in separating the anomeric glucosides of gallic acid and their sulphated derivatives on both analytical and preparative scales.

EXPERIMENTAL

Chemicals

3,5-Diacetyl 4-O-(D-2′,3′,4′,6′-tetra-O-benzylglucopyranosyl)methylgallate was

[a] Present address: Department of Chemistry, Ecological Chemistry, University of Stellenbosch, Stellenbosch 7600, South Africa.

0021-9673/90/$03.50

synthesized [6] using the trichloroacetimidate method described by Schmidt [7]. Cleavage of the protecting groups was carried out in two steps: first, debenzylation by hydrogenolysis with hydrogen at room temperature and atmospheric pressure using Pd/C (10%) as catalyst, and second, cleavage of the acetyl groups and the methyl group with $Ba(OH)_2$ in concentrated aqueous solution in an inert gas atmosphere to give finally the α- and β-anomers of 4-O-(D-glucopyranosyl)gallic acid in a ratio of 1:1. The separated glucosides were sulphated using an SO_3–pyridine complex in absolute dimethylformamide as sulphating agent [8].

Water was purified by deionization on ion-exchange columns and passage through a Milli-Q water purification system. Methanol was donated by BASF (Ludwigshafen, F.R.G.) and was purified by rectification. Trifluoroacetic acid (TFA) for spectroscopy (Uvasol) was purchased from Merck (Darmstadt, F.R.G.).

HPLC systems

The chromatographic system for analytical separations consisted of an LDC ConstaMetric III HPLC pump and a Philips PU 4020 variable-wavelength absorbance detector. Chromatograms were recorded on a Merck/Hitachi Model D 2000 integrator. Columns were 250 mm × 8 mm I.D., stainless steel, laboratory-packed with Nucleosil C_{18} (5 μm, 100 Å) purchased from Macherey-Nagel (Düren, F.R.G.). The chromatographic system for separations on a preparative scale consisted of a Model HD-2-200 HPLC pump (Besta, Heidelberg, F.R.G.) and an LDC Spectro-Monitor III variable-wavelength absorbance detector. The column, purchased from Macherey-Nagel, was 250 mm × 20 mm I.D., stainless steel, packed with Nucleosil C_{18} (7 μm, 100 Å) coupled with a precolumn of 30 mm × 16 mm I.D., stainless steel, packed with Nucleosil C_{18} (5 μm, 100 Å).

RESULTS AND DISCUSSION

4-O-(α-D-Glucopyranosyl)gallic acid (**1**α), 4-O-(β-D-glucopyranosyl)gallic acid (**1**β) and their sulphated derivatives (**2**α and **2**β) were separated by reversed-phase

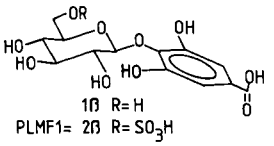

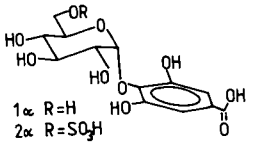

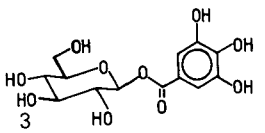

TABLE I

REVERSED-PHASE SEPARATION OF THE ANOMERIC GLUCOSIDES OF GALLIC ACID

Eluents: I = methanol–water (15:85, v/v) containing 2 m*M* TFA; II = methanol–water (12:88, v/v) containing 2 m*M* TFA; III = methanol–water (10:90, v/v) containing 3 m*M* TFA; IV = methanol–water (12:88, v/v) containing 3 m*M* TFA. a, Analytical system, flow-rate 3 ml/min; b, preparative system, flow-rate 16 ml/min.

Compound	Retention time (min)[a]			
	Ia	IIa	IIIa	IVb
1α	11.0 ± 0.2	13.0 ± 0.3	17.0 ± 0.5	20.4 ± 0.6
1β	13.3 ± 0.3	16.2 ± 0.4	20.9 ± 0.6	26.3 ± 0.7
2α		10.0 ± 0.5	11.3 ± 0.2	
2β		11.8 ± 0.6	14.0 ± 0.3	

[a] Mean values ± standard error.

chromatography. The retention times of these substances obtained with different chromatographic systems are presented in Table I. In all instances the α-anomer elutes first (Fig. 1). Complete separation of the anomers **1**α and **1**β on a prepparative scale was achieved within 30 min. The amount of substance separated with this sys-

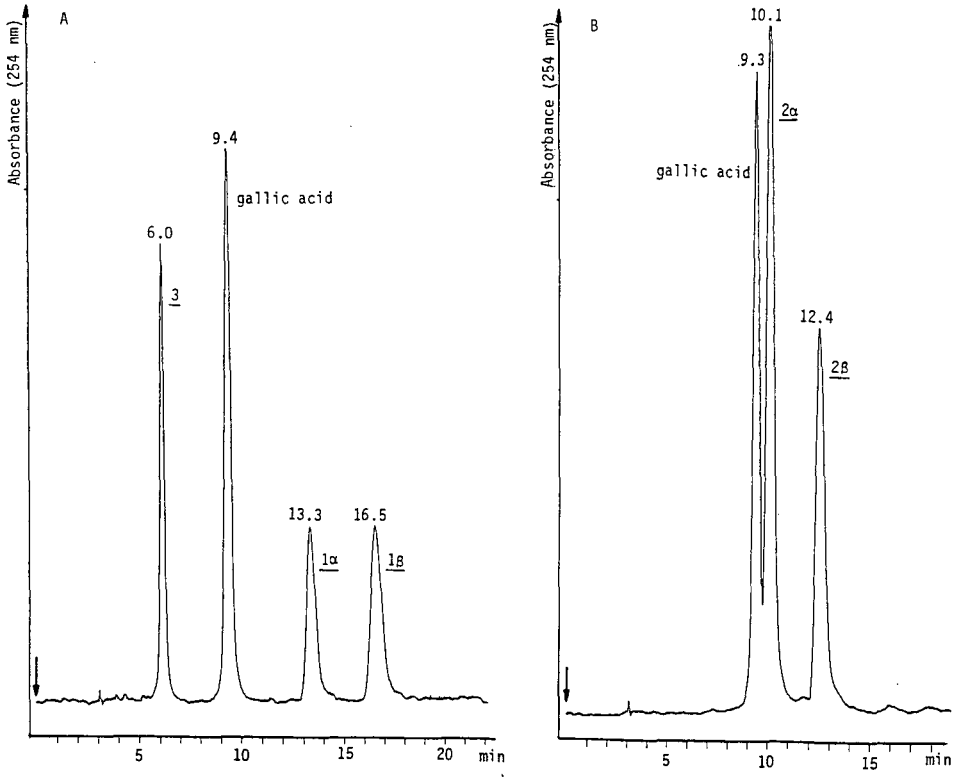

Fig. 1. Typical analytical separation of (A) compounds **3**, **1**α and **1**β (B) and compounds **2**α and **2**β. Gallic acid was added as an internal standard in both runs. Eluent, methanol–water (12:88, v/v) containing 2mM TFA; flow-rate, 3 ml/min; column, 250 mm × 8 mm I.D., Nucleosil C_{18} (5 μm, 100 Å).

tem was usually 15 mg per run. During the scale-up of the analytical system, a column of 250 mm × 16 mm I.D. packed with Nucleosil C_{18} (5 μm, 100 Å) was used. On this column 3 mg were separated per run using methanol–water (12:88, v/v), containing 2 m*M* TFA as eluent at a flow-rate of 10 ml/min (results not shown).

Of major importance was the incorporation of TFA in the eluent, as it provides some advantages over glacial acetic acid. Only small amounts of TFA (1–3 m*M*) were needed to obtain a high resolution. It also prevented tailing of peaks eluting with higher retention times. Further, TFA is more convenient to use for preparative separations, as it is easier to evaporate than glacial acetic acid.

Increasing the TFA content in a given mobile phase in 1 m*M* steps resulted in an increase in the retention time of the acidic compounds owing to greater protonation of their acid groups [9]. This influence could be demonstrated by comparing **1**β with its isomer 1-galloyl-β-D-glucopyranose (**3**), in which β-D-glucose is connected to the carboxylic group of gallic acid [10,11]. As **1**β possesses a carboxyl group, its dissociation can be suppressed by the addition of TFA, which shifts the equilibrium in the direction of the less polar undissociated acid having a longer retention time on the reversed-phase column. In the isomeric compound **3** the carboxyl group is esterified with β-D-glucose, thus largely eliminating the influence of TFA on the retention time of this substance. Whereas the retention time of **1**β was 16.2 ± 0.4 min with solvent system IIa, 1-galloyl-β-D-glucopyranose eluted after 5.8 ± 0.3 min using the same system (Fig. 1A) [6]. As illustrated by the retention times of the sulphated glucosides **2**α and **2**β with system IIIA, the separation of strongly acidic compounds is also possible.

The HPLC systems presented here are helpful for the separation and purification of glucosides of phenolic acids. Scale-up from an analytical scale to the described preparative separation is possible without any problems. The preparative separation of the anomeric glucosides of gallic acid yields pure compounds that can be used without further purification.

ACKNOWLEDGEMENTS

We thank Martina Schickedanz and Gerhard Schaller of our HPLC laboratory for valuable technical assistance and helpful advice. Financial support from the Bundesminister für Forschung und Technologie (BMFT), the Fonds der Chemischen Industrie and the Deutsche Forschungsgemeinschaft (DFG) is gratefully acknowledged.

REFERENCES

1 H. R. Bode, *Planta*, 51 (1958) 440.
2 H. Schildknecht, *Spektrum der Wissenschaft*, No. 11 (1986) 44.
3 P. Kallas, W. Meier-Augenstein and H. Schildknecht, *Naturwiss. Rundsch.*, 42 (1989) 309.
4 P. Kallas, W. Meier-Augenstein and H. Schildknecht, *J. Plant Physiol.*, 136 (1990) 225.
5 H. Schildknecht and R. Milde, *Carbohydr. Res.*, 164 (1987) 23.
6 W. Meier-Augenstein, *Ph. D. Thesis*, University of Heidelberg, 1989.
7 R. R. Schmidt, *Angew. Chem., Int. Ed. Engl.*, 25 (1986) 212.
8 H. Schildknecht, *Angew. Chem. Int. Ed. Engl.*, 22 (1983) 695.
9 G. Schaller, personal communication.
10 E. Fischer and M. Bergmann, *Chem. Ber.*, 51 (1918) 1760.
11 O. Th. Schmidt and H. Reuss, *Justus Liebigs Ann. Chem.*, 649 (1961) 137.

Journal of Chromatography, 518 (1990) 258–263
Elsevier Science Publishers B.V., Amsterdam

CHROM. 22 654

Note

Optimal conditions for long-term storage of biogenic amines for subsequent analysis by column chromatography with electrochemical detection

D. L. PALAZZOLO and S. K. QUADRI*
Neuroendocrine Research Laboratory, Department of Anatomy and Physiology (VMS 228), Kansas State University, Manhattan, KS 66506 (U.S.A.)
(First received October 31st, 1989; revised manuscript received June 26th, 1990)

The optimal conditions for storage of biogenic amines in solutions are not known. Temperature and pH of the solvents and length of storage have dramatic effects on stabilities of amines [1–3], yet the variability in the storage conditions used by various investigators is rather striking [4–6]. These amines have been stored in a variety of weak acids and buffers, including perchloric acid, hydrochloric acid, formic acid, and acetic acid, with molarities of 0.1 to 0.5; at temperatures ranging from room temperature to −80°C; and for periods of 12 h to several weeks or months [1–3, 7–11]. Not surprisingly, the results have been highly variable. Another complicating factor has been the fact that not all biogenic amines behave uniformly under similar storage conditions. We have noticed that catecholamines remain stable for weeks in acidic solutions under refrigeration but indoleamines undergo fast degradation under the same conditions. The aims of the present study were (1) to determine stabilities of biogenic amines in Krebs–Ringer–Hensleit (KRH) saline under various combinations of pH, temperature, and length of storage, and (2) to investigate the conditions optimum for storage of catecholamines and indoleamines together in KRH which is a commonly used medium for studying release of biogenic amines.

EXPERIMENTAL

Experiment 1

This experiment was performed to determine the stabilities at room temperature of biogenic amines and the internal standard, dihydroxybenzylamine (DHBA), dissolved in KRH of various pHs. Dopamine (DA, 11.70 mg), norepinephrine (NE, 11.48 mg), epinephrine (EPI, 11.30 mg), serotonin (5-HT, 11.40 mg), and DHBA (14.96 mg) each were dissolved separately in 100 ml of 0.05 *M* perchloric acid. From each of these solutions, 50 μl were withdrawn and mixed with 99.95 ml of each of the following four solvents: (1) 0.05 *M* perchloric acid (pH 1.40), (2) KRH and 1 *M* perchloric acid in a ratio of 25:1 (v/v) (pH 1.96), (3) KRH and 1 *M* perchloric acid in a

0021-9673/90/$03.50

ratio of 50:1 (v/v) (pH 5.81), and (4) KRH (pH 7.81). KRH consisted of 117 m*M* NaCl, 4.7 m*M* KCl, 1.2 m*M* $MgSO_4$, 1.2 m*M* KH_2PO_4, 2.5 m*M* $CaCl_2$, 24.8 m*M* $NaHCO_3$ and 11.1 m*M* glucose. The solutions were kept at room temperature (22°C). From each of them, 15 μl were withdrawn at 0, 30, 60 and 90 min, and their amine content was determined by column chromatography with electrochemical detection. The percent recovery of each amine was calculated by comparison with its recovery in freshly made 0.05 *M* perchloric acid.

Experiment 2

This experiment was performed to determine the effects of refrigeration on the recovery of the above amines. They were prepared in four solutions as described above and refrigerated (4°C). Within 2 h of refrigeration on day 0 and then on days 1, 2, 4, 7, 14 and 28 after refrigeration, 15-μl aliquots were withdrawn from each solution and analyzed in duplicate.

Experiment 3

This experiment was performed to investigate the effects of freezing (−60°C) on the recovery of amines. They were prepared as described in experiment 1 and immediately frozen. Within 30 min after freezing on day 0 and again on days 1, 2, 4, 7, 14 and 28 after freezing, 15-μl aliquots were withdrawn from each solution and analyzed in quadruplicate. Before injection into the high-performance liquid chromatography (HPLC)–electrochemical detection (ED) system, each solution was thawed for 1 min at 60°C.

Column chromatography with electrochemical detection

This procedure has been described in detail previously [12]. The mobile phase (pH 3.1) included monochloroacetic acid (14.15 g/l), sodium hydroxide (4.675 g/l), EDTA (250 mg/l), octanesulfonic acid (300 mg/l), tetrahydrofuran (1.4%) and acetonitrile (3.5%). The sensitivity of the detector was 1 nA full scale, and the potential of the working electrode was 0.8 V with respect to a Ag/AgCl reference electrode. The temperatures of the column and mobile phase reservoir were maintained at 29.3–30.1°C and 43.2–44.0°C, respectively [12].

RESULTS

Effects of pH on stability of amines at room temperature

Percent recoveries of amines in KRH saline of various pH values after a 90-min storage at room temperature are shown in Fig. 1. There were no significant differences in recoveries at 0 min or after storage for 30, 60 and 90 min; therefore, results for these four time intervals were combined to calculate average percent recoveries for the 90-min period. As shown in Fig. 1, when the amines were stored in pure KRH saline (pH 7.81), marked reductions occurred in the recoveries of all catecholamines and DHBA as compared to their recoveries in 0.05 *M* perchloric acid (pH 1.40). These reductions were 46% (DA), 34% (NE), 46% (EPI), and 22% (DHBA). In contrast, this pH had no effect on the recovery of 5-HT. In acidic KRH (pH 5.81), DA, NE, and DHBA remained almost 100% stable, but EPI decreased by 10%, and 5-HT increased by 16%. In highly acidic KRH (pH 1.96), recoveries of DA, NE, and

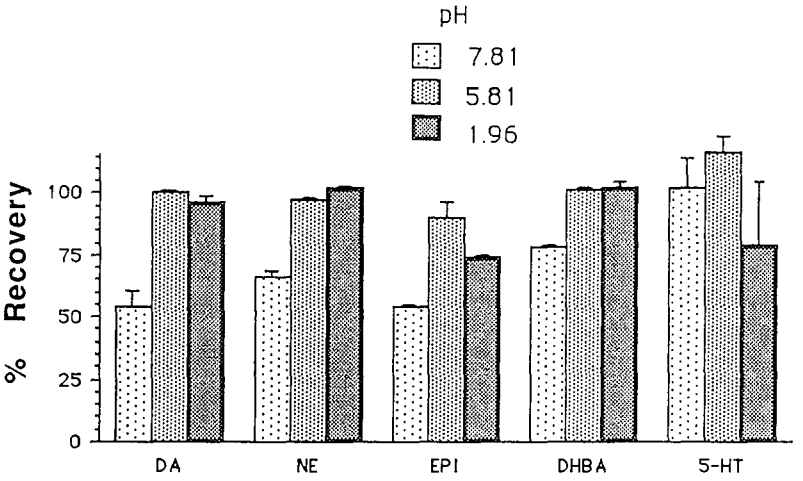

Fig. 1. Percent recoveries of dopamine (DA), norepinephrine (NE), epinephrine (EPI), dihydroxybenzylamine (DHBA) and serotonin (5-HT) after 90 min at room temperature (22°C) in Krebs–Ringer–Hensleit (KRH) saline of pH 7.81, 5.81 and 1.96.

DHBA were again almost 100%, but EPI and 5-HT decreased by 26% and 21%, respectively.

Effects of pH on stability of amines under refrigeration

In alkaline KRH saline (pH 7.81), all the catecholamines and DHBA suffered 100% loss by day 2 (Fig. 2). On the other hand, 5-HT decreased more gradually, until it became undetectable by day 28. In acidic KRH saline (pH 5.81), the decline in the recoveries remained essentially the same, except that 5-HT became undetectable earlier (day 14) than before. In highly acidic KRH saline (pH 1.96), recoveries of all the amines improved considerably and more than 50% of DA, NE and DHBA and more than 20% of EPI and 5-HT were recovered on day 28. In 0.05 *M* perchloric acid (pH 1.4), 5-HT declined rapidly and was undetectable by day 14, whereas DA and EPI declined more gradually and NE and DHBA suffered only minor losses by day 28.

Effect of pH on stability of amines under freezing

Freezing had remarkable stabilizing effects on all the catecholamines and DHBA. They remained completely stable up to 28 days under all the pHs tested (Fig. 2). However, the losses in 5-HT were very significant and very rapid under acidic conditions. Recoveries of this amine decreased by more than 75% in acidic KRH (pH 1.96) and by more than 50% in 0.05 *M* perchloric acid (pH1.4) within 1 day. However, like catecholamines, 5-HT remained completely stable for up to 28 days in KRH solutions of pHs 5.81 and 7.81.

DISCUSSION

The results presented above demonstrate that the stabilities of biogenic amines in solutions are affected not only by pH, temperature and length of storage, but also

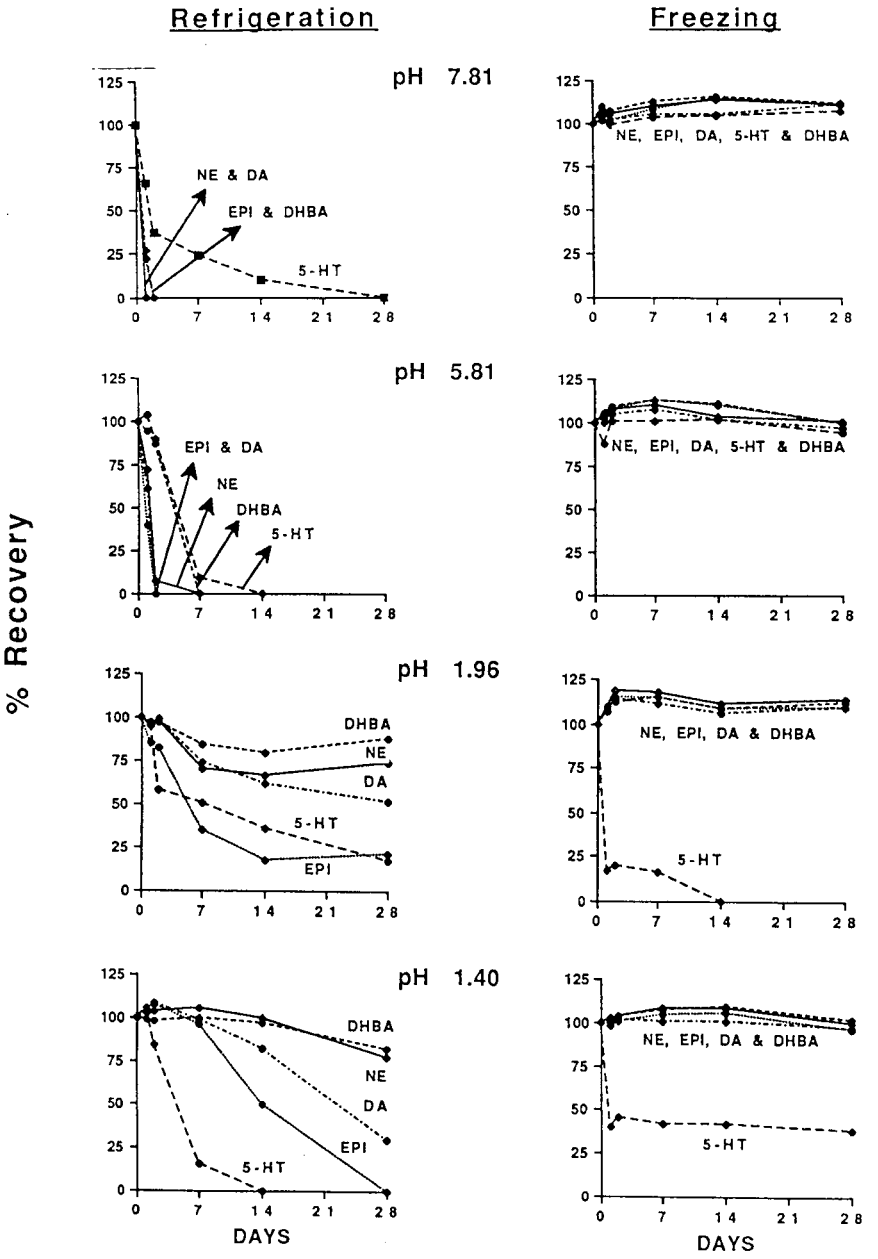

Fig. 2. Percent recoveries of dopamine (DA), norepinephrine (NE), epinephrine (EPI), dihydroxybenzylamine (DHBA) and serotonin (5-HT) under refrigeration (4°C) and under freezing (−60°C) for variable periods of time in Krebs–Ringer–Hensleit (KRH) saline of pH 7.81, 5.81 and 1.96 and in 0.05 *M* perchloric acid (pH 1.4).

by slight differences in structures of amines. At room temperature, DA and NE remained stable for at least 90 min in acidic KRH saline (pH 1.96). But, this was not true for the other catecholamine, EPI, indicating that minor differences in structure can lead to major differences in stabilities. Interestingly, the loss of this catecholamine was almost identical to the loss of the indoleamine, 5-HT, under the same conditions, making it difficult to relate stability to chemical structure with confidence.

The results indicate that catecholamines are more stable in acidic solutions. However, acid solutions do not confer stability for indefinite periods of time [1,3,5,6]. In 0.4 *M* perchloric acid, NE recovery decreases by 50% in 4 months [1]. Also, there is a limit to acidity of the solvents before it becomes detrimental to stability of catecholamines. According to one report, at room temperature, NE was stable for several hours in the pH range of 4–5, but losses occurred below pH 3 [3].

Our observation that 5-HT is not stable in strong acidic solutions is consistent with earlier reports [1,3]. Acidic solutions are also not suitable for storage of 5-HT metabolites. In dilute hydrochloric acid, 5-hydroxyindoleacetic acid (5-HIAA) suffered losses at room temperature, 4°C, and −20°C, and these losses were greater in stronger acidic solutions [3].

Our results give a clear demonstration of the advantages of low temperature for storing amines. In alkaline KRH (pH 7.81), DA and NE decreased by 30–45% at room temperature but remained stable for up to 28 days at −60°C. In acidic KRH (pH 1.96), EPI decreased by more than 25% in 90 min at room temperature, but remained more than 80% stable for 2 days at 4°C and was 100% stable for 28 days at −60°C. Other investigators also have recognized the beneficial effects of low temperatures on the stability of amines [1–3].

Low temperatures, however, do not always guarantee stability. The behavior of 5-HT is a case in point. In acidic KRH (pH 1.96), it decreased by 25% in 90 min at room temperature, remained 50% stable for 7 days at 4°C, but suffered a loss of more than 75% in 1 day at −60°C. In 0.05 *M* perchloric acid (pH 1.4), it decreased by 84% in 7 days at 4°C but lost more than 60% of its content within 1 day at −60°C. Taken together, these examples indicate that for each amine, there is a combination of pH and low temperature that is most conductive to its stability.

The results of this study demonstrate that it is possible to devise conditions that maintain stability of catecholamines and indoleamines in the same solution. DA, NE, EPI, and 5-HT remained 100% stable for 28 days at −60°C if stored in KRH saline of pH 5.81 or 7.81. We feel that pH of 5.81 is more suitable, because at that pH all of the amines also remained stable for at least 90 min at room temperature, whereas at pH 7.81 catecholamines decreased by more than 25% in 90 min at room temperature. Thus, pH 5.81 would permit short delays in freezing without any losses.

ACKNOWLEDGEMENT

This is contribution No. 90-170-J from the Kansas Agricultural Experiment Station.

REFERENCES

1 L. M. Gunne, *Acta Physiol. Scand.*, 58, Suppl. 204 (1963) 5.

2 C. F. Saller and A. I. Salama, *J. Chromatogr.*, 309 (1984) 287.
3 A. S. Welch and B. L. Welch, *Anal. Biochem.*, 30 (1969) 161.
4 N. E. Anden and T. Magnusson, *Acta Physiol. Scand.*, 69 (1967) 87.
5 G. B. West, *J. Pharm. Pharmacol.*, 4 (1952) 560.
6 A. Bertler, A. Carlsson and E. Rosengren, *Acta. Physiol. Scand.*, 44 (1958) 273.
7 G. S. Mayer and R. E. Shoup, *J. Chromatogr.*, 255 (1983) 533.
8 P. Herregodts and Y. Michotte, *J. Chromatogr.*, 345 (1985) 33.
9 W. A. Hunt and T. K. Dalton, *Anal. Biochem.*, 135 (1983) 269.
10 V. M. Gregory, *J. Chromatogr.*, 345 (1985) 140.
11 V. J. Aloyo and R. F. Walker, *J. Endocrinol*, 114 (1987) 3.
12 D. L. Palazzolo and S. K. Quadri, *J. Chromatogr.*, 479 (1989) 216.

Journal of Chromatography, 518 (1990) 264–267
Elsevier Science Publishers B.V., Amsterdam

CHROM. 22 572

Note

Investigation of interfering products in the high-performance liquid chromatographic determination of polyamines as benzoyl derivatives

SATORU WATANABE* and TAIICHI SAITO
Department of Pharmacology, Kawasaki Medical School, 577 Matsushima, Kurashiki City, Okayama 701–01 (Japan)
SHOICHI SATO, SUMIKA NAGASE and SATOSHI UEDA
Department of Medical Technology, Kawasaki College of Allied Health Professions, 316 Matsushima, Kurashiki City, Okayama 701–01 (Japan)
and
MASAFUMI TOMITA
Department of Legal Medicine, Kawasaki Medical School, 577 Matsushima, Kurashiki City, Okayama 701–01 (Japan)
(First received January 11th, 1990; revised manuscript received April 24th, 1990)

The determination of polyamines (putrescine, spermidine and spermine) in cells, tissues and organs is necessary in order to clarify the precise physiology of living organisms and the role of cell proliferations within them. Recently, several workers have employed benzoyl derivatization procedures [1–3] in the determination of these polyamines by high-performance liquid chromatography (HPLC). These procedures are both rapid and simple. In the course of our application of these benzoylation procedures to the determination of polyamines in rat organs, we observed slow-moving peaks at retention times of 7.8 and 17.0 min in addition to those of three benzoyl polyamines which were synthesized by the previous workers [1–3]. The size of these two peaks changed with the reaction time of benzoylation and the standing time of the benzoyl polyamines in methanol before measurement. These peaks influenced the peak area of N,N′-dibenzoylbutane-1,4-diamine and made accurate measurement of the polyamines impossible. If they could be eliminated, then precise measurements could be made.

EXPERIMENTAL

Equipment

HPLC studies were performed on an LC-6A chromatograph (Shimadzu, Kyoto, Japan) equipped with a Chromatopac C-R3A data processing system and an SPD-66A UV spectrophotometric detector operated at 254 nm under isocratic conditions.

0021-9673/90/$03.50

A reversed-phase column (Cosmosil 5 C_{18}) (150 × 3 mm I.D.) was purchased from Nakalai Tesque (Kyoto, Japan).

Polyamines and benzoyl chloride were obtained from Sigma (St. Louis, MO, U.S.A.) and Wako (Osaka, Japan), respectively.

Procedure[1]

To 50 μl of a sample containing 25 nmol of polyamines were added 2.0 ml of 2 *M* sodium hydroxide followed by 50 μl of benzoyl chloride. The mixture was well shaken with a vortex mixer until the disappearance of benzoyl chloride (5.0 min), after which it was allowed to stand for 3.0 h at 40°C. Next, 2.0 ml of saturated sodium chloride solution were added, followed by 2.0 ml of diethyl ether. The solution was well mixed and centrifuged at 700 *g* for 25 min to separate the layers, and the diethyl ether phase was removed by evaporation in a stream of nitrogen. The residue was dissolved in 100 μl of hot methanol (40–50°C) and 10 μl of the solution were charged to the HPLC system.

RESULTS AND DISCUSSION

Contrary to our expectations, the HPLC of the benzoylated polyamines showed two peaks with retention times of 7.8 and 17.0 min in addition to those of N,N′-dibenzoylbutane-1,4-diamine, N,N′,4-tribenzoyl-4-azaoctane-1,8-diamine and N,N′,4,9-tetrabenzoyl-4,9-diazadodecane-1,12-diamine, as shown in Fig. 1. The peak areas of N,N′-dibenzoylbutane-1,4-diamine at 4.0 min and of the unidentified peak at

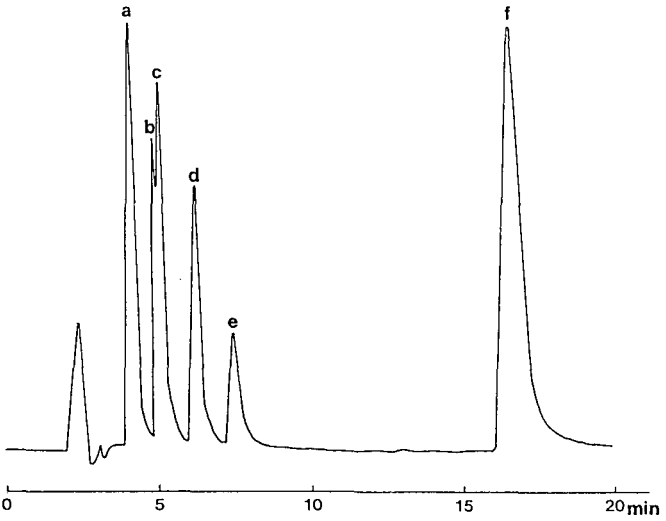

Fig. 1. Separation of benzoylated polyamine by HPLC. The reaction time was 3.0 h at 40°C. Operating conditions: column, 15 cm Cosmosil 5 C_{18}; mobile phase, water–acetonitrile–methanol (9:10:1) containing 0.2% trifluoroacetic acid; column temperature, ambient; flow-rate, 0.6 ml/min. Peaks: a = benzoylated putrescine; b = benzoylated 1,6-diaminohexane; c = benzoylated spermidine; d = benzoylated spermine; e = methyl benzoate; f = benzoic anhydride.

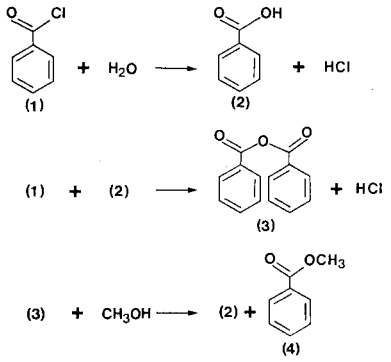

Fig. 2. Reactions producing benzoic acid, benzoic anhydride and methyl benzoate.

7.8 min increased with extended storage time in methanol, whereas the peak area at 17.0 min decreased. Therefore, these three peaks seem to be closely related to each other as shown in reactions poducing benzoic acid, benzoic anhydride and methyl benzoate (Fig. 2). Benzoyl chloride (1) reacted partly with polyamines and was hydrolysed to benzoic acid (2), then benzoyl chloride and benzoic acid condensed to give benzoic anhydride (3) which was extracted efficiently by diethyl ether. After evaporation of the diethyl ether, the benzoic anhydride immediately began to undergo solvolysis in methanol and produced methyl benzoate (4) and benzoic acid during storage, as shown in Fig. 3. The peaks with retention times of 4.0, 7.8 and 17.0 min were thus identified as benzoic acid, methyl benzoate and benzoic anhydride, respectively, by comparison with authentic samples.

Unfortunately, the peak of benzoic acid was superimposed on that of N,N′-dibenzoylbutane-1,4-diamine under our experimental conditions regardless of the application of different solvent systems. Therefore, care should be taken in using

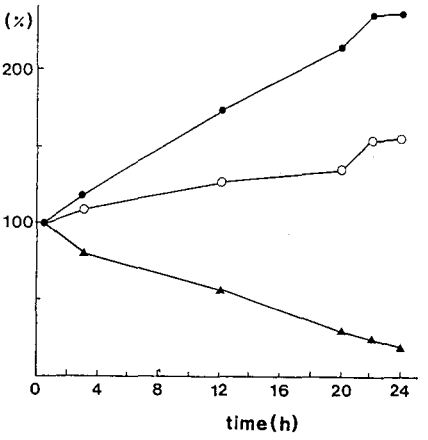

Fig. 3. Time course of the solvolysis of benzoic anhydride (▲) in methanol to benzoic acid (○) and methyl benzoate (●) at 25°C, as determined by HPLC. The ordinate represents the percentages of benzoic acid, methyl benzoate and benzoic anhydride *versus* the respective concentrations at 30 min after starting the reaction.

the benzoylation method for the determination of polyamines, as peaks of products occurring as a result of the reaction might be superimposed over those of the benzoylated polyamines in HPLC, leading to incorrect deductions. To eliminate this benzoic acid, it is necessary to decompose the benzoic anhydride produced in the solution by the benzoylation reaction before diethyl ether extraction of the benzoylated polyamines, as the benzoic anhydride solvolyses to benzoic acid and methyl benzoate in methanol. The decomposition of the benzoic anhydride produced in the reaction mixture seems to be dependent on the temperature and time of the benzoylation. When benzoylation was carried out overnight at 40°C with shaking of the mixture of benzoyl chloride and polyamines, benzoic anhydride was still observed. However, it was not present in the mixture when it was shaken vigorously overnight at 60°C. There were no differences in the concentrations of N,N′-dibenzoylbutane-1,4-diamine, N,N′,4-tribenzoyl-4-azaoctane-1,8-diamine and N,N′,4,9-tetrabenzoyl-4,9-diazadodecane-1,2-diamine due to the variations in temperature.

ACKNOWLEDGEMENTS

We thank Miss Y. Tachibana, M. Nishimaru, Y. Ueno and S. Kubota for technical assistance.

REFERENCES

1 J. W. Redmond and A. Tseng, *J. Chromatogr.*, 170 (1979) 479.
2 J. R. Clarke and A. S. Tyms, *Med. Lab. Sci.*, 43 (1986) 258.
3 C. F. Verkoelen, J. C. Romijn, F. H. Schroeder, W. P. van Schalkwijk and T. A. W. Splinter, *J. Chromatogr.*, 426 (1988) 41.

Journal of Chromatography, 518 (1990) 268–272
Elsevier Science Publishers B.V., Amsterdam

CHROM. 22 610

Note

Determination of iodide in dairy products and table salt by ion chromatography with electrochemical detection

RAJINDER K. CHADHA* and JAMES F. LAWRENCE
Food Research Division, Bureau of Chemical Safety, Food Directorate, Health Protection Branch, Health and Welfare Canada, Ottawa, Ontario K1A 0L2 (Canada)
(Received March 27th, 1990)

The use of iodine-containing feed supplements and teat dips in the farming industry has resulted in significant increases in the concentration of iodide in milk. Because of its toxicity, excessive intake of iodine is cause for health concern [1]. Since from 25% to more than 50% of the dietary intake [1,2] of iodine is from milk and dairy products in the form of iodide, a simple and reliable method for the routine determination of iodide in such products is desirable.

Several methods are available for the determination of iodide in milk. Microchemical methods require acid digestion [2] or alkaline ashing [3] of the sample prior to quantification based on the modified Sandell–Kolthoff reaction. A gas chromatographic method with electron-capture detection involves making an iodobutanone [4] or 2-iodoethanol [5] derivative. A differential-pulse polarographic method [6] also requires ashing. Iodide has been determined by ion chromatography with UV detection following combustion of the sample in a Schöninger flask [7]. Except for the gas chromatographic method, which determines inorganic iodine, the above methods give the total iodine content of milk.

As most of the iodide in milk is in the ionic form [8], iodide-specific electrodes [1,9] can be used and are the simplest of all the detection devices. However, the electrode response is slow at low iodide concentrations and the approach is subject to interference from free sulphydryl groups in pasteurized milk and dairy products [1].

In the method proposed here, precipitation of milk proteins and most of the fat is effected by addition of methanol. The remaining organics are removed by means of a C_{18} solid-phase extraction cartridge before ion chromatographic separation and electrochemical detection of iodide. Table salt is simply diluted, filtered and directly analysed by high-performance liquid chromatography (HPLC).

EXPERIMENTAL

Reagents

Degassed Milli-Q water (Millipore, Bedford, MA, U.S.A.) was used for making solutions. The mobile phase consisted of 0.0055 *M* KH_2PO_4 at its natural pH of about

0021-9673/90/$03.50

5. For solid-phase extraction clean-up, Waters Assoc. Sep-Pak C_{18} cartridges and 0.45-μm filters were used. A 500 μg/ml iodide stock solution was prepared from potassium iodide and dilutions were made as necessary. Milk and other samples were purchased from local supermarkets. Spiking of milk was done by diluting 0.2 ml of appropriate concentrated aqueous iodide standard to 100 ml with milk.

Liquid chromatography

The HPLC system consisted of a Beckman Model 112 solvent-delivery module, a Model 420 controller and a Model 340 organizer with a 50-μl loop. A Bioanalytical Systems LC-4B amperometric detector was used with a silver working electrode at 0.155 V and 0.005 in. film thickness. Peak areas were computed with a Spectra Physics SP 4270 integrator. A Vydac 302 IC (Separations Group, Hesperia, CA, U.S.A.), column (250 × 4.6 mm I.D) preceded by a Vydac ion guard column was used for separations. The mobile phase flow-rate was maintained at 2 ml/min.

Sample preparation

Milk. A 25-ml volume of milk was incubated in a 150-ml beaker in a water-bath for 3 min at 38°C. Following this, 50 ml of analytical-reagent grade methanol were added, the solution was mixed by swirling and the beaker was left in the bath for a further 3 min. The sample was allowed to stand at room temperature for 30 min and then filtered through Whatman No. 1 filter-paper. After another a further 30 min about 4 ml of clear filtrate were passed through a Sep-Pak C_{18} cartridge. The first 2 ml of the eluate were discarded and the remainder was filtered through a 0.45-μm filter for analysis.

Other samples. Yogurt and cream were treated in the same way as milk. For instant milk powder an 8–10% solution in water was prepared and then treated as for milk. For processed cheese, a 10-g sample of cut pieces of cheese was weighed in a 150 ml beaker and mixed with water to give about 50 ml of sample. The sample was homogenized (Polytron) for 1 min and the homogenate was diluted to 100 ml with methanol, homogenized again and filtered. A 4-ml volume of the filtrate was passed through a Sep-Pak C_{18} cartridge and the remainder of the procedure for milk was followed.

Procedure

A 100-μl aliquot of the sample filtrate was injected into the HPLC system. Iodide was determined by comparing the peak areas of the sample and the standard treated in exactly the same manner.

RESULTS AND DISCUSSION

Three different ion chromatographic columns were evaluated for the separation of iodide in milk sample extracts. Fig. 1 shows typical chromatograms obtained. Although all three columns performed well for pure iodide standards, there were signifiant differences when actual samples were analysed. With the Partisil 10 SAX column (Whatman) (A), the iodide peak was immediately preceded by another peak of almost equal height. In the case of the IC Pak Anion column (Waters Assoc.) (B). a huge matrix peak followed the iodide peak, thus affecting quantification. The best

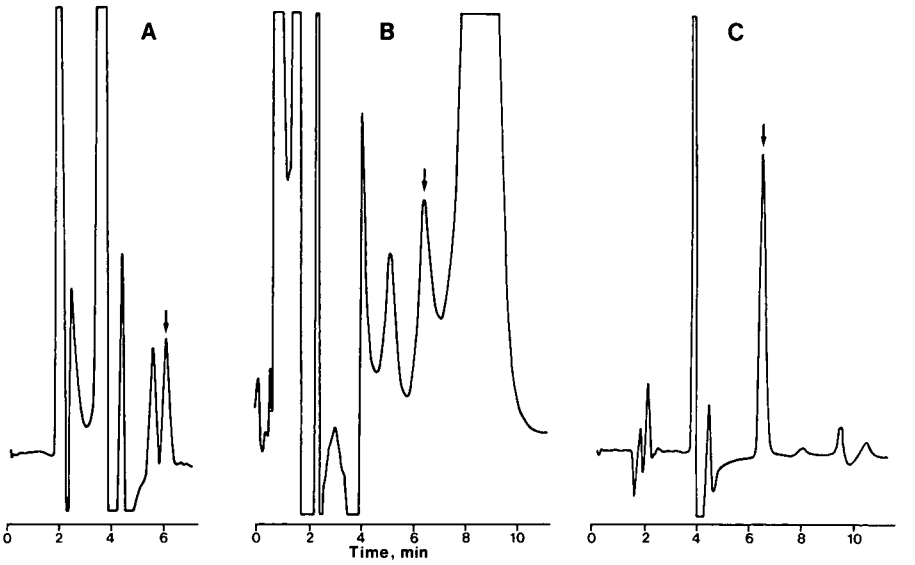

Fig. 1. Chromatograms of a whole-milk extract obtained under different conditions. (A) Partisil 10 SAX; mobile phase, 0.0065 *M* KH_2PO_4 (pH 6.2) at 2 ml/min. (B) IC Pak Anion; mobile phase, 0.005 *M* *p*-hydroxybenzoic acid (pH 10.5) at 0.9 ml/min. (C) Vydac 302 IC; mobile phase, 0.0065 *M* KH_2PO_4 (pH 6.3) at 2 ml/min.

TABLE I

IODIDE IN DAIRY PRODUCTS

Sample	Iodide (μg/l)
Milk:	
Brand A:	
Whole	363
2% fat	633
Skim	529
Brand B:	
Whole	730
2% fat	1074
Skim	480
Brand C:	
Whole	244
2% fat	236
Skim	273
Chocolate milk	350
Yoghurt	351
Half-and-half cream	350
Instant milk powder[a]	3000 μg/kg
Processed cheese (brick)	320 μg/kg

[a] Normally diluted *ca.* 10-fold before consumption.

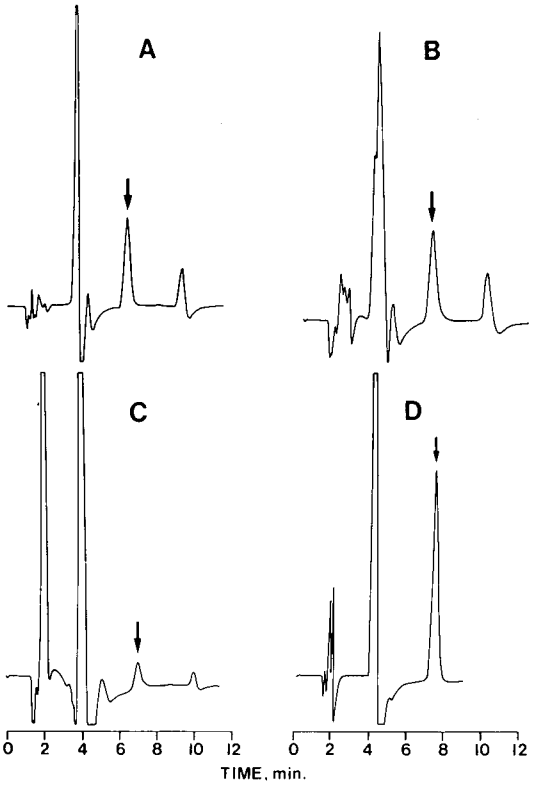

Fig. 2. Typical chromatograms obtained using the procedure described in the text. (A) Instant milk powder; (B) yogurt; (C) processed cheese; (D) table salt.

results were obtained with a Vydac 302 IC column (Separations Group) (C), where the iodide peak was clearly separated from the other sample components.

Several ionic reagents were checked for precipitation of proteins in milk. Some of them were found to be electroactive under the chromatographic conditions chosen and either gave a large response close to iodide elution time or resulted in a high background. Precipitation of proteins by adding an equal volume of acetonitrile [7] to milk was found to be satisfactory. However, it was observed that the response of iodide increased with repeated injections of filtrate. This effect was substantially reduced when methanol was used as the precipitant. No significant change in peak area was noticed on repeated injections over a 1-h period.

The detector response to iodide was linear in the range 2–100 ng injected. Replicate determinations on 25-ml aliquots of a whole milk sample gave a relative standard deviation of 3.3% at a level of 600 μg/l. The recovery of iodide at levels of 400 and 800 μg/l added to milk was 99% and 114%, respectively. Yogurt, chocolate milk, half-and-half cream, instant milk powder and processed cheese gave recoveries of 92, 100, 110, 99 and 103%, respectively. The detection limits were about 25 μg/l for the foods examined.

Table I presents results obtained for a variety of dairy products. The values for

milk ranged from 236 to 1074 μg/l iodide with an overall average of 507 μg/l, which compares well with earlier data for milk from this geographical area [2] obtained using a completely different technique. The wide range of values is probably due to the difference in the use of iodophors within the dairy industry. The concentration of iodide was not related to the fat content of the milk. The other dairy products analysed had iodide concentrations within the range found for the milk products (instant milk powder being diluted *ca.* 10-fold before consumption). Fig. 2 shows some typical chromatograms obtained using the described method. No interferences or technical problems were encountered with any of the sample types examined.

Confirmation of the iodide peak in selected samples was carried out by adding silver nitrate to the sample extract to precipitate the iodide. The extract was then passed through a cation-exchange solid-phase extraction tube (Supelco) to remove the silver ions and then an aliquot was injected into the HPLC system. The iodide peak was completely removed by the silver nitrate treatment indicating that it was, indeed, iodide (bromide, chloride and fluoride elute with different retention times).

Iodide in table salt was determined using the same HPLC system. Table salt was simply dissolved in water (0.2%, w/v), filtered and analysed for iodide. No interferences from chloride were observed (see Fig. 2). The recovery of iodide from table salt was 94% at a 100 μg/g spiking level. A similar technique using electrochemical detection with a platinum electrode and different chromatographic conditions has been reported recently [10].

The method described is simple, sensitive and selective. It may be adapted to the determination of ionic iodide in other food types.

REFERENCES

1 M. E. Dellavalle and D. M. Barbano, *J. Food Prot.*, 47 (1984) 678.
2 P. W. F. Fisher and A. Giroux, *Can. Inst. Food Sci. Technol. J.*, 20 (1987) 166.
3 R. Stabel-Taucher, *Finn. Chem. Lett.*, 1 (1976) 27.
4 H. J. Baker, *J. Assoc. Off. Anal. Chem.*, 60 (1977) 1307.
5 T. Stijve, J. M. Diserens and Ch. Blake, *Dtsch. Lebensm.-Rundsch.*, 84 (1988) 341.
6 A. R. Curtis and P. Hamming, *J. Assoc. Off. Anal. Chem.*, 65 (1982) 20.
7 W. J. Hurst, K. P. Snyder and R. A. Martin, Jr., *J. Liq. Chromatogr.*, 6 (1983) 2067.
8 E. W. Bretthauer, A. L. Mullen and A. A. Moghissi, *Health Phys.*, 22 (1972) 257.
9 D. E. Lacroix and N. P. Wong, *J. Food Prot.*, 43 (1980) 672.
10 K. Han, W. F. Koch and K. W. Pratt, *Anal. Chem.*, 59 (1987) 731.

Journal of Chromatography, 518 (1990) 273–276
Elsevier Science Publishers B.V., Amsterdam

CHROM. 22 603

Note

Stepwise gradient in thin-layer chromatography of *Chelidonium* alkaloids

G. MATYSIK* and L. JUSIAK
Department of Inorganic and Analytical Chemistry, Medical Academy, ul. Staszica 6, 20081 Lublin (Poland)
(First received March 23rd, 1990; revised manuscript received May 30th, 1990)

The application of gradient elution in thin-layer chromatography (TLC) has been found to be very effective in the separation of complex mixtures, *e.g.*, plant extracts [1–9], whose components have a wide range of polarity. Various methods of gradient elution have been elaborated, for instance, by preadsorption of solvent vapours in chambers devised by Geiss and Schlitt (see ref. 1), Kaiser [10] and De Zeeuw [1,12] or by the use of eluent distributors as described by Niederwieser and Honegger [2,3], Soczewiński and co-workers [13–15] and more recently Dzido and Soczewiński [16,17].

In all gradient techniques, if there are large differences in the eluent strengths of the component solvents of the mobile phase [A (weaker) and B (stronger)], deformation of the gradient profile is observed, owing to much stronger adsorption of component B in the layer, which is especially significant at low concentrations of solvent B. This effect leads to accumulation of spots in the zone of strong changes in the composition of the mobile phase [13].

In order to eliminate this undesirable effect, a combined polyzonal–stepwise gradient programme was applied in a recent paper [18]. As in ordinary stepwise gradients, the eluent is composed of two solvents, A (weaker) and B (stronger), the content of solvent B being increased stepwise; however, one component (or both) is composed of several solvents (*e.g.*, B_1, B_2 and B_3) of differentiated eluent strength ε^0, so that $\varepsilon^0_{B1} < \varepsilon^0_{B2} < \varepsilon^0_{B3}$. Under these conditions, solvents B_1–B_3 undergo frontal chromatography, as in polyzonal elution, thus reducing the sudden changes in the eluent strength along the layer.

In this paper, an analogous ternary stepwise gradient programme was applied to the analysis of *Chelidonium* alkaloids in the waste alkaloid fractions after industrial isolation of two dominant alkaloids used in therapy, chelidonine and protopine [19]. The extracts contain alkaloidal derivatives of benzophenanthridine, protoberberine, protopine and aporphine; some of them have interesting pharmacological properties [20] such as anticancer and spasmolytic (chelidonine and protopine), antimicrobial (chelerithrine) and anti-inflammatory properties (sanguinarine).

0021-9673/90/$03.50

EXPERIMENTAL

The industrial waste alkaloid fraction was obtained from Herbapol (Wroclaw, Poland). Reference alkaloids were prepared in this Department according to several procedures [21–23]. A chloroform solution of the mixture of alkaloids was spotted without preliminary purification on precoated silica gel plates (Si 60, 5 × 10 cm; E. Merck, Darmstadt, F.R.G.). The separated spots were detected under UV light (366 nm) or with Dragendroff's reagent.

A horizontal sandwich chamber with a glass distributor was used [13,14], equipped with a spiral PTFE capillary serving as a reservoir of eluent fractions [15]. The gradient programmes applied are given in Table I. Portions of 0.2 ml of six eluent fractions were introduced into six small test-tubes and sucked consecutively into the PTFE capillary in the reverse order (6–1) by moving the plunger of the syringe [15] backwards; to avoid mixing, each fraction was separated by a small air bubble. After introducing fraction under the distributor of the chamber and starting the development, the consecutive fractions of increasing eluent strength were sucked under the distributor by capillary forces so that stepwise gradient elution was produced.

A simpler method [13,14] consists in direct introduction of the consecutive eluent fractions 1–6 under the distributor from a micropipette, after complete absorption of the previous fraction by the layer. The PTFE capillary is then not necessary.

RESULTS AND DISCUSSION

Fig. 1 presents the chromatograms of the waste alkaloid extract obtained for a binary, six-step gradient programme (Table I). The spots are accumulated in the lower part of the chromatogram and a distinct eluent demixing front is visible. The use of fractions containing higher concentrations of methanol did not improve the separation.

Fig. 2 is the chromatogram obtained with the first ternary stepwise gradient programme given in Table I and Fig. 3 that obtained with the second ternary gradient programme given in Table I. It can be seen that the use of ethyl acetate as a compo-

TABLE I

SIX-STEP GRADIENT ELUTION PROGRAMMES WITH BINARY AND TERNARY ELUENTS

Eluent	Solvent	Eluent fraction No.					
		1	2	3	4	5	6
Binary	A = toluene	99	98	95	93	90	88
	B = methanol	1	2	5	7	10	12
Ternary	A = toluene–ethyl acetate (1:1)	99	98	95	93	92	90
	B = isopropanol	1	2	5	7	8	10
Ternary	A = toluene–ethyl acetate (1:1)	100	98	97	95	93	90
	B = methanol	–	2	3	5	7	10

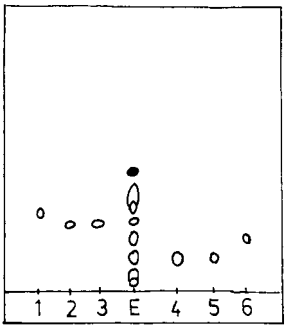

Fig. 1. Chromatogram of alkaloid extract (E) and reference solutes: (1) sanguinarine; (2) homochelidonine; (3) chelerithrine; (4) allocryptopine; (5) protopine; (6) chelidonine. Stepwise gradient according to Table I with binary eluent. White spots, visible under UV radiation and reacting with Dragendorff's reagent; black spots, visible only under UV radiation. Reference alkaloids, 4 μl of 0.1% (w/v) solution; extract, 8 μl of 0.5% solution.

nent of the mobile phase, owing to its moderate eluent strength, eliminated the effect of solvent demixing; the alkaloid spots are well shaped and compact, distributed along the whole chromatogram. Twelve spots reacting with Dragendorff's reagent are visible, including a large amount of chelidonine and trace amounts of three alkaloids (a, b and c) which could not be separated in isocratic systems and in systems reported in earlier papers [24,25]. These are presumably chelamine, chelamidine and coptisine [20]. The total number of separated spots visible under UV light is about 30. It is also noteworthy that two pairs of alkaloids are well separated in the system reported, *i.e.*, protopine–allocryptopine and chelerithrine–sanguinarine (pseudochelerithrine), with minor structural differences (dimethoxy or methylenedioxy groups). These pairs of alkaloids show small differences in R_F values in other systems [22–25].

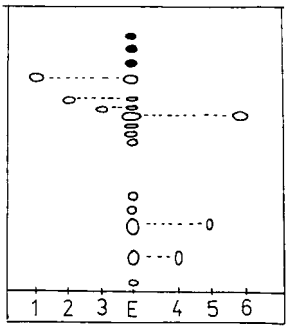

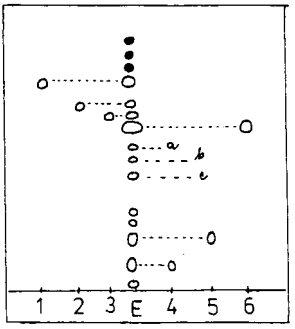

Fig. 2. As in Fig. 1, with gradient programme according to Table I using the first ternary eluent.

Fig. 3. As in Fig. 1, with gradient programme according to Table I using the second ternary eluent.

CONCLUSIONS

The separation efficiency in gradient TLC in the polyzonal–stepwise mode is much better, especially for complex samples containing solutes with a wide range of polarity, which requires a steep gradient with great differences in the polarities of component solvents A and B. Even the relatively simple ternary system is suitable also for the micropreparative TLC separation of alkaloids as reference compounds.

The method is suitable for direct TLC of waste alkaloid fractions without preliminary purification, which permits the detection of additional alkaloids present in trace amounts. It is also suitable for the analytical control of subsequent separation stages.

The concept of a polyzonal–stepwise gradient, where the component solvents A or B (or both) are mixtures of several solvents, can also be used in high-performance liquid chromatography for simple, two-compartment gradient generators.

REFERENCES

1 F. Geiss, *Fundamentals of Thin Layer Chromatography (Planar Chromatography)*, Hüthig, Heidelberg, 1987, p. 395.
2 A. Niederwieser and C. C. Honegger, *Adv. Chromatogr.*, 2 (1966) 123.
3 A. Niederwieser, *Chromatographia*, 2 (1969) 362.
4 G. Matysik and E. Soczewiński, *J. Chromatogr.*, 355 (1986) 363.
5 E. Soczewiński, G. Matysik and K. Glowniak, in R. E. Kaiser (Editor), *Instrumental High Performance Thin-Layer Chromatography, Proceedings of the 3rd international Symposium, Würzburg, April 1985*, Institut für Chromatographie, Bad Dürkheim, 1985, p. 413.
6 G. Matysik and E. Soczewiński, *Chromatographia*, 26 (1988) 178.
7 W. Cisowski, K. Glowniak, G. Matysik and E. Soczewiński, *Herba Pol.*, 33 (1987) 233.
8 T. Dzido, G. Matysik, E. Soczewiński, H. Wysokińska and U. Adamczyk, *Chromatographia*, 27 (1989) 24.
9 K. Glowniak, G. Matysik, M. Bieganowska and E. Soczewiński, *Chromatographia*, 22 (1986) 307.
10 R. E. Kaiser, in A. Zlatkis and R. E. Kaiser (Editors), *HPTLC—High Performance Thin-Layer Chromatography*, Elsevier, Amsterdam, 1977, p. 73.
11 *Desaga VP-Trennkammer nach De Zeeuw*, Druckschrift 171/71, Desaga, Heidelberg, 1971.
12 R. A. De Zeeuw, *Prog. Sep. Purif.*, 3 (1970) 1.
13 E. Soczewiński, in R. E. Kaiser (Editor), *Planar Chromatography*, Vol. 1, Hüthig, Heidelberg, 1986, p. 79.
14 G. Matysik and E. Soczewiński, *J. Chromatogr.*, 369 (1986) 19.
15 E. Soczewiński and G. Matysik, *J. Planar Chromatogr.*, 1 (1988) 354.
16 T. H. Dzido and E. Soczewiński, *J. Chromatogr.*, in press.
17 T. H. Dzido, *J. Planar Chromatogr.*, 3 (1990) 144.
18 E. Soczewiński and G. Matysik, *J. Planar Chromatogr.*, in press.
19 J. Jusiak, J. Kuczyński, E. Soczewiński, T. Gersz and S. Popiołek, *Pol. Pat.*, 261 306, 1985.
20 I. W. Southon and J. Buckingham (Editors), *Dictionary of Alkaloids*, Chapman and Hall, London, New York, 1989.
21 L. Jusiak, E. Soczewiński, J. Respondek, T. Żaba, M. Ciesielski and P. Sieradzki, *Pol. Pat.*, 129 822, 1981.
22 J. Jusiak, E. Soczewiński and M. Ciesielski, *Pol. Pat.*, 136 290, 1985.
23 L. Jusiak, A. Rompala, *Pol. Pat.*, 141 868, 1987.
24 L. Jusiak, *Acta Pol. Pharm.*, 39 (1982) 249.
25 B. Szabelska, L. Jusiak and G. Matysik, *Acta Pol. Pharm.*, 38 (1981) 329.

Journal of Chromatography, 518 (1990) 277–281
Elsevier Science Publishers B.V., Amsterdam

CHROM. 22 625

Letter to the Editor

Effect of ^2H_2O on the resolution of the optical isomers of ibuprofen on an α_1-acid glycoprotein column

Sir,

Recently we have been working with an α_1-Acid glycoprotein (α_1-AGP) column (purchased from Chrom Tech) for the chiral separation of a variety of molecules. We are interested in the mechanism of chiral recognition processes involved in the resolution of optical isomers as we feel that such an understanding will facilitate the prediction of the correct choice of analytical column for a particular separation. Unfortunately, as in the case of other immobilised protein systems the mechanism of chiral recognition by α_1-AGP is complex and not yet known in detail. Although hydrophobic and electrostatic interactions are thought [1] to affect chiral discrimination by protein columns, other interactions can also be of importance. To enhance our understanding of the mechanisms of interaction on α_1-AGP we have investigated the influence of replacing H_2O by ^2H_2O as the mobile phase on the separation of the enantiomers of a model carboxylic acid, namely ibuprofen.

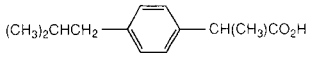

Ibuprofen

We carried out the chiral resolution of the enantiomers of ibuprofen using phosphate buffer as the mobile phase. This consisted of 0.01 *M* KH_2PO_4 adjusted to the required pH with 0.01 *M* K_2HPO_4. The acidity (p^2H) of ^2H_2O solutions was measured with an ordinary glass electrode by adding 0.40 to the observed reading of a pH meter which was calibrated with standard buffers in aqueous solution [2]. The flow-rate of the mobile phase was maintained at 0.5 ml min^{-1} in all experiments. The temperature of the column was 25°C and UV detection was at a wavelength of 225 nm. Results are tabulated in Tables I and II.

It is known [3] that the retention of carboxylic acids is increased on the α_1-AGP column with a decrease in pH. This has been confirmed in our studies and may be due either to an increase in the unionised form of ibuprofen or to an increase in the number of positive charges on α_1-AGP or to a combination of both effects. Fig. 1 shows that the largest change in the capacity factors of the two enantiomers of ibuprofen (labelled k_A and k_B) occurs around a pH of 6.5. As the pK_a of ibuprofen is about 4.5, this molecule is expected to exist largely in the unionised form in the pH range of 5.6 to 7.5. Moreover, amine groups on the protein derived from lysine and

0021-9673/90/$03.50

TABLE I

RESOLUTION OF THE ENANTIOMERS OF IBUPROFEN USING H_2O IN THE MOBILE PHASE

k_A and k_B values are averages of two experiments.

pH	k_A	k_B	$k_B - k_A$	α
5.99	11.93	15.86	3.93	1.33
6.30	7.44	9.10	1.86	1.26
6.49	5.54	7.23	1.69	1.31
6.71	3.71	4.90	1.20	1.32
7.00	2.19	2.81	0.62	1.28
7.28	1.60	2.01	0.41	1.26
7.50	1.31	1.53	0.22	1.17

TABLE II

RESOLUTION OF THE ENANTIOMERS OF IBUPROFEN USING ^2H_2O

k_A and k_B values are averages of two experiments.

p^{2}H	k_A	k_B	$k_B - k_A$	α
6.17	21.63	28.51	6.89	1.32
6.50	12.58	17.12	4.54	1.36
6.80	8.47	11.36	2.89	1.34
7.30	4.37	5.46	1.09	1.25

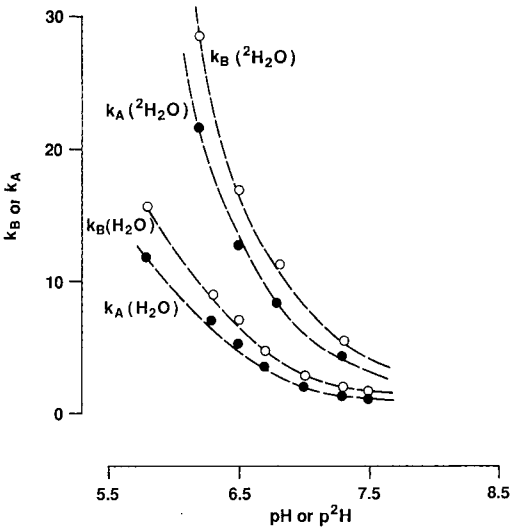

Fig. 1. Variation of k_A and k_B with pH using either H_2O or ^2H_2O as the mobile phase.

arginine residues have pK_a values of about 10.5 and over 12, respectively, so that in the pH region mentioned such amino groups are expected to be fully protonated. On the other hand, the basic site on a histidine residue will accept a proton to form a conjugate acid of $pK_a \approx 6.4$–7.0 and carrying a positive charge. A wider pH profile could have given a better indication on whether a histidine residue plays a role in the chiral separation of the antipodes of ibuprofen. Low pH values have an adverse effect on the stability of the α_1-acid glycoprotein column.

Fig. 1 also shows that both enantiomers of ibuprofen are retained more in ^2H_2O rather than in H_2O solutions of the same acidity. This isotope effect is further illustrated in the chromatograms shown in Fig. 2 for chiral resolutions carried out at pH or p^2H values close to 7.3; in this case almost baseline resolution of the enantiomers of ibuprofen is only obtained in ^2H_2O solution. The magnitude of the isotope effect is again demonstrated in Fig. 3 by plotting the difference in the capacity factors ($k_B - k_A$) either in ^2H_2O or H_2O solutions *versus* pH or p^2H.

As shown in Tables I and II the separation factor α does not change appreciably over a range of pH or p^2H values. In contrast the resolution factor R_s changes markedly with acidity and varies linearly as shown by other workers [4]. R_s values have been plotted *versus* pH or p^2H in Fig. 4. These were found to be generally higher in ^2H_2O compared to H_2O in the acidity region of 6–7, usually recommended for the α_1-AGP column. Moreover, the slope of R_s against p^2H is steeper than that of R_s against pH. We have performed repeated analyses of α_1-AGP using ^2H_2O with no apparent effect on the stability of the column although we have no knowledge about the effect of this solvent in altering the conformation of the protein via changes in hydrogen and hydrophobic bonds.

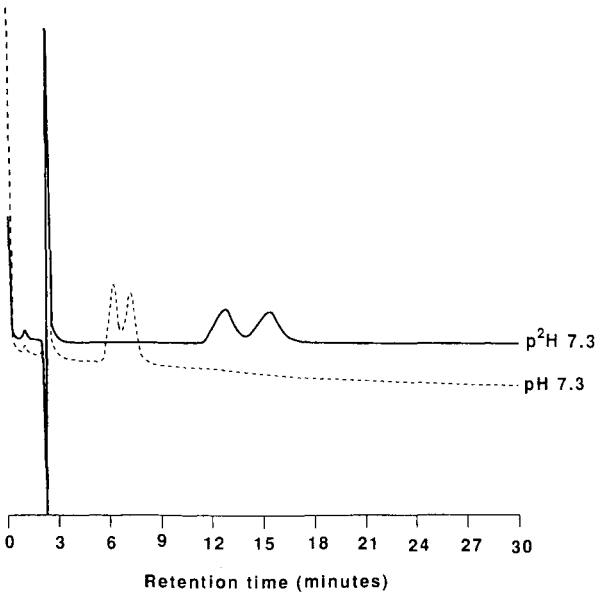

Fig. 2. Chromatograms of ibuprofen at a pH or p^2H around 7.3 (see Tables I and II for accurate acidity values).

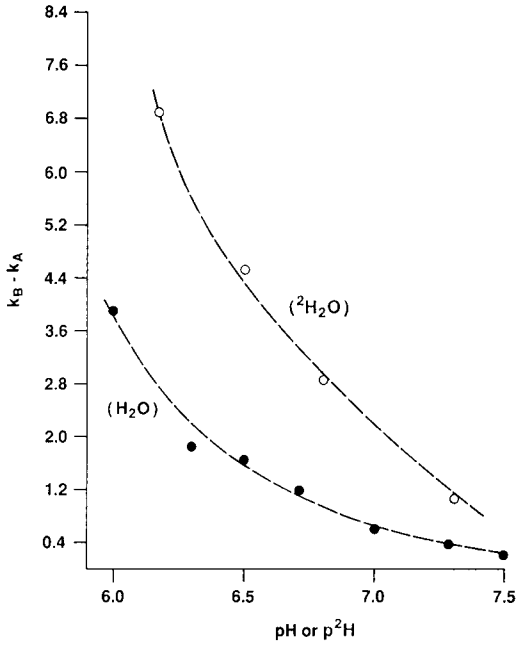

Fig. 3. A plot of $k_B - k_A$ *versus* pH or p^2H.

We feel that changes in retention characteristics of the enantiomers of a molecule observed on replacing H_2O with ^2H_2O as the mobile phase can have analytical advantages in that it can be used to improve chiral resolution, apparently by increasing the number of theoretical plates in a column, although the occurrence of such an effect is not universal with all compounds. In fact, preliminary studies carried out on Atenolol, which contains a secondary amine substituent, does not show any

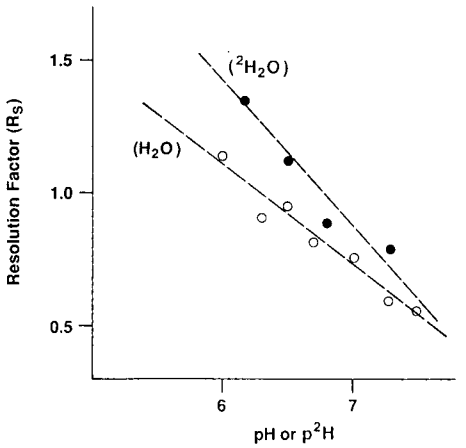

Fig. 4. Illustration of the increase of the resolution factor, R_s, with a decrease in acidity.

significant increase in resolution of the respective enantiomers using ^2H_2O as the mobile phase. Presently we are investigating the magnitude of a ^2H_2O effect on the chiral resolution of other acids and we shall report this data in due course.

Separation and Detection Methods Section,
SmithKline Beecham, The Frythe,
Welwyn, Herts. AL6 9AR (U.K.)

PATRICK CAMILLERI*
CATHERINE DYKE

1 S. Allenmark, in A. M. Krstulovic (Editor), *Chiral Separation by HPLC, Applications to Pharmaceutical Compounds,* Ellis Horwood, Chichester, New York, 1989, p. 285.
2 P. K. Glasoe and F. A. Long, *J. Phys. Chem.*, 64 (1960) 188.
3 S. Allenmark, B. Bomgren and H. Boren, *J. Chromatogr.*, 316 (1984) 617.
4 K. Balmer, B.-A. Persson and G. Schill, *J. Chromatogr.*, 477 (1989) 107.

(First received May 8th, 1990; revised manuscript received June 11th, 1990)

15 th International

Symposium

on Column Liquid

Chromatography

Convention Center

Basel, Switzerland

June 3–7, 1991

HPLC '91 Basel

Chairman

Dr. Fritz Erni

Secretariat

Swiss Industries Fair
Congress Department
P. O. Box
CH-4021 Basel
Switzerland

Telephone
++41 61/686 28 28
Telefax
++41 61/691 80 49

ANNOUNCEMENT AND CALL FOR PAPERS

12th INTERNATIONAL MASS SPECTROMETRY CONFERENCE

Amsterdam, The Netherlands

26–30 August 1991

The scientific programme will cover all aspects of mass spectrometry: theory, fundamental studies, applications, and instrumentation. An important aim of the Organizing Committee is to provide an atmosphere which will stimulate the exchange of information between the attending scientists.

Plenary lectures will be given by invited speakers who will review areas in mass spectrometry such as instrumentation, theory, multi-photon ionisation, gas phase ion chemistry, desorption and hyphenated methods and biochemical applications. Shorter keynote lectures, also to be presented by invited speakers, will consist of specialized reviews covering similar subjects, and topics such as high masses, clusters, organometallics, thermochemistry, isotope dilution and surface analysis, reaction dynamics, pyrolysis, geochemistry, environmental and forensic applications, biochemical and biomedical studies, and chemometrics.

Contributed papers will be accepted for poster sessions only. All those intending to contribute to the conference are invited to submit papers. All contributed papers will be refereed. The final date for submission of abstracts is **15 January 1991** and for revised/extended abstracts **1 June 1991**.

The proceedings of the Conference, comprising all plenary and keynote lectures in full, will be published by Elsevier Science Publishers as a hard-cover book, entitled "*Advances in Mass Spectrometry, Volume 12*" and as two consecutive volumes of the *International Journal of Mass Spectrometry and Ion Processes*. These will be published after the conference. A book containing the revised/extended abstracts of all contributed papers will be made available to registered participants at the conference. There will be an extensive exhibition of scientific equipment, including mass spectrometers in operation, and of the relevant literature.

The registration fee will be Dfl.500 if paid on or before **30 June 1991** and Dfl.550 if paid at a later date. The accompanying person's fee is Dfl.150. The registration fee for students working for a research degree will be Dfl.250 if paid on or before 30 June 1991. Students are encouraged to present a poster.

For further details, contact:

Conference Secretariat IMSC-XII
c/o RAI Organisatie Bureau Amsterdam bv
Europaplein 12
1078 GZ Amsterdam
The Netherlands

PUBLICATION SCHEDULE FOR 1990

Journal of Chromatography and Journal of Chromatography, Biomedical Applications

MONTH	J	F	M	A	M	J	J	A	S	O	N	D[a]
Journal of Chromatography	498/1 498/2 499	500 502/1	502/2 503/1 503/2 504/1	504/2 505/1	505/2 506 507 508/1	508/2 509/1 509/2 510	511 512 513	514/1 514/2 515	516/1 516/2 517 518/1	518/2 519/1	519/2 520 521/1 521/2	
Cumulative Indexes, Vols. 451–500		501										
Bibliography Section		524/1		524/2		524/3		524/4		524/5		
Biomedical Applications	525/1	525/2	526/1	526/2 527/1	527/2	528/1 528/2	529/1	529/2 530/1	530/2	531 532/1	532/2 533	

[a] The publication schedule for further issues will be published later.

INFORMATION FOR AUTHORS

(Detailed *Instructions to Authors* were published in Vol. 513, pp. 413–416. A free reprint can be obtained by application to the publisher, Elsevier Science Publishers B.V., P.O. Box 330, 1000 AH Amsterdam, The Netherlands.)

Types of Contributions. The following types of papers are published in the *Journal of Chromatography* and the section on *Biomedical Applications:* Regular research papers (Full-length papers), Notes, Review articles and Letters to the Editor. Notes are usually descriptions of short investigations and reflect the same quality of research as Full-length papers, but should preferably not exceed six printed pages. Letters to the Editor can comment on (parts of) previously published articles, or they can report minor technical improvements of previously published procedures; they should preferably not exceed two printed pages. For review articles, see inside front cover under Submission of Papers.

Submission. Every paper must be accompanied by a letter from the senior author, stating that he is submitting the paper for publication in the *Journal of Chromatography*. Please do not send a letter signed by the director of the institute or the professor unless he is one of the authors.

Manuscripts. Manuscripts should be typed in double spacing on consecutively numbered pages of uniform size. The manuscript should be preceded by a sheet of manuscript paper carrying the title of the paper and the name and full postal address of the person to whom the proofs are to be sent. As a rule, papers should be divided into sections, headed by a caption (*e.g.*, Abstract, Introduction, Experimental, Results, Discussion, etc.). All illustrations, photographs, tables, etc., should be on separate sheets.

Introduction. Every paper must have a concise introduction mentioning what has been done before on the topic described, and stating clearly what is new in the paper now submitted.

Abstract. Full-length papers and Review articles should have an abstract of 50–100 words which clearly and briefly indicates what is new, different and significant. (Notes and Letters to the Editor are published without an abstract.)

Illustrations. The figures should be submitted in a form suitable for reproduction, drawn in Indian ink on drawing or tracing paper. Each illustration should have a legend, all the *legends* being typed (with double spacing) together on a *separate sheet*. If structures are given in the text, the original drawings should be supplied. Coloured illustrations are reproduced at the author's expense, the cost being determined by the number of pages and by the number of colours needed. The written permission of the author and publisher must be obtained for the use of any figure already published. Its source must be indicated in the legend.

References. References should be numbered in the order in which they are cited in the text, and listed in numerical sequence on a separate sheet at the end of the article. Please check a recent issue for the layout of the reference list. Abbreviations for the titles of journals should follow the system used by *Chemical Abstracts*. Articles not yet published should be given as "in press" (journal should be specified), "submitted for publication" (journal should be specified), "in preparation" or "personal communication".

Dispatch. Before sending the manuscript to the Editor please check that the envelope contains four copies of the paper complete with references, legends and figures. One of the sets of figures must be the originals suitable for direct reproduction. Please also ensure that permission to publish has been obtained from your institute.

Proofs. One set of proofs will be sent to the author to be carefully checked for printer's errors. Corrections must be restricted to instances in which the proof is at variance with the manuscript. "Extra corrections" will be inserted at the author's expense.

Reprints. Fifty reprints of Full-length papers, Notes and Letters to the Editor will be supplied free of charge. Additional reprints can be ordered by the authors. An order form containing price quotations will be sent to the authors together with the proofs of their article.

Advertisements. Advertisement rates are available from the publisher on request. The Editors of the journal accept no responsibility for the contents of the advertisements.